Chemiluminescence detection of cytotoxic drugs and their hydrolysis products

A thesis submitted for fulfilment of the degree of Doctor of Philosophy

Tiffany A. Reeves
BSc (Forens&AnalytChem)(Hons)

Flinders
UNIVERSITY

Faculty of Science and Engineering
School of Chemical and Physical Sciences

August 2016

Declaration

I certify that this thesis does not incorporate without acknowledgment any material previously submitted for a degree or diploma in any university; and that to the best of my knowledge and belief it does not contain any material previously published or written by another person except where due reference is made in the text.

Tiffany A. Reeves

…… ……..

Signed Date

Acknowledgements

Firstly, I would like to thank my supervisors Claire and Rachel. Your support both academically and personally has been incredible. You have been so understanding of my situations throughout the years. Thank you for being referees for numerous house and job applications. And especially thank you for the amazing work you both put in towards the end to ensure I could submit my thesis by the deadline I had imposed on myself. I would not have been able to achieve this without your amazing organisation and extra effort.

To Helen Webb, Sean Graney, and David Vincent, thank you for your help in gaining the necessary approval and permits required to use the cytotoxics in this research. Thank you also to Angela Binns and the Flinders Medical Centre for allowing me to use their cytotoxic preparation facilities to prepare my samples under these guidelines.

For training, advice, and access to analytical instrumentation I'd like to thank Rachel Hughes for the SIA chemiluminescence instrument, Martin Johnston for ^{31}P NMR experiments, and Tristan Kilmartin, Daniel Jardine, and Flinders Analytical for LC-MS/MS and UHPLC-UV/CAD analysis. Also a big thank you to Kimberley Patterson for training on the UHPLC-UV in Flinders Analytical, and for running the analysis on the LC-MS/MS at Thermo-Fischer in Melbourne for me. Another big thank you also to Caitlyn Rogers for analysing some of my samples on the LC-MS/MS at Forensic Science South Australia (FSSA). Also, thank you to Owen Osborne and Darko Bogdanovic for writing and developing the instrumentation and software that was the basis for the majority of this research.

Cheers to all the other PhD students from our year and others, especially Kimmi, Tim, Caroline, Russell, David, and Chris. It's been great getting to know you all. I'm really going to miss all of the sunshine lunch times, ice-cream binges while marking, getting distracted with videos, and all the good chats/venting sessions. Thanks for all your support guys!

Finally, to my friends and family, especially Mum, Dad, Andrew, Josh, and Mal. You've been the most amazing support and encouragement even when I was absolutely hating this. Thanks so much for not caring what I do, but just wanting me to be happy and content. Without you I definitely would not have been able to finish this.

Abstract

Cytotoxics are drugs used in chemotherapy to prevent growth and replication of cancerous cells via interacting with DNA and other cell processes. This action is non-specific, affecting both cancerous and healthy cells, and hence giving rise to harmful side effects. Cytotoxics have been of increasing concern to environmental chemists because many of these drugs are excreted unchanged and hence released into wastewaters. Their removal by wastewater treatment plants is also often inefficient, resulting in their release into surface waters, where they have the potential to have mutagenic and carcinogenic effects on aquatic organisms. Knowledge of these effects, however, is quite limited. This is in part due to lack of sensitivie analytical methods amenable to real-time, in-situ environmental analysis. Chemiluminescence is a technique with numerous advantages in environmental analysis, however it has had limited use in cytotoxic drug detection. This thesis describes development of chemiluminescence detection for three of the most commonly used cytotoxic drugs in Australia; cyclophosphamide, 5-fluorouracil, and imatinb.

Potassium permanganate, tris-2,2'-bipyridyl ruthenium (II) chloride ($Ru(bipy)_3Cl_2$), manganese dioxide, and cerium sulphate were investigated for their potential as chemiluminescence oxidising reagents of each cytotoxic. $Ru(bipy)_3Cl_2$ when prepared using either PbO_2 or $Ce(SO_4)_2$ produced the most intense chemiluminescence for each analyte. Further investigation into the use of $Ru(bipy)_3Cl_2$ prepared with $Ce(SO_4)_2$ indicated that side reactions were occurring between the cytotoxics and $Ce(SO_4)_2$. This detection method would therefore not offer analytical utility. The use of $Ru(bipy)_3Cl_2$ oxidised with PbO_2 was therefore explored.

While detection of imatinib using this reagent proved unsuccessful, detection methods for both 5-fluorouracil and cyclophosphamide were successfully developed. A new chemiluminescence detection method for 5-fluorouracil using $Ru(bipy)_3Cl_2$ oxidised with PbO_2 was developed using flow injection analysis (FIA). The limits of detection and quantitation were 6.06×10^{-8} M and 1.16×10^{-6} M, respectively. This was a 4-fold decrease in detection limit compared with previously reported methods [1]. Interference from Na^+, K^+, Mg^{2+}, Ca^{2+}, Fe^{3+}, Cl^-, Br^-, and I^- spiked into 5-fluorouracil solutions was observed, with all but Ca^{2+} resulting in emission quenching. These interferences were found to be removed via sequential strong anion SPE (STRATA-X-A) and strong cation SPE (STRATA-X-C) of the sample prior to analysis. The method was applied to spiked tap and lake water samples. The presence of organic interfering compounds results in recoveries of 27.5 % and 34.1 % from tap and lake water, respectively. However, these compounds could be easily separated from 5-flurouracil using UHPLC, and hence the developed method has great potential for detection of 5-fluorouracil in surface waters.

A new method for the chemiluminescence detection of cyclophosphamide in aqueous solution was also developed using $Ru(bipy)_3Cl_2$ oxidised with PbO_2. While poor linearity of response was achieved for fresh cyclophosphamide solutions, high correlation between cyclophosphamide concentration and chemiluminescence signal was obtained when analysing 24-hour-old solutions (R^2 of 0.9995). This was found to be due to hydrolysis of cyclophosphamide to compounds 7, 9, and 10 (see below) over 24 hours when stored at room temperature in the absence of light.

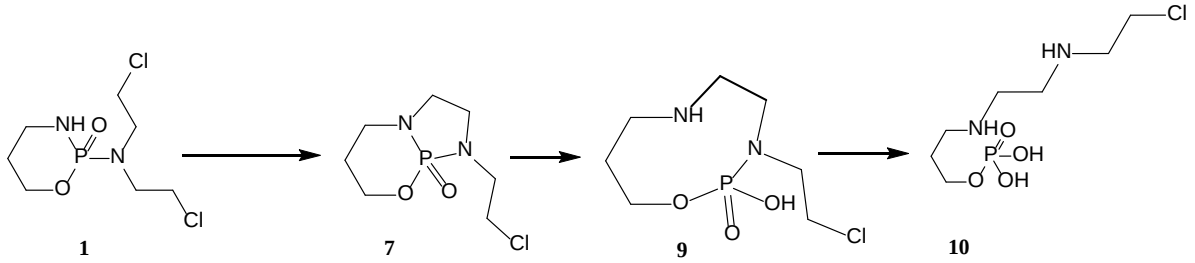

In summary, alternative sensitive analysis methods for cytotoxic drugs are required in order to conduct a true risk assessment on their potential harmful effects in surface waters. Here new chemiluminescence detection methods for the common cytotoxics cyclophosphamide and 5-fluorouracil were developed using $Ru(bipy)_3Cl_2$ prepared with PbO_2 as the oxidising reagent. A four-fold decrease in detection limits compared with previous methods was obtained for 5-fluorouracil detection, while chemiluminescence detection of cyclophosphamide proved valuable in monitoring its aqueous degradation. With these new methods further insight into their aqueous stability, and hence fate in surface waters, can be obtained, which would provide valuable information in assessing their effects on aquatic organisms in surface waters.

“In life, as in running, it’s all about the third bend;

how deep you dig.

It’s easy to explode out of the blocks, and the finish

line pulls us towards it with an almost magnetic

force,

But the hardest part is when you can’t remember

the beginning, or see the end.”

~Tom Hiddleston~

Contents

List of Figures

List of Tables

List of Abbreviations

Abbreviation	Meaning
HMP	hexametaphosphate
UHPLC	ultra high pressure liquid chromatography
SIA	sequential injection analysis
UV/Vis	ultra-violet/ visible
MS	mass spectrometry
NMR	nuclear magnetic resonance
FIA	flow injection analysis
LC-MS/MS	liquid chromatography tandem mass spectrometry
IC	ion chromatography
CAD	charged aerosol detector
PTFE	polytetrafluoroethylene

List of Chemicals

Chemical	Grade	Purity	Supplier
cyclophosphamide monhydrate	Analytical	97-100 %	Sigma Aldrich Pty Ltd.
5-fluorouracil	Analytical	>99 %	Sigma Aldrich Pty Ltd.
imatinib mesylate	Analytical	>99 %	Sapphire Bioscience
deuterium oxide	Reagent	100 %	Sigma Aldrich Pty Ltd.
sodium deuteroxide	Analytical	>98 %	Sigma Aldrich Pty Ltd.
deuterium chloride	Analytical	35 %	Sigma Aldrich Pty Ltd.
humic acids	Technical	-	Sigma Aldrich Pty Ltd.
potassium permanganate	Analytical	>99 %	Chem-Supply
tris-2,2'-bipyridyl ruthenium (II) chloride	Analytical	>98 %	Strem Chemicals
sulfuric acid	Reagent	95-97 %	Sigma Aldrich Pty Ltd.
hydrochloric acid	Ultra-Pure	37 %	Choice Analytical
sodium hydroxide	Analytical	98 %	Chem-Supply
sodium hydrogen carbonate	Laboratory	100 %	Merck Pty Ltd.
sodium borate decahydrate	Analytical	99 %	Amersham Australia Pty. Ltd
sodium dihydrogen phosphate	Analytical	98.50 %	Merck Pty Ltd.
disodium hydrogen phosphate	Analytical	98.5 %	Chem-Supply
perchloric acid	Analytical	70 %	Chem-Supply
acetonitrile	HPLC	99 %	Rowe Scientific
methanol	Analytical	99.80 %	Chem-Supply
formic acid	Ultra-Pure	90 %	Chem-Supply
formaldehyde	Analytical	37 %	Chem-Supply
ethanol	Analytical	>99 %	Chem-Supply
cerium(IV) sulfate	Analytical	99 %	Sigma Aldrich Pty Ltd.
sodium perchlorate	Puriss	>98 %	Sigma Aldrich Pty Ltd.
vanillin	Unknown	98 %	unknown
sodium oxalate	Puriss	<99.5 %	Sigma Aldrich Pty Ltd.
lead dioxide	Analytical	95 %	Chem-Supply
tris(hydroxymethyl)aminomethane	analytical	>99.5 %	Merck Pty Ltd.
Triton X100	Analytical	100 %	Sigma Aldrich Pty Ltd.
orthophosphoric acid	Reagent	85 %	Chem-Supply
sodium thiosulfate	Analytical	unknown	Chem-Supply
sodium hexametaphosphate	Reagent	100 %	Ajax Finechem
sodium chloride	Technical	unknown	Chem-Supply
potassium chloride	Analytical	99 %	Chem-Supply
magnesium chloride	Analytical	99 %	Merck Pty Ltd.
potassium iodide	Analytical	99 %	Ajax Finechem
potassium bromide	Analytical	99.5 %	Ajax Finechem
copper sulphate heptahydrate	Analytical	99 %	unknown
iron (III) chloride hexahydrate	analytical	99 %	Chem-Supply
calcium chloride dihydrate	Analytical	>99 %	Sigma Aldrich Pty Ltd.

Safety Considerations

All work was conducted in accordance with Section 56 of the Controlled Substances Act 1984. A Research Instruction Training or Analysis Permit was obtained (Permit Number: 2013-80161).

Chapter 1:

Introduction

1. Introduction

1.1 Cytotoxic Drugs

Cancer is one of the most common causes of death in Australia, accounting for 30 % of Australian deaths in 2013 [2]. It is caused by the rapid, uncontrollable division of body cells to form masses (tumours) or liquid cancers, such as in the blood and bone marrow [2]. These cancerous cells invade and damage neighbouring tissues and can spread to other parts of the body, which, if uncontrolled, can lead to death [3, 4]. It is predicted that 1 in 2 Australians will develop cancer before the age of 85, and 1 in 5 of these people will die from it. There is therefore a great and urgent need to develop effective cancer treatments [2].

There are currently three main treatments for cancer: surgery, chemotherapy, and radiotherapy, all of which can also be used in combination [4, 5]. Chemotherapy is the most common cancer treatment [6] and is defined as the use of anti-cancer drugs, or antineoplastics, to kill cancer cells, or to prevent their growth and spread [4]. This type of therapy began in the 1940's with the use of nitrogen mustards, which are alkylating agents capable of destroying DNA [4]. Since then, many different anti-cancer agents have been developed and utilised, each with various sites and modes of action [4].

There are two main classes of anticancer drugs: endocrine therapies and cytotoxic drugs [4, 7-9]. Endocrine drugs are used to treat hormone-dependent cancers, and can be either hormone analogues or hormone antagonists, and related compounds [9]. Cytotoxic drugs, on the other hand, are designed to either interact with DNA to prevent DNA and cell replication; hence preventing the spread of cancerous cells [4]. Alternately they may act on other cell components, such as structural proteins, resulting in cell death. Those that interact with DNA include alkylating agents and cross-linkers, antimetabolites, intercalating agents, and DNA cleaving agents. Those that do not interact with DNA include monoclonal antibodies, anti-protein kinases, anti-tubulin agents, and topoisomerase inhibitors [4]. Cytotoxics are non-selective, damaging the DNA and cell components of both healthy and cancerous cells [10]. They are therefore considered to be carcinogenic, genotoxic, and mutagenic themselves, and many have also been shown to exhibit teratogenicity, resulting in birth defects [5].

Cytotoxics encompass a large range of chemical compounds, with typical structures given in Figure 1-1. They can be classified according to the Anatomical Therapeutic Chemical (ATC) classification system from the World Health Organisation (WHO) [7], as shown in Figure 1-2. In Australia, the most commonly used class of cytotoxic drugs is pyrimidine analogues, followed by protein kinase inhibitors, "other" antineoplastic agents, and nitrogen mustards, as shown in Table 1-1. Cyclophosphamide, imatinib mesylate, and 5-fluorouracil (the active drug of capecitabine), are the

most commonly used cytotoxic drugs for each of the top 4 cytotoxic classes. These drugs were therefore selected as target analytes for this research, and will be the remaining focus of this literature review.

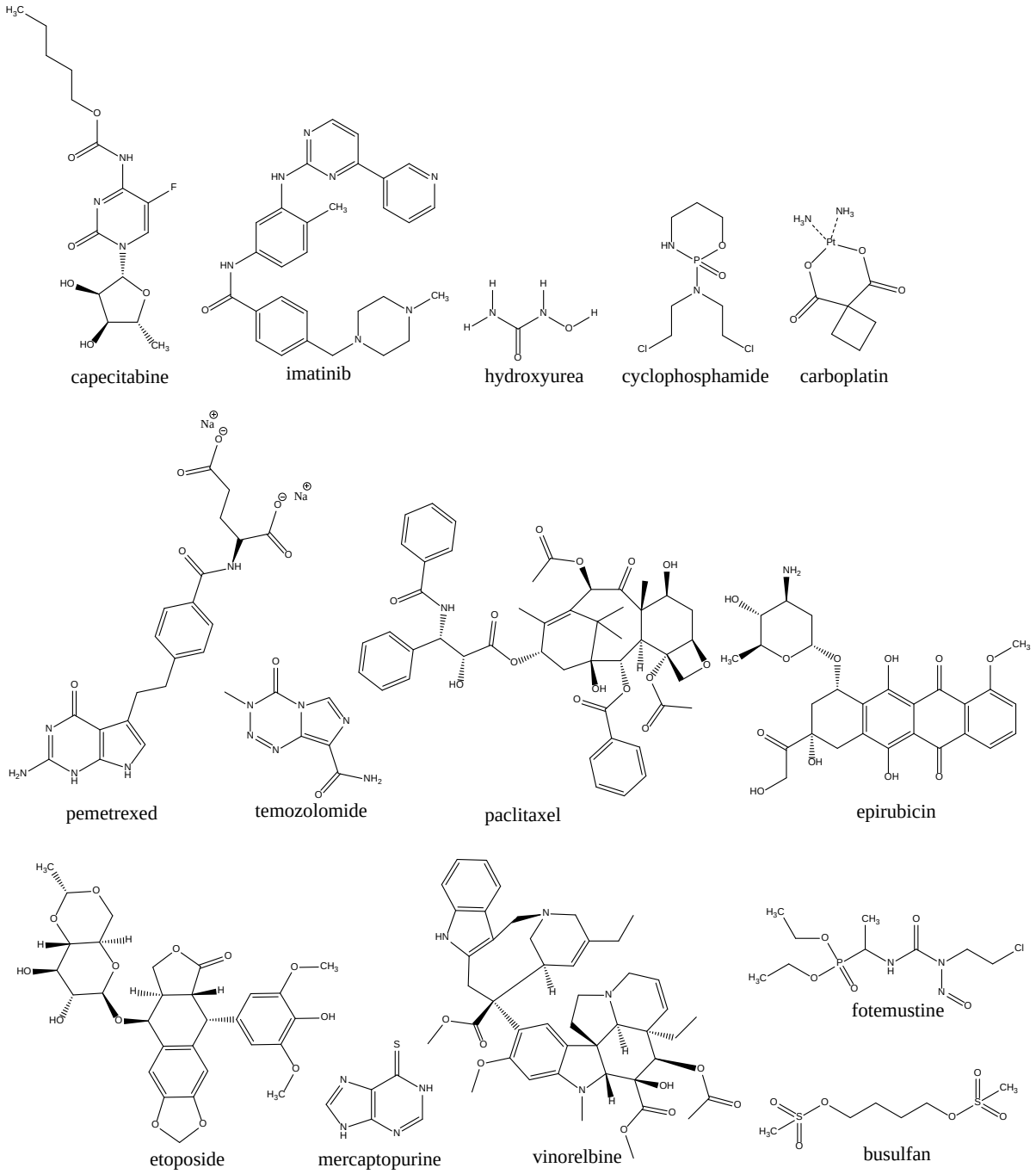

Figure 1-1. Structures of the most commonly used cytotoxic drugs of each class

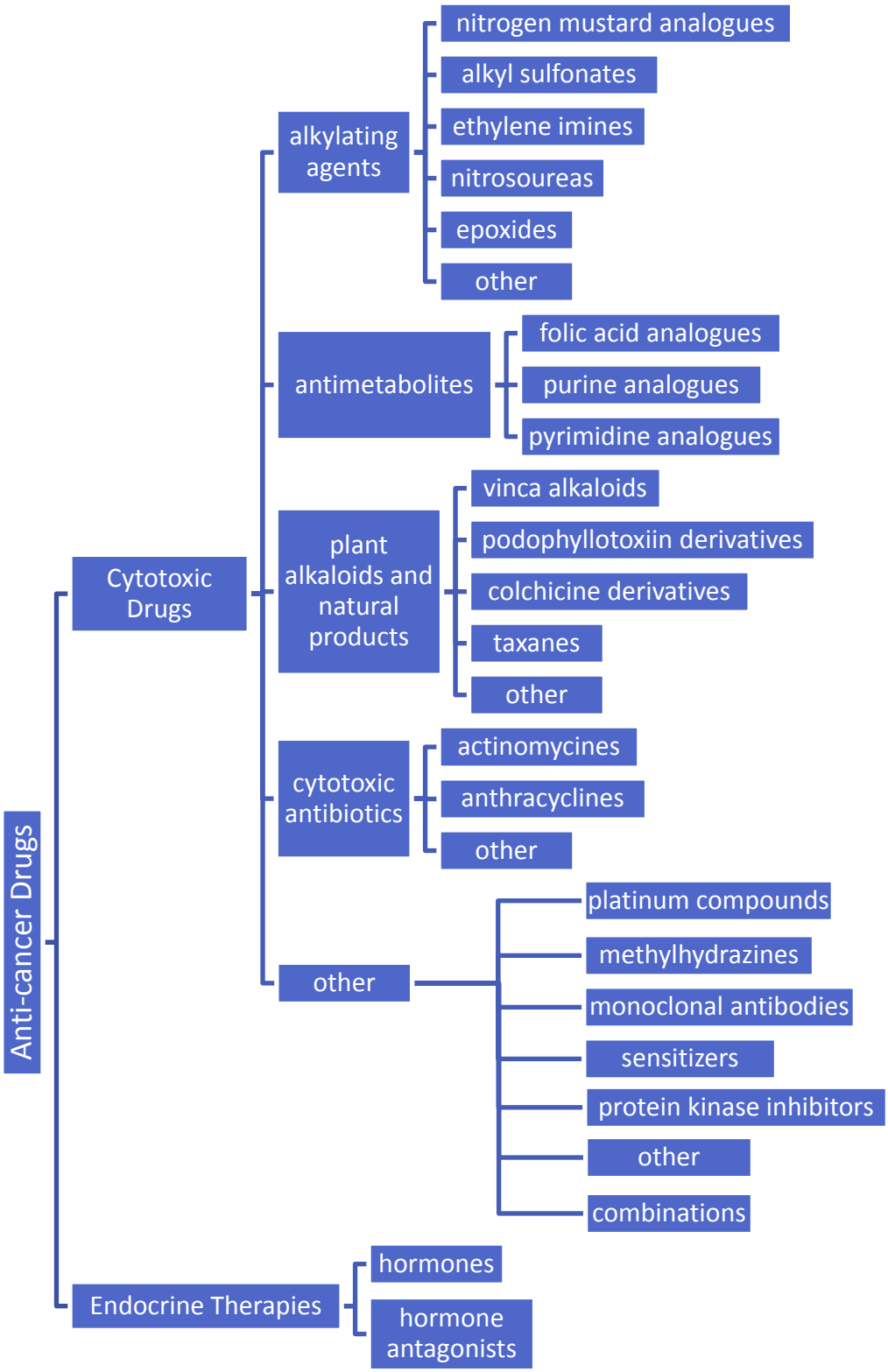

Figure 1-2. Classification of cytotoxic drugs according to the Anatomical Therapeutic Chemical (ATC) classification system of the World Health Organisation (WHO)[6].

Table 1-1. Usage of cytotoxic drug classes in Australia in 2010 based on per cent of total grams of cytotoxics sold and per cent of total prescriptions of cytotoxics, as well as the most commonly used cytotoxics of each class and their corresponding usage based on per cent of total mass of all cytotoxics sold [11]

Class	Grams (% Total)	Prescriptions (% Total)	Most Common of Class	Grams (% Total)
pyrimidine analogues	74.8	23.0	Capecitabine (CAP)	64.0
protein kinase inhibitors	16.1	3.82	Imatinib (imatinib)	10.6
other antineoplastic agents	2.60	5.68	hydroxyurea	0.804
nitrogen mustards	2.54	5.21	Cyclophosphamide (cyclophosphamide)	2.11
monoclonal antibodies	1.38	11.3	rituximab	0.905
platinum compounds	0.899	9.32	carboplatin	0.442
folic acid analogues	0.584	23.4	pemetrexed	0.388
other alkylating agents	0.385	1.13	temozolomide	0.385
Taxanes	0.291	7.14	paclitaxel	0.210
Anthracyclines	0.197	4.70	epirubicin hydrochloride	0.109
podophyllotoxin derivatives	0.159	1.49	etoposide	0.159
purine analogues	6.47×10^{-2}	2.05	mercaptopurine	4.11×10^{-2}
vinca alkaloids	4.45×10^{-3}	1.57	vinorelbine	2.92×10^{-3}
Nitrosoureas	3.78×10^{-3}	8.54E-02	fotemustine	3.78×10^{-3}
alkyl sulfates	4.36×10^{-5}	4.68E-02	busulfan	4.36×10^{-5}

1.2 Cytotoxic Action and Metabolism

1.2.1 Cyclophosphamide

Cyclophosphamide (Figure 1-3) is one of the most widely used cytotoxic drugs worldwide. It is used to treat various cancers including Hodgkins lymphoma, various types of leukaemia, ovarian, breast, and lung cancers [12]. It may also be used to treat non-cancerous diseases, such as nephrotic syndrome in children, in patients who have not shown improvement with other treatments or exhibit intolerable side-effects with other drugs [12].

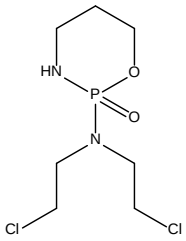

Figure 1-3 Chemical structure of cyclophosphamide

Cyclophosphamide is administered to patients either intravenously or in tablet form. It is administered as a racemate, having a chiral centre at the phosphorus. It is an alkylating agent, and hence brings about its therapeutic effect by destroying DNA and preventing it from replicating. As such, cyclophosphamide is listed as a restricted carcinogen in Australia. Prescription of this drug for

the treatment of non-cancerous diseases is therefore used with high discretion. Cyclophosphamide may also produce various adverse side-effects, such as nausea and vomiting, weight loss, hair loss, painful urination, difficulty breathing, skin yellowing, swelling of extremities, and infection-like symptoms.

Between 5 and 25 % of administered cyclophosphamide is excreted unchanged in the urine. A further 31 to 66 % of administered cyclophosphamide is excreted unchanged in the faeces, thus cyclophosphamide is able to enter wastewater via sewage outlets. The remaining cyclophosphamide is metabolised in the body to form 4-hydroxycyclophosphamide and its tautomer (aldophosphamide) as the major metabolites [13]. This compound then undergoes spontaneous, non-enzymatic elimination to produce acrolein and the phosphoramide mustard (N,N-bis-2-(2-chlorethyl) phosphorodiamidic acid), as shown in Figure 1-4 [13, 14]. It is the acrolein which is responsible for toxicity in the bladder, while phosphoramide is an active DNA-cross-linking agent itself [15]. There is also a minor metabolic pathway that eventually results in the production of chloroacetaldehyde, which is a neurotoxin.

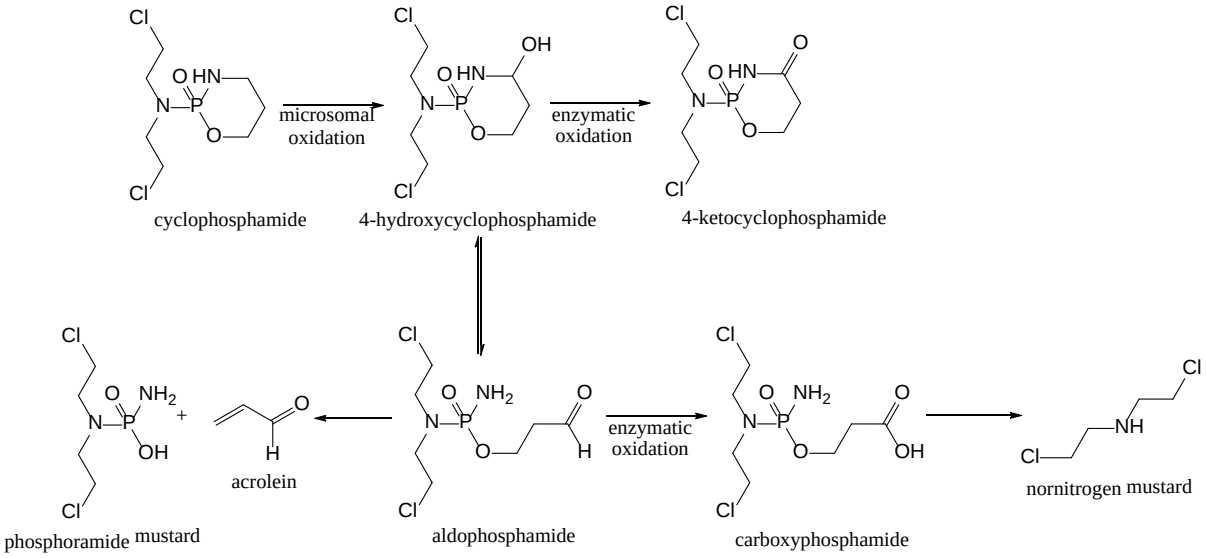

Figure 1-4. Metabolism pathway of cyclophosphamide [16]

1.2.2 5-Fluorouracil

Capecitabine (Figure 1-5) is the most commonly used drug in Australia, constituting 64.1 % of the drug mass distributed in 2010 [11]. Unlike cyclophosphamide, which acts directly on the body, capecitabine is a pro-drug, meaning that it is inactive and metabolised in the body into the reactive species (5-fluorouracil). It is the 5-fluorouracil that gives rise to the physiological effect. Approximately 95.5 % of capecitabine is converted to 5-flurouracil, and hence only low concentrations of capecitabine are excreted [17]. 5-fluorouacil can be also administered directly, constituting 10.6 % of the total cytotoxic drug mass used in Australia in 2010 [11]. It is an antimetabolite that is used in combination with other

medications to treat advanced colon and rectal cancers, pancreas and stomach cancers, as well as some forms of breast cancer after radiation therapy or surgery [18].

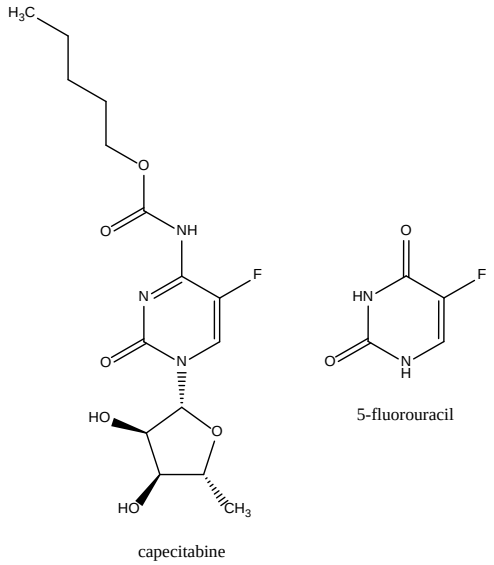

Figure 1-5. Chemical structure of 5-fluorouracil and its pro-drug capecitabine

5-fluorouracil brings about its cytotoxic effect via multiple reaction chains within the cell, with the predominant mechanism resulting in its conversion to fluorodeoxyuridine diphosphate (FdUDP). FdUDP inhibits the enzyme thymidylate synthetase, a critical enzyme in DNA replication and repair [19]. Although the metabolism of 5-fluorouracil is complex and consists of multiple alternate pathways, all of the active metabolites have been shown to be converted into inactive compounds before excretion, with urea, carbon dioxide, and α-fluoro-β-alanine being the most common [20, 21]. Approximately 10-20 % of administered 5-fluorouracil (or that obtained from capecitabine administration), however, is excreted in the urine unchanged, and hence is able to enter wastewaters [20, 21].

1.2.3 Imatinib

Protein kinase inhibitors are the second most commonly used cytotoxic drug class in Australia by drug mass. Of this class, imatinib (Figure 1-6) is the most predominant, constituting 64 % of protein kinase inhibitors used by mass in Australia in 2010 [11]. Imatinib is used to treat certain leukaemias and gastrointestinal tumours, as well as dermatofibrosarcoma protuberans in cases when the tumour cannot be surgically removed [22]. Imatinib brings about its effect by binding to tyrosine kinases, which are responsible for phosphorylating adenosine triphosphate (ATP) [23]. This binding therefore inhibits activation of growth receptors in the cell, preventing cell signalling and resulting in cell death.

It is known that up to 68 % of administered imatinib is excreted by humans unchanged, and much of what is not directly eliminated is metabolised to N-desmethylimatinib [24]. This compound has an

equally-potent biological activity to that of imatinib [24]. The administration of imatinib therefore results in the release of high amounts of harmful compounds into sewage systems.

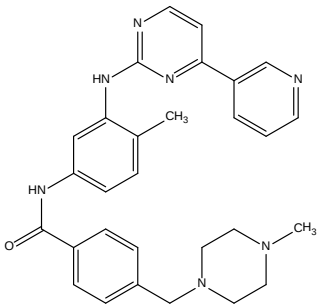

Figure 1-6 Chemical structure of imatinib

The potential of cytotoxics and their metabolites to cause harm to non-cancerous cells, and hence organisms, as well as their known high excretion rates, has given rise to increasing interest in what happens to these compounds when excreted into the sewage system. If cytotoxic drugs can not be removed from wastewater in wastewater treatment plants they could then be released into surface waters, such as rivers and lakes. Here these drugs could have mutagenic, teratogenic, and carcinogenic effects on aquatic organisms. The remainder of this review will detail current knowledge of cytotoxic fate in sewage treatment plants and the aquatic environment, as well as explore current analytical methods for their detection in these matrices.

1.3 Cytotoxic Fate During Wastewater Treatment

1.3.1 Cyclophosphamide

Cyclophosphamide is one of the most commonly investigated cytotoxic in wastewater treatment plants (WWTPs) [25-28]. It has been shown to be highly persistent in a variety of WWTPs, predominantly due to its resistance to biodegradation [29]. Lab-scale batch experiments, including the Zahn-Wellens test, have been conducted to monitor the concentration of cyclophosphamide over time when incubated with activated sludge (used in wastewater treatment plants) using cyclophosphamide concentrations between 100 ng/L to 160 mg/L. No significant change in cytotoxic concentration was observed over 28 days [25, 30]. The cyclophosphamide concentrations were low enough to ensure the observed clearance rates were not due to high concentrations of the cytotoxic having toxic effects on the microorganisms in the activated sludge, which is known to produce false negative results [25]. Multiple investigations into real WWTPs with activated sludge have also been conducted, with each supporting the observation that cyclophosphamide is not effectively removed by this treatment [29, 31-34]. Cyclophosphamide has been detected in WWTP effluents at concentrations between 2.1 and 14.5 ng/L [31, 33]. The cyclophosphamide concentrations in the

influents, however, were not made clear in these studies, and hence removal efficiencies could not be determined. Garcia-Ac *et al.* [29], however, detected cyclophosphamide at a concentration of 9 ng/L in the influent of STPs in Quebec and Montreal, but were unable to detect cyclophosphamide in the effluent. The authors suggested that this loss was unlikely to be due to biodegradation because cyclophosphamide is known to be resistant to biodegradation [35], and hence a different abiotic transformation, such as direct or indirect photolysis, was proposed. The detected cyclophosphamide concentration of 9 ng/L, however, was equal to the LOD determined for the utilised LC-MS/MS method in WWTP effluents [29], and hence it is also possible that this was the reason for the inability to detect cyclophosphamide in the effluent samples.

Lab-scale experiments using membrane bioreactors, however, which combine activated sludge treatment with advanced filtration processes, appear to show contradictory results [36-39]. Delgado *et al.* [37-39] observed that up to 80 % of cyclophosphamide was removed using a lab-scale membrane bioreactor. The membrane filter used in this system had a pore size of 0.1 µm, which would be large enough to allow cyclophosphamide and its metabolites through, hence eliminating size exclusion as the mechanism of removal. It was found that the removal was instead achieved via adsorption onto activated sludge. Also, the concentration of the cyclophosphamide metabolite 4-ketocyclophosphamide was actually observed to increase after treatment, which indicated that the cyclophosphamide was undergoing degradation. It was suggested that because the cyclophosphamide was present at such low concentrations, it was more likely to have been co-metabolically degraded. As these results contradicted all of those previously reported further investigation is required in order to determine why this occurred, and to confirm if cyclophosphamide can in-fact be removed in WWTPs. It was also observed in this study that the presence of cyclophosphamide also promoted the production of more extracellular polymeric substances (EPS) by the microorganisms in the sludge as a protection mechanism, which resulted in an increase in bio-fouling of the microfiltration (MF) membrane of the system, as well as an increased retention of humic substances. The efficiency of the membrane bioreactor (MBR) system, however, remained constant throughout the study. It was suggested that this was due to the long activated sludge retention times possible with MBR systems allowing adaptation of the microorganisms to occur to produce microorganisms with a wider range of physiological capabilities. Similar findings were also obtained by Avella *et al.* [36] in their lab-scale MBR.

Cyclophosphamide removal by various other treatment techniques has also been reported. Cyclophosphamide is generally accepted to be resistant to UV degradation in WWTPs. Negligible decrease in cyclophosphamide concentration from 3.7 ng/L down to 3.5 ng/L after UV treatment was

determined by Llewellyn *et al.* [40]. Metcalfe *et al.* [41], however, were unable to detect cyclophosphamide in the effleunts of a WWTP using UV treatment. No analysis of the influents, however, was conducted, and hence this result may be due to cyclophosphamide having been present at concentrations lower than the LOD in both the influents and effluents, rather than due to UV degradation of this compound.

The removal of cyclophosphamide by more advanced secondary wastewater treatments such as reverse osmosis membranes and nanofiltration has also been investigated. These studies have shown that up to 90 % of cyclophosphamide can be removed using reverse osmosis treatments methods [42, 43]. Nanofiltration has been shown to remove between 20 and 40 % of influent cyclophosphamide, and this removal efficiency can be increased up to 60 % via the use of a membrane bioreactor prior to nanofiltration [43].

The removal of cyclophosphamide by AOPs has also been investigated by multiple researchers, such as Garcia-Ac *et al.* [44] who performed lab-scale ozonation experiments. They found that cyclophosphamide degradation under ozone was slow, with a rate constant of only 3.3 $M^{-1}s^{-1}$, and suggesting this was due to the lack of functional groups in cyclophosphamide that would react readily with ozone, such as nitrogen-containing aromatic rings, aromatics, and amino groups. They found that an ozone concentration of 46 mg.min/L was required to achieve 96 % removal of cyclophosphamide, which is much higher than the 1.0 mg.min/L usually used for drinking water disinfection, and hence this would not be a viable removal option for this compound. The addition of H_2O_2 did increase the reaction rate, but very long contact times would still be required. Fernandez *et al.* [45] observed similar results in their batch ozonation experiments with cyclophosphamide with ozone concentrations of 45 mg min L^{-1}. They found that when tert-butanol, a radical scavenger, was added, the level of degradation decreased, hence suggesting that a radical oxidation mechanism was taking place. Increasing the pH of the solution and the addition of H_2O_2 were found to increase the degradation rate by the same proportion, and hence basifying was suggested to be the best choice because of its simplicity. 4-ketocyclophosphamide, the major human metabolite of cyclophosphamide as mentioned previously, was identified as the major ozonation product. Tuerk *et al.* [46] also investigated cyclophosphamide removal by ozonation and UV/H_2O_2 treatment, observing that 95 % removal could be achieved within 40 min. The concentrations of ozone used, however, were again very high (115 g/L). Lester *et al.* [47] used ozone concentrations closer to those used in real treatment plants (0.1-1 mg/L), and observed that cyclophosphamide degradation did occur, but very slowly with a rate constant of 0.008 min^{-1}. They also found that the addition of 2 mg/L H_2O_2 increased the

degradation rate, and the application of UV treatment increased this even further, however no removal efficiencies were provided.

1.3.2 5-Fluorouracil

Similarly to cyclohosphamide investigations, research into 5-fluorouracil removal via activated sludge treatment has shown mixed responses. Rowney *et al.* [48] found that 90 % of 5 mg/L 5-fluorouracil was transformed in activated sludge within 10 hours. Straub [49] also observed complete degradation of 5-fluorouracil during batch incubation with activated sludge, even when other cytotoxics were also present. The biodegradability of 5-fluorouracil was also observed by Kosjek *et al.* [50] when investigating a laboratory-scale activated sludge treatment plant. They observed 99.99 % removal of this drug within 40 hours; corresponding to a half-life of about 8 hours. It was also noted that no transformation products of this biodegradation were detected, which could have been a result of these products being more biodegradable than the parent drug, and hence difficult to detect. Kummerer and Al-Ahmad [51], however, demonstrated that this drug was non-biodegradable using the closed bottle test and the Zahn-Wellens test (OECD 302B).

Straub [49] compiled a review in 2009 in an attempt to explain the inconsistencies in biodegradation results of 5-fluorouracil. He compiled the results of 5 biodegradability tests on 5-fluorouracil of concentrations between 9 and 854 mg/L and found there to be no biodegradation in any of them. He suggested that at the high concentrations used 5-fluorouracil could have toxic effects on the microorganisms in the sludge, in the same way as described for cyclophosphamide, hence producing false negative results. It is therefore advisable to use lower concentrations when performing these simulation and batch tests, especially considering the expected concentrations of cytotoxics in the environment are much lower than mg/L.

Mahnik *et al.* [52] performed batch experiments on 5-fluorouracil in activated sludge and analysed the influent and effluent water as well as the sludge and container walls in order to determine if biodegradation was indeed the mechanism of 5-fluorouracil removal in WWTPs. They reported degradation to below limits of detection within 24 hours, however only 2-5 % of the 5-fluorouracil was detected in the sludge itself. 25 % was actually detected in the soda lime (mixture of calcium oxide and sodium hydroxide), which had been added to trap any CO_2 by microorganisms in order to monitor biodegradation [52]. The detection of 5-fluorouracil with soda lime therefore suggested that biodegradation, rather than adsorption to sludge, was the predominant removal mechanism. It was also observed that there was no adsorption of 5-fluorouracil to any suspended solids in the water, hence eliminating this as a potential mechanism of removal. This was in correlation with the investigations of Kosjek *et al.* [5] in 2011, which demonstrated that adsorption of 5-fluorouracil to

suspended solids and sludge is negligible. Kiffmeyer *et al.* [35] determined the biodegradation of 5-fluorouracil in activated sludge using the OECD confirmatory test, which involved the use of a laboratory-scale activated sludge treatment plant. Complete degradation was observed within a few days, but the rate of this degradation was found to be dependent on the original concentration of 5-fluorouracil, with higher concentrations resulting in lower removal rates. This dependence on concentration could also be a cause of the inconsistent biodegradation results for this compound. Investigation into 5-fluorouracil removal in real activated sludge treatment plants was also conducted on one occasion. Kosjek *et al.* [50] reported the detection of 5-fluorouracil at 4.7 and 14 ng/L in the influent of an activated sludge STP, however its concentration was below the limits of detection in the effluent, hence indicating that the 5-fluorouracil had been removed by the activated sludge.

Research into 5-fluorouracil removal via other WWTP techniques has also been conducted. Kosjek *et al.* [50] conducted UV degradation batch experiments on 5-fluorouracil in distilled water and found that when only exposed to UV light 5-fluorouracil had a short half-life of 15 minutes. They also found that the addition of the strong oxidising agent H_2O_2 resulted in 99.6 % removal of 5-fluorouracil from the distilled water after 10 minutes, suggesting that it may also be successfully removed by UV treatment in WWTPs. A few transformation products were also identified after UV degradation for 5-fluorouracil, which indicated the need to assess transformation products produced during wastewater treatment as well as the usual human metabolites and surface water transformation products in order to gain a complete understanding of the environmental effects of cytotoxics. Mahnik *et al.* [52] investigated the fate of 5-fluorouracil in an MBR with UF and activated sludge by attaching a pilot MBR to selected effluent from a university hospital in Vienna. Concentrations of 5-fluorouracil in the hospital wastewater were between 8.6 and 124 µg/L, and these were decreased to below limits of detection after MBR treatment, hence demonstrating the highly efficient removal of 5-fluorouracil by activated sludge and MBR. Finally, Rey *et al.* [53] investigated the removal of this compound via ozonation, finding that it could be decreased to below limits of detection within 30 min using 16-18 mg/L of ozone; concentrations which are similar to those used in real WWTPs. Despite controversies over 5-fluorouracil removal by activated sludge it had therefore been demonstrated that advanced treatment methods could be used for effective 5-fluorouracil removal from wastewater.

1.3.3 Imatinib

The high excretion rate and formation of an active metabolite have made imatinib of growing interest to researchers. However, very little research into the fate of imatinib or its metabolites in wastewater treatment plants or surfaces waters has been conducted. Imatinib and N-desmethylimatinib were included in the investigation of Negreira *et al.* [54], who developed a solid-phase extraction-liquid chromatography-tandem mass spectrometry (SPE-LC-MS/MS) method for the simultaneous detection

of cytotoxics in wastewater. Both compounds, however, were below the limits of detection in real wastewater samples. This research was conducted in Catalonia, Spain, where the use of imatinib is much less prevalent, and hence this drug is still of interest to Australian researchers. This therefore represents a significant gap in the knowledge that must be filled in order to gain an accurate understanding of the effects of cytotoxics on waterways.

1.4 Cytotoxic Fate in Surface Waters

The low efficiency of removal of cytotoxic drugs by WWTPs results in their release into surface waters. Cyclophosphamide has been detected in surface waters at concentrations of 50 pg/L up to 65 ng/L [9, 25, 28, 41, 55-58]. Investigations into the presence of 5-fluorouracil in surface waters have also been conducted, however this drug was below detection limits (0.16-34 ng/L) [50, 59]. Determination of the presence of imatinib in surface waters, however, has not yet been conducted.

Despite knowledge of the existence of cytotoxics in surface waters, there has been very little research into their subsequent fate in these environments [10]. This is most likely due to their low expected concentrations, especially in comparison to other pharmaceuticals and micropollutants. There is very little knowledge, however, about whether these compounds undergo transformations in surface waters to compounds that could also show cytotoxicity or other activity [5, 60-62]. There has also been no research conducted into the effects of interactions between multiple different cytotoxics and pharmaceuticals when present at low concentrations, and hence there could be adverse effects that are going unnoticed [9, 60]. Finally, only acute toxicity assays have been performed on cytotoxics, and hence there is no information about the chronic effects of exposure to small concentrations of these chemicals over long time periods [60]. Further investigation into cytotoxic transformation and distribution in the aquatic is therefore vital in order to gain a realistic comprehension of the risks they pose.

A small number of studies on the potential transformation of cyclophosphamide and 5-fluorouracil have been conducted. Imatinib transformation, however, has not yet been investigated. The potential abiotic transformation of cyclophosphamide and 5-fluorouracil has been investigated in lab-scale batch experiments. Kosjek *et al.* [50] found 5-fluorouracil (1 mg/L) undergoes photodegradation in distilled water under UV light with a half-life of 15 min. This rate was also found to increase in the presence of H_2O_2. Six transformation products of 5-fluorouracil, formed via photo-addition of water, defluorination, and hydroxylation, were also detected. The toxicity of these compounds and their potential presence in surface waters, however, has not yet been determined. This study therefore highlights the wide range of reactions that could take place in surface waters, and the need to

investigate and include transformation products when assessing the impact of a particular cytotoxic on the environment.

Lin *et al.* [63] also investigated the phototransformation of 5-fluorouracil by conducting batch experiments of this compound (0.38 µM in distilled water) in a sunlight simulator (290-800 nm) at pH 7. The same experiment was also conducted separately using cyclophosphamide (0.19 µM). It was observed that 5-fluorouracil was degraded slowly by direct photolysis with a half-life of 36 hours, while no degradation of cyclophosphamide was observed at all within 26 hours. The slower degradation rate of 5-fluorouracil observed in this study compared with that obtained by Kosjek et al. [50] was most likely due to the 5-fluorouracil concentration used by Kosjek being 1000 times higher than those used by Lin. It was suggested that the observed stability of cyclophosphamide was due to cyclophosphamide exhibiting minimal light absorbance between 250 and 300 nm. 5-fluorouracil, however, exhibits maximum absorbance at 265 nm, as shown in Table 1-2, and hence is able to undergo photodegradation. The indirect photolysis of each compound was also investigated via the addition of sodium bicarbonate ($[HCO_3^-]$ = 0.2-10 mM), sodium nitrate ($[NO_3^-]$ = 1-10 mg/L), and fulvic acid (1-10 mg C/L) in order to simulate the presence of bicarbonate, nitrate, and dissolved organic matter in the water respectively. In the presence of nitrate the photodegradation of both cytotoxics increased, most likely due to the formation of HO· upon irradiation. Bicarbonate, which acts as a radical scavenger, was found to decrease the photodegradation of cyclophosphamide; indicating that HO· was important in the degradation of this compound. The overall very slow degradation of cyclophosphamide suggested that, unless present in a very shallow water body with high levels of sunlight and high residence times, photodegradation would not be the predominant form of dispersion of this compound in natural waterways.

Buerge *et al.* [25] confirmed the high persistence of cyclophosphamide when analysing river samples various distances from an STP; finding that cyclophosphamide could still be detected in the most distant sample 6 km downstream from the plant. The degradation of 5-fluorouracil, however, increased in the presence of bicarbonate and nitrate; indicating that CO_3^-·, which is itself a selective oxidant, could also be significant in the degradation of 5-fluorouracil. These same conditions were also monitored in samples of river water and the same effects were observed. During these experiments it was found 5-fluorouracil produced an unknown transformation product, which was further degraded by the present radicals. Despite of this conversion, and the degradation of 5-fluorouracil by up to 93 %, the total organic carbon remained steady throughout incubation, hence indicating that persistent unknown transformation products were being formed. Further investigation into the identities and toxicities of these products is required.

The distribution of 5-fluorouracil in soils was investigated by Mamouni *et al.* [64] using the pond water/river system fate test according to OECD 308 under aerobic conditions. It was found that 9.0 and 6.6 % of the original 5-fluorouracil partitioned in river and pond sediments respectively, hence indicating that this was an unlikely distribution mechanism for this cytotoxic in surface waters. This correlated well with the low log K_{ow} of 5-fluorouracil of 0.1-0.34 at environmental pH, as shown in Table 1-2 [49]. No other cytotoxic drugs have been investigated in soils or sediments; however predictions have been made on the fate of others in these media based on physiological data and other observations.

Similarly to the biodegradation of 5-fluorouracil in WWTPs, there is still no consensus on the biodegradability of this cytotoxic in surface waters [65]. Lutterbeck *et al.* [65] conducted the closed bottle test (OECD, 1992b) on 5-fluorouracil and its forced photodegradation products at 20 ± 1 °C in the absence of light for 28 days. They observed that 5-fluorouracil did not undergo biodegradation during the incubation period. Similarly, Kummerer *et al.* [51] found 5-fluorouracil was not biodegradable in the closed bottle test (OECD 301 D) or the Zahn-Weelens test (OECD 302 B). This was contradictory to the study by Kiffmeyer *et al.* [35] in which 5-fluorouracil was found to undergo complete biodegradation within 14 days in a lab-scale activated sludge treatment plant.

Table 1-2. Physiochemical properties of cyclophosphamide, 5-fluorouracil, and imatinib used to predict environmental fate [61]

Cytotoxic	Water Solubility (mg/L)	BCF	pK_a	K_{ow}	K_{oc}	Atmospheric OH rate ($x10^{-11}$ cm^3/ molecule.s)	UV Max (nm)
cyclophosphamide	4×10^4	2.1-3	2.84	0.63	52-59	7.03	200
5-fluorouracil	1.11×10^4	3-3.6	pK_{a1} 8.0 pK_{a2} 13	-0.89	8	0.583	266
imatinib	200	n.d.	pK_{a1} 8.07 pK_{a2} 13.45	2.89	7.9	n.d.	260

1.5 Chemiluminescence

1.5.1 Basic Theory

The phenomenon of luminescence has been known for many centuries, with the first observations of its existence involving the emission of light from living organisms, such as glow worms [66]. The first scientific observation of luminescence from a synthetic chemical reaction was by Radziszewski in 1877, who observed the production of green light during the reaction of lophine with oxygen. The term "chemiluminescence" was first used to describe this phenomenon by Weidemann in 1888, who defined it as "luminescence caused by a chemical reaction". This was in order to differentiate it from other light emissions, such as photoluminescence, caused by the absorption of light by a molecule.

More specifically, chemiluminescence is now defined as a process by which a chemical reaction produces an intermediate or product in the excited state, which, as it relaxes to the ground state, either emits electromagnetic radiation or donates its energy to another molecule which then emits light [66]. The former example is termed "direct" chemiluminescence, while the latter is termed "indirect" or "sensitised" chemiluminescence [66, 67]. The emitted radiation can be ultra-violet, visible, or infra-red [66].

There are several factors that determine if a chemical reaction can produce light. Firstly, the reaction must produce sufficient energy and follow a favourable pathway to allow for the formation of an electronically excited state [66]. Secondly, the most favourable relaxation process of the excited state must be light emission, compared to non-radiative relaxation processes [67]. Oxidation reactions generally meet these criteria, and hence oxidising reagents are the most commonly utilised chemiluminescence reagents [68].

The overall efficiency of light production, termed quantum efficiency or quantum yield, is what determines the intensity of chemiluminescence. This is dependent on the efficiency of formation of the excited species (ϕ_{ex}), defined as the fraction of the chemiluminescence pre-cursor (A) that is converted to an excited species. It is also dependent on the efficiency of subsequent luminescence from this excited species (ϕ_L), and hence can be described by the equation below. In the case of indirect chemiluminescence, ϕ_{ex} also includes the efficiency of the energy transfer.

$$\Phi_{\mathrm{CL}} = \Phi_{\mathrm{ex}}\Phi_{\mathrm{L}} \quad (1)$$

Chemiluminescence intensity (I_{CL}) can then be described by the following equation, where $-\mathrm{d}A/\mathrm{d}t$ is the rate of consumption of the chemiluminescence precursor. For chemiluminescence to occur ϕ_{CL} must generally be between 0.001 and 0.1.

$$I_{\mathrm{CL}} = \Phi_{\mathrm{CL}} \frac{-\mathrm{d}A}{\mathrm{d}t} \quad (2)$$

This relationship therefore demonstrates that the intensity of chemiluminescence emission is directly proportional to the concentration of the chemiluminescence precursor, ie; any reagent involved in the production of the excited state. Detection of the emitted light can therefore be used to detect any compounds participating in the chemiluminescence, such as the substrates or precursors, oxidants, fluorophores or analytes derivatised to contain fluorophores, as well as possible inhibitors or activators of the reaction.

Chemiluminescence detection offers several advantages over absorptiometric techniques. As it is an emission process it does not require an external light source, and hence background interferences,

source instability, and problems with light scattering and unselective excitation are eliminated [66, 67]. The low background signal also greatly increases the sensitivity of chemiluminescence detection, making it up to 100,000 times more sensitive than spectroscopic techniques [68]. Due to its dependence on emission during a chemical reaction, chemiluminescence detection also generally has a very large linear dynamic range, from the minimum detectable concentration up to the concentration at which it is no longer possible to maintain the reagents in excess compared to the analyte [67]. The linear range can therefore spread over up to 6 orders of magnitude [67]. The software and hardware required for chemiluminescence instrumentation is also often very simple and cheap, making this detection method easily accessible to most laboratories.

Chemiluminescence does, however, have several limitations that must be considered. Slight changes in pH, temperature, solvent composition, or ionic strength, for instance, can strongly influence the chemiluminescence reaction, and hence these factors must be tightly controlled [66, 68]. Also, light emission by a molecule is known to increase to a point and then gradually decrease for each chemiluminescence event, rather than instantaneously increasing and decreasing, and hence the chemiluminescence varies with time [69]. The chemiluminescence must therefore only be detected at strict time periods in order to obtain a consistent response. Finally, the chemiluminescence reaction is non-selective, because the oxidising agents are generally able to react with multiple compounds [68]. This can often be overcome by the incorporation of an enzyme that selectively binds to the target compound; however this drastically limits the possible analytes. Chemiluminescence detection is also commonly coupled to chromatographic separation such as high performance liquid chromatography (HPLC) or capillary electrophoresis (CE) in order to separate interfering compounds from the target analyte [68, 70, 71].

The analytical applications of chemiluminescence have been investigated extensively. Thorough reviews have recently been written on the applications of chemiluminescence detection to pharmaceuticals [72], controlled drugs [73], food products [74], clinical and biomedical studies ([70, 71], and environmental samples [71].

1.5.2 Instrumentation

In order for chemiluminescence to have analytical utility, instrumentation must be developed to allow for tight control of the reaction conditions, as well as efficient detection of the emitted light at a precise time period [66]. Although commercial chemiluminescence instruments do exist, in-house built instrumentation is most commonly utilised and provides the same detection capabilities and control [75]. The basic requirements are various tubing lines through which each reagent can be

delivered individually, a reaction cell in which the reagents can be mixed, and a detection device directly adjacent to this detector cpabale of converting the emitted light into an electrical signal.

Flow Injection Analysis (FIA):

There are three main methods used for the delivery and mixing of reagents in chemiluminescence detection; flow injection analysis (FIA), sequential injection analysis (SIA), and batch injection analysis (BIA) [75].

FIA involves the continual pumping of reagents through a reaction coil and flow-through detector. If all reagents required for the chemiluminescence reaction are continually pumped a continuous chemiluminescence emission is produced. Commonly, however, a precise volume of one of the reagents is injected into the stream, resulting in transient emission over a precise time period [68, 75]. The reagent injected can be either the oxidising reagent, the analyte, or any enhancer or sensitising reagent. The initial reagent stream is generally a chosen carrier solution, which is continually mixed with the analyte or oxidiser at a defined junction on-line. Theoretically, however, the carrier solution, injected reagent, and any other merging streams can contain any of the chosen reagents, depending on the mixing orders, rates, and volumes found to be required for the particular chemiluminescence reaction in question. The composition, pH, concentration, flow rates, and delivery points of each reagent can therefore be manipulated to develop the optimum method for detection of a target analyte [66, 76]. FIA has the advantages of allowing precise control over reagent flow rates and volumes using simple instrumentation [66]. The continual-flow nature of FIA also permits on-line treatment of particular reagents, for instance derivatisation of analytes, or activation of oxidising reagents [66]. FIA is also more easily coupled to liquid chromatography techniques [66]. The continual flow of reagents in FIA does, however, result in the need for much larger reagent volumes than SIA or stopped-flow analysis, as well as the generation of larger volumes of waste [77]. FIA was recently thoroughly reviewed by Trojanowicz *et al.* [75], covering basic methodology as well as the most notable achievements and concepts from FIA investigations in the last fifteen years.

Sequential Injection Analysis (SIA):

SIA involves the sequential withdrawal of reagents into a mixing cell by a high-precision bidirectional pump to produce “segments” of individual reagents, prior reversal of the pump direction to deliver all reagents to the reaction coil, where they mix and undergo the chemiluminescence reaction [75, 78].

SIA has several advantages over FIA. Specifically, the volumes of reagents consumed during SIA are far lower than in FIA, due to elimination of the need for continual flow of reagents [78]. Logistically, the instrumentation required for SIA is generally simpler than that for FIA. For instance, in SIA if

changes in reagent volumes, mixing order, or timing are required, this is generally achievable by changing the valve and pump parameters using the computer program [78]. In FIA, however, this often involves physically changing the configuration of the reagent lines and merging points themselves [78]. This makes SIA a much more robust technique for a wide range of analytical applications.

Similarly to FIA, SIA allows for precise and accurate control of reagent flow rates and volumes, as well as online reagent treatment [78]. SIA does, however, have disadvantages. In particular, sample throughput has been shown to be between only 30 and 50 % of that achievable using FIA, due to the longer time required for aspiration of all reagents [78]. This makes coupling of SIA to liquid chromatography methods more difficult.

Batch Injection Analysis (BIA) or Stopped-Flow Analysis:

The alternative to flow-based methods is batch analysis. This involves the introduction of all reagents into a single reaction cell adjacent to the detection device (inside a light-proof housing), where they are held while all emitted light is detected over a defined time-period [79]. This can be achieved via a variety of methods. Selected reagents can be pre-mixed in the reaction cell before the final reagent required for chemiluminescence is injected, or, in a method of batch analysis known as stopped-flow analysis, precise volumes of reagents can be injected simultaneously into the reaction cell. This can also be conducted using SIA manifolds by programming the reagent mixture to be held in the reaction cell prior to flow to waste {Hartwell, 2012 #210}.

Batch analysis has several advantages over flow-based chemiluminescence techniques. For instance, it is particularly applicable to detection of rapid or short-lived chemiluminescence emissions, which would otherwise be missed in flow-based methods [80, 81]. Similarly, slow reactions requiring longer reaction times can be more easily detected using batch analysis [82]. It also solves several logistical problems associated with flow-based methods, such as the need for valves and bidirectional pumps, and the large reagent volumes required [83]. It is for this reason that batch chemiluminescence is often the method of choice for coupling to capillary electrophoresis (CE) separation. Tsukagoshi and co-workers [84-89] have worked extensively on development of reaction cells suitable for batch chemiluminescence for CE detection. This was in order to solve problems encountered in matching flow rates between CE and detection, and connecting capillaries to flow devices.

The signal obtained during batch analysis differs from that obtained using SIA and FIA. In SIA or FIA light emission at a single point in time is detected, resulting in the production of a Gaussian-like peak shape as the reagent mixture flows through the reaction cell past the detector. In batch analysis,

however, the full extent of the reaction is detected, including the formation of the emitting species and its eventual consumption [76]. Chemiluminescence signals from batch analysis therefore typically consist of a sharp increase in light intensity followed by a gradual decrease, as shown in Figure 1-7. The slope of the initial increase in light intensity therefore corresponds to the rate of formation of the chemiluminescence-emitting species [90]. The slope of the tail corresponds to the rate of consumption of this emitting species, or the rate of decay of the chemiluminescence emission [90]. These signal components can be used to investigate the effect of different analytes, reagents, enhancers, inhibitors, and well as temperature and pH effects on the reaction rates [76]. This information can then be used to elucidate the potential chemiluminescence mechanisms involved. It is for this reason that batch analysis is commonly used for reaction kinetics investigations [76, 79, 91-100].

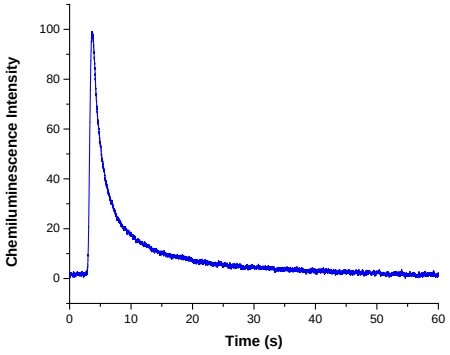

Figure 1-7. Typical chemiluminescence emission profile obtained during batch-analysis

Differences in chemiluminescence reaction kinetics can also be used to detect compounds that are difficult to separate from a mixture. Garcia Sanchez *et al.* [101], for instance, observed that interferences during batch chemiluminescence analysis of asulam (a common pesticide) in surface water samples were negligible because these interfering compounds were not able to react on the same short time-scale as the target analyte. Multicomponent analysis of the initial chemiluminescence reaction rate has also been used on multiple occasions to simultaneously determine the concentration of compounds in a mixture, based on their varying contributions to the overall chemiluminescence emission rate [69, 102-105].

Finally, batch chemiluminescence can be used in the same way as SIA and FIA for the detection and concentration determination of analytes [100, 106-108]. However, several pieces of information are now available for correlation to analyte concentration, including the maximum intensity of light emission, the initial rate of the light-emitting reaction and its decay, as well as the total chemiluminescence emission [109]. Target analytes can therefore be detected indirectly based on their inhibition or enhancement of chemiluminescence reaction rate, rather than just changes in maximum chemiluminescence emission. Penicillin compounds, for instance, are known to inhibit the

chemiluminescence reaction between luminol and iodine. Ventura *et al.* [110] therefore utilised this knowledge for the detection of penicillins by measuring the rate of formation and decay of light-emitting species in the luminol-iodine chemiluminescence reaction using stopped-flow analysis.

Batch analysis does, however, have several disadvantages. Unlike in continuous-flow-based methods, it is difficult to achieve rapid and complete mixing of reagents using batch methods [111]. Also, batch processes are less easily automated, resulting in lower sample through-put [111]. There is also limited ability for online preparation of reagents, which can be required when their stability is poor [111].

Pump Considerations:

Typically in FIA, SIA, and stopped-flow experiments smooth laminar flow of reagents is desired in order to control partial dispersion of reagents. This is most commonly achieved via use of either peristaltic pumps or syringe pumps. These pumping systems allow for simple and robust instrumentation, tight control of reagent volumes and flow rates, and rapid and reproducible reagent mixing [112]. Syringe pumps, however, can require manual re-filling, which decreases the obtainable analysis through-put frequencies. Peristaltic pumps also have disadvantages, in that they are known to produce variable flow rates over time due to pump aging and wear [112]. Lewis *et al.* [112] developed an alternative pumping method called pulsed flow. This involved the use of short pressure pulses to produce bursts of solution flow, interspersed between longer static periods. This system allowed for tight control of reagent ratios within each pulse, which eliminated the need for an injection valve. This allowed for rapid and efficient mixing of reagents directly adjacent to the detector, making it highly applicable to fast, short-lived chemiluminescence reactions. Other advantages include high precision, high sampling frequency, compact instrumentation, and low reagent consumption [113]. Pulsed flow has had several applications in chemiluminescence analysis including pharmaceutical formulations [114-116] and biological samples [117].

Reaction Cells and Detectors:

The reaction cell geometry required is determined predominantly by which type of analysis (FIA, SIA, or batch analysis) is used. In batch analysis the whole reagent mixture is injected into a reaction cell and held for a defined time period before being expelled to waste. The geometry of the reaction cell is therefore quite different to those employed when using SIA or FIA, in which flow-through cells are required to allow pumping of the reagent mixture through the cell during detection.

The size and geometry of this cell has a large effect on the efficiency of propagation of the chemiluminescence light from the reagent mixture to the detection device [71, 118]. While larger reaction cells increase the total number of emitted photons, they also introduce a dilution effect, and

hence a compromise must be reached [118]. Most commonly in flow-through chemiluminescence systems the cell geometry is a flat spiral (Figure 1-8) made of either plastic, quartz, or glass, to allow all sections of the coil to be "visible" to the detector while providing adequate geometry for reagent mixing [118, 119].

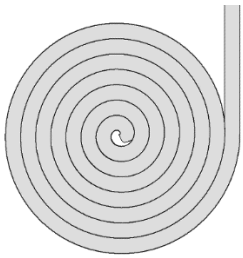

Figure 1-8. Schematic of a flat spiral reaction cell

A wide range of detectors can be used for chemiluminescence, such as photomultiplier tubes (PMTs), photo-counting systems, scintillation counters, fibre optics, or photodiodes [66].

Common detection devices include photomultiplier tubes (PMTs), photon counting systems, photodiodes, and scintillation counters [120]. More complex systems can instead utilise charged coupled devices (CCD) detectors or fibre optics in order to increase performance [66]. This detection device must be contained inside a light-proof housing to prevent interferences from ambient light and to minimise loss of chemiluminescence signal. The FIA, SIA, or BIA systems with one of these detectors can then be used as a detection technique for chromatographic or other separation techniques, such as LC, GC, or CE. These systems can also be incorporated into sensors or immunoassays.

Immobilisation on supports:

Chemiluminescence can be quite non-selective, due to the ability of numerous compounds to react with a given oxidising reagent. One method by which the selectivity can be greatly increased is via the use of enzymatic reactions and immobilisation techniques. In these systems, the target analyte is a substrate of the enzymatic reaction. The desired enzyme is immobilised on a solid support or column through which the analyte is passed [66]. The analyte then undergoes a reaction catalysed by the enzyme to produce a product capable of undergoing a chemiluminescence reaction with a chosen oxidising reagent [66]. A common example of immobilised chemiluminescence is for the detection of glucose [121]. Glucose undergoes a reaction to form H_2O_2, catalysed by glucose oxidase. The H_2O_2 is then able to react strongly with luminol to produce a chemiluminescence signal.

Chemiluminescence sensors are an extension of immobilisation methods, in which the surface is incorporated with a transducer. This allows for detection of analytes in a continuous, reversible, and reproducible manner [66]. Chemiluminescence sensors can typically be divided into batch- and flow-

based sensors. Flow-based sensors are the most commonly used due to their ability to more tightly control the reagents, faster analysis times, increased reproducibility, and their being highly suited to automation [66]. Batch sensors, in which the sensing surface is simply immersed into the analyte solution and the emission detected by an optical fibre, are also utilised [66].

Chemiluminescence Immunoassays:

Another method by which the sensitivity of chemiluminescence can be increased is through immunoassays. Any species participating in the desired chemiluminescence reaction can be coupled to an antigen or antibody [66]. This coupled-reagent is then used in a competitive or non-competitive binding assay, before the addition of the remaining reagents results in the chemiluminescence reaction. Chemiluminescence immunoassays have the advantage of having a wide dynamic range and being highly sensitive, especially in comparison to radiolabelling immunoassay techniques. This is because the use of an enzyme can result in the production of a large number of product molecules capable of undergoing chemiluminescence from a single enzyme molecule [66].

Coupling to chromatography and other techniques:

Chemiluminescence detection is also quite commonly coupled to chromatographic techniques as an alternative to UV or flurourescence detection. The most commonly used instrumentation for this purpose is flow injection analysis (FIA). This involves delivering the chemiluminescence reagent into the analyte stream as it emerges from the separation column, before it enters a flow cell placed directly in front of the optical window of the detector. The chemiluminescence produced is then detected at a fixed time after mixing of the analyte and chemiluminescence reagent. This set-up results in high sensitivities, robustness, and precision, as well as a rapid response. It also allows for separation of organic sample components that may interfere with analyte detection with much higher sensitivity. It has been shown that the sensitivity obtained when coupled to LC analysis can be increased by 10 to 100-fold compared with conventional fluorescence detection. FIA can also be utilised for on-line conversion of the analyte to a product capable of undergoing chemiluminescence via physical or chemical treatment [66]. This therefore expands the range of possible analytes while minimising manual handling that could introduce error. Detection sensitivity and limits of FIA chemiluminescence can be optimised via manipulation of the dimensions of the mixing and reaction coils, reagent flow rates and merging geometries, as well as factors not directly controlled by FIA, such as temperature, and reagent concentration and pH.

The most commonly used separation technique is liquid chromatography, either LC or HPLC, due to the ease with which it can be coupled to flow injection systems. There are several factors, however,

that must be considered and may limit the ability to couple chemiluminescence detection to LC. In particular, the chemical conditions used are highly critical in eliciting a chemiluminescence response from a chosen analyte. These include pH, temperature, reagent concentrations, and solvents. These conditions must therefore be compatible between the chromatographic and chemiluminescence systems [66, 71]. Compromises therefore generally have to be made in order to develop an effective detection system. The use of tris-2,2'-bipyridyl ruthenium(II) as the chemiluminescence oxidising reagent, for instance, generally requires highly acidic conditions, which are not compatible for LC separations requiring basic buffers such as phosphate [122]. Many of the solvents used in LC techniques are also not compatible with chemiluminescence analysis. Methanol, for instance, is known to produce high background emission in chemiluminescence detection, hence hindering detection of the analytes [122]. Mobile phase additives to aid in separation, such as the surfactant SDS, may also cause suppression of the chemiluminescence signal [122]. Finally, compromises in flow rates may also need to be made to allow adequate time for chemiluminescence reagent mixing while still producing reasonable chromatographic peak shapes and separation [122].

1.5.3 Oxidising Reagents

1.5.3.1 Permanganate (Mn(VII)):

Permanganate chemiluminescence is one of the most commonly used oxidising reagent systems [123-125]. Its use can be traced back to the research by Harvey *et al.* in 1917 and that of Grinberg *et al.* in 1920 [123]. Since then its applications have growth substantially. Comprehensive reviews of its mechanisms, targeted functional groups, enhancers, and vast applications have been conducted by the Barnett research group at Deakin University [123, 124, 126], with the most recent being in 2014.

Permanganate chemiluminescence in acidic solution produces characteristic red light at a wavelength of 734 ± 5 nm, when variations in instrument sensitivity in this wavelength range have been corrected for [125, 126]. Permanganate chemiluminescence in basic solution has also been conducted, however this is far less common, and results in emission of light of a different wavelength range [126]. The acidic permanganate reagent is most commonly prepared in sulfuric acid [123], however hydrochloric, perchloric, and orthophosphoric acid have also been used. The optimum acid composition and concentration has been found to be dependent on the analyte as well as the instrument configuration and other reagents used [123]. The acidic permanganate chemiluminescence mechanism is known to be quite complex due to the large number of valence states possible for manganese, which have all been shown to undergo different chemistry [125]. Several papers have suggested the reaction occurs via production of a singlet oxygen [1, 127, 128]. Unequivocal proof of a mechanism involving relaxation of the Mn(II) excited state to the ground state, however, has been produced by several

groups [125, 126]. In particular, the spectral distribution of the red emission from permanganate chemiluminescence does not match that typical of singlet oxygen emission. Singlet oxygen emission contains bands with maxima at 1268 nm from the unimolecular singlet oxygen transition, and 703 and 633 nm from the dimeric species [126]. Weak peaks at 578 nm and 786 nm also due to bimolecular singlet oxygen emission are also observed [126]. The emission spectrum from permanganate chemiluminescence, however, contains a single band with maximum at 734 ± 5 nm. The band at 1268 nm has not been able to be detected during permanganate chemiluminescence [129, 130]. Permanganate chemiluminescence emission does, however, match that observed for laser-induced phosphorescence of Mn(II) in $MnCl_2$, as well as for the reduction of Mn(IV) and Mn(III) to Mn(II) [130, 131]. Other evidence for light emission involving electronically excited Mn(II) include the independence of this emission on the analyte in question, as opposed to the singlet oxygen mechanism, which was greatly influenced by analyte properties [126]. Permanganate reactions are also not strongly influenced by the concentration of dissolved oxygen or oxygen radical scavengers [130, 132]. Other postulated mechanisms have involved analyte oxidation products, and compounds to which energy is transferred from excited intermediates during the reaction [123]. Emission through Mn(II)* is, however, now the most widely accepted mechanism for acidic permanganate chemiluminescence [126].

The general reaction scheme for chemiluminescence through this intermediate is depicted in Figure 1-9 [126]. It is thought that the analyte originally reacts with permanganate to form reactive radical intermediates and Mn(III), with a rate that is dependent on the analyte (step 1). These intermediates then undergo single electron transfer to the Mn(III) intermediate to form the electronically-excited Mn(II)* emitter (step 2). This species then relaxes back to the ground state, which is accompanied by the characteristic red light emission (step 3). It is clear from this scheme that permanganate chemiluminescence is highly dependent on the concentration of Mn(III). Significant enhancement can therefore be achieved by the addition of compounds capable of increasing Mn(III) concentration. The strong reducing agents formaldehyde and formic acid, as well as other low molecular weight aldehydes, have been shown to greatly enhance permanganate chemiluminescence due to increasing Mn(III) production. Similarly, the preparation of permanganate in sodium thiosulfate has been found to provide enhancement by up to two orders of magnitude, particularly for analytes that undergo slow reactions with permanganate [126]. The addition of fluorescence compounds, such as rhodamine 6G and rhodamine B, has also been shown to provide enhancement of permanganate chemiluminescence on some occasions. This is generally thought to occur via formation of fluorescent products derived from the analyte, or via electron transfer to the more efficient fluorophore [126]. Nanoparticles have also been used extensively in recent years as

permanganate chemiluminescence enhancers [126]. This is again thought to be due to their ability to increase the formation of Mn(III) [126].

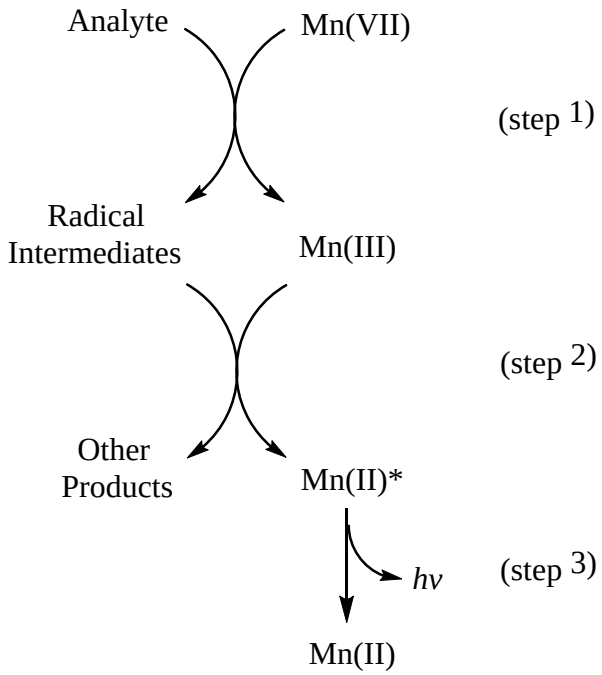

Figure 1-9. General reaction scheme for acidic permanganate chemiluminescence [126]

The most commonly used enhancers of permanganate chemiluminescence are polyphosphates, such as sodium hexametaphosphate, generally adjusted to a pH between 2 and 4 using sulfuric acid [123]. Polyphosphates are known to enhance chemiluminescence by 50-fold when present in large excess. This enhancement has been shown to be accompanied by a shift in the maximum emission wavelength of light from 734 nm ± 5 nm to 689 ± 5 nm [125]. A mechanism for the chemiluminescence reaction occurring in the presence of polyphosphates was postulated by Hindson *et al.* 2010 [125] (Figure 1-10). This mechanism involves initial reaction of the analyte/substrate with Mn(VII) to generate a radical intermediate of the substrate as well as a polyphosphate-stabilised trivalent manganese species (Mn(III)PP). The radical intermediate then further reduces this species then produces the divalent species (Mn(II)PP*) in the $^4T_1$ excited state together with the oxidised substrate. Relaxation of the Mn(II)PP* species to the ground state results in the emission of light at 689 ± 5 nm [125, 126], as opposed to emission at 734 ± 5 nm in the absence of polyphosphates. The enhancing effect is thought to occur via both stabilisation of the Mn(III) species to prevent flocculation of Mn(IV) oxides, as well as protection of the Mn(II)* emitter from undergoing non-radiative relaxation processes [133]. The latter effect is believed to be a function of polyphosphate chain length, with shorter ortho- and pyro-phosphates being less able to provide enhancement [133]. Investigation into the effect of polyphosphate chain length on this enhancement was conducted by Holland *et al.* 2014 [133]. This group found that the polyphosphate chain length needed to be at least 6, however increasing the

chain length beyond this did not result in significant differences in enhancement. The optimum concentration of polyphosphate required for enhancement was found to be dependent on the analyte, provided there was a high proportion of chains of length of at least 6.

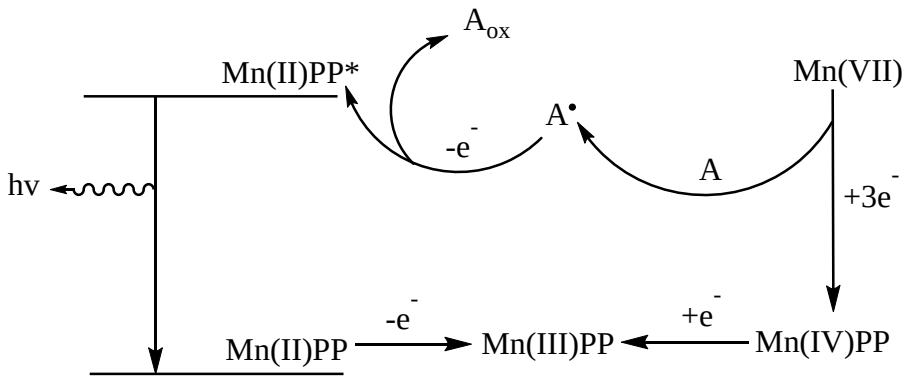

Figure 1-10. Proposed mechanism of permanganate chemiluminescence in the presence of polyphosphates

The addition of Mn(II) reagents (such as $MnSO_4$) has also been shown to enhance permanganate chemiluminescence, hence providing further support for emission via a Mn(II)* emitter [134]. This enhancement was found to increase over 24 hours after reagent mixing before levelling off. UV/Vis monitoring has suggested that this is due to a slow reaction to produce Mn(III) [134]. Perez-Benito *et al.* [135] found that the reaction of permanganate with sodium thiosulfate could also yield Mn(III) with the same absorption and enhancement properties. This reaction occurred almost instantaneously, hence providing a viable alternative preparation method for chemiluminescence analysis. Slezak *et al.* [136] found that the concentrations of thiosulfate and permanganate required for this reaction varied with the analyte.

The analytical applications of permanganate chemiluminescence have been investigated extensively. Thorough reviews have recently been written on the applications of chemiluminescence detection to pharmaceuticals [72], controlled drugs [73], food products [74], clinical and biomedical studies [70, 71], and environmental samples [71].

The most commonly-targeted analytes in permanganate chemiluminescence are phenols, however a very wide range of both organic and inorganic analytes have also been reported extensively. Generally, most organic analytes containing phenolic or amine functionalities are capable of undergoing permanganate chemiluminescence reactions [71]. Exact relationships between analyte functionalities and chemiluminescence intensity have been difficult to determine due to differences in reaction conditions and instrumental set-ups between laboratories. It has been found, however, that the limits of detection achievable for morphine are generally significantly lower than those for other analytes.

1.5.3.2 Mn(IV)

Permanganate chemiluminescence (Mn(VII) is by far the most commonly used manganese oxidising reagent in chemiluminescence, however recently chemiluminescence reactions utilising manganese dioxide (Mn(IV)) have been receiving increasing attention. Mn(IV) has been known to be capable of oxidising a wide range of organic compounds for many years [137, 138]. Its analytical applications, however, were originally quite limited due to its non-stoichiometric nature and low solubility in most solvents [139, 140]. There have therefore been numerous attempts to prepare a soluble form of Mn(IV) for use in analysis, which was recently reviewed by Brown *et al.* [140]. Jáky *et al.* [137, 138] were able to prepare a brown-translucent solution of Mn(IV) phosphate, with particle sizes less than 2 nm. They did this by first preparing MnO_2 via reduction of potassium permanganate with sodium formate, followed by dissolution of this product in 3 M orthophosphoric acid, shaking for 30 minutes, and filtration to remove any remaining solid particles. The high orthophosphoric acid concentration was required to prevent formation of a colloid. Brown *et al.* [38] repeated these experiments and found that dissolution times of 1-3 days at room temperature were required to produce the final product. Alternatively, ultra-sonication for 30 minutes followed by heating at 80 °C for 1 hour also resulted in dissolution. Although particles were detected in these solutions with sizes between 150 and 350 nm, solutions with MnO_2 concentrations less than 0.01 M did indeed remain translucent for several months. The absorption of phosphate ions to the particle surface was found to stabilise the solution. The preparation of this reagent is, however, quite complex and time-consuming, which does not permit same-day analysis when used in chemiluminescence detection. Perez-Benito *et al.* [135], however, developed a simpler and faster method for preparation of this reagent. This group reduced potassium permanganate using sodium thiosulfate in neutral aqueous solution according to the reaction in Equation (3).

$$8MnO_4^- + 3S_2O_3^{2-} + 2H^+ \rightarrow 8MnO_2 + 6SO_4^{2-} + H_2O \quad (3)$$

This produced a dark-brown transparent colloid containing particles with diameters between 89 and 193 nm, and remained transparent for several months. This colloid was also shown to have the same UV/Vis spectrum characteristic of Mn(IV). Several groups have therefore used this preparation method for chemiluminescence analysis [141, 142].

As with other manganese-based reagents, the exact mechanism involved in Mn(IV) chemiluminescence is still not completely known [129]. Du and Wang [143] found that the corrected maximum emission wavelength of Mn(IV) when reacted with various organic compounds was between 725 and 740 nm. This was independent on the analyte or the presence of formaldehyde as an enhancer. They also observed that this emission could be quenched by singlet oxygen scavengers

such as sodium azide and 1,4-diazabicyclo[2.2.2]octane. This suggested that the Mn(IV) reaction occurred through emission by a singlet oxygen species. The observed emission wavelengths in these studies, however, also closely match those observed using other manganese-based reagents, for which there is strong evidence for a mechanism involving Mn(II)*, rather than a singlet oxygen species [129]. It should be noted here that this information was gained from the review by Adcock *et al.* [129], rather than the original paper, due to this paper not being available in English.

Mn(IV) chemiluminescence analysis is most commonly conducted using formaldehyde as an enhancer, typically with concentrations between 0.2 and 3.0 M [144]. Formaldehyde, however, is carcinogenic, and hence cannot be used in routine analysis. Numerous other compounds have been investigated as alternatives, including formic acid, various surfactants, sodium thiosulfate, quinine sulphate, and β-cyclodextrin, but with little success. Other enhancers, including sulfite, polyphosphates, and rhodamine B, however, have been successfully used as Mn(IV) chemiluminescence enhancers for selected reagents. Recently, Smith *et al.* [144] found that ethanol could be an even more effective enhancer than formaldehyde for a wide range of organic analytes. They observed that chemiluminescence signal enhancement when analysing 20 different organic compounds was generally 20-60 % greater than the enhancement resulting from formaldehyde addition (2 M). For some analytes, however, namely glutathione, glutathione disulphide, and methionine, the enhancement could be between 200 and 544 % higher than that using formaldehyde. Selectivity for certain analytes particularly thiols, was also observed to differ when using ethanol compared to formaldehyde enhancement. The mechanism for both formaldehyde and ethanol enhancement are yet to be fully determined. It is hypothesised to occur via increasing the rate of formation of the Mn(II) precursor, which is the case for permanganate chemiluminescence enhancement using formaldehyde. This hypothesis was supported by the observation that the spectral distributions of chemiluminescence obtained using Mn(IV) with formaldehyde and ethanol enhancement are identical to those obtained from permanganate chemiluminescence [144]. The reasons for lower enhancement by other reducing agents similar to ethanol and formaldehyde, however, are yet to be explained.

The use of Mn(IV) as a chemiluminescence reagent has recently been reviewed by Adcock *et al.* [129], and hence the majority of this review will detail applications since 2014. Mn(IV) was first used as a chemiluminescence reagent by Barnett *et al.* [139] for the detection of 25 different organic and inorganic analytes. Mn(IV) was prepared using the preparation method of Jáky *et al.* [137, 138] and formaldehyde was used as an enhancer. Since then, this reagent has been used in the detection of a wide range of organic analytes, including thiols, disulfides, antioxidants, alkaloids, and phenols. Typical detection limits have been between 1×10^{-9} M and 8×10^{-5} M, depending on the analyte [129].

This detection has been applied to a wide range of matrices, including tablets, capsules, and other pharmaceutical formulations, plant extracts, urine, blood, beverages, and food [129]. Mn(IV) chemiluminescence has generally been found to be less selective than that using other Mn species, with coupling to chromatographic separation prior to detection often required for complex matrices, such as plant extracts or clinical samples [129]. Since 2014 four additional papers using Mn(IV) have been published, all by Nalewajko-Seiliwoniuk and co-workers [145-148]. These studies were focussed on detection of phenolic compounds in plant-based food samples using a Mn(IV)-formaldehyde-hexametaphosphate system.

1.5.3.3 Mn Acetate (Mn(III)):

Manganese acetate (Mn(III)) can be prepared via either reduction of Mn(IV) or Mn(VII), or oxidation of Mn(II) [140]. The Mn(III), however, is quite unstable and can disproportionate to Mn(II) or Mn(IV). This can be minimised by the addition of Mn(II), complexation with sulphate, oxalate, or EDTA anions, or by maintaining the solution at an acidic pH [140]. For instance, oxidation of $MnSO_4$ with $KMnO_4$ in H_2SO_4 has been previously used to produce Mn(III) via the equation below, provided that the Mn(II) concentration and acidity is high [149].

$$MnO_4^- + 4Mn^{2+} + 8H^+ \rightarrow 5Mn^{3+} + 4H_2O \quad (4)$$

Mn(III) is commonly used as a single electron oxidant in synthetic chemistry, however it has also been applied to chemiluminescence detection on numerous occasions. It has been applied to a range of organic analytes, with detection limits ranging from 4 x 10^{-9} M to 2 x 10^{-6} M, as summarised in the review by Brown *et al.* [140]. Various sample matrices have been investigated, including pharmaceutical formulations, beer, urine, and air [140]. Mn(III) has scarcely been used since the review in 2008 for chemiluminescence detection. Tsaplev *et al.* [149, 150] did, however, investigate its reaction mechanisms and quenching.

The emissions spectrum resulting from Mn(III) chemiluminescence has again been shown to be very similar to those obtained during Mn(VII) and Mn(IV) reactions, with maxima between 680 and 720 nm [140, 149, 151]. This therefore suggests the same mechanism through electronically excited Mn(II) is occurring [151]. Tsaplev *et al.* [149] conducted a thorough investigation into the kinetics and reaction pathways of Mn(III) chemiluminescence with malic acid using batch chemiluminescence methods. They suggested that the reaction occurred via complexation between malic acid and the Mn(III), followed by one-electron oxidation of malic acid to form a radical intermediate and Mn^{2+}. This was then followed by reaction of the malic acid radical with O_2 to form malic acid hydroperoxide and the peroxide radical. This group also studied the effects of the presence of HF and acetonitrile on Mn(III)

chemiluminescence emission from citric acid [150]. They observed that addition of HF reduced the rate of light emission, but not the intensity of emission, hence indicating that HF acted as an inhibitor, rather than a quencher. This was suggested to be due to competition between the citric acid and the HF for complexation to Mn^{3+}, hence supporting the hypothesis of a reaction mechanism involving participation of Mn(III). Acetonitrile was found to quench the chemiluminescence reaction, however the exact mechanism involved is still unclear [150].

1.5.3.4 Tris-2,2'-bipyridyl ruthenium:

Another commonly used chemiluminescence oxidising agent is tris-2,2'-bipyridyl ruthenium (II) chloride ($Ru(bipy)_3Cl_2$), which is known to produce chemiluminescence upon reaction with tertiary amines, among other functional groups [122]. The active compound in this chemiluminescence reaction is the 3+ oxidation state ($[Ru(bipy)_3]^{3+}$), which must first be produced via oxidation of tris-2,2'-bipyridyl ruthenium (II) chloride ($[Ru(bipy)_3]^{2+}$) (Equation 5), which is accompanied by a colour change from orange to green [152]. It is then the $[Ru(bipy)_3]^{3+}$ that reacts with the target analyte to form an excited intermediate (Equation 6), which, upon relaxation, releases light energy and regenerates the original $[Ru(bipy)_3]^{2+}$ (Equation 7) [152]. The maximum light emission occurs at 610 nm [122].

$$[\mathrm{Ru(bipy)_3}]^{2+} \xrightarrow{oxidation} [\mathrm{Ru(bipy)_3}]^{3+} + e^- \quad (5)$$

$$[\mathrm{Ru(bipy)_3}]^{3+} \xrightarrow{target\ analyte} [\mathrm{Ru(bipy)_3}]^{2+*} \quad (6)$$

$$[\mathrm{Ru(bipy)_3}^{2+}]^* \rightarrow [\mathrm{Ru(bipy)_3}]^{2+} + hv \quad (7)$$

The initial oxidation step can be performed in a number of ways, either chemically or via electrogeneration [122]. The most simple chemical method of generating $[Ru(bipy)_3]^{3+}$ is via mixing an acidic solution of $Ru(bipy)_3Cl_2$ with solid lead dioxide (PbO_2), followed by filtration to remove the solid. This method had been applied to a large variety of analytes with good success. There are, however, several drawbacks. The $[Ru(bipy)_3]^{2+}$* state is highly reactive, and hence can react with any water in the system to convert back to the 3^+ form. This decreases the concentration of $[Ru(bipy)_3]^{2+}$*, hence decreasing the chemiluminescence emission over time. Other chemical oxidation methods include reaction with cerium (IV) sulphate ($Ce(SO_4)_2$) or potassium permanganate ($KMnO_4$) [122]. In contrast to PbO_2, $Ce(SO_4)_2$ and $KMnO_4$ reagents are solutions and hence can be mixed with the $Ru(bipy)_3Cl_2$ online. This maximises the time of contact between the reagents, and minimises the time between reagent mixing and emission detection, hence decreasing the effect of a low-stability $[Ru(bipy)_3]^{3+}$ state. $Ce(SO_4)_2$ is a very strong oxidising reagent itself, and hence can actually act to oxidise analytes or other compounds present in the reaction mixture [153]. Analytes may therefore

be able to react with $Ce(SO_4)_2$ to form products that are then capable of undergoing chemiluminescence with $Ru(bipy)_3Cl_2$, that could otherwise not be detected. $Ce(SO_4)_2$ does have a limitation, however, in that it is poorly soluble at pH levels greater than 3 [153]. This makes detection of analytes that must be held under alkaline conditions more complicated, however still achievable. The composition and concentration of acid used to prepare the $Ce(SO_4)_2$ has been shown to be highly critical in determining the chemiluminescence emission obtained [153]. This influence has also been shown to vary depending on the analyte [153]. Although the exact reaction mechanism is still unclear, it has been noted that organic acids containing a hydroxyl group alpha to a carboxylic acid are capable of undergoing chemiluminescence with $Ru(bipy)_3Cl_2$ oxidised with $Ce(SO_4)_2$ [153].

Electro-generation involves generation of $[Ru(bipy)_3]^{3+}$ at an electrode surface. This can be conducted either separately from the analyte, referred to as electrochemical oxidation, or in the same vessel as the analyte, referred to as in-situ electrochemiluminescence [154]. Electrochemical oxidation has been shown to produce similar problems to the use of PbO_2, in that the stability of the $[Ru(bipy)_3]^{3+}$ is low. This has been overcome on several occasions via the use of on-line continual regeneration using flow-through electrochemical cells [154, 155]. Electrochemiluminescence, however, allows for continual generation of the $[Ru(bipy)_3]^{3+}$ state, hence increasing its lifetime. It also has similar advantages to $Ce(SO_4)_2$ and $KMnO_4$ in that it allows for oxidation of both the oxidising reagent and the analyte, hence opening up the possibility of a larger range of analytes. Electrochemiluminescence is even more advantageous in this aspect because a wider range of analytes can be oxidised using this method, compared with the limited number capable of chemically reacting with $KMnO_4$ or $Ce(SO_4)_2$ [153]. Electrochemiluminescence does have several disadvantages, however. For instance, the initial oxidation reactions are dependent on the diffusion of the analytes and reagents to the electrodes. Also, only a small concentration of $[Ru(bipy)_3]^{3+}$ relative to the size of the experiment is generally produced, which limits the chemiluminescence reactions that can occur [153]. Although more sophisticated than chemical generation, both electrochemical oxidation and electrochemiluminescence methods have been shown to produce equivalent figures of merit [122]. The choice of $[Ru(bipy)_3]^{3+}$ generation method is therefore often dependent on the desired applications and available instrumentation.

1.5.3.5 Cerium Sulphate (Ce(IV)):

Cerium sulphate (Ce(IV) is a well-established oxidising reagent, which has been utilised extensively in organic synthesis. Ce(IV) as a chemiluminescence reagent was recently reviewed by Kaczmarek [156] in 2015, including reaction mechanisms and the use of sensitisers and enhancers. The chemiluminescence reaction and mechanism of Ce(IV) are highly dependent on the analyte in question. The emitting species of these reactions can generally be classified into 5 groups: Ce(III),

electronically-excited sulphur dioxide (SO_2*), excited oxidation products of the analyte, fluorophores, and dimols of singlet oxygen [156]. Reaction through Ce(III) results in emission at approximately 355 nm. Sulfites and other inorganic sulphur oxides, however, are the most commonly used systems in Ce(IV) chemiluminescence. These reactions occur through production of electronically-excited sulphur dioxide (SO_2*), as shown in the equation below.

$$Ce(IV) + HSO_3^- \rightarrow HSO_3^{\cdot} + Ce(III) \quad (1)$$

$$2HSO_3^{\cdot} \rightarrow S_2O_6^{2-} + 2H^+ \quad (2)$$

$$S_2O_6^{2-} \rightarrow SO_4^{2-} + SO_2^* \quad (3)$$

The SO_2* undergoes a very weak emission of light between 300 and 450 nm, and hence often requires the addition of enhancers, to which the energy can be effectively transferred [156]. Common enhancers include benzamides, silver nanoclusters, gold nanoparticles, and carbon dots. Surfactants have also been utilised extensively for their ability to protect the emitting species from reacting with other compounds in the reaction mixture. These include sodium dodecylbenzenesulphonate (SDBS), sodium dodecylsulphate (SDS), and cetyltrimethylammonium bromide (CTAB).

The direct oxidation of analytes by Ce(IV) to produce intense chemiluminescence without the need for enhancers has also been reported on a few occasions. These analytes have included tryptophan, naproxen, and norfloxacin, with the structures given in Figure 1-11. In the case of tryptophan, the predominant emitter was an oxidation product of tryptophan. Emission spectra from norfloxacin, however, were typical of singlet oxygen dimols, thought to be generated by the transfer of energy between a reaction intermediate and dissolved oxygen. The exact reaction scheme is detailed in [156].

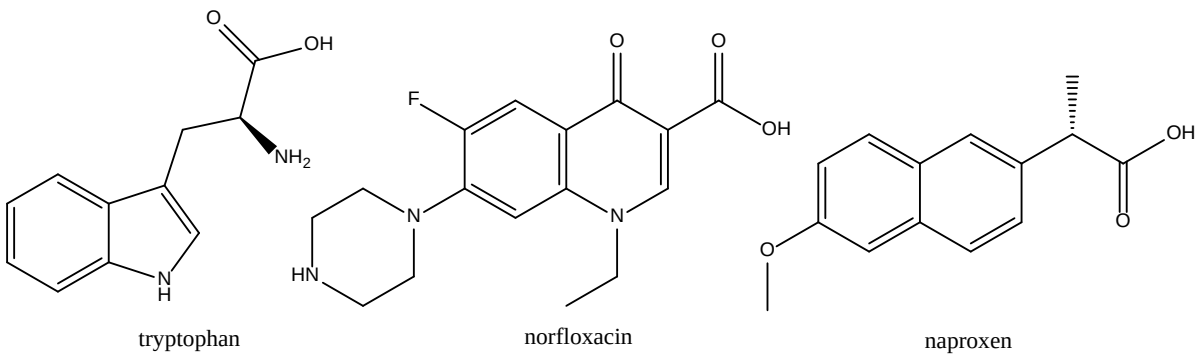

tryptophan norfloxacin naproxen

Figure 1-11. Structures of tryptophan, norfloxacin, and naproxen

1.5.3.6 Luminol:

Luminol (5-amino-2,3-dihydrophthalazine-1,4-dione) is the most commonly-used chemiluminescence reagent across a wide range of disciplines [111]. Unlike the reagents previously described, however,

luminol itself is not an oxidising reagent. Rather, it is itself oxidised by a chosen compound, such as hydrogen peroxide, chlorate persulphate, dichlorocyanurate, N-bromosuccinimide, permanganate, hexacyanoferrate, and electro-generated hypobromite [111]. No matter which reagent is used to oxidise luminol, the light-producing pathway is the same; going through the electronically excited 3-aminopthalate anion, as shown in Figure 1-12 [111]. This results in light emission with maximum intensity at 425 nm [111, 157].

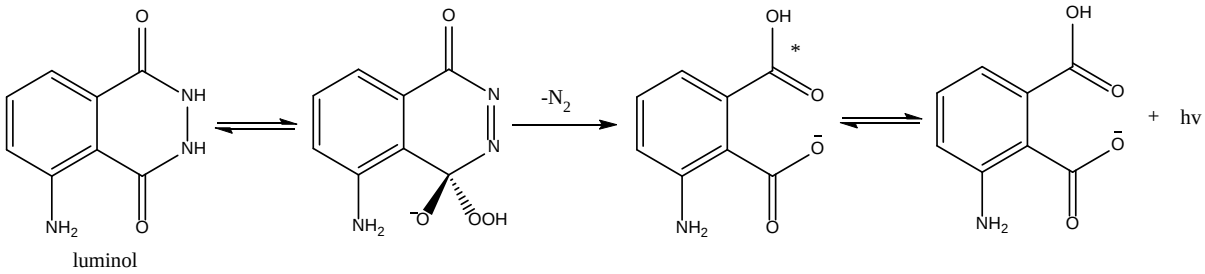

Figure 1-12. General mechanism of luminol chemiluminescence [67]

Luminol chemiluminescence is therefore not commonly used for direct detection of an analyte. Rather, the properties of this well-defined reaction are used as indicators to investigate enhancers, inhibitors, and catalysts of the reaction [111]. The oxidation of mon-, di-, and polyhydric phenols, for instance, results in the production of superoxide radicals, which can undergo luminol chemiluminescence. This oxidation is catalysed by polyphenol oxidases, enzymes present in plant juices, and hence luminol chemiluminescence is commonly used to monitor the action of these enzymes [111]. H_2O_2 is a common product of many biological reactions, and hence the luminol-H_2O_2 reaction has been extensively applied to biochemistry-based analytical sensors, such as biosensors, immunosensors, microarrays, and immunoassays [67].

There are various catalysts of luminol chemiluminescence, including ozone, halogens, persulfates, xanthide oxidase, singlet oxygen, Fe(III) complexes, and various other metal ions [67]. Again, these compounds are therefore often exploited for use in detection of other compounds. Cu(II), for example, catalyses the luminol-H_2O_2 reaction [157]. Cu(II) is also known to form complexes with methimazole and carbimazole, hence suppressing its catalytic ability. Changes in chemiluminescence intensity can therefore be correlated with the concentrations of these complexing drugs [111].

1.5.4 Application of Chemiluminescence Techniques to Surface Waters

Chemiluminescence has several advantages when applied to the analysis of surface waters. These include high selectivity, which decreases matrix effects, portability, allowing for real-time in-situ analysis, and high sensitivity [71]. Since then several groups have applied chemiluminescence detection to a range of environmental analyses, and demonstrated its excellent detection limits. Xu *et al.* [158] detected hydroquinone down to concentrations of 0.17 nM using Co(II)-catalysed luminol

chemiluminescence, with recoveries in tap, lake, and river water samples obtained between 95 and 106 %. Catala-Icardo *et al.* [159] developed detection for carbamate pesticides using Ce(IV), with recoveries in surface- and ground-water between 87 and 110 %. The limits of detection were between 5 and 80 ng/L. This group was also able to detect quinmerac down to concentrations of 0.6 ng/mL using sodium sulphite and Ce(IV) in acidic media, with surface- and ground-water recoveries between 78.1 and 94.5 % [160]. Wang *et al.* [161] developed chemiluminescence detection for calcein with a limit of detection of 0.01 µM using a novel CNOOH-calcein-modified kaclin system. Recoveries in tap and river water were between 96.9 and 105.2 %. Linnik *et al.* [162] was able to determine the levels of dissolved copper using luminol chemiluminescence in surface water. Durand *et al.* [163] also developed chemiluminescence detection for copper using 1,10-phenanthroline as the oxidising reagent, with a detection limit of 4×10^{-8} M in surface water. Chemiluminescence has also been used for the detection of pesticides in environmental matrices on numerous occasions, as recently reviewed by Liang *et al.* [164]. Zhihua and Jiaguo [165] developed a novel electrochemiluminescence sensor for the detection of tripropylamine using $Ru(bipy)_3$ immobilised on TiO_2 nanotube arrays, however this was not applied to real water samples.

In environmental analysis chemiluminescence detection is most commonly coupled with chromatography in order to further eliminate matrix effects. The application of HPLC-chemiluminescence techniques to the analysis of environmental samples was recently reviewed In 2009 by Gámiz-Gracia *et al.* [71]. This coupling does, however, limit the portability of the analysis technique. Čapka *et al.* [166], however, demonstrated that coupling to chromatography need not limit the use of chemiluminescence detection in the field. This group developed a novel micro-column liquid chromatography system with chemiluminescence detection for the detection of nitramine-, nitroester-, and nitroaromatic-based explosives in surface waters and soil that was able to be taken out into the field. The chemiluminescence was based on the reaction between luminol and the products of photolytic conversion of the explosives post-column. Nitrates are a large component of environmental samples, particularly soils, and are known to cause large interferences during chemiluminescence analysis of other analytes containing similar functionalities. In order to overcome this Čapka *et al.* [166] developed a novel chromatographic method in which 5 µL of a weak mobile phase (15 % v/v methanol/water) was injected into the solvent stream after injection of the sample, prior to elution with a strong mobile phase (55 % v/v methanol/water). This resulted in all nitrate compounds being eluted in the weak mobile phase while the explosive compounds were delayed, before then being eluted by the strong mobile phase. This group therefore demonstrated the applicability of chemiluminescence detection even in matrices with large concentrations of interfering compounds.

1.5.5 Chemiluminescence Detection of Cytotoxics

Despite their obvious advantages, chemiluminescence methods have had very limited use in cytotoxic analysis. Sun *et al.* [1, 127, 128] developed chemiluminescence reaction systems for 5-fluorouracil and mitomcyin-C, finding that the use of 5 x 10^{-4} M $KMnO_4$ and 2 M HCl or 1 M HNO_3 for 5-fluorouracil and mitomycin-C, respectively, could produce high levels of chemiluminescence at a wavelength of 639 nm. Maximum emission and optimal precision were obtained with a sample volume of 120 µL and flow rate of 3 mL/min. HCOH (2.5 %) was the only sensitiser tested that was able to enhance the signal. The LOD obtained was 30 µg/L; much higher than those obtained using LC-MS/MS techniques. It was suggested, however, that if this detection had been couple to a separation technique, the LODs obtained could have been greatly decreased. The developed method was used to analyse pharmaceutical formulations for these drugs. The authors proposed a mechanism involving a singlet oxygen species (Equations 8-12), where $^1O_2{}^1O_2(^1\Delta_g{}^1\Delta_g)$ is single-state bimolecular oxygen, $^1O_2(^1\Delta_g)$ is singlet state oxygen, and $^3O_2(^3\Sigma_g)$ is triplet-state oxygen. This mechanism was postulated due to the maximum chemiluminescence emission occurring at 639 nm, which was very similar to the 645 nm reported for singlet-oxygen systems [1]. The characteristic peaks at 578 and 786 nm due to bimolecular-oxygen, respectively, however, were not detected. The wavelength range assessed (360-730 nm) was also too narrow for detection of the peak at 1268 nm typical of singlet-oxygen reactions [126]. It is therefore possible that this reaction was in fact occurring through electronically-excited Mn(II), for which there is strong evidence for permanganate chemiluminescence [167]. It is possible that the discrepancy between the maximum emission wavelength of 639 nm observed by Sun *et al.* [1] and the 734 ± 5 nm expected for Mn(II)* chemiluminescence was due to differences between instrument sensitivity in this wavelength range [126].

$$MnO_4^- + H^+ + \text{5-fluorouracil} \longrightarrow {}^1O_2(^1\Delta_g) + Mn^{2+} + \text{5-fluorouracil}^{\bullet} + H_2O \quad (8)$$

$$2MnO_4^- + 6H^+ + 5CHOH + 2H_2O \longrightarrow 5HOCH_2OOH + 2Mn^{2+} \quad (9)$$

$$HOCH_2OOH \longrightarrow HOCH_2OO^- + H^+ \quad (10)$$

$$2HOCH_2OO^- + \text{5-fluorouracil}^{\bullet} \longrightarrow HCHO + HCOOH + {}^1O_2(^1\Delta_g) + \text{5-fluorouracil} + H_2O \quad (11)$$

$${}^1O_2(^1\Delta_g) + {}^1O_2(^1\Delta_g) \longrightarrow {}^1O_2{}^1O_2(^1\Delta_g{}^1\Delta_g) \quad (12)$$

$${}^1O_2{}^1O_2(^1\Delta_g{}^1\Delta_g) \longrightarrow {}^3O_2(^3\Sigma_g) + hv \quad (13)$$

Dong *et al.* [168] also reported the chemiluminescence detection of 5-fluorouracil, as well as uracil and 1-methyl-uracil. They used ECL in an FIA manifold and attempted to elucidate the mechanism via monitoring with UV/Vis spectroelectrochemistry (SEC). It was found that the chemiluminescence reactions of each uracil were highly affected by pH, with no chemiluminescence being observed in

acidic media. In alkaline media, however, intense chemiluminescence was produced, and increased substantially with increasing pH. This suggested that the chemiluminescence mechanism required deprotonation of the substrates. The mechanism in Figure 1-13 was proposed for uracil and 5-fluorouracil [168]. This was vastly different for the known mechanism occurring with aliphatic amines. As this was an investigative study of the electrochemiluminescence mechanism, no detection limits or linearity were reported.

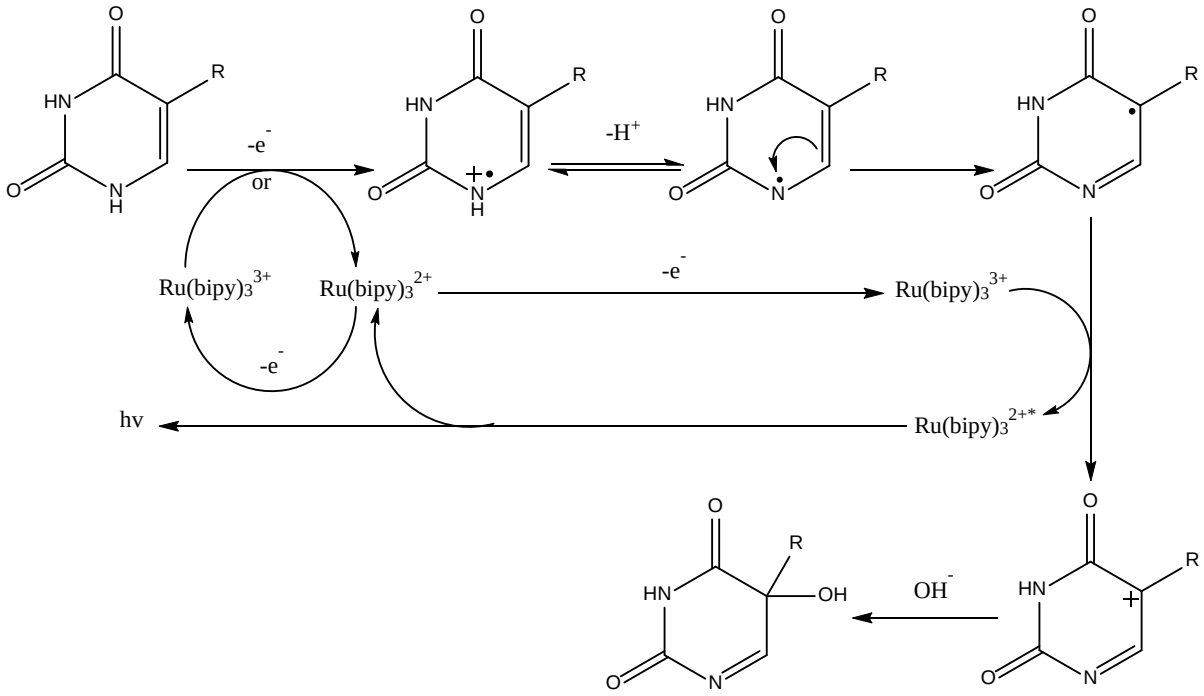

Figure 1-13. Proposed electrochemiluminescence mechanism of uracil (R = H) and 5-fluorouracil (R = F) with $Ru(bipy)_3^{2+}$ [168]

This mechanism involves the oxidiation of the uracil compound by $[Ru(bipy)_3]^{3+}$, here electrogenerated, to form a cationic intermediate. Deprotonation at N1 then occurs to produce a neutral radical intermediate. The presence of strong electron-withdrawing groups, such as fluorine in 5-fluorouracil, is thought to enhance this deprotonation by decreasing the negative charge density on N1. The radical centre is then transferred from N1 to C5, before this radical reduces $[Ru(bipy)_3]^{3+}$ to the excited $[Ru(bipy)_3]^{2+*}$ compound and forms another cationic intermediate. It is this relaxation/reduction step that is accompanied by the emission of light.

Luminol and lucigenin oxidation reactions have also been utilised to monitor the effects of doxorubicin, etoposide, paclitaxel, and cisplatin on neutrophils in cells [169-171] and the effects of 5-fluorouracil on oxygen production in leukocytes [172]. An assay based on chemiluminescence production via phosphorylation has also been used previously to determine the interactions of vindesine, vinorelbine, paclitaxel, 5-fluorouracil, MET, etoposide, antinomycin-D, amsacrine, DOX, mitomycin-C, bleomycin, chlorambucil, melphalan, and mitoxantrone with cellular DNA [173, 174].

The use of chemiluminescence methods in environmental analysis of cytotoxics, however, has never been investigated, despite being shown to be amenable to in situ analysis of aquatic systems [175].

Neither cyclophosphamide nor imatinib have been detected using chemiluminescence. Their chemical structures, however, suggest they may have potential for reactions with certain oxidising reagents. Imatinib contains several secondary and tertiary amines, which could be highly reactive with $Ru(bipy)_3Cl_2$. Cyclophosphamide also contains a secondary and a tertiary amine, and hence could possibly react with $Ru(bipy)_3Cl_2$. The vast range of compounds detectable using permanganate chemiluminescence also opens up the possibility for detection of these cytotoxics.

1.6 Project Aims

It is clear that there are large gaps in our understanding of the fate of cytotoxics in the environment, particularly surface waters. More concerning is the fact that many of the un-researched cytotoxics are used quite predominantly in Australia, and hence could have a large impact on the environment. There is therefore a need for the development of new analytical methods for the detection of cytotoxics in surface waters. These methods could then be used to monitor the degradation, transformation, and distribution of these drugs in environmental waters, in order to advise authorities on the true risks associated with these drugs. Chemiluminescence is a detection method with numerous advantages for environmental monitoring, but which has had limited use in the detection of cytotoxics. The research presented in this thesis is therefore focussed on development of chemiluminescence detection for three of the most commonly used cytotoxic drugs in Australia; cyclophosphamide, 5-fluorouracil, and imatinib. These three drugs exhibit vastly different chemical and physical properties, and hence could act as effective markers for a range of cytotoxics in surface waters.

These aims will be achieved via the following project components:

1. Preliminary investigation into the suitability of various chemilumnescence oxidising reagents for the detection of cyclophosphamide, 5-fluorouracil, and imatinib.

2. Systematic development of chemiluminescence detection for each cytotoxic in surface waters.

3. Investigation of the degradation of cyclophosphamide in aqueous solutions using the developed chemiluminescence detection method, together with LC-MS/MS and NMR techniques.

Chapter 2:

Preliminary Investigation into the Feasibility of Chemiluminescence Detection for Cyclophosphamide, 5-Fluorouracil, and Imatinib

2. Preliminary Investigation into the Feasibility of Chemiluminescence Detection for Cyclophosphamide, 5-Fluorouracil, and Imatinib

2.1 Introduction

Cytotoxic drugs, such as cyclophosphamide, 5-fluorouracil, and imatinib, are used in chemotherapy to prevent the growth and replication of cancerous cells [4]. They bring about this effect via influencing DNA replication and translation, or by inhibiting other cell processes vital for growth [4]. This action is non-specific, and hence cytotoxic drugs are often carcinogenic, mutagenic, and teratogenic (resulting in birth defects) [5, 10]. Many common cytotoxics are excreted from the body unchanged, and hence enter wastewater. Their removal from wastewater by common treatment methods is often inefficient, resulting in their release into surface waters [9, 176]. Here, cytotoxic drugs have the potential to cause harm to aquatic organisms. Knowledge of the effects of cytotoxics in surface waters is limited. This is in-part due to lack of instrumentation suitable for real-time, in-situ analysis. There is therefore need for development of new, simple, sensitive, and potentially portable analysis methods for environmental monitoring of cytotoxic drugs.

Chemiluminescence analysis is a technique highly suited to environmental analysis. It involves simple instrumentation, low detection limits, high selectivity, and capabilities of in-situ real-time analysis [66-68]. Chemiluminescence involves reaction of the analyte with one or more chosen reagents, typically an oxidising reagent, in order to form an intermediate in the excited state. Upon relaxation of this intermediate the excess energy is released as light, which can be detected to determine the presence of the target analyte [66]. There are a variety of oxidising reagents that can be used, including potassium permanganate ($KMnO_4$), tris-2,2'-bipyirdyl ruthenium ($Ru(bipy)_3$), cerium sulphate ($Ce(SO_4)_2$), and manganese dioxide (Mn(IV)) [66, 73, 76]. Each reagent proceeds via a different mechanism and has different selectivities to analyte functionalities [122, 123, 140, 156]. The way in which the oxidising reagent is prepared and the use of enhancers can also strongly influence detection sensitivity, selectivity, linear range, and repeatability. For example, $[Ru(bipy)_3]^{3+}$ prepared using $Ce(SO_4)_2$ or $KMnO_4$, has been shown to produce markedly different selectivity for analytes than $[Ru(bipy)_3]^{3+}$ prepared using PbO_2 [153]. Similarly, $KMnO_4$ combined with sodium hexametaphosphate as an enhancer has very different selectivity and analytical responses than $KMnO_4$ prepared in the absence of the enhancer [123, 125].

Despite its advantages chemiluminescence detection has not yet been applied to monitoring of cytotoxic drugs in the environment. This research is therefore focussed on investigation of the suitability of this technique to the detection of the cytotoxic drugs cyclophosphamide, 5-fluorouracil,

and imatinib. Of these three cytotoxic drugs, only 5-fluorouracil has been studied for its potential to be detected using chemiluminescence. Two of these studies used $KMnO_4$ as the oxidant, whilst the other used $Ru(bipy)_3$ [1, 127, 168]. The detection method using $KMnO_4$ produced a detection limit of 2.31×10^{-6} mol/L in aqueous solution [1]. The reaction mechanism was suggested to occur via a singlet-oxygen species [1], however there is strong evidence for a pathway involving electronically-excited Mn(II) instead [126]. The $Ru(bipy)_3Cl_2$ reaction was suggested to have occurred via reaction with N1 in 5-fluorouracil [168]. As this was an investigative study into reaction mechanisms, however, no limits of detection or other method validation was conducted.

Chemiluminescence detection for cyclophosphamide and imatinib has not yet been reported. Imatinib contains two secondary amines, two tertiary amines, and three aromatic amines, and hence has strong potential for reaction with $[Ru(bipy)_3]^{3+}$ [154]. Similarly, cyclophosphamide contains a secondary and a tertiary amine, which could also undergo chemiluminescence with $[Ru(bipy)_3]^{3+}$. The wide range of analytes possible for $KMnO_4$, Mn(IV), and Ce(IV) chemiluminescence [71, 137, 138, 156], however, also makes these oxidising reagents viable options for detection of cyclophosphamide and imatinib. The first step in development of chemiluminescence detection is selection of the oxidising reagent.

This chapter describes a comprehensive investigation to determine the most suitable oxidising reagent to use for chemiluminescence detection of each of cyclophosphamide, 5-fluorouracil, and imatinib. The oxidising reagents considered were $KMnO_4$, Mn(IV), $Ce(SO_4)_2$, and $Ru(bipy)_3Cl_2$. This study involved investigation into each oxidising reagent separately to determine the effect of reagent concentrations and preparation methods, the use of enhancers, and instrumental settings (reagent volumes and flow rates) on the chemiluminescence signal. The most suitable reagent and instrumental conditions determined for each oxidising reagent were then compared for each cytotoxic to determine the most suitable oxidising reagent.

2.2 Experimental

2.2.1 Chemicals and Reagents

All reagents were analytical grade unless otherwise stated. 5-fluorouracil, cyclophosphamide monohydrate, cerium(IV) sulphate, and Triton X100 were purchased from Sigma Aldrich (Castle Hill, NSW, Australia). Imatinib mesylate was purchased from Sapphire Bioscience (Waterloo, NSW, Australia). Tris-2,2'-bipyridyl ruthenium (II) chloride hexahydrate was purchased from Strem Chemicals (Newburyport, MA, USA). Potassium permanganate, sulfuric acid (98 %), ethanol, (99.9 % HPLC-grade), lead dioxide, formaldehyde, orthophosphoric acid, disodium hydrogen phosphate, and sodium thiosulfate were purchased from Chem-Supply (Gillman, SA, Australia). Hydrochloric acid (37

%) was purchased from Choice Analytical (Thornleigh, NSW, Australia). Acetonitrile (HPLC grade) was purchased from Rowe Scientific Pty. Ltd (Lonsdale, SA, Australia). Tris(hydroxymethyl)aminomethane, sodium hydrogen carbonate, and sodium dihydrogen phosphate were purchased from Merck Pty. Ltd (Bayswater, Victoria, Australia). Sodium borate decahydrate was purchased from Amersham Australia Pty. Ltd (Baulkham Hills, NSW, Australia). Sodium hexametaphosphate was purchased from Ajax Finechem (Taren Point, NSW, Australia). All solutions were prepared using deionised water (18 MΩ) unless otherwise stated.

2.2.2 Standards

Stock solutions of cyclophosphamide, 5-fluorouracil, and imatinib mesylate ($1x10^{-3}$ M) were prepared daily and stored in sealed glass bottles in the absence of light. These were prepared in either deionised water, $Ce(SO_4)_2$ (0.5×10^{-3} – 2×10^{-3} M in 0.4 M H_2SO_4), or $Ru(bipy)_3Cl_2$ (0.5×10^{-4} – 2×10^{-3} M in deionised water). These solutions were then diluted (1×10^{-5} – 1×10^{-4} M) as required immediately prior to analysis using these solvents.

2.2.3 Preparation of Oxidising Reagents

$KMnO_4$ (1×10^{-3} M) was prepared via dissolution of solid $KMnO_4$ in aqueous sodium hexametaphosphate (1 % m/v, pH 2.25 (H_2SO_4)). $KMnO_4/Na_2S_2O_3$ was prepared as described by Francis *et al.* [177] and Terry *et al.* [178] in which $KMnO_4$ (1.9×10^{-3} M, 100mL) was prepared in aqueous sodium hexametaphosphate (1 % m/v, pH 2.25 (H_2SO_4)) and subsequently mixed with $Na_2S_2O_3$ (6×10^{-4} M, 600 µL). $[Ru(bipy)_3]Cl_2$ (1×10^{-3} M) was prepared by dissolution of the solid reagent in 0.1 M H_2SO_4. The reagent was oxidised to the 3+ oxidation state via three approaches: i) batch oxidation with solid PbO_2, ii) on-line generation using $Ce(SO_4)_2$, and iii) on-line generation using $KMnO_4$. Batch oxidation with solid PbO_2 was achieved by mixing the solid with $[Ru(bipy)_3]Cl_2$ (1×10^{-3} M in 0.1 M H_2SO_4) at a ratio of 0.1 g: 20 mL. The solid material was subsequently removed via filtration (0.45 µm, nylon) immediately prior to analysis. On-line generation using $Ce(SO_4)_2$ was achieved via the sequential aspiration of $Ce(SO_4)_2$ (1×10^{-3} M in 0.05 M H_2SO_4) and $Ru(bipy)_3Cl_2$ (1×10^{-3} M in deionised water) into the SIA system using the reagent volumes inTable 2-1. On-line generation using $KMnO_4$ was achieved via the sequential aspiration of $KMnO_4$ (1×10^{-3} M in 0.05 M H_2SO_4) and $[Ru(bipy)_3]Cl_2$ (1×10^{-3} M in deionised water). Solid $[Ru(bipy)_3]ClO_4$ was prepared according to the method described by McDermott *et al.* [179]. $[Ru(bipy)_3]Cl_2.6H_2O$ (400 mg in 6 mL water) mixed with solid $NaClO_4$ (200 mg), before being cooled on an ice bath for 5 min. The resulting $[Ru(bipy)_3]ClO_4$ solid was collected via filtration and washed twice with ice water (2 mL). $[Ru(bipy)_3]ClO_4$ solutions (1.0×10^{-3} M) were prepared in $HClO_4$ (0.05 M in acetonitrile) and oxidised with PbO_2 (0.1 g/ 20 mL). The solid was allowed to settle to the bottom, and the resulting deep green solution was taken directly from above the PbO_2 layer and used without filtering. Mn(IV) was prepared using the simplified method developed by

Smith *et al.* [141], in which $KMnO_4$ (0.1 M, 1.25 mL) and $Na_2S_2O_3$ (1.88×10^{-2} M, 2.5 mL) were mixed and diluted to 250 mL with deionised water. The resulting brown-orange colloid was used as prepared. Ce(IV) was prepared by dissolving $Ce(SO_4)_2$ (1-1.5 x 10^{-4} M) in 0.1 M H_2SO_4. Triton X100 (10 % v/v), formaldehyde (0.1-1.0 M), and formic acid (0.1-0.75 M) were prepared by dissolution in deionised water.

2.2.4 Instrumentation

Sequential injection analysis:

All experiments were conducted using an in-house built Sequential Injection Analysis (SIA) instrument (Figure 2-1) developed by Bogdanovic *et al.* [180]. This consisted of a bi-directional MilliGAT™ pump (Global FIA, Fox Island, WA, USA), a Valco 10-port multiposition valve (Global FIA, Fox Island, WA, USA), a 29 mm diameter photomultiplier tube (PMT) (Electron Tubes Limited, 9828SB, Uxbridge, England). A reaction coil (100 µL) adjacent to the PMT inside the light-proof housing was made from PTFE tubing (ID 0.76 mm) (Pro Tech Group, Coolum, Australia). PTFE tubing (0.02 mm I.D.) (Global FIA, Fox Island, WA, USA) was used as the hold cell, and for connections between reagents, the valve, and the pump. The pump was connected to a computer via a RS232 serial port. The instrument was controlled via software written in-house using National Instruments LabVIEW® version 8.2 (Austin, TX, USA). This was based on software written by Osborne *et al.* [181] and Bogdagonic *et al.* [180]. Precise volumes of each reagent (specified using the LabVIEW® program) were sequentially aspirated into the holding coil by the pump. The direction of the pump was then reversed and the hold-cell contents pumped via a carrier solution into the reaction coil. At this time data acquisition was automatically commenced by the program and continued for 15 seconds. A Chebyshev low-pass filter was utilised with a cut-off frequency of 1 Hz. The PMT voltage was maintained at 800 V throughout all experiments. The signal gain was 2 ± 0.1 V. The carrier solutions used for each reagent, the enhancers tested for each, and the ranges of reagent volumes and flow rates trialled during the oxidising reagent screen are detailed in Table 2-1. The ranges of reagent volumes and flow rates tested during screening of $[Ru(bipy)_3]^{3+}$ generation methods are described in Table 2-2. The reagents in the tables are sorted in ascending aspiration order. Unless otherwise stated, the oxidising reagent was withdrawn first, followed by the $[Ru(bipy)_3]^{3+}$ generator (when utilised), followed by the sample, and then followed by an enhancer (when utilised). The chemiluminescence signal of voltage (mV) over data acquisition time (s) was imported into Origin® version 9.0 (Northampton, MA, USA) for data analysis. Baseline subtraction using a constant value of the minimum recorded voltage was conducted before plots were constructed, in order to eliminate differences due to ambient light. The peak area and maximum peak intensity of each baseline-subtracted plot was calculated and the average and standard deviation of these values for each experiment were determined (n=3). All analyses were performed in triplicate.

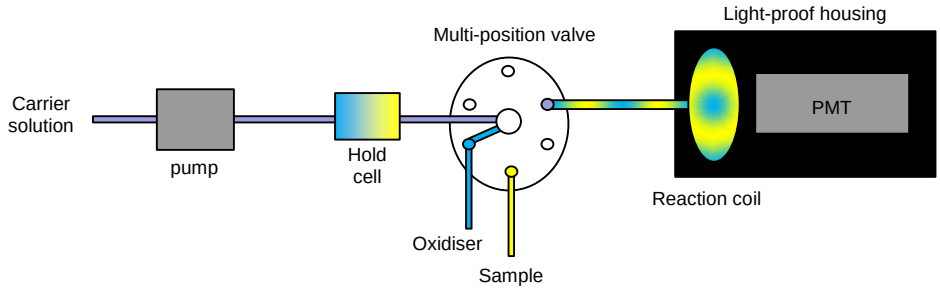

Figure 2-1. Schematic of in-house-built sequential injection analysis (SIA) manifold utilised for oxidising reagent screen.

Table 2-1. Oxidising reagents and corresponding standards, enhancers, and carrier solutions used, and the reagent volume and flow rate ranges tested during preliminary oxidising reagent screen for analysis of cyclophosphamide, 5-fluorouracil, and imatinib (1 x 10^{-3} M in deionised water) using SIA chemiluminescence. The reagent volumes and flow rates found to be optimal are given in brackets.

Oxidising Reagent		Composition	Concentration	Solvent	Volume (µL)	Flow Rate (µL)
$KMnO_4$	**Oxidiser**	$KMnO_4$	1 x 10^{-3} M	aqueous sodium hexametaphosphate (1 % m/v in 5 x 10^{-3} H_2SO_4)	10-100	1-20 (20)
	Standards	cyclophosphamide, 5-fluorouracil, imatinib	1 x 10^{-3} M	deionised water	20-200 (50)	1-20 (20)
	Enhancers	None formaldehyde HCl	- 0.1-1.0 M (0.01 M) 2 M	- deionised water	- 200	- 20 20
	Carrier	sodium hexametaphosphate	1 % (m/v)	H_2SO_4 (2 x 10^{-3}-0.1 M)	500-1300 (1000)	1-100 (100)
$KMnO_4$/ $Na_2S_2O_3$	**Oxidiser**	$KMnO_4/Na_2S_2O_3$	1.9 x 10^{-3} M/ 6 x 10^{-4} M (respectively)	deionised water	30	10-50 (20)
	Standards	cyclophosphamide, 5-fluorouracil, imatinib	1 x 10^{-3} M	deionised water	50	10
	Enhancers	none	-	-	-	-
	Carrier	sodium hexametaphosphate	1 % (m/v)	H_2SO_4 (5 x 10^{-3} M)	1000	50-100 (100)
$[Ru(bipy)_3]Cl_2$	**Oxidiser**	$[Ru(bipy)_3]Cl_2$	1 x 10^{-3} M	H_2SO_4 (0.1 M)	50	50
	Standards	cyclophosphamide, 5-fluorouracil, imatinib	1 x 10^{-3} M	Deionised water	50	50
	Enhancers	none	-	-	50	50
	$[Ru(bipy)_3]^{3+}$ Generator	PbO_2 (off-line) $KMnO_4$ (on-line) $Ce(SO_4)_2$ (on-line)	0.1 g/ 20 mL 1 x 10^{-3} M 1 x 10^{-3} M	- H_2SO_4 (0.05 M) H_2SO_4 (0.05 M)	- 50 20-70	- 10 5-30
	Carrier	H_2SO_4	0.1 M	deionised water	400-1000	50-120

$[Ru(bipy)_3]ClO_4$	**Oxidiser**	$[Ru(bipy)_3]ClO_4$	1 x 10^{-3} M	$HClO_4$ (0.05 M in acetonitrile)	50	50
	Standards	cyclophosphamide, 5-fluorouracil, imatinib	1 x 10^{-3} M	deionised water	50	50
	Enhancers	none	-	-	-	-
	$[Ru(bipy)_3]^{3+}$ Generator	PbO_2 (off-line)	0.1 g/ 20 mL	-	-	-
	Carrier	$HClO_4$	0.05 M	acetonitrile	1000	50
Mn(IV)	**Oxidiser**	Mn(IV)	5 x 10^{-4} M	deionised water	50	10
	Standards	cyclophosphamide, 5-fluorouracil, imatinib	1 x 10^{-3} M	deionised water	50	10
	Enhancers	none ethanol	- 100 %	- -	- 50	- 10
	Carrier	H_3PO_4	3 M	deionised water	1000	100
$Ce(SO_4)_2$	**Oxidiser**	$Ce(SO_4)_2$	1 x 10^{-4} M	H_2SO_4	10	10
	Standards	cyclophosphamide, 5-fluorouracil, imatinib	1 x 10^{-3} M	deionised water	10	10
	Enhancers	none	-	-	-	-
	Carrier	H_2SO_4	0.1 M	deionised water	1000	100

Table 2-2. $[Ru(bipy)_3]^{3+}$ generation methods and corresponding carrier solutions and reagent volume and flow rate ranges tested

$[Ru(bipy)_3]^{3+}$ Generation Method		**Composition**	**Concentration (M)**	**Volume (µL)**	**Flow Rate (µL/s)**
PbO_2	**Oxidiser**	$[Ru(bipy)_3]Cl_2$	1 x 10^{-3}	50-100	15-50
	Standard	5-FU	1 x 10^{-3}	50-100	1-50
	Carrier	H_2SO_4	0.05	300-1000	50
$KMnO_4$	**Oxidiser**	$[Ru(bipy)_3]Cl_2$	1 x 10^{-4}	50	10
	$[Ru(bipy)_3]^{3+}$ Generator	$KMnO_4$	1 x 10^{-3}	50	10
	Standard	5-FU	1 x 10^{-3}	50	10
	Carrier	H_2SO_4	0.05	1000	100
$Ce(SO_4)_2$	**Oxidiser**	$[Ru(bipy)_3]Cl_2$	1-1.5 x 10^{-3}	20-70	5-30
	$[Ru(bipy)_3]^{3+}$ Generator	$Ce(SO_4)_2$	1-1.5 x 10^{-3}	20-70	5-30
	Standard	5-FU	1 x 10^{-3}	20-70	5-30
	Carrier	H_2SO_4	0.4	400	50-120

Stopped-Flow Chemiluminescence:

Stopped flow experiments were conducted using an in-house-built stopped-flow manifold consisting of a syringe pump (Chemyx, Stafford, TX, USA), two 10 mL plastic syringes (Livingstone International Pty Ltd, Rosebery, NSW, Australia), and a 29 mm diameter photomultiplier tube (PMT) (Electron Tubes Limited, 9828SB, Uxbridge, England) encased in a light-proof housing. The instrument set-up is shown in Figure 2-2. The PMT was run at 800 V using a modular power supply (Electron Tubes Limited, PS1800/12F, Uxbridge, England). A custom-made glass spiral coil (I.D. 2mm) with an internal volume of 400 µL was used as the reaction cell adjacent to the PMT inside the light-proof housing. PTFE tubing (0.02 mm I.D.) (Global FIA, Fox Island, WA, USA) was used for connections between reagents, the valve, and the pump. The instrument was controlled using software written in National Instruments LabVIEW® version 8.2 (Austin, TX, USA) by Bogdanovic *et al.* [180]. Prior to each analysis the reagents were loaded into the syringe using the software with a 1000 µL infusion volume for each. The pump then simultaneously delivered 75 µL from each syringe into tubing that met at a T-piece before entering the reaction coil. The data acquisition was commenced simultaneously with reagent injection and continued for 60 seconds to ensure detection of entire chemiluminescence reaction. The flow rate from each syringe was 250 µL/s. The raw chemiluminescence signal of voltage (mV) over data acquisition time (s) was imported into Origin® version 9.0 (Northampton, MA, USA). Baseline subtraction using a constant value of the minimum recorded voltage was conducted before plots were constructed. The peak area and maximum peak intensity of each baseline-subtracted plot was calculated and the average and standard deviation of these values for each experiment were determined (n=3). The combinations of reagents delivered from each syringe are given in Table 2-3. Blanks in which no cytotoxic sample was added to each sample medium were also analysed for each combination. All analyses were performed in triplicate.

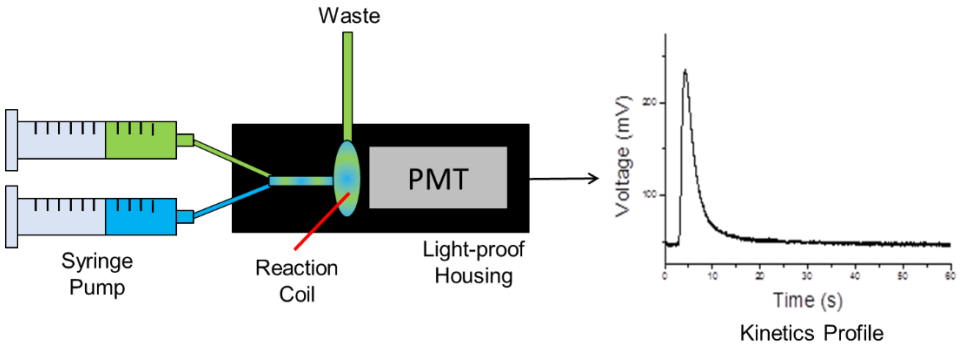

Figure 2-2. Schematic of stopped-flow chemiluminescence manifold used in kinetics experiments

Table 2-3 Combinations of reagents and analytes analysed via stopped-flow chemiluminescence, where analyte refers to individual solutions of cyclophosphamide, 5-fluorouracil (1 x 10^{-3} M), or 1 x 10^{-4} M imatinib unless otherwise stated

Experiment	Syringe 1	Syringe 2
Effect of $Ce(SO_4)_2$ concentration with pre-mixed oxidising reagents	Analyte in deionised water	1:1 (v/v) $Ru(bipy)_3Cl_2$ (1 x 10^{-3} M in deionised water)/ $Ce(SO_4)_2$ (0.5 x 10^{-4} M - 2 x 10^{-3} M in 0.4 M H_2SO_4)
Effect of $Ce(SO_4)_2$ concentration with analyte prepared in $Ru(bipy)_3Cl_2$	Analyte in $Ru(bipy)_3Cl_2$ (1 x 10^{-3} M in deionised water)	$Ce(SO_4)_2$ (0.5 x 10^{-4} M - 1 x 10^{-3} M in 0.4 M H_2SO_4)
Effect of $Ru(bipy)_3Cl_2$ concentration with analyte prepared in $Ru(bipy)_3Cl_2$	Analyte in $Ru(bipy)_3Cl_2$ (0.5 x 10^{-4} - 2 x 10^{-3} M in deionised water)	$Ce(SO_4)_2$ (1 x 10^{-3} M in 0.4 M H_2SO_4)
Effect of analyte concentration with analyte prepared in $Ru(bipy)_3Cl_2$	Analyte (0.5 x 10^{-4} - 1 x 10^{-3} M) in $Ru(bipy)_3Cl_2$ (1 x 10^{-3} M in deionised water)	$Ce(SO_4)_2$ (1 x 10^{-3} M in 0.4 M H_2SO_4)
Effect of analyte concentration when analyte prepared in $Ce(SO_4)_2$	Analyte (1 x 10^{-5} - 1 x 10^{-3} M) in $Ce(SO_4)_2$ (1 x 10^{-3} M in 0.4 M H_2SO_4)	$Ru(bipy)_3Cl_2$ (1.5 x 10^{-3} M in deionised water)

2.3 Results and Discussion

2.3.1 Preliminary Experiments

$KMnO_4$, $Ru(bipy)_3Cl_2$, $Ru(bipy)_3ClO_4$, Mn(IV), and $Ce(SO_4)_2$ were tested individually using SIA for their ability to produce chemiluminescence upon reaction with each of cyclophosphamide, 5-fluorouracil, and imatinib. For each oxidising reagent various factors were manipulated, including reagent flow rates and volumes, solvents, concentrations, and addition of enhancers.

2.3.1.1 Permanganate Chemiluminescence

Prior research has demonstrated the chemiluminescence detection of 5-fluorouracil using 5 x 10^{-4} M $KMnO_4$ in an FIA system [1, 127]. In that work, HCl (2 M) and formaldehyde (2.5 %) were used as sensitisers [1, 127], with the analyte and formaldehyde solutions being pre-mixed at a Y-piece prior to injection into a mixture of $KMnO_4$ and the HCl. There has been no report of the use of $KMnO_4$ chemiluminescence for the determination of imatinib or cyclophosphamide. Solutions of cyclophosphamide, 5-fluorouracil, and imatinib (1 x 10^{-3} M) were tested, with the experimental conditions given in Table 2-4. The initial SIA sequence comprised aspirating the analyte and formaldehyde first, followed by the HCl and $KMnO_4$, before delivery to the reaction coil. This order was chosen to best emmulate reagent conditions used in the FIA instrument used by Sun *et al.* [1, 127]. The resulting net chemiluminescence peak heights are given in Figure 2-3. 5-fluorouracil and imatinib produced chemiluminescence with average net peak heights of 1.93 ± 0.7 mV and 4.34 ± 0.6 mV, respectively. Cylophosphamide did not produce a signal larger than the blank. Despite signals being obtained for 5-fluorouracill, they were much less intense than those obtained by Sun *et al.* [1,

127]. This discrepancy was most likely the result of differences in instrumental and reagent conditions. Specifically, Sun and co-workers used FIA in which the delay time between mixing of the reagents and detection in the reaction cell would be shorter than that in the SIA used here. The chemiluminescence reaction may be occurring too quickly to be detected by SIA compared with FIA. Also, in the method of Sun *et al.* [1] the analyte and formaldehyde were merged at a Y-piece separately prior to a small volume of this mixture being injected into a stream of $KMnO_4$ and HCl. The $KMnO_4$ and HCl were therefore present in a large excess with respect to the analyte and formaldehyde. In the SIA experiments, however, the formaldehyde, HCl, and $KMnO_4$ were present at approximately equal volumes. Various volumes of each reagent were trialled in the SIA instrument (Appendix A), however no increase in chemiluminescence peak area was obtained.

The pre-mixing of the $KMnO_4$ with the HCl and the 5-fluorouracil with the formaldehyde was most likely also critical. $KMnO_4$ is known to react strongly with HCl to form manganese dioxide (MnO_2), which then reacts further to form manganese chloride ($MnCl_2$) in the presence of excess acid [182]. If the $KMnO_4$ was unable to react completely with the acid in the SIA instrument the second reaction to $MnCl_2$ may have been unable to occur. MnO_2 is known to form insoluble oxides, which cause flocculation and prevent propagation of the chemiluminescence emission to the detector [125]. This could have resulted in the low chemiluminescence signals detected. The mechanism of formaldehyde enhancement is still unknown [123]. In the detection of 5-fluorouracil Sun *et al.* [1] suggested the formaldehyde acted to increase the rate of generation of singlet-state oxygen, despite there being strong evidence of permanganate chemiluminescence occurring through electronically excited Mn(II) [123, 125]. Nevertheless the pre-mixing of formaldehyde with the 5-fluorouracil may have been ciritical in obtaining a chemiluminescence response.

Table 2-4. SIA reagents, volumes, and flow rates used for analysis of cyclophosphamide, 5-fluororuacil, and imatinib (1 x 10^{-3} M) using $KMnO_4$ and the oxidising reagent and formaldehyde and HCl as enhancers

Reagent	Composition	Volume (µL)	Flow Rate (µL/s)
Analyte	1 x 10^{-3} M cyclophosphamide, 5-fluorouracil, imatinib in deionised water	50	20
Enhancer 1	Formaldehyde (0.1 M in deionised water)	200	20
Enhancer 2	HCl (2 M)	200	20
Oxidising Reagent	1 x 10^{-3} M $KMnO_4$ in deionised water	200	20
Carrier Solution	Deionised water	1000	100

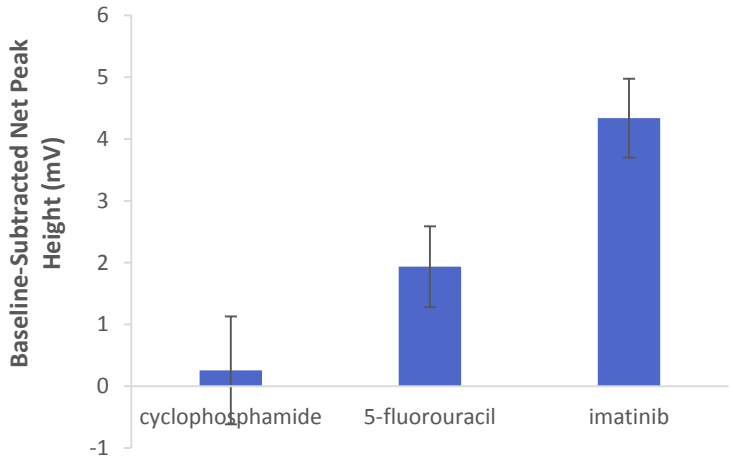

Figure 2-3. Baseline-subtracted average peak height (n=3) of SIA chemiluminescence signals obtained from cyclophosphamide, 5-fluorouracil, and imatinib (1 x 10^{-3} M in deionised water) using $KMnO_4$ (1 x 10^{-3} M in sodium hexametaphosphate (1 % m/v in H_2SO_4) as the oxidising reagent and HCl (2 M) and formaldehyde (0.01 M) as enhancers. Error bars = ± 1 standard deviation.

As just discussed, HCl and $KMnO_4$ are known to undergo side-reactions, which can inhibit the chemiluminescence reaction [180]. In order to test this the HCl stream was removed and each cytotoxic was subsequently analysed using only formaldehyde as the enhancer. The conditions used are given in Table 2-8. More intense chemiluminescence (3.58 ± 0.3 mV) was obtained for 5-fluorouracil compared to when using HCl. Both cyclophosphamide and imatinib both did not produce signals beyond the blank. The loss of the imatinib signal upon removal of the HCl stream indicates that the HCl was critical in eliciting chemiluminescence from imatinib. Acidic conditions are known to stabilise the Mn(II)* emitter in permanganate chemiluminescence, hence increasing chemiluminescence emission [125]. The presence of strong acid also prevents flocculation of Mn(IV) formed during the reaction of Mn(II) with residual Mn(VII), hence increasing the likelihood of emission and minimising interferences for light transfer to the detector [125]. Removal of the HCl stream would have therefore decreased the chemiluminescence detected.

Table 2-5. SIA reagents, volumes, and flow rates used for analysis of cyclophosphamide, 5-fluororuacil, and imatinib (1 x 10^{-3} M) using $KMnO_4$ and the oxidising reagent and formaldehyde of various concentrations as the enhancer

Reagent	Composition	Volume (µL)	Flow Rate (µL/s)
Analyte	1 x 10^{-3} M cyclophosphamide, 5-fluorouracil, imatinib in deionised water	50	20
Enhancer	Formaldehyde (0.1 M in deionised water)	200	20
Oxidising Reagent	1 x 10^{-3} M $KMnO_4$ in deionised water	200	20
Carrier Solution	Deionised water	1000	100

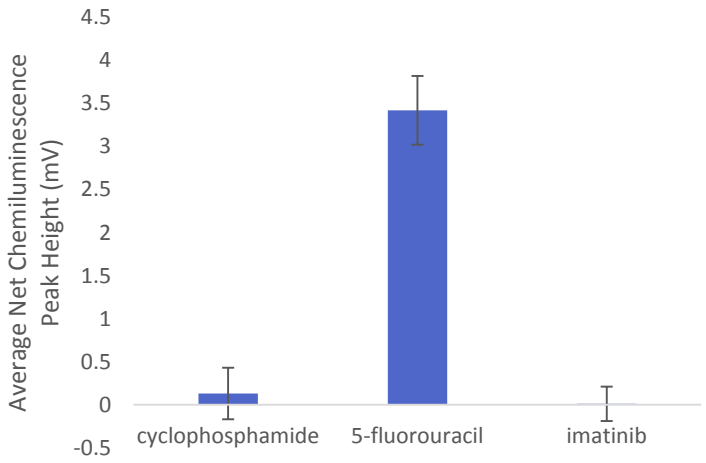

Figure 2-4. Baseline-subtracted average net peak height (n=3) of SIA chemiluminescence signals obtained from cyclophosphamide, 5-fluorouracil, and imatinib (1 x 10^{-3} M in deionised water) using $KMnO_4$ (1 x 10^{-3} M in sodium hexametaphosphate (1 % m/v in H_2SO_4) as the oxidising reagent and formaldehyde (0.01 M) as enhancers. Error bars = ± 1 standard deviation.

The most commonly used enhancer of $KMnO_4$ chemiluminescence is sodium hexametaphosphate [123, 125]. This is typically prepared in H_2SO_4 [123]. Experiments in which this enhancer was used rather than formaldehyde were therefore conducted. The experimental conditions are detailed in Table 2-6. The resulting net chemiluminescence peak heights are given in Figure 2-5. Weak chemiluminescence emission with average peak height of 7.32 ± 0.2 mV was observed for 5-fluorouracil. Imatinib and cyclophosphamide did not yield a response larger than the blank. Manipulation of analyte and oxidising reagent volumes did not improve the emission response from 5-fluorouracil (see Appendix B). This was in contrast to the use of formaldehyde and HCl as sensitisers (Figure 2-3), in which both 5-fluorouracil and imatinib produced chemiluminescence signals. Permanganate chemiluminescence is known to occur through the Mn(II)* emitter when using either formaldehyde or hexametaphosphate as the enhancer [123, 125, 133, 183]. The signals from 5-fluorouracil and inability to detect cyclophosphamide using both systems was therefore to be expected. Imatinib, however, produced chemiluminescence using the formaldehyde/HCl system, but not the hexametaphosphate/H_2SO_4 system. As the emitting species would be the same this suggested that the change in acid may be the cause. The type of acid used has been shown to be highly influential in obtaining chemiluminescence from particular analytes [1, 123]. The reaction of permanganate with imatinib may therefore be more favourable in the presence of HCl than H_2SO_4.

Table 2-6. SIA reagents, volumes, and flow rates used for first test of $KMnO_4$ as an oxidising reagent for cyclophosphamide, 5-fluororuacil, and imatinib detection

Reagent	Composition	Volume (µL)	Flow Rate (µL/s)
Analyte	1 x 10^{-3} M cyclophosphamide, 5-fluorouracil, imatinib in deionised water	50	20
Enhancer	Sodium hexametaphosphate (1 % m/v in 5 x 10^{-3} M H_2SO_4)	100	20
Oxidising Reagent	1 x 10^{-3} M $KMnO_4$ in sodium hexametaphosphate (1 % m/v in 5 x 10^{-3} M H_2SO_4)	200	20
Carrier Solution	Sodium hexametaphosphate (1 % m/v in 5 x 10^{-3} M H_2SO_4)	1000	100

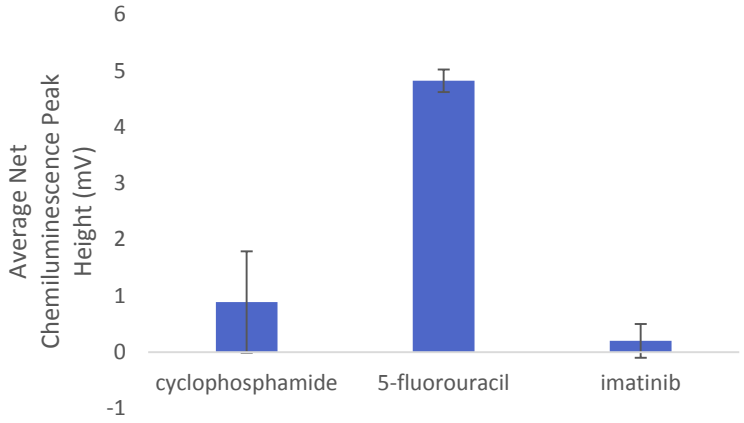

Figure 2-5. Average net peak height (n=3) of SIA chemiluminescence signals obtained from cyclophosphamide, 5-fluorouracil, and imatinib (1 x 10^{-3} M in deionised water) using $KMnO_4$ (1 x 10^{-3} M in sodium hexametaphosphate) as the oxidising reagent and sodium hexametaphosphate (1 x 10^{-3} M in 1 % m/v in H_2SO_4) as the enhancer. Error bars = ± 1 standard deviation.

It is known that pH can significantly affect the emission intensity from permanganate chemiluminescence, with the optimum acid concentration varying depending on the analyte [123]. Consequently, a range of H_2SO_4 concentrations ranging from 1x10^{-4} M to 0.1 M (final pH between 5.93 and 1.38) in 1% (v/v) sodium hexametaphosphate were tested in the oxidiser, enhancer, and carrier streams simultaneously, as described in Table 2-7. Cyclophosphamide and imatinib again produced signals no more intense than the blank. As shown in Figure 2-6, chemiluminescence peak height from 5-fluorouracil increased with increasing H_2SO_4 concentration up to 0.01 M, beyond which the signal plateaued. This is a similar trend to those previously observed for permanganate chemiluminescence intensity when increasing the acid concentration [184, 185]. This suggested that the H_2SO_4 could be participating in the reaction, either with the analyte or the $KMnO_4$, with increasing concentrations allowing this reaction to occur more readily. Above a certain concentration the permanganate is fully consumed, hence limiting the reaction and preventing further increase in chemiluminescence with increasing acid concentration. A H_2SO_4 concentration of 0.01 M was point at which the chemiluminescence began to plataue, and hence was selected for subsequent analyses.

Table 2-7. SIA reagents, volumes, and flow rates used for chemiluminescence analysis of cyclophosphamide, 5-fluororuacil, and imatinib (1 x 10^{-3} M in deionised water) using $KMnO_4$ as the oxidising reagent, and varying the concentration of H_2SO_4 in the enhancer, carrier, and oxidising reagent solutions.

Reagent	Composition	Volume (µL)	Flow Rate (µL/s)
Enhancer	Sodium hexametaphosphate (1 % m/v in H_2SO_4 (1 x 10^{-4} M – 0.1 M)	100	20
Analyte	1 x 10^{-3} M cyclophosphamide, 5-fluorouracil, imatinib in deionised water	50	20
Oxidising Reagent	1 x 10^{-3} M $KMnO_4$ in sodium hexametaphosphate (1 % m/v in H_2SO_4 (1 x 10^{-4} M – 0.1 M)	200	20
Carrier Solution	Sodium hexametaphosphate (1 % m/v in H_2SO_4 (1 x 10^{-4} M – 0.1 M)	1000	100

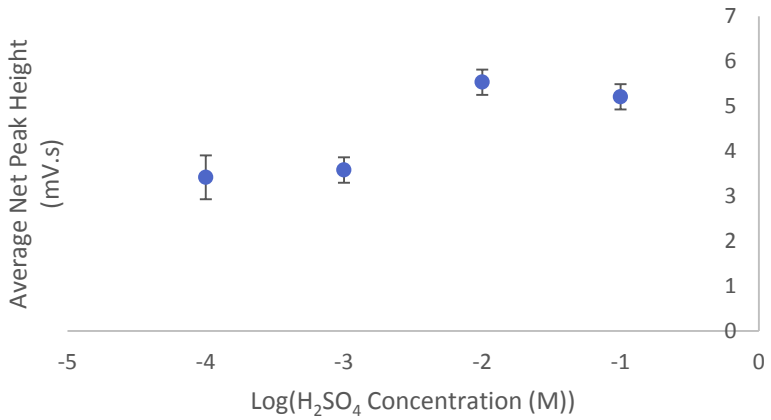

Figure 2-6. Baseline-subtracted average peak height (n=3) of SIA chemiluminescence signals obtained from 5-fluorouracil (1 x 10^{-3} M in deionised water) using $KMnO_4$ (1 x 10^{-3} M in sodium hexametaphosphate (1 % m/v in H_2SO_4) as the oxidising reagent and varying the H_2SO_4 concentration (1 x 10^{-4} M – 0.1 M) in the sodium hexametaphosphate solution used for the oxidiser, enhancer, and carrier solutions. Error bars = ± 1 standard deviation. H_2SO_4 concentration is on a $\log_{10}$ scale.

The use of formaldehyde together with sodium hexametaphosphate has also shown analytical utility on some occasions [186, 187]. Consequently experiments in which formaldehyde was introduced on-line as an enhancer, while the carrier solution and $KMnO_4$ solutions still contained sodium hexametaphoshate were conducted. This was done using a range of formaldehyde concentrations between 0.1 M and 1 M. The conditions used are given in Table 2-8, and the resulting net chemiluminescence peak areas are given in Figure 2-7. The chemiluminescence peak height increased with increasing formaldehyde concentration up to 0.4 M, before gradually decreasing. Increasing formaldehyde concentration most likely increased the reaction rate, resulting in increased chemiluminescence. Beyond a certain formaldehyde concentration, however, the chemiluminescence emission may occur too quickly to be detected, resulting in an apparent decrease in chemiluminescence intensity. As a formaldehyde concentration of 0.4 M resulted in the most intense chemiluminescence this concentration was selected for subsequent analyses.

Table 2-8. SIA reagents, volumes, and flow rates used for analysis of cyclophosphamide, 5-fluororuacil, and imatinib (1 x 10^{-3} M) using $KMnO_4$ and the oxidising reagent and formaldehyde of various concentrations as the enhancer

Reagent	Composition	Volume (µL)	Flow Rate (µL/s)
Enhancer	Formaldehyde (0.1-1.0 M in deionised water)	200	20
Analyte	1 x 10^{-3} M cyclophosphamide, 5-fluorouracil, imatinib in deionised water	50	20
Oxidising Reagent	1 x 10^{-3} M $KMnO_4$ in sodium hexametaphosphate (1 % m/v in 5 x 10^{-3} M H_2SO_4)	200	20
Carrier Solution	Sodium hexametaphosphate (1 % m/v in 5 x 10^{-3} M H_2SO_4)	1000	100

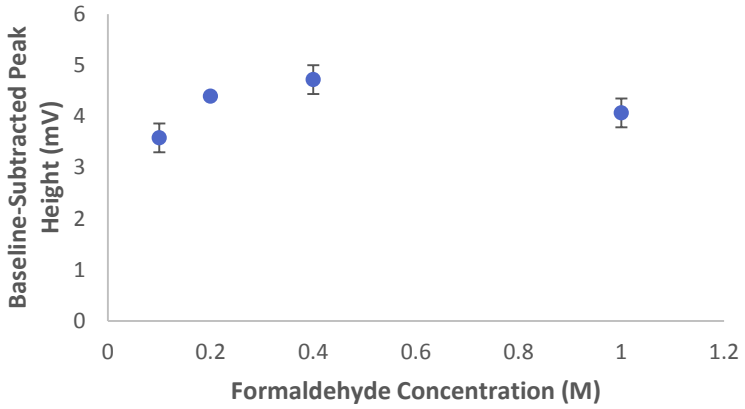

Figure 2-7. Baseline-subtracted average peak height (n=3) of SIA chemiluminescence signals obtained from 5-fluorouracil (1 x 10^{-3} M in deionised water) using $KMnO_4$ (1 x 10^{-3} M in sodium hexametaphosphate (1 % m/v in H_2SO_4) as the oxidising reagent and formaldehyde of various concentrations (0.1-1 M). Error bars = ± 1 standard deviation.

Francis *et al.* [134] demonstrated that the addition of a small volume of sodium thiosulfate to the $KMnO_4$ reagent greatly enhanced chemiluminescence emission during analysis of a range of analytes, due to increased formation of Mn(II)*. Consequently the addition of thiosulfate was trialled for each cytotoxic in an attempt to increase the chemiluminescence signals. The experimental conditions used are detailed in Table 2-9. Resulting chemiluminescence peak intensities are given in Figure 2-8. The addition of thiosulphate resulted in a signal larger than that of the blank from imatinib, while cyclophosphamide and 5-fluorouracil produced signals lower than the blank. This was in contrast to results obtained when using only $KMnO_4$ in hexametaphosphate, in which only 5-fluorouracil produced a signal. The addition of thiosulphate does not change the emitting species, but rather increases formation of Mn(II) [124, 125]. It would therefore be expected that analytes able to undergo reaction with $KMnO_4$ would still undergo this reaction in the presence of $Na_2S_2O_3$. It is possible that in the case of 5-fluorouracil and cyclophosphamide the addition of the sodium thiosulphate enhancer resulted in a chemiluminescence reaction that was too fast to be detected in the SIA system, resulting in the production of a signal lower than that of the blank. Sample and oxidiser volume and withdrawal rates, as well as the flow rate to the detector were therefore manipulated in

an attempt to improve these signals. No increase in imatinib signal, however, was obtained. Similarly, chemiluminescence signals from 5-fluorouracil and cyclophosphamide could not be obtained.

Table 2-9. SIA reagents, volumes, and flow rates used for analysis of cyclophosphamide, 5-fluorouracil, and imatinib (1 x 10^{-3} M) using $KMnO_4/Na_2S_2O_3$ as the oxidising reagent

Reagent	Composition	Volume (µL)	Flow Rate (µL/s)
Analyte	1 x 10^{-3} M cyclophosphamide, 5-fluorouracil, imatinib in deionised water	50	20
Oxidising Reagent	1.9 x 10^{-3} M $KMnO_4$ in sodium hexametaphosphate (1 % m/v in 5 x 10^{-3} M H_2SO_4) with 3.6 x 10^{-6} M sodium thiosulphate	200	20
Carrier Solution	Sodium hexametaphosphate (1 % m/v in 5 x 10^{-3} M H_2SO_4)	1000	100

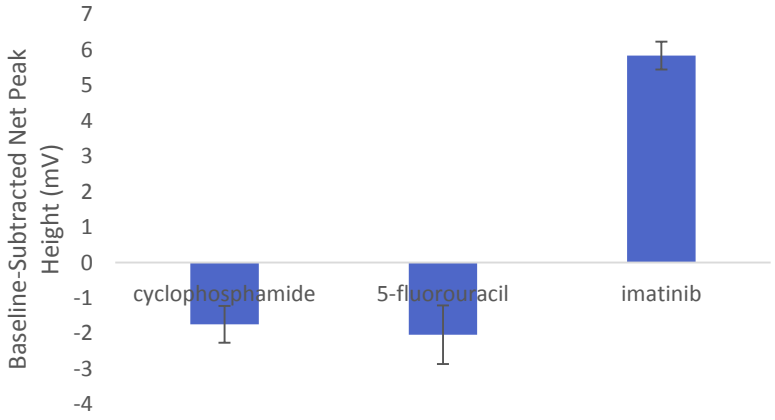

Figure 2-8. Baseline-subtracted average net peak height (n=3) of SIA chemiluminescence signals obtained from cyclophosphamide, 5-fluorouracil, and imatinib (1 x 10^{-3} M in deionised water) using 1.9 x 10^{-3} M $KMnO_4$ in sodium hexametaphosphate (1 % m/v in 5 x 10^{-3} M H_2SO_4) with 3.6 x 10^{-6} M sodium thiosulphate as the oxidising reagent. Error bars = ± 1 standard deviation.

Overall, the experimental conditions in Table 2-10 and Table 2-11 produced the highest chemiluminescence intensity for 5-fluorouracil and imatinib, respectively. Emission larger than the blank was not obtained for cyclophosphamide under any of the conditions tested. The maximum signals obtained from 5-fluorouracil and imatinb were very weak (peak heights of 5.53 ± 0.3 mV and 5.84 ± 0.4 mV for 5-fluorouracil, and imatinib, respectively) and hence would not offer any analytical utility. It was therefore decided that permanganate chemiluminescence would not be a viable detection for these cytotoxics using this SIA instrument.

Table 2-10. SIA reagents, volumes, and flow rates found to produce the most intense chemiluminescence signal from 5-fluororuacil (1 x 10^{-3} M in deionised water) using $KMnO_4/Na_2S_2O_3$ as the oxidising reagent

Reagent	Composition	Volume (µL)	Flow Rate (µL/s)
Analyte	1 x 10^{-3} M 5-fluorouracil in deionised water	50	20
Enhancer	Sodium hexametaphosphate (1 % m/v in 0.01 M H_2SO_4)	100	20
Oxidising Reagent	1 x 10^{-3} M $KMnO_4$ in sodium hexametaphosphate (1 % m/v in 5 x 10^{-3} M H_2SO_4)	200	20
Carrier Solution	Sodium hexametaphosphate (1 % m/v in 5 x 10^{-3} M H_2SO_4)	1000	100

Table 2-11. SIA reagents, volumes, and flow rates found to produce the most intense chemiluminescence signal from imatinib (1 x 10^{-3} M in deionised water) using $KMnO_4$ as the oxidising reagent

Reagent	Composition	Volume (µL)	Flow Rate (µL/s)
Analyte	1 x 10^{-3} M cyclophosphamide, 5-fluorouracil, imatinib in deionised water	50	20
Oxidising Reagent	1.9 x 10^{-3} M $KMnO_4$ in sodium hexametaphosphate (1 % m/v in 5 x 10^{-3} M H_2SO_4) with 3.6 x 10^{-6} M sodium thiosulphate	200	20
Carrier Solution	Sodium hexametaphosphate (1 % m/v in 5 x 10^{-3} M H_2SO_4)	1000	100

2.3.1.2 Manganese (IV)

Although proceeding through the same Mn(II)* emitter, Mn(IV) chemiluminescence is known to have markedly different selectivity than permanganate [125, 130, 140]. Consequently, Mn(IV) prepared using the method of Perez-Benito *et al.* [135] was tested for its potential as an oxidising reagent of cyclophosphamide, 5-fluorouracil, and imatinib. The reagent conditions used are given in Table 2-12. Ethanol (99.9 %, HPLC-grade), which has been shown to be a highly effective enhancer of Mn(IV) chemiluminescence [144], was used as an enhancer. The resulting average net chemiluminescence peak areas are given in Figure 2-9. Imatinib was found to produce chemiluminescence of greater intensity than that of the blank, both cyclophosphamide and 5-fluorouracil quenched the background emission. This correlated well with the results obtained when using permanganate prepared in hexametphosphate and mixed with $Na_2S_2O_3$ (Section 2.3.1.1, Figure 2-8), in which only imatinb produced a chemiluminescence signal. When $Na_2S_2O_3$ is added to $KMnO_4$ prepared in polyphosphates, as was done in Section 2.3.1.1, Mn(II) is produced, which increases the chemiluminescence emission due to increased Mn(II)* formation. In the absence of polyphosphates, as was the case in this section, colloidal Mn(IV) is formed [134, 188], however the chemiluminescence reaction still proceeds through the same Mn(II)* intermediate. It would therefore be reasonable that similar results be obtained when reacting the same analytes with either of $KMnO_4/Na_2S_2O_3$ or Mn(IV). In Section 2.3.1.1

5-fluorouracil was able to elicit a chemiluminescence response when reacted with $KMnO_4$ prepared in hexmetaphosphate. The loss of signal when using Mn(IV) in this section therefore highlights the large differences in selectivities obtained using Mn(IV) compared with permanganate, despite both reactions proceeding through the same emitter [140].

The volumes of the ethanol enhancer were then manipulated between 1 µL and 100 µL in an attempt to increase the chemiluminescence signal, with no success. As no signals from cyclophosphamide or 5-fluorouracil had been obtained, and only weak emission from imatinib was detected, it was decided that manganese-based chemiluminescence reagents would not be effective in detecting the target cytotoxics.

Table 2-12. SIA reagents, volumes, and flow rates used for analysis of cyclophosphamide, 5-fluororuacil, and imatinib (1 x 10^{-3} M in deionised water) using Mn(IV) (5 x 10^{-4} M in deionised water) as the oxidising reagent, and 3 M orthophosphoric acid as the carrier solution

Reagent	Composition	Volume (µL)	Flow Rate (µL/s)
Oxidising Reagent	Mn(IV) (5 x 10^{-4} M in deionised water)	50	10
Analyte	1 x 10^{-3} M cyclophosphamide, 5-fluorouracil, or imatinib in deionised water	50	10
Enhancer	Ethanol (99.9 %)	50	10
Carrier Solution	3 M orthophosphoric acid	1000	100

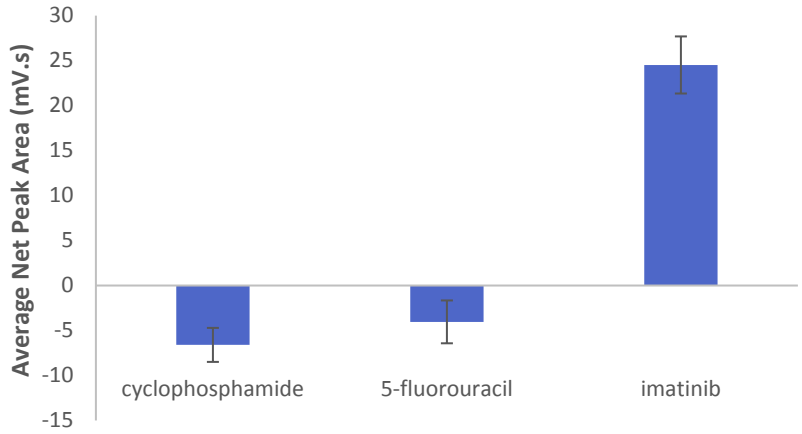

Figure 2-9. Average net peak area (n=3) obtained via SIA chemiluminescence analysis of cyclophosphamide, 5-fluorouracil, and imatinib (1 x 10^{-3} M in distilled water) using Mn(IV) (5 x 10^{-4} M in 0.1 M H_2SO_4) as the oxidising reagent and 3 M orthophosphoric acid as the carrier solution. Error bars = ± 1 standard deviation.

2.3.1.3 Cerium (IV) Sulphate

Brief investigation into the potential of $Ce(SO_4)_2$ for chemiluminescence detection of the cytotoxics was conducted. Individual solutions of cyclophosphamide, 5-fluorouracil, and imatinib were analysed using SIA with the reagent conditions in Table 2-13. The resulting net chemiluminescence peak areas are given in Figure 2-10. None of the cytotoxics produced signals significantly larger than the blank (within ± 1 standard deviation). Imatinib was found to completely quench the background emission

(Figure 2-11), which may be due to absorption of the emitted light. $Ce(SO_4)_2$ produces chemiluminescence with an emission profile with maximum between 300 and 450 nm. This overlaps closely with the absorption profile of imatinib with peaks at 230-238 nm and 268-274 nm, and an additional band being observed at 380 to 440 nm at pH levels below 2 [189]. It was therefore decided that $Ce(SO_4)_2$ would not be an effective oxidising reagent for use in detecting these cytotoxics.

Table 2-13. SIA reagents, volumes, and flow rates used for analysis of cyclophosphamide, 5-fluororuacil, and imatinib (1 x 10^{-3} M in deionised water) using $Ce(SO_4)_2$ (1 x 10^{-4} M in 0.1 M H_2SO_4) as the oxidising reagent and 0.1 M H_2SO_4 as the carrier solution.

Reagent	Composition	Volume (µL)	Flow Rate (µL/s)
Analyte	1 x 10^{-3} M cyclophosphamide, 5-fluorouracil, or imatinib in deionised water	50	10
Oxidising Reagent	1 x 10^{-4} M $Ce(SO_4)_2$ in 0.1 M H_2SO_4	50	10
Carrier Solution	0.1 M H_2SO_4	1000	100

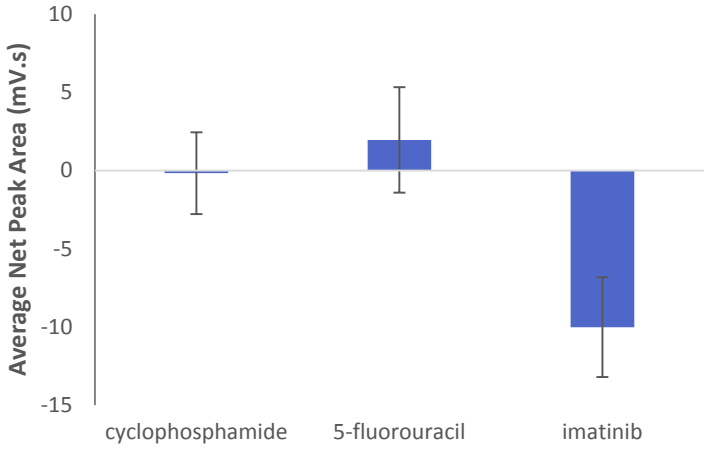

Figure 2-10. Average net peak area of SIA chemiluminescence signals obtained from cyclophosphamide, 5-fluorouracil, and imatinib (1 x 10^{-3} M in deionised water) using $Ce(SO_4)_2$ (1 x 10^{-4} M in 0.1 M H_2SO_4) as the oxidising reagent and 0.1 M H_2SO_4 as the carrier solution. Error bars = ± 1 standard deviation.

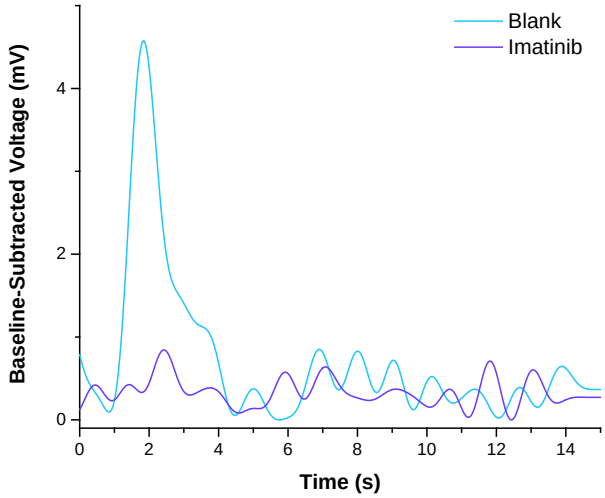

Figure 2-11. Baseline-subtracted SIA-chemiluminescence signals from analysis of imatinib (1x10^{-3} M in distilled water) using $Ce(SO_4)_2$ (1 x 10^{-4} M in 0.1 M H_2SO_4) as the oxidising reagent and 0.1 M H_2SO_4 as the carrier solution.

2.3.1.4 Tris-2,2'-bipyridyl ruthenium (II) chloride

Tris-2,2'-bipyridyl ruthenium (II) chloride ($Ru(bipy)_3Cl_2$) is known to elicit intense chemiluminescence upon reaction with amine functionalities [122]. The amine groups in cyclophosphamide, 5-fluorouracil, and imatinib therefore have the potential to also react with this oxidising reagent, and hence investigations using $Ru(bipy)_3Cl_2$ were conducted. There are multiple methods by which the reactive $[Ru(bipy)_3]^{3+}$ species can be formed, with the most common chemical methods being reaction with solid lead dioxide, or reaction with solutions of either $Ce(SO_4)_2$ or $KMnO_4$ [122]. These three preparation methods were therefore investigated individually for their effectiveness in eliciting a chemiluminescence response from each cytotoxic.

Preparation using PbO_2 was conducted off-line, whereas preparation using $Ce(SO_4)_2$ and $KMnO_4$ was conducted on-line. The experimental conditions are detailed in Table 2-14, Table 2-15, and Table 2-16. The resulting net chemiluminescence peak areas for each cytotoxic using each $[Ru(bipy)_3]^{3+}$ preparation method are given in Figure 2-12.

Table 2-14. SIA reagents, volumes, and flow rates used for initial analysis of cyclophosphamide, 5-fluororuacil, and imatinib using $Ru(bipy)_3Cl_2$ oxidised off-line with PbO_2

Reagent	Composition	Volume (µL)	Flow Rate (µL/s)
Oxidising Reagent	$Ru(bipy)_3Cl_2$ (1×10^{-3} M in 0.1 M H_2SO_4) oxidised with PbO_2 (0.1 g/20 mL)	50	15
Analyte	1×10^{-3} M cyclophosphamide, 5-fluorouracil, or imatinib in deionised water	50	15
Carrier Solution	0.05 M H_2SO_4	1000	100

Table 2-15. SIA reagents, volumes, and flow rates used for initial analysis of cyclophosphamide, 5-fluororuacil, and imatinib using $Ru(bipy)_3Cl_2$ oxidised online with $KMnO_4$

Reagent	Composition	Volume (µL)	Flow Rate (µL/s)
Oxidising Reagent 1	$Ru(bipy)_3Cl_2$ (1×10^{-3} M in 0.1 M H_2SO_4)	50	15
Oxidising Reagent 2	$KMnO_4$ (1×10^{-3} M in 0.05 M H_2SO_4)		
Analyte	1×10^{-3} M cyclophosphamide, 5-fluorouracil, or imatinib in deionised water	50	15
Carrier Solution	0.05 M H_2SO_4	1000	100

Table 2-16. SIA reagents, volumes, and flow rates used for initial analysis of cyclophosphamide, 5-fluororuacil, and imatinib using $Ru(bipy)_3Cl_2$ oxidised on-line with $Ce(SO_4)_2$

Reagent	Composition	Volume (µL)	Flow Rate (µL/s)
Oxidising Reagent 1	$Ru(bipy)_3Cl_2$ (1×10^{-3} M in 0.1 M H_2SO_4)	50	15
Oxidising Reagent 2	$Ce(SO_4)_2$ (1×10^{-3} M in 0.4 M H_2SO_4)		
Analyte	1×10^{-3} M cyclophosphamide, 5-fluorouracil, or imatinib in deionised water	50	15
Carrier Solution	0.05 M H_2SO_4	1000	100

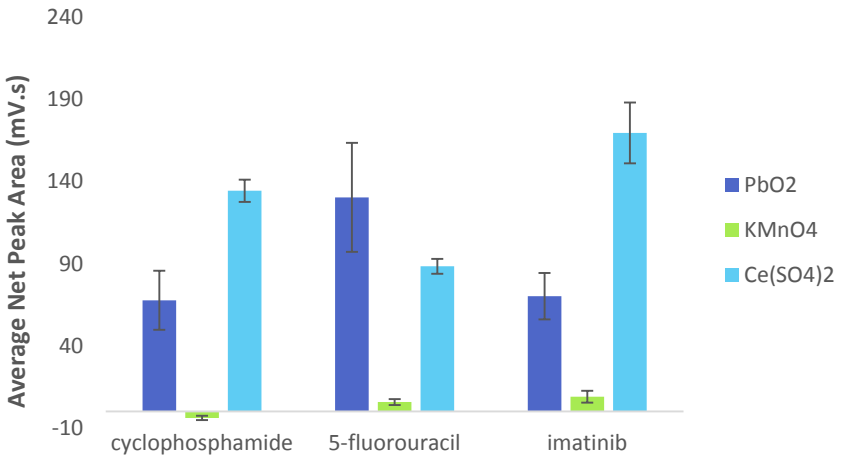

Figure 2-12. Average net peak area (n=3) obtained via SIA chemiluminescence analysis of cyclophosphamide, 5-fluorouracil, and imatinib (1 x 10^{-3} M in distilled water) using $Ru(bipy)_3Cl_2$ (1x10^{-3} M in 0.1 M H_2SO_4) oxidised using either solid PbO_2 (0.1 g/mL), $KMnO_4$ (1 x 10^{-3} M in 0.05 M H_2SO_4), or $Ce(SO_4)_2$ (1 x 10^{-3} M in 0.4 M H_2SO_4) as the oxidising reagent. Error bars = ± 1 standard deviation.

Out of the three $[Ru(bipy)_3]^{3+}$ preparation methods, $KMnO_4$ produced the least promising results. Low net peak areas of 5.72 ± 4 mV.s and 8.95 ± 1 mV.s were obtained for 5-fluorouracil and imatinib, respectively, while cyclophosphamide produced a peak area less than that of the blank. The use of either solid PbO_2 or $Ce(SO_4)_2$, however, produced peak areas significantly larger than that of the blank for each cytotoxic. The lower signals obtained using $KMnO_4$ preparation could have been a result of incomplete on-line oxidation of the $Ru(bipy)_3Cl_2$. Ce(IV) and PbO_2 have standard reduction potentials (E°) of +1.61 V and +1.69 V, respectively. These are slightly larger than that of MnO_4^- (+1.51 V), hence indicating that Ce(IV) and PbO_2 are stronger oxidising reagents [190]. $KMnO_4$ may be less able to completely oxidise the $Ru(bipy)_3Cl_2$ than Ce(IV) or PbO_2, hence resulting in lower chemiluminescence signals. This could be improved by pre-mixing the $KMnO_4$ and $Ru(bipy)_3Cl_2$, rather than using an on-line method, to increase the contact time and hence increase the likelihood of a complete reaction. It is also possible that the $KMnO_4$ was able to react with the analytes themselves, hence preventing the oxidation of $Ru(bipy)_3Cl_2$. Weaker emission via the $KMnO_4$ mechanism rather than that observed for $[Ru(bipy)_3]^{3+}$ chemiluminescence would therefore occur.

The production of a chemiluminescence signal lower than that of the blank for cyclophosphamide is unlikely to be due to light absorption. Cyclophosphamide absorbs the maximum light at 200 nm [61], whereas $[Ru(bipy)_3]^{3+}$ chemiluminescence is known to have an emission spectrum with maximum intensity at 610 nm [122]. It is therefore possible that reaction kinetics played a role in the lower chemiluminescence detected. The rate of reaction of the blank solution (deionised water) with $Ru(bipy)_3Cl_2$ may be different to that of cyclophosphamide. The maximum emission by cyclophosphamide may therefore be before or after detection by the PMT in the current instrument manifold, hence resulting in detection of a signal lower than that of the blank (see Figure 2-13).

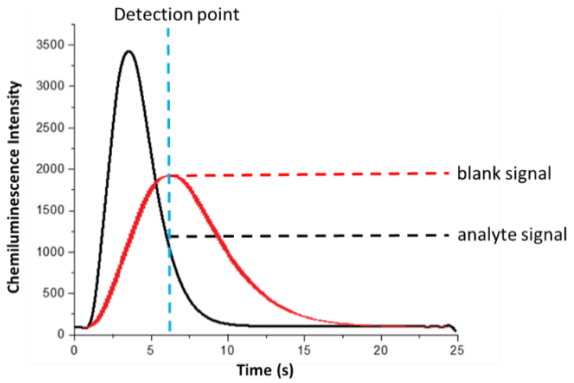

Figure 2-13. Schematic of possible differences chemiluminescence emission profiles between analytes that could result in variations in detected light intensity during chemiluminescence analysis

In general, the use of $Ce(SO_4)_2$ produced lower variation in signal, with percentage relative standard deviation (%RSD) (n=3) of peak area being 6.7, 4.6, and 18 % for cyclophosphamide, 5-fluorouracil, and imatinib respectively. The %RSD (n=3) of peak area obtained when using PbO_2 for $[Ru(bipy)_3]^{3+}$ preparation, however, was 27, 25, and 20 % for cyclophosphamide, 5-fluorouracil, and imatinib, respectively. This may have indicated that the on-line mixing of $Ce(SO_4)_2$ with the $Ru(bipy)_3Cl_2$ was more reproducible than the manual mixing with PbO_2. This could be in-part due to precise control over mixing velocities in-line compared with manual mixing, as well as tighter control over the time of contact between the reagents, and the time before analysis.

2.3.1.5 Overall Comparison

When directly comparing the maximum chemiluminescence instensities obtained for each cytotoxic using each oxidising reagent (Figure 2-14), it is clear that $Ru(bipy)_3Cl_2$ prepared using either PbO_2 or $Ce(SO_4)_2$ produced the most intense chemiluminescence for each.

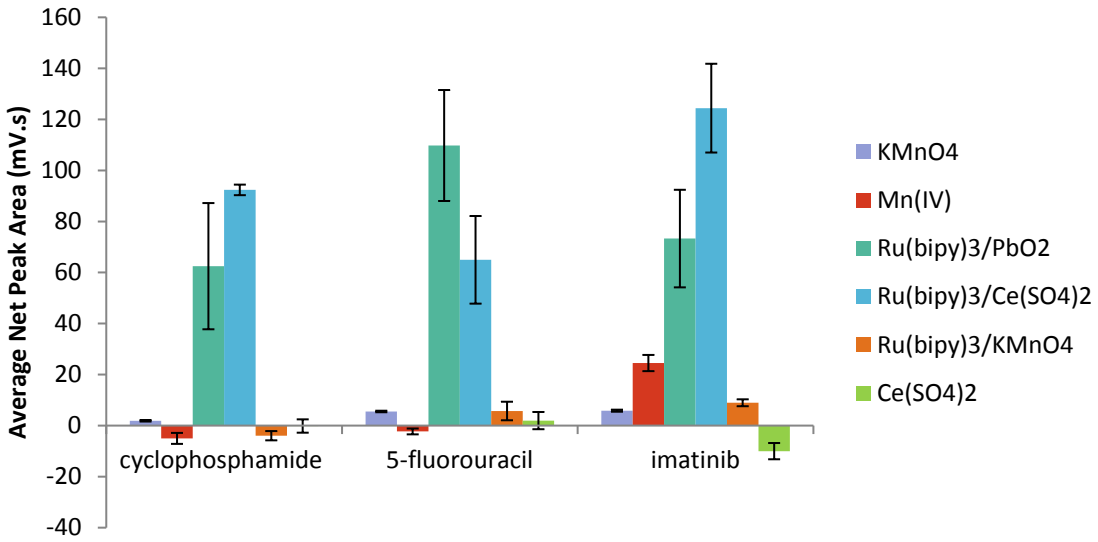

Figure 2-14. Comparison of the most intense average net chemiluminescence peak area (n=3) obtained via SIA of cyclophosphamide, 5-fluorouracil, and imatinib (1 x 10^{-3} M) using each of the different oxidising reagents tested. Error bars = ± 1 standard deviation.

2.3.2 Ce(IV)/Ru(bipy)$_3$Cl$_2$ Chemiluminescence and Kinetics

2.3.2.1 SIA-CL Method Development

$[Ru(bipy)_3]^{3+}$ prepared using $Ce(SO_4)_2$ gave the most reproducible signals for each cytotoxic when compared to preparation using solid PbO_2. This reagent system was therefore investigated more thoroughly. Firstly, the effect of analyte volume was investigated via analysis of cyclophosphamide, 5-fluorouracil, and imatinib standards using the conditions described in Table 2-17. The resulting net peak areas are given in Figure 2-15. For each cytotoxic net chemiluminescence peak area increased with increasing analyte volume up to 50 µL. Above 50 µL the net peak area remained relatively constant, within ± 1 standard deviation. This was to be expected because when using volumes larger than 50 µL the analyte would have been present in molar excess with respect to the oxidising reagent, and hence the Ru(bipy)$_3$Cl$_2$ would be the limiting reagent. The variation in net peak area was quite large when using an analyte volume of 70 µL compared to lower volumes. This may have been due to incomplete mixing of the larger volume with the relatively smaller 50 µL of oxidising reagent. An analyte volume of 50 µL was therefore chosen for subsequent analyses.

Table 2-17. SIA reagents, volumes, and flow rates used for analysis of cyclophosphamide, 5-fluororuacil, and imatinib (1 x 10^{-3} M in deionised water) using Ru(bipy)$_3$Cl$_2$ (1 x 10^{-3} M in 0.1 M H_2SO_4) oxidised online with $Ce(SO_4)_2$ (1 x 10^{-3} M in 0.4 M H_2SO_4) as the oxidising reagent, and varying the analyte volume

Reagent	Composition	Volume (µL)	Flow Rate (µL/s)
Oxidising Reagent	Ru(bipy)$_3$Cl$_2$ (1 x 10^{-3} M in deionised water)	50	10
Analyte	cyclophosphamide, 5-fluorouracil, or imatinib (1 x 10^{-3} M in deionised water)	20-70	10
Carrier Solution	$Ce(SO_4)_2$ (1 x 10^{-3} M in 0.4 M H_2SO_4)	400	100

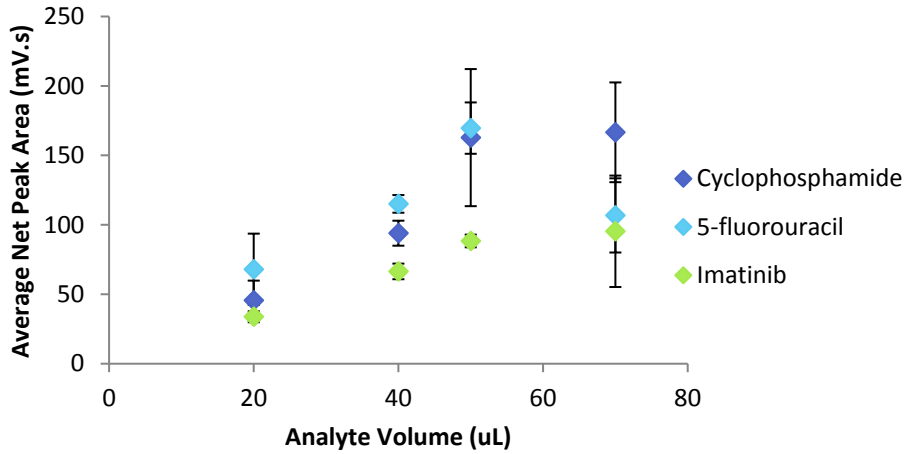

Figure 2-15. Effect of analyte volume on the average net peak area (n=3) of SIA-chemiluminescence signals obtained for individual standards of cyclophosphamide, 5-fluorouracil, and imatinib (1 x 10^{-3} M in deionised water) using $Ce(SO_4)_2$ (1 x 10^{-3} M in 0.4 M H_2SO_4) and Ru(bipy)$_3$Cl$_2$ (1.5 x 10^{-3} M in deionised water) as the oxidising reagents. Error bars = ± 1 standard deviation.

The effect of oxidising reagent volume was then investigated via analysis of cyclophosphamide, 5-fluorouracil, and imatinib standards using the conditions described in Table 2-18. The resulting net

peak areas are given in Figure 2-16. For both cyclophosphamide and imatinib increasing the oxidising reagent volume up to 50 µL increased the net peak area. When using 70 µL, however, the net peak area then decreased for all cytotoxics. This was most likely due to the same reasons as the trends when changing the analyte concentration. 50 µL was the volume at which the oxidising reagent and analytes would be present in equal molarities, hence allowing for complete reaction between the compounds. An oxidising reagent volume of 50 µL was therefore selected for subsequent analyses.

Table 2-18. SIA reagents, volumes, and flow rates used for analysis of cyclophosphamide, 5-fluororuacil, and imatinib (1 x 10^{-3} M in deionised water) using $Ru(bipy)_3Cl_2$ (1 x 10^{-3} M in 0.1 M H_2SO_4) oxidised online with $Ce(SO_4)_2$ (1 x 10^{-3} M in 0.4 M H_2SO_4) as the oxidising reagent, and varying the oxidising reagent volume

Reagent	Composition	Volume (µL)	Flow Rate (µL/s)
Oxidising Reagent	$Ru(bipy)_3Cl_2$ (1 x 10^{-3} M in deionised water)	20-70	10
Analyte	cyclophosphamide, 5-fluorouracil, or imatinib (1 x 10^{-3} M in deionised water)	50	10
Carrier Solution	$Ce(SO_4)_2$ (1 x 10^{-3} M in 0.4 M H_2SO_4)	400	100

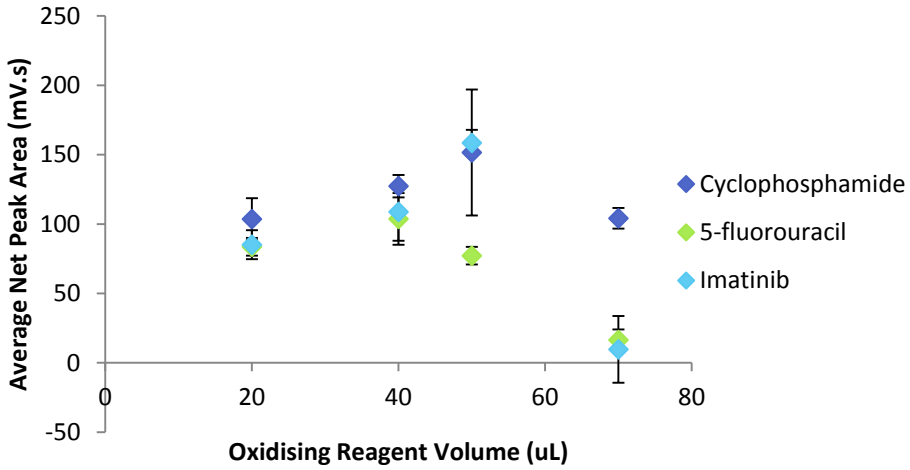

Figure 2-16 Effect of oxidiser volume on the average net peak area of SIA-chemiluminescence signals obtained for individual standards of cyclophosphamide, 5-fluorouracil, and imatinib (1 x 10^{-3} M in deionised water) using $Ce(SO_4)_2$ (1 x 10^{-3} M in 0.4 M H_2SO_4) and $Ru(bipy)_3Cl_2$ (1.5 x 10^{-3} M in deionised water) as the oxidising reagents. Error bars = ± 1 standard deviation.

The effect of the rate of withdrawal of both the oxidising reagent and analyte was then investigated simultaneously via analysis of cyclophosphamide, 5-fluorouracil, and imatinib standards using the conditions described in Table 2-19. The resulting average net peak areas are given in Figure 2-17. The net chemiluminescence peak area was found to increase with increasing sample and oxidiser aspiration rate up to 10 µL/s, before then decreasing. An aspiration rate of 10 µL/s was therefore used for all subsequent analyses.

Table 2-19. SIA reagents, volumes, and flow rates used for analysis of cyclophosphamide, 5-fluororuacil, and imatinib (1 x 10^{-3} M in deionised water) using $Ru(bipy)_3Cl_2$ (1 x 10^{-3} M in 0.1 M H_2SO_4) oxidised online with $Ce(SO_4)_2$ (1 x 10^{-3} M in 0.4 M H_2SO_4) as the oxidising reagent, and varying the analyte and oxidising reagent flow rates

Reagent	Composition	Volume (µL)	Flow Rate (µL/s)
Oxidising Reagent	$Ru(bipy)_3Cl_2$ (1 x 10^{-3} M in deionised water)	50	5-30
Analyte	cyclophosphamide, 5-fluorouracil, or imatinib (1 x 10^{-3} M in deionised water)	50	5-30
Carrier Solution	$Ce(SO_4)_2$ (1 x 10^{-3} M in 0.4 M H_2SO_4)	400	100

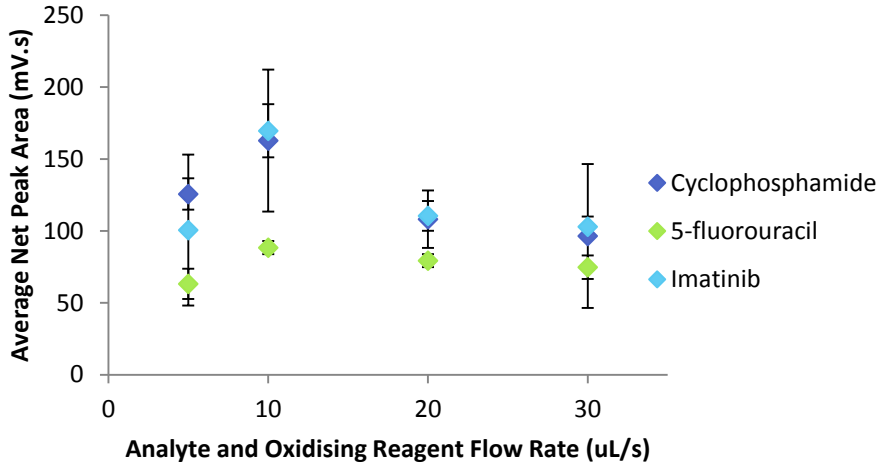

Figure 2-17 Effect of sample and oxidiser flow rate on the average net peak area (n=3) of SIA-chemiluminescence of individual standards of cyclophosphamide, 5-fluorouracil, and imatinib (1 x 10^{-3} M in deionised water) using $Ce(SO_4)_2$ (1 x 10^{-3} M in 0.4 M H_2SO_4) and $Ru(bipy)_3Cl_2$ (1.5 x 10^{-3} M in deionised water) as the oxidising reagents. Error bars = ± 1 standard deviation.

Finally, the effect of the rate at which the reagent mixture was delivered to the detector by the carrier solution was investigated via analysis of cyclophosphamide, 5-fluorouracil, and imatinib standards using the conditions described in Table 2-20. The resulting net peak areas are given in Figure 2-18. The net peak area appeared to fluctuate differently for each cytotoxic with increasing carrier flow rate up to 100 µL/s. At the highest flow rate tested (120 µL/s), however, the net peak area was below zero for all cytotoxics. This drop was most likely due to an increase in backpressure at this high flow rate, resulting in poor mixing between the reagents and formation of air pockets. This would ultimately decrease the efficiency of the chemiluminescence reaction, hence decreasing the net peak area. It was observed, however, that the shape of the chemiluminescence peak was much broader and did not return to the baseline when using the lower flow rates, as shown in an example plot comparing 100 µL/s and 50 µL/s for imatinib analysis in Figure 2-19. This may have indicated that these flow rates were too slow to allow for complete mixing of the reagents and detection of light at the time of maximum emission. A final carrier flow rate of 100 µL/s, which resulted in a desirable peak shape, was therefore chosen.

Table 2-20. SIA reagents, volumes, and flow rates used for analysis of cyclophosphamide, 5-fluororuacil, and imatinib (1 x 10^{-3} M in deionised water) using $Ru(bipy)_3Cl_2$ (1 x 10^{-3} M in 0.1 M H_2SO_4) oxidised online with $Ce(SO_4)_2$ (1 x 10^{-3} M in 0.4 M H_2SO_4) as the oxidising reagent, and varying the flow rate of the carrier solution

Reagent	Composition	Volume (µL)	Flow Rate (µL/s)
Oxidising Reagent	$Ru(bipy)_3Cl_2$ (1 x 10^{-3} M in deionised water)	50	10
Analyte	cyclophosphamide, 5-fluorouracil, or imatinib (1 x 10^{-3} M in deionised water)	50	10
Carrier Solution	$Ce(SO_4)_2$ (1 x 10^{-3} M in 0.4 M H_2SO_4)	400	50-120

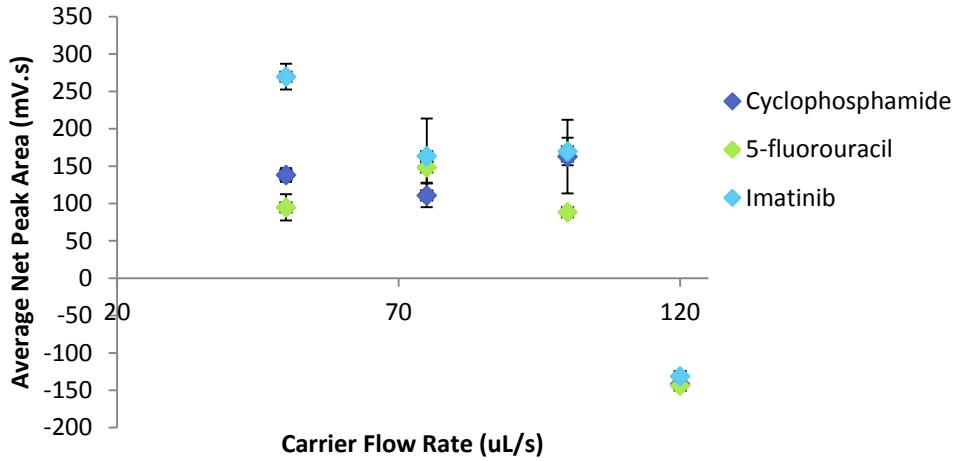

Figure 2-18 Effect of carrier flow rate on the average net peak area (n=3) obtained via SIA-chemiluminescence of individual standards of cyclophosphamide, 5-fluorouracil, and imatinib (1 x 10^{-3} M in deionised water) using $Ce(SO_4)_2$ (1 x 10^{-3} M in 0.4 M H_2SO_4) and $Ru(bipy)_3Cl_2$ (1.5 x 10^{-3} M in deionised water) as the oxidising reagents. Error bars = ± 1 standard deviation.

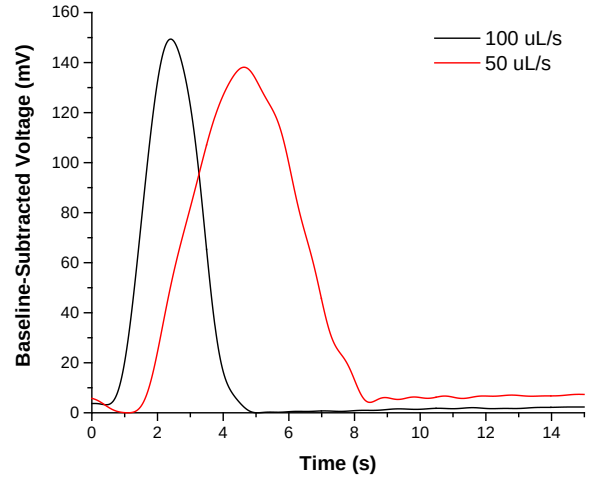

Figure 2-19. Baseline-subtracted chemiluminescence signals for imatinib (1 x 10^{-3} M in deionised water) using $Ce(SO_4)_2$ (1 x 10^{-3} M in 0.4 M H_2SO_4) and $Ru(bipy)_3Cl_2$ (1.5 x 10^{-3} M in deionised water) as the oxidising reagents, comparing two carrier solution flow rates.

The final experimental conditions found to be optimal (Table 2-21) were then used to construct calibration curves for each of the cytotoxics at concentrations between 1x10^{-4} M and 1x10^{-3} M in deionised water, as shown in Figure 2-20. These curves, however, showed no linearity. The variation between replicates was also quite high, with %RSD values for net peak area up to 60.7 %.

Table 2-21. SIA reagents, volumes, and flow rates found to be optimal for analysis of cyclophosphamide, 5-fluororuacil, and imatinib in deionised water using $Ru(bipy)_3Cl_2$ (1 x 10^{-3} M in 0.1 M H_2SO_4) oxidised online with $Ce(SO_4)_2$ (1 x 10^{-3} M in 0.4 M H_2SO_4) as the oxidising reagent

Reagent	Composition	Volume (µL)	Flow Rate (µL/s)
Oxidising Reagent	$Ru(bipy)_3Cl_2$ (1 x 10^{-3} M in deionised water)	50	10
Analyte	cyclophosphamide, 5-fluorouracil, or imatinib (1 x 10^{-4} - 1 x 10^{-3} M in deionised water)	50	10
Carrier Solution	$Ce(SO_4)_2$ (1 x 10^{-3} M in 0.4 M H_2SO_4)	400	100

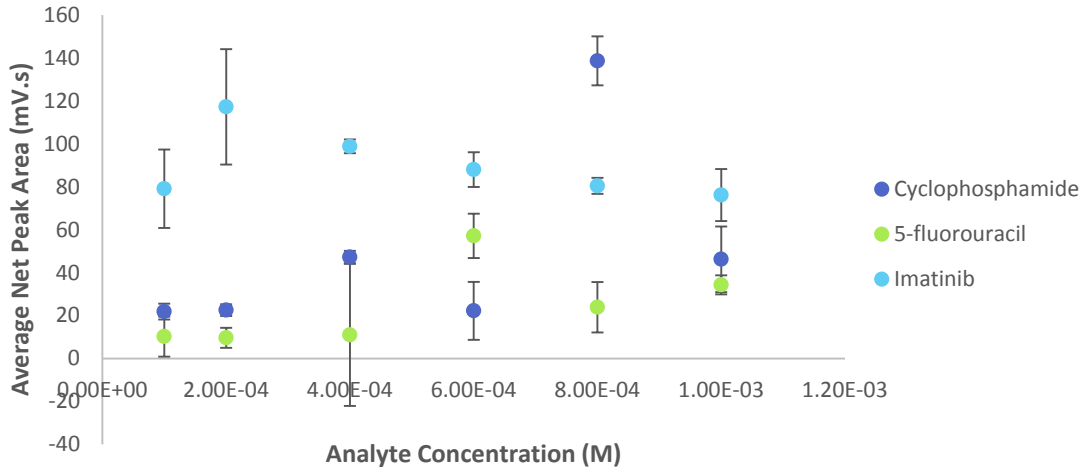

Figure 2-20. Effect of analyte concentration on the average net peak area (n=3) obtained via SIA chemiluminescence of cyclophosphamide, 5-fluorouracil, and imatinib using $Ce(SO_4)_2$ (1 x 10^{-3} M in 0.4 M H_2SO_4) and $Ru(bipy)_3Cl_2$ (1.5 x 10^{-3} M in deionised water) as the oxidising reagents. Error bars = ± 1 standard deviation.

It was suggested that mixing of the analytes with the $Ce(SO_4)_2$ may be critical in obtaining a chemiluminescence response, and hence may improve linearity. Consequently, experiments were conducted in which the $Ce(SO_4)_2$ was withdrawn prior to the sample, and then a H_2SO_4 carrier used to propel the reagent mixture to the detector. The conditions used are in Table 2-22. The use of the H_2SO_4 carrier solution resulted in more obvious relationships between net peak area and analyte concentration (Figure 2-21). For instance, the net peak area was found to increase with increasing concentration of both cyclophosphamide and 5-fluorouracil. The linearity of this response, however, was poor, with R^2 of 0.975 and 0.547 being calculated for linear regression lines for cyclophosphamide and 5-fluorouracil, respectively. Interestingly, all signals obtained from imatinib analysis were smaller than that of the blank. These signals also increased with increasing imatinib concentration, however because the blank signal was constant, this resulted in the net signal decreasing with increasing imatinib concentration. This was most likely a result of differences in reaction kinetics between the blank deionised water and the imatinib. It is possible the imatinib emission occurred at a different rate to that of the deionised water, and hence at the time of detection the imatinib emission could have appeared to be less intense than that of the blank (see Figure 2-13). It is also possible that imatinib was undergoing a reaction with the $Ce(SO_4)_2$ itself, which may have resulted in signal

quenching or consumption of the $Ce(SO_4)_2$ reagent. It was therefore clear that $Ce(SO_4)_2$ was playing a critical role in the chemiluminescence reactions of these cytotoxics.

Table 2-22. SIA reagents, volumes, and flow rates used for analysis of cyclophosphamide, 5-fluororuacil, and imatinib using $Ru(bipy)_3Cl_2$ (1 x 10^{-3} M in 0.1 M H_2SO_4) oxidised online with $Ce(SO_4)_2$ (1 x 10^{-3} M in 0.4 M H_2SO_4) as the oxidising reagent

Reagent	Composition	Volume (µL)	Flow Rate (µL/s)
Oxidising Reagent 1	$Ru(bipy)_3Cl_2$ (1.5 x 10^{-3} M in deionised water)	50	10
Oxidising Reagent 2	$Ce(SO_4)_2$ (1 x 10^{-3} M in 0.4 M H_2SO_4)	50	10
Analyte	cyclophosphamide, 5-fluorouracil, or imatinib (1 x 10^{-3} - 1 x 10^{-3} M in deionised water)	50	10
Carrier Solution	0.4 M H_2SO_4	400	100

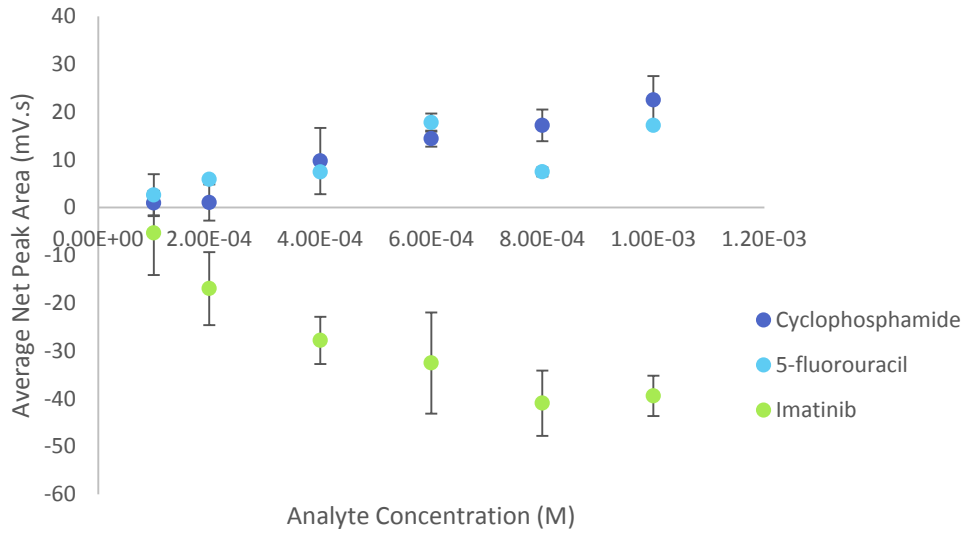

Figure 2-21. Effect of analyte concentration on the average net peak area (n=3) obtained via SIA chemiluminescence of cyclophosphamide, 5-fluorouracil, and imatinib using $Ce(SO_4)_2$ (1 x 10^{-3} M in 0.4 M H_2SO_4) and $Ru(bipy)_3Cl_2$ (1.5 x 10^{-3} M in deionised water) as the oxidising reagents and 0.04 M H_2SO_4 as the carrier solution. Error bars = ± 1 standard deviation.

In order to investigate the role each reagent was playing in the chemiluminescence reaction, the effect of the uptake order of each reagent was investigated. The order in which the $Ru(bipy)_3Cl_2$ and $Ce(SO_4)_2$ were withdrawn was swapped, as described in Table 2-23. This would result in the imatinib solution making contact with the $Ru(bipy)_3Cl_2$ first, rather than the $Ce(SO_4)_2$. Various imatinib concentrations were then analysed. The resulting plots of average net chemiluminescence peak area versus imatinib concentration are given in Figure 2-22. The net peak areas obtained were greatly different to those obtained using the previous reagent uptake order. The trend of decreasing net peak area with increasing imatinib concentration was no longer observed. The variation between replicates was also larger, with %RSD of net peak area being between 7.93 and 361 %, compared with between 10.7 and 164 % obtained previously. This therefore supported the hypothesis that the $Ce(SO_4)_2$ was playing a role in the chemiluminescence reactions observed in addition to oxidising the $Ru(bipy)_3Cl_2$. It was

therefore decided that a further investigation into the role of each oxidising reagent be conducted for each of the cytotoxics.

Table 2-23. SIA reagents, volumes, and flow rates used for analysis of imatinib using $Ru(bipy)_3Cl_2$ (1 x 10^{-3} M in 0.1 M H_2SO_4) oxidised online with $Ce(SO_4)_2$ (1 x 10^{-3} M in 0.4 M H_2SO_4) as the oxidising reagent

Reagent	Composition	Volume (µL)	Flow Rate (µL/s)
Oxidising Reagent 1	$Ce(SO_4)_2$ (1 x 10^{-3} M in 0.4 M H_2SO_4)	50	10
Oxidising Reagent 2	$Ru(bipy)_3Cl_2$ (1.5 x 10^{-3} M in deionised water)	50	10
Analyte	Imatinib (1 x 10^{-4} - 1 x 10^{-3} M in deionised water)	50	10
Carrier Solution	0.4 M H_2SO_4	400	100

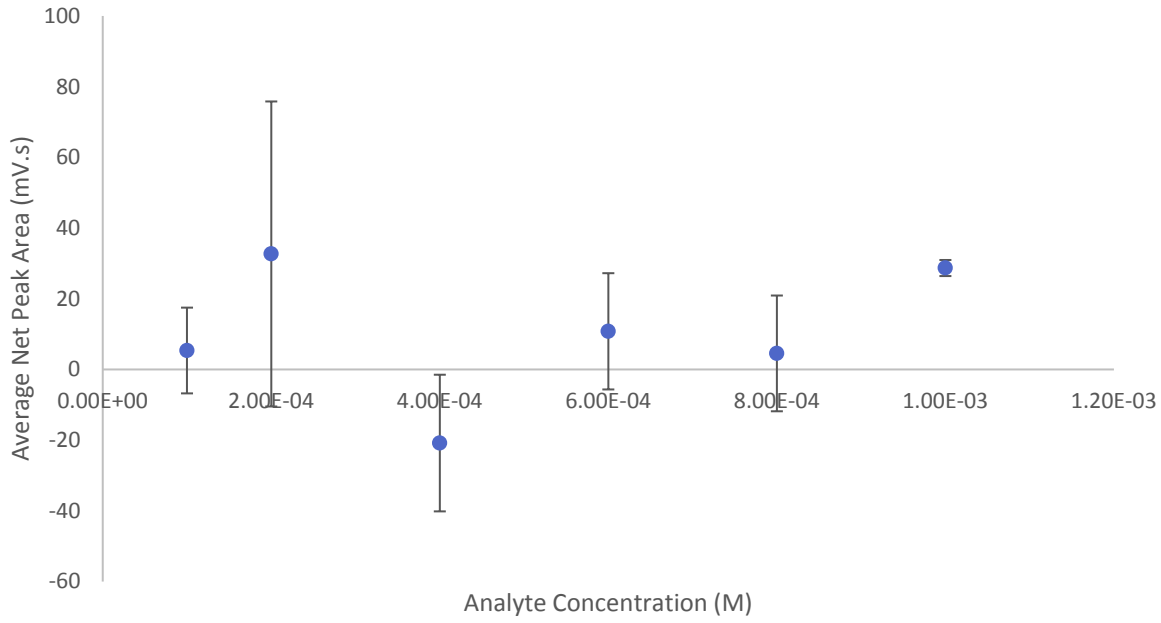

Figure 2-22. Effect of imatinib concentration on the average net peak area (n=3) obtained via SIA chemiluminescence using $Ce(SO_4)_2$ (1 x 10^{-3} M in 0.4 M H_2SO_4) and $Ru(bipy)_3Cl_2$ (1.5 x 10^{-3} M in deionised water) as the oxidising reagents and 0.04 M H_2SO_4 as the carrier solution. Error bars = ± 1 standard deviation.

2.3.2.2 Kinetics Studies and Investigation of the Role of Each Oxidising Reagent

It was hypothesised that reactions between the $Ce(SO_4)_2$ and the cytotoxics may be occurring, resulting in poor linearity in chemiluminescence response. In order to investigate this, experiments were conducted in which the cytotoxics were prepared using either deionised water, $Ce(SO_4)_2$, or $Ru(bipy)_3Cl_2$ as the solvent before being reacted with the remaining oxidising reagent. This would allow for control over which oxidising reagent the cytotoxics were able to react with first, hence giving an indication of the role of each reagent in the chemiluminescence reaction. The reagent conditions are summarised in Table 2-24, Table 2-25, and Table 2-26. It should be noted that when imatinib was prepared in $Ce(SO_4)_2$ at concentrations greater than 1 x 10^{-3} M, complete loss of the signal was observed, producing only noise, as shown in Figure 2-24. It was suspected that this was the result of

light absorption by the imatinib. Preparation of the imatinib in $Ce(SO_4)_2$ would have allowed a chemiluminescence reaction via the $Ce(SO_4)_2$ pathway to occur, the emission of which could have been absorbed by the imatinib, as observed during the preliminary oxidising reagent screen. In order to obtain signals usable for method development imatinib solutions with concentrations of $1x10^{-4}$ M instead of 1×10^{-3} M were used. The resulting net chemiluminescence peak areas are given in Figure 2-23. Signals larger than the blank were obtained for all cytotoxics when prepared in either deionised water or $Ru(bipy)_3Cl_2$. When prepared in $Ce(SO_4)_2$ all signals were equal to or lower than the blank (2.39 ± 7 mV.s, -7.82 ± 14 mV.s, and -66.4 ± 6 mV.s for cyclophosphamide, 5-fluorouracil, and imatinib, respectively). This suggested that there was indeed a reaction taking place between each analyte and the $Ce(SO_4)_2$. These reactions may have formed products less able to undergo a chemiluminescence reaction with $Ru(bipy)_3Cl_2$. It is also possible that these reactions resulted in consumption of the $Ce(SO_4)_2$, hence preventing its oxidation of the $Ru(bipy)_3Cl_2$ to the active 3+ oxidation state, and hence preventing the chemiluminescence reaction from occurring. Finally, in the case of imatinib absorption of the emitted light could have been the cause. This would not be possible for cyclophosphamide and 5-fluorouracil, however, because the absorbance profiles of these drugs do not overlap with the emissions profile of $Ru(bipy)_3$ or $Ce(SO_4)_2$ chemiluminescence. It was also noted that the 5-fluorouracil solution prepared in $Ce(SO_4)_2$, when left to stand, changed from a translucent yellow colour to a clear and colourless solution. Solutions of Ce(IV) are known to be yellow in colour, whereas Ce(III) solutions are clear and colourless [191]. The observed colour change therefore suggested that the Ce(IV) was oxidising the 5-fluorouracil when left to stand, hence being reduced to Ce(III) itself.

The largest chemiluminescence peak areas were obtained when the cytotoxics were able to react with the $Ru(bipy)_3$ first (28.5 ± 8 mV.s, 14.7 ± 6 mV.s, and 40.8 ± 9 mV.s for cyclophosphamide, 5-fluorouracil, and imatinib, respectively). This suggested the pre-oxidiation of the cytotoxics may be required to obtain chemiluminescence.

Table 2-24. SIA reagents, volumes, and flow rates used for analysis of cyclophosphamide, 5-fluorouracil, and imatinib using pre-mixed $Ru(bipy)_3Cl_2$ and $Ce(SO_4)_2$

Aspiration Order	Reagent	Composition	Volume (µL)	Flow Rate (µL/s)
1	Oxidising Reagent	50:50 (v/v) $Ce(SO_4)_2$ (1×10^{-3} M in 0.4 M H_2SO_4):$Ru(bipy)_3Cl_2$ (1.5×10^{-3} M in deionised water)	50	10
2	Analyte	Cyclophosphamide, 5-fluorouracil, or imatinib (1×10^{-3} M in deionised water)	50	10
3	Carrier Solution	0.4 M H_2SO_4	400	100

Table 2-25. SIA reagents, volumes, and flow rates used for analysis of cyclophosphamide, 5-fluorouracil, and imatinib prepared in $Ce(SO_4)_2$, using $Ru(bipy)_3Cl_2$ as the oxidising reagent

Aspiration Order	Reagent	Composition	Volume (µL)	Flow Rate (µL/s)
1	Oxidising Reagent	$Ru(bipy)_3Cl_2$ (1.5×10^{-3} M in deionised water)	50	10
2	Analyte	Cyclophosphamide, 5-fluorouracil (1×10^{-3} M) or imatinib (1×10^{-4} M) in $Ce(SO_4)_2$ (1×10^{-3} M in 0.4 M H_2SO_4)	50	10
3	Carrier Solution	0.4 M H_2SO_4	400	100

Table 2-26. SIA reagents, volumes, and flow rates used for analysis of cyclophosphamide, 5-fluorouracil, and imatinib prepared in $Ru(bipy)_3Cl_2$, using $Ce(SO_4)_2$ using as the oxidising reagent

Aspiration Order	Reagent	Composition	Volume (µL)	Flow Rate (µL/s)
1	Oxidising Reagent	$Ce(SO_4)_2$ (1×10^{-3} M in 0.4 M H_2SO_4)	50	10
2	Analyte	Cyclophosphamide, 5-fluorouracil (1×10^{-3} M) or imatinib (1×10^{-4} M) in $Ru(bipy)_3Cl_2$ (1.5×10^{-3} M in deionised water)	50	10
3	Carrier Solution	0.4 M H_2SO_4	400	100

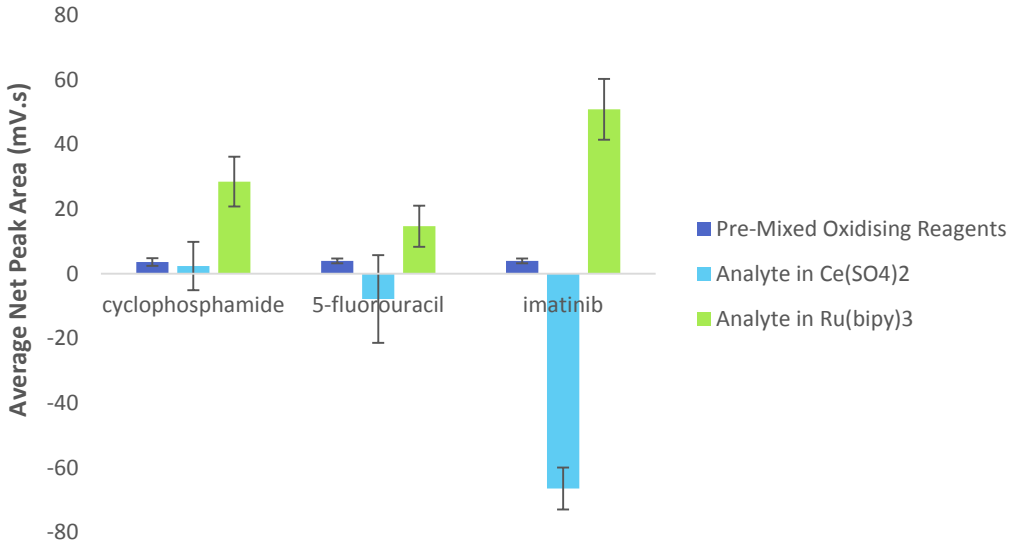

Figure 2-23. Average net peak area (n=3) of SIA-chemiluminescence signals from cyclophosphamide, 5-fluorouracil (1×10^{-3} M), and imatinib (1×10^{-4} M) prepared in either $Ru(bipy)_3Cl_2$ (1.5×10^{-3} M in deionised water), $Ce(SO_4)_2$ (1×10^{-3} M in 0.4 M H_2SO_4), or deionised water, and reacted with the remaining oxidising reagent. Error bars = ± 1 standard deviation

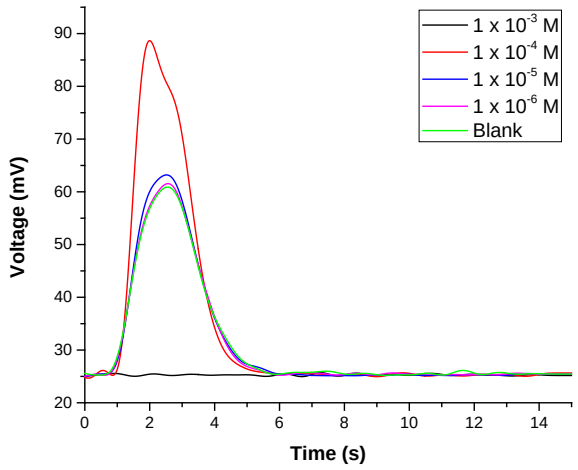

Figure 2-24. Raw chemiluminescence signals obtained via SIA-chemiluminescence analysis of imatinib solutions of various concentration prepared in $Ce(SO_4)_2$ (0.4 M H_2SO_4), using $Ru(bipy)_3$ (1.5 x 10^{-3} M in deionised water) as the oxidant

In order to confirm this, individual standards of 5-fluorouracil, imatinib, and cyclophosphamide were prepared in $Ce(SO_4)_2$ and analysed using SIA periodically over 20 hours. Again, a concentration of $1x10^{-4}$ M of imatinib was utilised in order to obtain usable signals. The experimental conditions used are detailed in Table 2-27, with the resulting average net peak areas given in Figure 2-25.

Table 2-27. SIA reagent conditions, volumes, and flow rates used to monitor the reaction of cyclophosphamide, 5-fluorouracil, and imatinib with $Ce(SO_4)_2$ over 20 hours

Aspiration Order	Reagent	Composition	Volume (µL)	Flow Rate (µL/s)
1	Oxidising Reagent	$Ru(bipy)_3Cl_2$ (1.5 x 10^{-3} M in deionised water)	50	10
2	Analyte	Cyclophosphamide, 5-fluorouracil (1 x 10^{-3} M) or imatinib (1 x 10^{-4} M) in $Ce(SO_4)_2$ (1 x 10^{-3} M in 0.4 M H_2SO_4)	50	10
3	Carrier Solution	0.4 M H_2SO_4	400	100

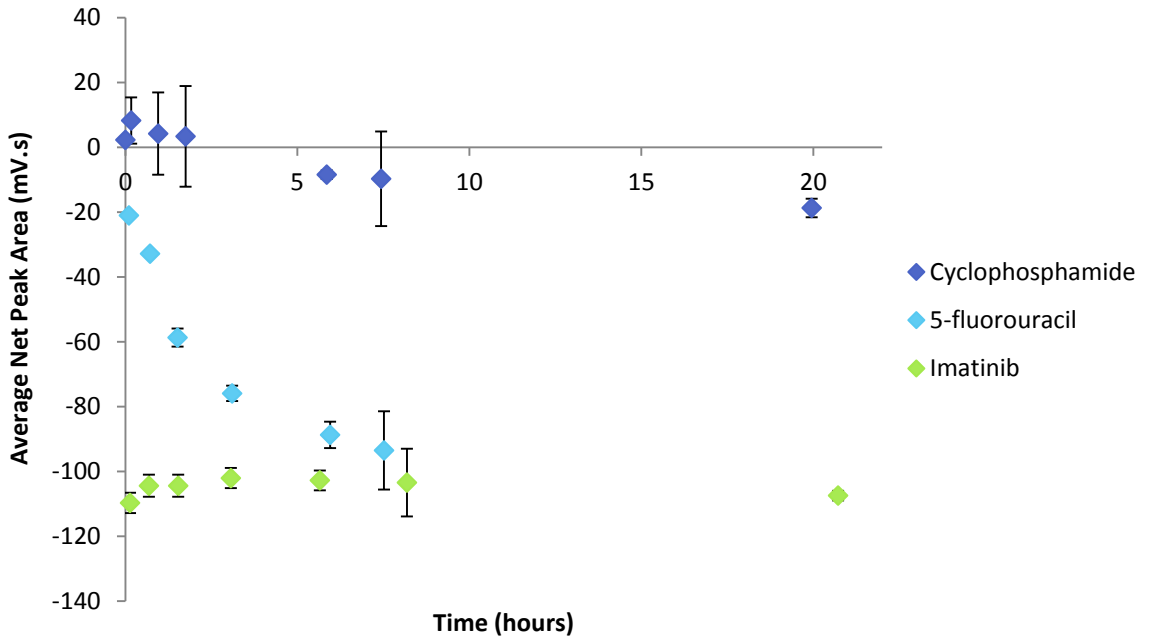

Figure 2-25. Average net peak area (n=3) of SIA-chemiluminescence signals from individual aqueous cyclophosphamide, 5-fluorouracil (1 x 10^{-3} M), and imatinib (1 x 10^{-4} M) prepared in $Ce(SO_4)_2$ (1 x 10^{-3} M in 0.4 M H_2SO_4), using Ru(bipy)3 (1.5 x 10^{-3} M in deionised water) as the oxidising reagent, and analysed periodically over 20 hours. Error bars = ± 1 standard deviation

The signal from both cyclophosphamide and 5-fluorouracil decreased over 20 hours, with the rate of decrease being faster for 5-fluorouracil. This indicated that there was a slow reaction occurring between these cytotoxics and the $Ce(SO_4)_2$. The reaction between Ce(IV) and uracil (structurally similar to 5-fluorouracil) has been investigated previously. Lakshmi and Renganathan [192] found that uracil (and other pyrimidines) could undergo electrophilic attack by Ce(IV) on the C5 of the keto form of the uracil (Figure 2-26), following the reaction scheme in Figure 2-27. This reaction may therefore be occurring between 5-flurouracil and Ce(IV), resulting in consumption of the $Ce(SO_4)_2$, and hence decreased formation of $[Ru(bipy)_3]^{3+}$.

a)

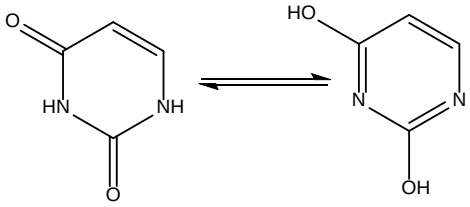

keto enol

b)

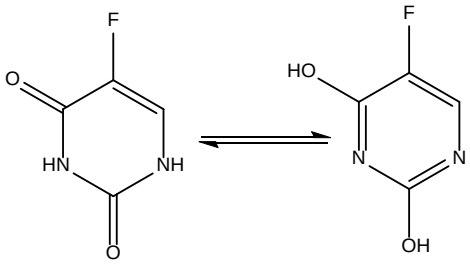

keto enol

Figure 2-26. Keto and enol forms of uracil (a) and 5-fluorouracil (b)

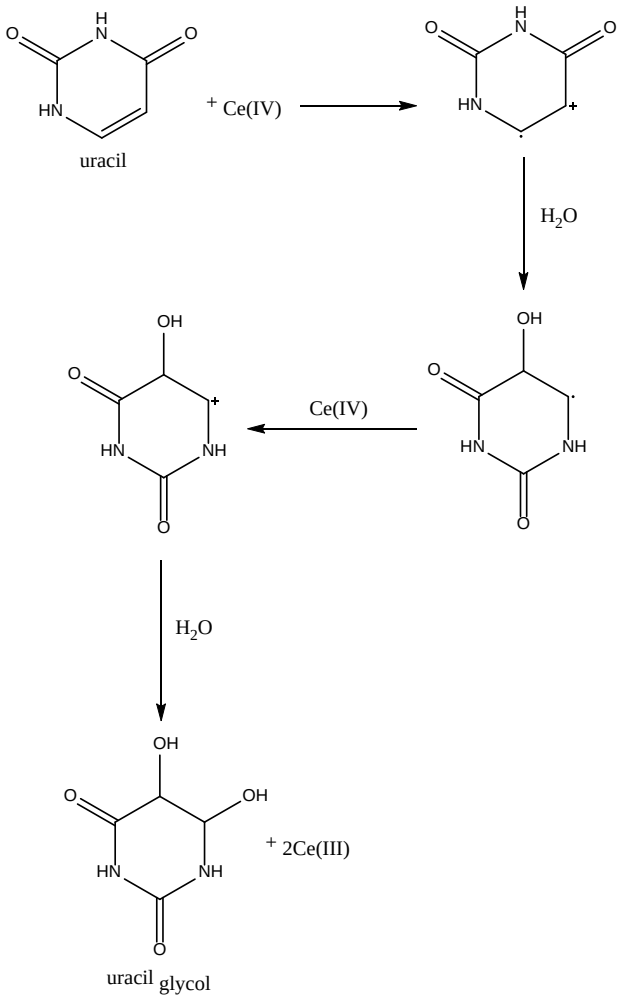

Figure 2-27. Reaction of uracil with Ce(IV) [192]

Cyclophosphamide, however, is an electrophile, and hence would not undergo this electrophilic attack by Ce(IV) [193]. It is therefore more likely that the observed decrease in chemiluminescence signal over time was due to instability of the cyclophosphamide itself, which is known to undergo hydrolysis in aqueous solution [194]. This would explain why the rate of decrease was very slow compared to that of imatinib and 5-fluorouracil.

In the case of imatinib a signal could only be detected in the first analysis, which was 6 minutes after the solution was prepared, after which complete quenching was obtained. When repeating this experiment for imatinib over a shorter time interval (50 minutes) a decreasing trend in chemiluminescence signal over time was observed (Figure 2-28). It should be noted that replicates of each analysis time could not be taken due to the minimum time taken for each analysis, and hence data points represent a single analysis. This therefore suggested that a similar but more rapid reaction may be occurring to that observed for the other cytotoxics. This result could also possibly explain the inability to obtain greater than background signals when analysing imatinib concentrations greater than 1×10^{-3} M. At high imatinib concentrations the suggested reaction between imatinib and $Ce(SO_4)_2$ could occur extremely rapidly, resulting in the loss of chemiluminescence ability before analysis could be conducted.

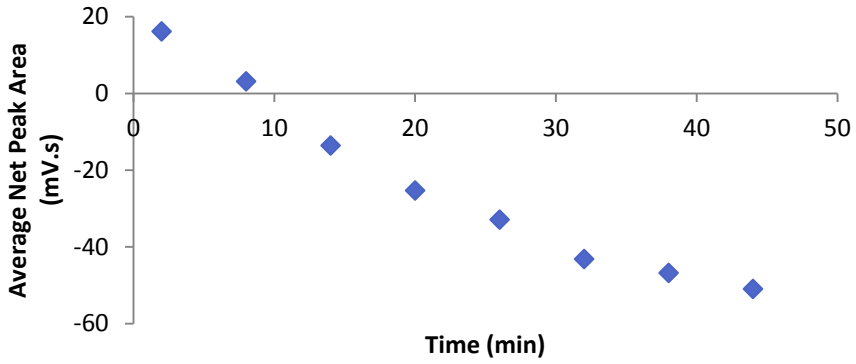

Figure 2-28. Net peak area (n=3) obtained via SIA-chemiluminescence of imatinib ($1x10^{-4}$ M in $Ce(SO_4)_2$ in 0.4 M H_2SO_4) using $Ru(bipy)_3$ as the oxidising reagent over 50 minutes.

In light of these findings it was decided that the kinetics and overall emission profiles of these reactions be investigated further using stopped-flow analysis. Individual solutions of cyclophosphamide, 5-fluorouracil, and imatinib were prepared in each of distilled water, $Ru(bipy)_3Cl_2$, and $Ce(SO_4)_2$ with a range of concentrations. Various combinations of these solutions were then analysed using the stopped-flow analysis instrument described in Section 2.2.4, in order to gain an understanding of the role of each reagent in the chemiluminescence reaction. The reagent combinations and concentrations investigated are detailed throughout the following sections.

Firstly, each analyte was prepared in deionised water and reacted with pre-mixed (1:1 v/v) $Ru(bipy)_3Cl_2$ (1×10^{-3} M in distilled water) and $Ce(SO_4)_2$ (in 0.4 M H_2SO_4). The concentration of $Ce(SO_4)_2$ was varied, as detailed in Table 2-28, in order to change the molar ratio between $Ru(bipy)_3$ and $Ce(SO_4)_2$. Resulting kinetics profiles and maximum chemiluminescence peak intensities for each cytotoxic are given in Figure 2-29 and Figure 2-30, respectively.

Table 2-28. Reagents delivered from each syringe during stopped-flow analysis of cyclophosphamide, 5-fluorouracil, and imatinib using pre-mixed oxidising reagents

Syringe 1	Syringe 2
Cyclophosphamide, 5-fluorouracil (1×10^{-3} M), or imatinib (1×10^{-4} M) in deionised water	1:1 (v/v) $Ru(bipy)_3$ (1×10^{-3} M in distilled water)/ $Ce(SO_4)_2$ (0.5×10^{-3} M - 2×10^{-3} M in 0.4 M H_2SO_4)

When reacting with pre-mixed oxidisers cyclophosphamide produced the most intense chemiluminescence, followed by 5-fluorouracil, and then imatinib. This correlated well with the linearity of response and preliminary detection limits obtained for each cytotoxic when using SIA (Figure 2-21). Cyclophosphamide showed the best linearity and lowest detection limit, followed by 5-fluorouracil, and imatinib produced quite poor results. This indicated that in the SIA manifold the two oxidising reagents were reacting together first, prior to mixing with the analyte, hence producing similar trends to those observed in this stopped-flow analysis. This was expected because in the SIA manifold the $Ru(bipy)_3Cl_2$ was withdrawn first, followed by the $Ce(SO_4)_2$, and then the analyte, before being delivered to the reaction cell.

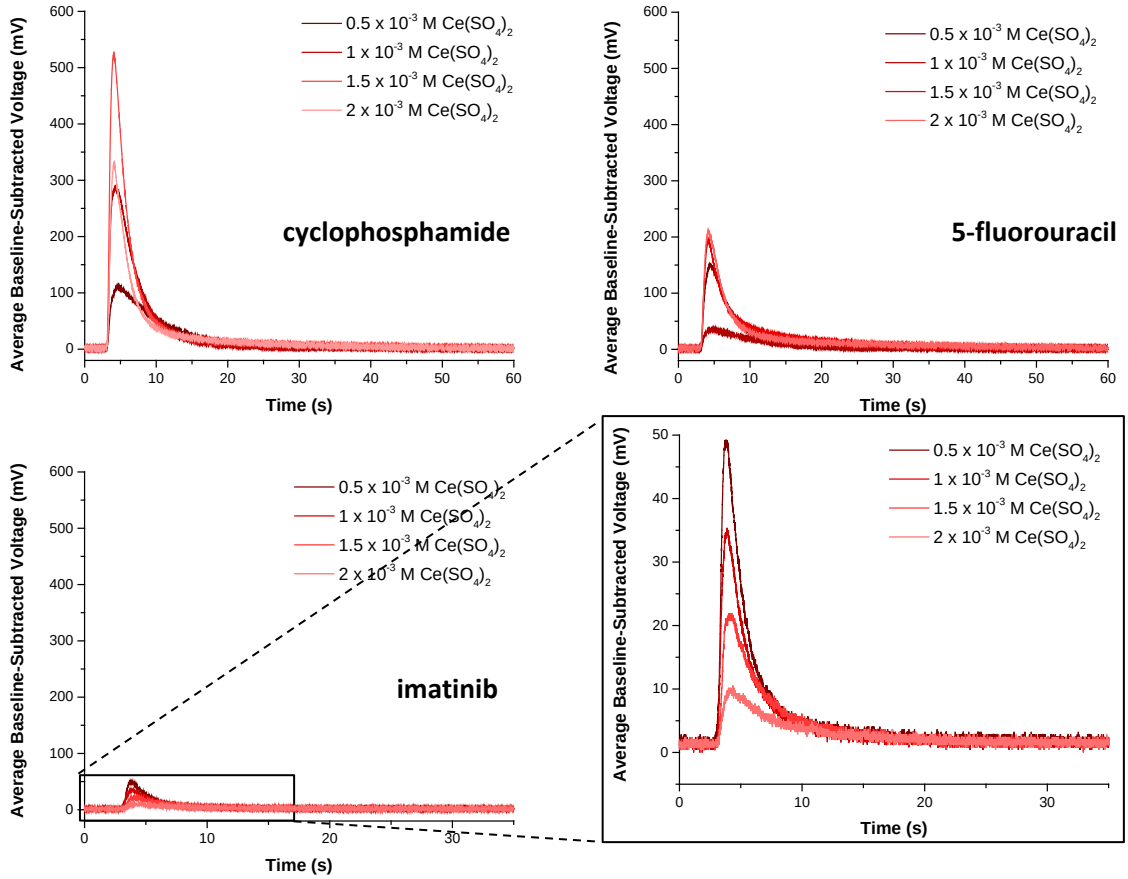

Figure 2-29. Chemiluminescence kinetics profiles of cyclophosphamide, 5-fluorouracil (1 x 10^{-3} M in deionised water), and imatinib (1 x 10^{-4} M in deionised water) reacted with 50:50 (%v/v) $Ru(bipy)_3Cl_2$ (1.5 x 10^{-3} M in deionised water):$Ce(SO_4)_2$ (0.5 x 10^{-3} M – 2 x 10^{-3} M in 0.4 M H_2SO_4)

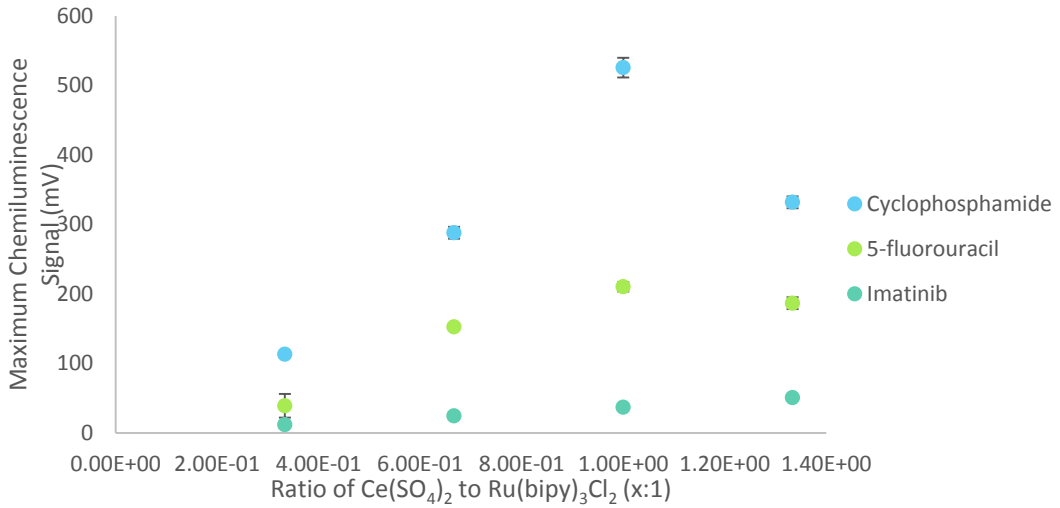

Figure 2-30. Effect of $Ce(SO_4)_2$:$Ru(bipy)Cl_2$ ratio on maximum of the chemiluminescence signal obtained via stopped-flow analysis of cyclophosphamide, 5-fluorouracil (1 x 10^{-3} M) and imatinib (1 x 10^{-4} M) in in one syringe and pre-mixed $Ce(SO_4)_2$ (in 0.4 M H_2SO_4)/1.5 x 10^{-3} M $Ru(bipy)_3Cl_2$ (1.5 x 10^{-3} M) in the other. Error bars = ± 1 standard deviation.

Experiments were then conducted on analytes prepared in the $Ru(bipy)_3Cl_2$ itself before being mixed with the $Ce(SO_4)_2$ in order to determine if an initial oxidation of the sample by the $Ru(bipy)_3$ was occurring. Firstly, the $Ru(bipy)_3$ concentration was held constant and the $Ce(SO_4)_2$ concentration

changed. The experimental conditions used are detailed in Table 2-29, and resulting kinetics profiles are given inFigure 2-31. The maximum chemiluminescence peak height obtained for each $Ce(SO_4)_2$ concentration is also given in Figure 2-32.

Table 2-29. Reagents delivered from each syringe during stopped-flow analysis of cyclophosphamide, 5-fluorouracil, and imatinib prepared in $Ru(bipy)_3Cl_2$

Syringe 1	Syringe 2
Cyclophosphamide, 5-fluorouracil (1×10^{-3} M), or imatinib (1×10^{-4} M) in $Ru(bipy)_3Cl_2$ (1×10^{-3} M in distilled water)	$Ce(SO_4)_2$ (0.5×10^{-4} M – 1×10^{-3} M in 0.4 M H_2SO_4)

It was observed that as the $Ce(SO_4)_2$ concentration was increased the maximum chemiluminescence intensity also increased for each cytotoxic. This suggested that the reaction was indeed dependent on the presence of $Ce(SO_4)_2$, rather than $Ru(bipy)_3$ alone. This was likely due to an increase in the formation of $[Ru(bipy)_3]^{3+}$ with increasing $Ce(SO_4)_2$ concentration. At the highest $Ce(SO_4)_2$ concentration tested (1×10^{-3} M) the overall shape of the kinetics profiles of both imatinib and cyclophosphamide also appeared to change, with a second shoulder being produced. This shoulder was much more pronounced in imatinib, having almost the same intensity as the first peak. This suggested that a second reaction was occurring at these higher $Ce(SO_4)_2$ concentrations. It is possible that the $Ce(SO_4)_2$ first oxidises the analyte, which undergoes chemiluminescence, and then at high enough concentrations any remaining $Ce(SO_4)_2$ can then oxidise the $Ru(bipy)_3Cl_2$ to form the active 3+ oxidation state, with which the analyte can also react, hence producing shouldered peaks. Similarly, the $Ce(SO_4)_2$ could be reacting with the $Ru(bipy)_3Cl_2$ first to form the active 3+ oxidation state, and then any excess $Ce(SO_4)_2$ could then oxidise the analytes. This correlated well with the previous observation of a rapid reaction between imatinib and $Ce(SO_4)_2$ over 24 hours. 5-fluorouracil was also observed to undergo a reaction with $Ce(SO_4)_2$ over 24 hours, however in these kinetics experiments no peak shouldering was observed. This may have been a result of the reaction occurring too slowly to be detectable within the analysis time. Cyclophosphamide, however, was not observed to undergo a fast reaction with $Ce(SO_4)_2$ in previous experiments, and hence the peak shouldering observed here is interesting.

No peak shouldering was observed in the previous experiments using pre-mixed oxidising reagents. This further supported the idea that this shouldering was due to secondary reactions between the analyte and either of the oxidising reagents, which would not be able to occur if the oxidising reagents had already reacted with each other.

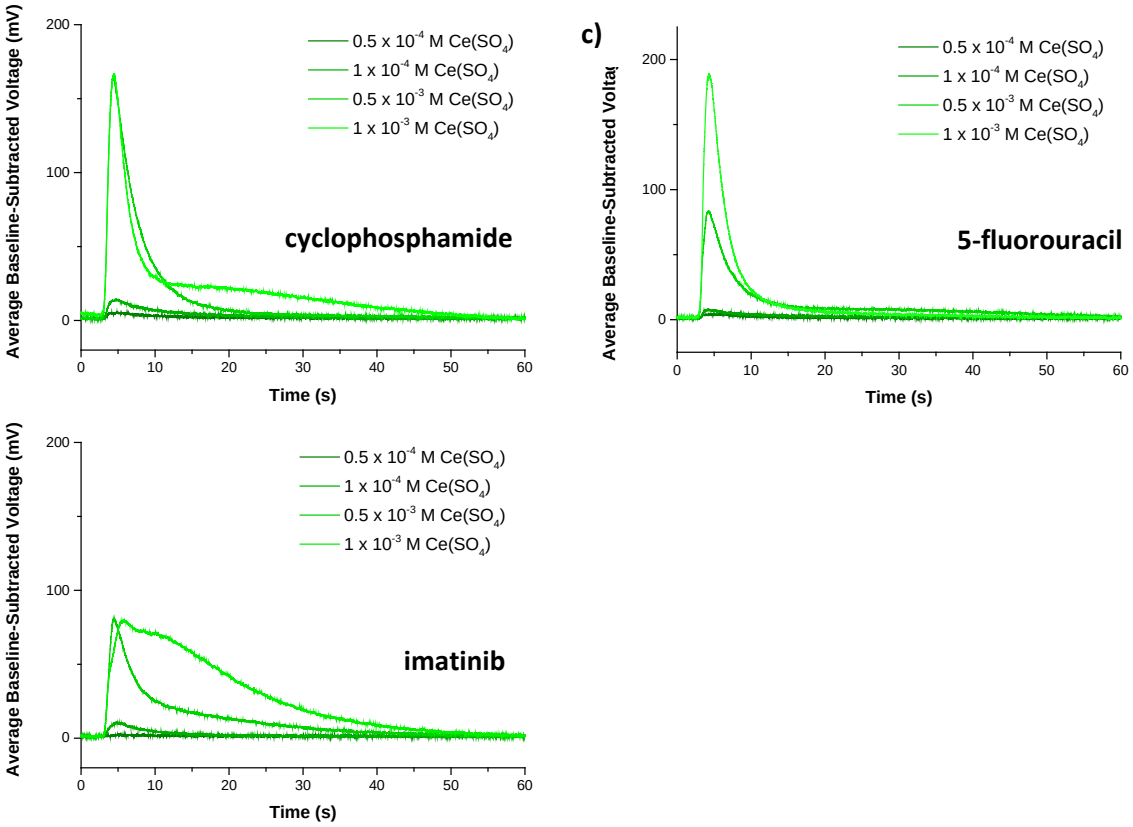

Figure 2-31. Chemiluminescence kinetics profiles of cyclophosphamide, 5-fluorouracil (1 x 10^{-3} M), and imatinib (1 x 10^{-4} M) prepared in $Ru(bipy)_3Cl_2$ (1.5 x 10^{-3} M in deionised water) and reacted with various concentrations of $Ce(SO_4)_2$ (in 0.4 M H_2SO_4)

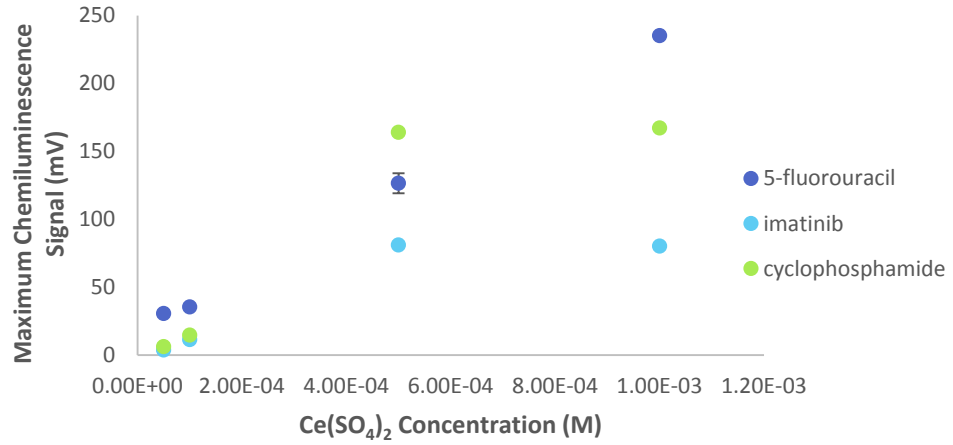

Figure 2-32. Effect of $Ce(SO_4)_2$ concentration (in 0.4 M H_2SO_4) on maximum of the chemiluminescence signal obtained via stopped-flow analysis of 5-fluorouracil (1 x 10^{-3} M in 1.5 x 10^{-3} M $Ru(bipy)_3Cl_2$ in deionised water) in one syringe and $Ce(SO_4)_2$ (in 0.4 M H_2SO_4) in the other. Error bars = ± 1 standard deviation.

The effect of $Ru(bipy)_3Cl_2$ concentration was then investigated via preparation of each cytotoxic in various $Ru(bipy)_3Cl_2$ concentrations and analysis using $Ce(SO_4)_2$ (1 x 10^{-3} M in 0.4 M H_2SO_4), as detailed in Table 2-30. Resulting kinetics profiles and maximum chemiluminescence peak height are given in Figure 2-33 and Figure 2-34, respectively. It was observed that maximum chemiluminescence

intensity increased with increasing $Ru(bipy)_3Cl_2$ concentration up to 1.5 x 10^{-3} M for both cyclophosphamide and 5-fluorouracil, before decreasing again. Imatinib also showed a similar trend, but with maximum chemiluminescence intensity beginning to decrease at a lower $Ru(bipy)_3Cl_2$ concentration.

Table 2-30. Reagents delivered from each syringe during stopped-flow analysis of cyclophosphamide, 5-fluorouracil, and imatinib prepared in $Ce(SO_4)_2$

Syringe 1	Syringe 2
Cyclophosphamide, 5-fluorouracil (1 x 10^{-3} M), or imatinib (1 x 10^{-4} M) in $Ru(bipy)_3$ (0.5 x 10^{-4} - 2 x 10^{-3} M in distilled water)	$Ce(SO_4)_2$ (1 x 10^{-3} M in 0.4 M H_2SO_4)

The shape of the kinetics profiles also changed dramatically with increasing $Ru(bipy)_3Cl_2$ concentration. Tailing of the chemiluminescence peak was observed for each of the cytotoxics. For cyclophosphamide, this tailing increased with increasing $Ru(bipy)_3Cl_2$ concentration up to 1.5 x 10^{-3} M, before decreasing dramatically at 2 x 10^{-3} M. This correlated well with the pattern observed for maximum signal height. For 5-fluorouracil this peak-tailing was more pronounced, and did not follow such a straight-forward trend. A small degree of peak tailing occurred at 0.5 x 10^{-3} M, before increasing to its maximum extent at 1 x 10^{-3} M. Tailing then decreased to its lowest extent at 1.5 x 10^{-3} M, before again decreasing at 2 x 10^{-3} M. Imatinib showed the largest peak tailing, which increased with increasing $Ru(bipy)_3Cl_2$ concentration. This tailing again suggested a secondary reaction was occurring for each of the cytotoxics, and that this reaction was highly dependent on the stochiometric ratio between either the cytotoxic, the $Ru(bipy)_3Cl_2$, and/or the $Ce(SO_4)_2$.

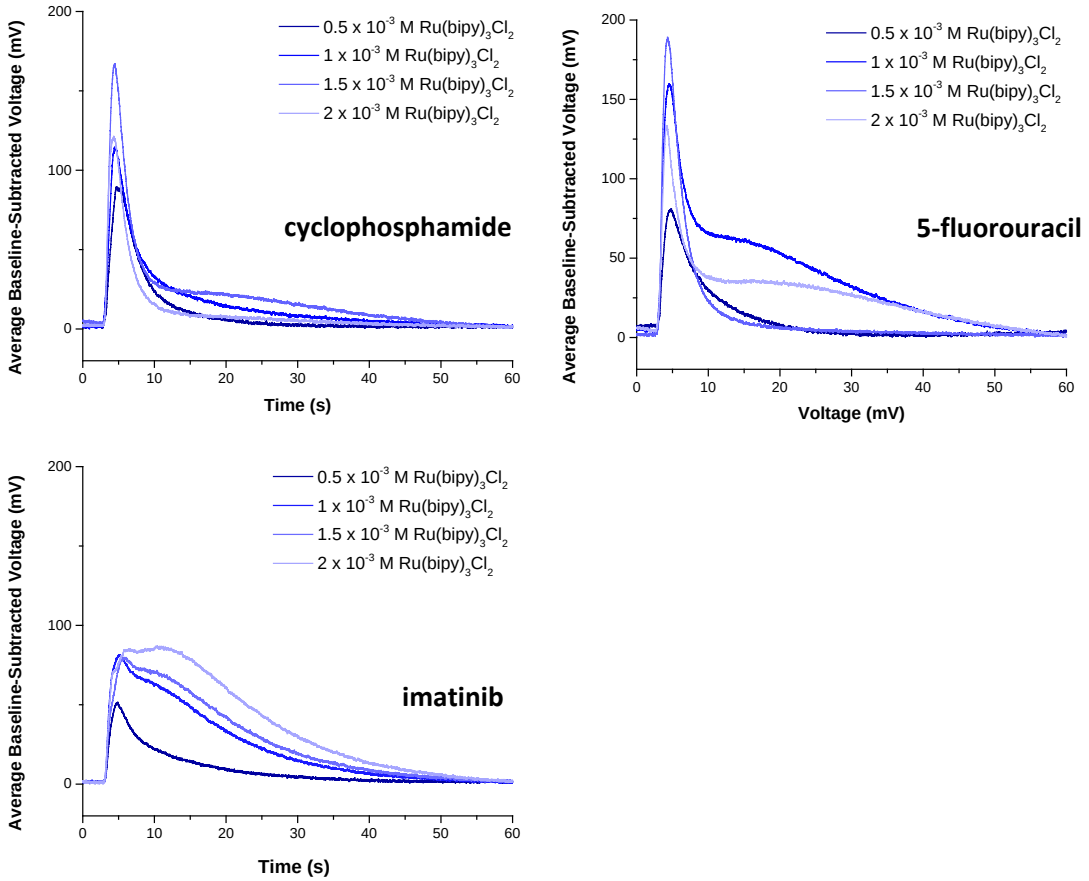

Figure 2-33. Chemiluminescence kinetics profiles of cyclophosphamide (a), 5-fluorouracil (1 x 10^{-3} M) (b), and imatinib (1 x 10^{-4} M)(c) prepared in various concentrations of $Ru(bipy)_3Cl_2$ (in deionised water) and reacted with $Ce(SO_4)_2$ (1 x 10^{-3} M in 0.4 M H_2SO_4)

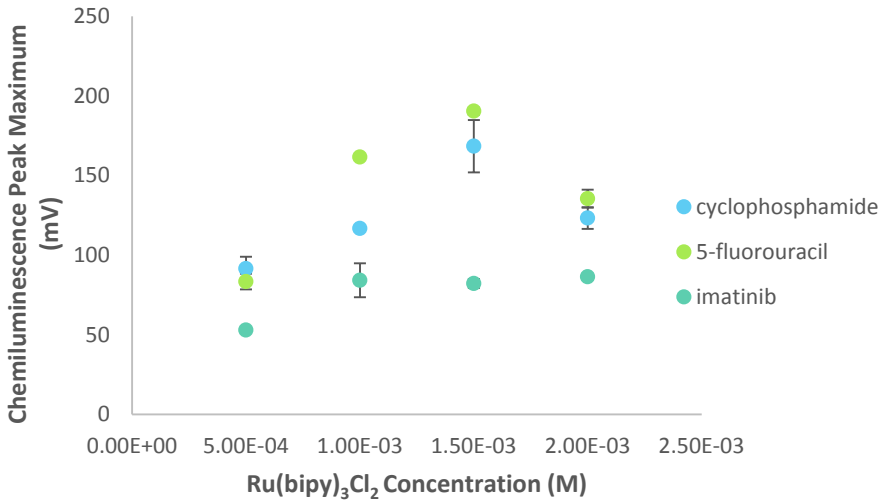

Figure 2-34. Effect of $Ru(bipy)_3Cl_2$ concentration on chemiluminescence kinetics profiles of cyclophosphamide, 5-fluorouracil (1 x 10^{-3} M), and imatinib (1 x 10^{-4} M) prepared in $Ru(bipy)_3Cl_2$ of varying concentrations and mixed with $Ce(SO_4)_2$ (1 x 10^{-3} M in 0.4 M H_2SO_4) in stopped-flow analysis. Error bars = ± 1 standard deviation.

Finally, the effect of cytotoxic concentration was investigated via preparation of cytotoxic solutions between 0.5 x 10^{-4} M and 1 x 10^{-3} M in $Ru(bipy)_3Cl_2$ (1.5 x 10^{-3} M in deionised water) and subsequent stopped-flow analysis using $Ce(SO_4)_2$ (1 x 10^{-3} M in 0.4 M H_2SO_4). The experimental conditions are

detailed in Table 2-31. Resulting kinetics profiles and maximum chemiluminescence intensities are given in Figure 2-35. Again, peak shouldering was observed during imatinib analysis. The shape of this shouldering, however, changed with changing imatinb concentration. At lower imatinib concentrations the kinetics profile was composed of two more distinct peaks relative to those obtained at higher imatinib concentrations. It is possible that at higher imatinib concentrations the second reaction was favoured, resulting in a more singular peak shape. At lower concentrations, however, the first reaction may have been able to occur to a greater extent, resulting in two peaks corresponding to the first and second reactions. This change in peak shape was also observed for cyclophosphamide to a lesser extent. No change in peak shape was observed during 5-fluorouracil analysis, hence suggesting that the observed reactions were less dependent on 5-fluorouracil concentration than in the case of cyclophosphamide and imatinib.

Table 2-31. Reagents delivered from each syringe during stopped-flow analysis of cyclophosphamide, 5-fluorouracil, and imatinib prepared in $Ce(SO_4)_2$

Syringe 1	Syringe 2
Cyclophosphamide, 5-fluorouracil or imatinib (0.5×10^{-4} - 1×10^{-3} M) in $Ru(bipy)_3Cl_2$ (1.5×10^{-3} M in distilled water)	$Ce(SO_4)_2$ (1×10^{-3} M in 0.4 M H_2SO_4)

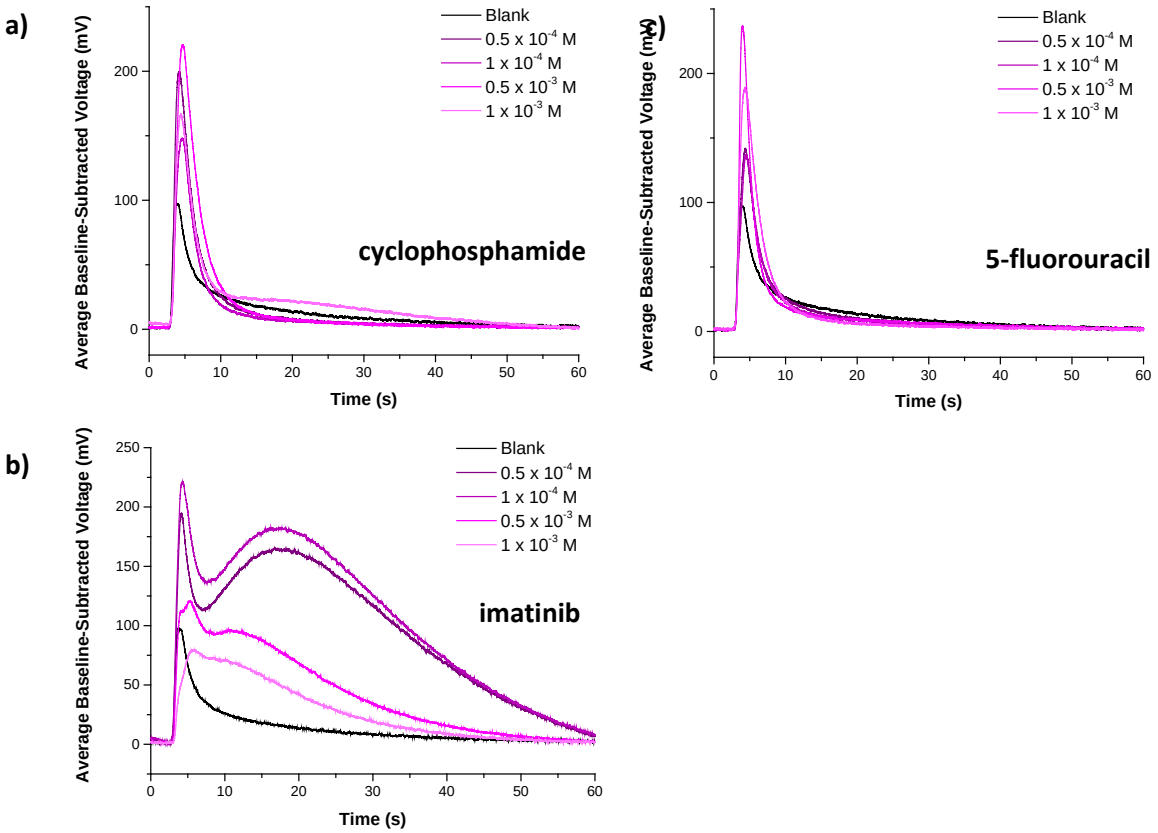

Figure 2-35. Chemiluminescence kinetics profiles of cyclophosphamide (a), 5-fluorouracil (b), and imatinib (c) of various concentrations prepared in $Ru(bipy)_3Cl_2$ (in deionised water) and reacted with $Ce(SO_4)_2$ (1×10^{-3} M in 0.4 M H_2SO_4)

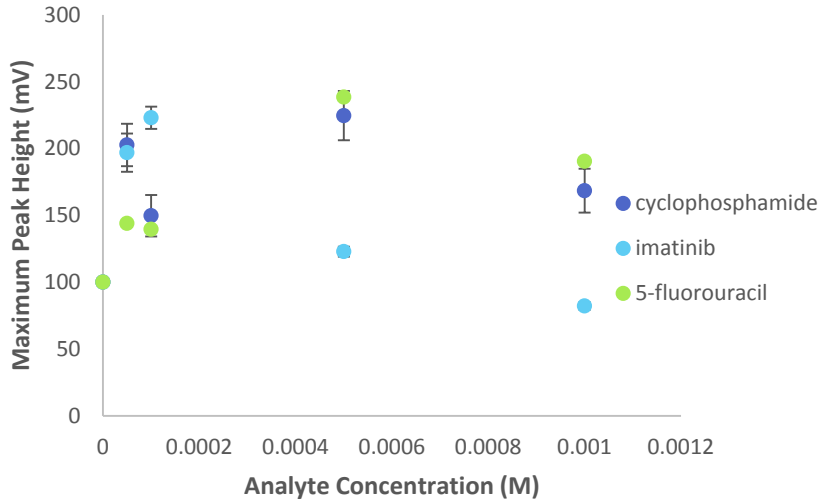

Figure 2-36. Effect of analyte concentration on maximum chemiluminescence intensity of cyclophosphamide, 5-fluorouracil, and imatinib prepared in $Ru(bipy)_3Cl_2$ (1.5×10^{-3} M in deionised water) and analysed with $Ce(SO_4)_2$ (1×10^{-3} M in 0.4 M H_2SO_4) using stopped-flow analysis. Error bars = ± 1 standard deviation.

In order to support these explanations, experiments in which the cytotoxics were prepared in the $Ce(SO_4)_2$ first, and then reacted with the $Ru(bipy)_3Cl_2$ were conducted, in order to determine if they could indeed react separately with the $Ce(SO_4)_2$. The experimental conditions are detailed in Table 2-32. In these experiments cyclophosphamide and 5-fluorouracil produced maximum chemiluminescence signals only slightly larger than that of the blank. This suggested that there was indeed a reaction occurring between the cytotoxics and the $Ce(SO_4)_2$, which was resulting in an overall decrease in the chemiluminescence emission.

Table 2-32. Reagents delivered from each syringe during stopped-flow analysis of cyclophosphamide, 5-fluorouracil, and imatinib prepared in $Ce(SO_4)_2$

Syringe 1	Syringe 2
Cyclophosphamide, 5-fluorouracil or imatinib (0.5×10^{-4} - 1×10^{-3} M) in $Ce(SO_4)_2$ (1×10^{-3} M in 0.4 M H_2SO_4)	$Ru(bipy)_3$ (1.5×10^{-3} M in distilled water)

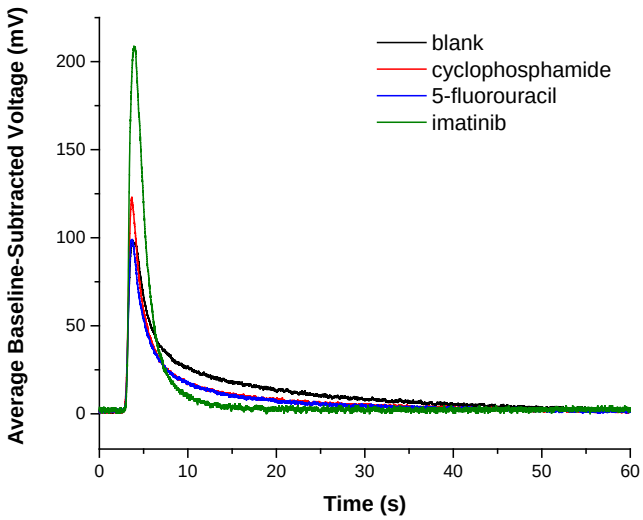

Figure 2-37. Chemiluminescence kinetics profiles of cyclophosphamide, 5-fluorouracil (1 x 10^{-3} M), and imatinib (1 x 10^{-4} M) prepared in $Ce(SO_4)_2$ (1 x 10^{-3} M in 0.4 M H_2SO_4)

Imatinib produced a larger signal, however, as in other experiments, the imatinib concentration used was 1 x 10^{-4} M rather than 1 x 10^{-3} M. Experiments in which the concentration of imatinib was varied (when prepared in $Ce(SO_4)_2$) were therefore conducted. Experimental conditions used are detailed in Table 2-33. Resulting kinetics profiles maximum emission intensities are given in Figure 2-38 and Figure 2-39, respectively. It was observed that as the imatinib concentration increased up to 1 x 10^{-4} M the chemiluminescence intensity increased, before being completely lost at 1 x 10^{-3} M. There was, however, no peak shouldering observed, suggesting that both of the reactions observed previously could not occur when imatinib was first able to react with $Ce(SO_4)_2$. This could have been due to the reaction between $Ce(SO_4)_2$ and imatinib occurring so rapidly that all $Ce(SO_4)_2$ was consumed before it was able to react further. The peak shapes obtained here closely matched the first section of the kinetics profiles obtained previously. This suggested that the first part of the kinetics profile described the reaction with $C(SO_4)_2$, while the second peak shoulder was due to reaction with $Ru(bipy)_3Cl_2$.

Table 2-33. Reagents delivered from each syringe during stopped-flow analysis of imatinib of various concentrations prepared in $Ce(SO_4)_2$

Syringe 1	Syringe 2
Imatinib (1 x 10^{-5} - 1 x 10^{-3} M) in $Ce(SO_4)_2$ (1 x 10^{-3} M in 0.4 M H_2SO_4)	$Ru(bipy)_3Cl_2$ (1.5 x 10^{-3} M in distilled water)

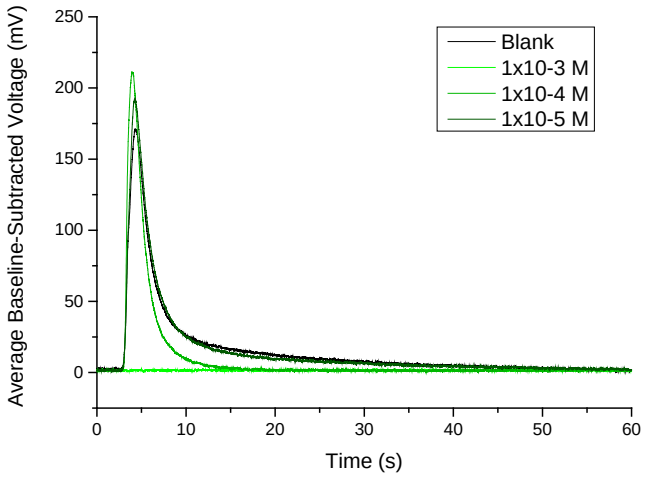

Figure 2-38. Chemiluminescence kinetics profiles of imatinib prepared in $Ce(SO_4)_2$ (1 x 10^{-3} M in 0.4 M H_2SO_4) at various concentrations and reacted with $Ru(bipy)_3Cl_2$ (1.5 x 10^{-3} M in deionised water) using stopped-flow analysis.

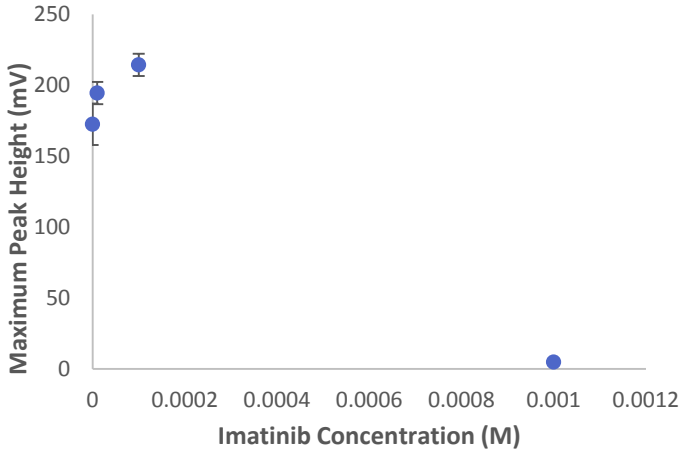

Figure 2-39. Effect of imatinib concentration on maximum chemiluminescence emission when prepared in $Ce(SO_4)_2$ (1 x 10^{-3} M in 0.4 M H_2SO_4) and reacted with $Ru(bipy)_3Cl_2$ (1.5 x 10^{-3} M in deionised water) using stopped-flow analysis. Error bars = ± 1 standard deviation.

As a final test to determine if $Ru(bipy)_3Cl_2$ had a role in the observed reaction of imatinib, experiments in which imatinib (prepared in deionised water) was reacted with $[Ru(bipy)_3]^{3+}$ prepared using PbO_2, rather than $Ce(SO_4)_2$, were conducted. $Ru(bipy)_3ClO_4$ salt was used instead of $Ru(bipy)_3Cl_2$ as it has been reported to produce a much more stable active 3+ state [122], and hence would minimise any possible reagent instability effects. Imatinib (1 x 10^{-4} M and 1 x 10^{-5} M) was analysed using $Ru(bipy)_3ClO_4$ (1 x 10^{-3} M in 0.05 M $HClO_4$ in 50 % acetonitrile) oxidised with solid PbO_2 (0.1 g/20 mL) (Table 2-34). Resulting kinetics profiles obtained for various imatinib concentrations are given in Figure 2-40. In these experiments the chemiluminescence signal again increased with increasing imatinib concentration before dramatically decreasing at a concentration of 1 x 10^{-3} M. Unlike when using $Ce(SO_4)_2$ oxidation, however, complete loss of the signal was not observed. This therefore suggested that the presence of the $Ce(SO_4)_2$ did indeed have a role in the observed quenching. Interestingly, the rate of decay of chemiluminescence obtained using $Ru(bipy)_3Cl_2/PbO_2$ was much slower than that obtained using $Ru(bipy)_3Cl_2/Ce(SO_4)_2$, with the chemiluminescence emission failing

to return to the baseline within the 60 second analysis time at imatinib concentrations of 1 x 10^{-4} M and 1 x 10^{-5} M. This indicated a different reaction mechanism may be occurring in each case.

Table 2-34. Reagents delivered from each syringe during stopped-flow analysis of imatinib of various concentrations prepared using PbO_2 oxidising reagent preparation

Syringe 1	Syringe 2
Imatinib (1 x 10^{-5} - 1 x 10^{-3} M) in deionised water	$Ru(bipy)_3ClO_4$ (1 x 10^{-3} M in 0.05 M $HClO_4$ in 50 % acetonitrile) oxidised with solid PbO_2 (0.1 g/20 mL)

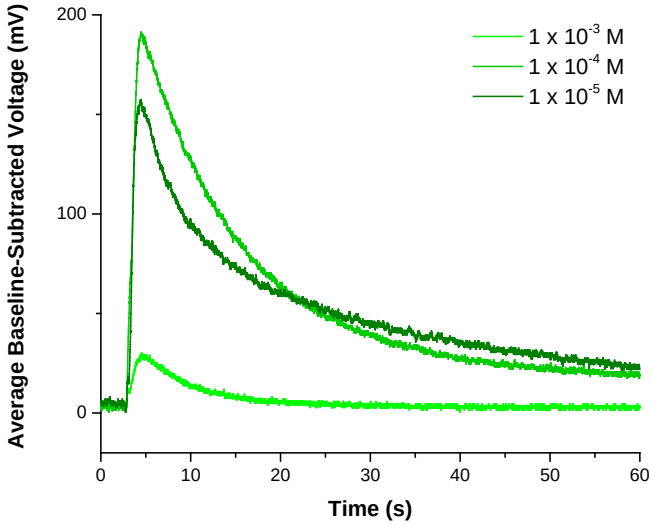

Figure 2-40. Chemiluminescence kinetics profiles of imatinib prepared in deionised water and reacted with $Ru(bipy)_3Cl_2$ (1 x 10^{-3} M in 0.05 M $HClO_4$ in 50 % acetonitrile) that had been oxidised suing solid PbO_2 (0.1 g/20 mL)

Overall, several conclusions could be drawn from these experiments. It was clear a reaction of 5-fluorouracil, imatinib, and possibly cyclophosphamide was occurring with $Ce(SO_4)_2$. This was demonstrated by peak shouldering in chemiluminescence kinetics profiles and a decrease in chemiluminescence detected when the analytes were able to react with $Ce(SO_4)_2$ prior to reaction with $Ru(bipy)_3Cl_2$. When the oxidising reagents were mixed first, however, maximum chemiluminescence intensity was obtained for cyclophosphamide and 5-fluorouracil (525.7 ± 14 mV.s and 210.4 ± 7 mV.s respectively). This was likely because reaction of $Ce(SO_4)_2$ with $Ru(bipy)_3Cl_2$ prevented the competing reaction of $Ce(SO_4)_2$ with the cytotoxics. The molar ratio between $Ce(SO_4)_2$ and $Ru(bipy)_3Cl_2$ was found to greatly affect the chemiluminescence profiles, with a ratio of 1.5:1 producing the most intense chemiluminescence when pre-mixed oxidising reagents were used. A ratio of 1:1.5, however, was found to produce maximum chemiluminescence intensity when the analytes were first prepared in $Ru(bipy)_3Cl_2$. This was most likely because an excess of $Ru(bipy)_3Cl_2$ was required to promote the reaction of $Ce(SO_4)_2$ with $Ru(bipy)_3Cl_2$ rather than the analytes.

It was therefore decided that FIA instrumentation may be more suited to the reaction kinetics in chemiluminescence detection of these cytotoxics. Method development using an in-house built FIA instrument was conducted using each cytotoxic analyte, however only very low signal intensities were obtained (see Appendix C). It was therefore decided that the use of $Ru(bipy)_3Cl_2$ oxidised with $Ce(SO_4)_2$ would not be effective in chemiluminescence detection of cyclophosphamide, 5-fluorouracil, or imatinib. $Ru(bipy)_3Cl_2$ oxidised with PbO_2, which also produced intense chemiluminescence from each cytotoxic during the preliminary oxidising reagent investigation, was therefore investigated individually for each analyte.

2.3.3 Preliminary Imatinib Detection using $Ru(bipy)_3Cl_2/PbO_2$

Systematic method development for chemiluminescence detection of imatinib using $Ru(bipy)_3Cl_2$ oxidised with PbO_2 was undertaken using SIA. The effect of the oxidising reagent volume was investigated via analysis of imatinib (1×10^{-5} M in 50 % acetonitrile) using the conditions in Table 2-35. Oxidising reagent volumes of 10 and 20 µL produced similar net peak areas (696.6 ± 15 mV.s and 691.6 ± 70 mV.s), however 10 µL produced less variation between replicates. 10 µL was therefore selected for subsequent analyses.

Table 2-35. SIA reagents, volumes, and flow rates used to investigate effect of oxidising reagent volume on imatinib chemiluminescence signal using $Ru(bipy)_3ClO_4$ oxidised with PbO_2

Reagent	Composition	Volume (µL)	Flow Rate (µL/s)
Analyte	1×10^{-5} M imatinib in 50 % acetonitrile	50	10
Oxidising Reagent	$Ru(bipy)_3ClO_4$ (1×10^{-3} M in 0.05 M $HClO_4$ in acetonitrile) oxidised with PbO_2 (0.1 g/20 mL)	5-20	10
Carrier Solution	0.05 M $HClO_4$ in acetonitrile	1000	100

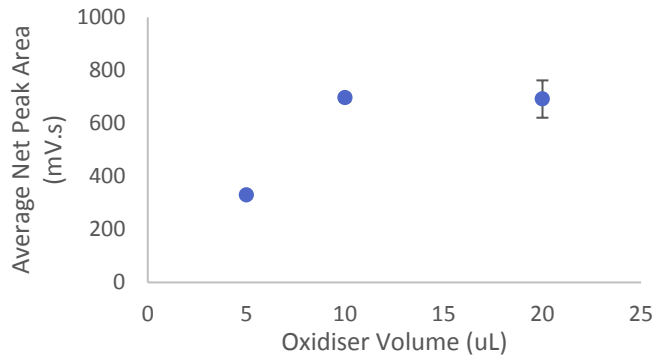

Figure 2-41. Effect of oxidiser volume on the average net chemiluminescence peak area (n=3) obtained via SIA of imatinib (1×10^{-5} M) using $Ru(bipy)_3ClO_4$ (1×10^{-3} M in 0.05 M $HClO_4$ in acetronitrile) as the oxidising reagent. Error bars = ± 1 standard deviation.

The effect of the analyte and oxidising reagent aspiration rate was investigated via analysis of imatinib (1×10^{-5} M in 50 % acetonitrile) using the conditions in Table 2-36. No significant difference in net peak area was obtained using different analyte and oxidising reagent flow rates (Figure 2-42). A flow

rate of 5 µL/s produced the lowest variation between replicates (%RSD 2.16 %) and hence was selected for subsequent analyses.

Table 2-36. SIA reagents, volumes, and flow rates used to investigate effect of analyte and oxidising reagent aspiration flow rate on imatinib chemiluminescence signal using $Ru(bipy)_3ClO_4$ oxidised with PbO_2

Reagent	Composition	Volume (µL)	Flow Rate (µL/s)
Analyte	1 x 10^{-5} M imatinib in 50 % acetonitrile	50	5-20
Oxidising Reagent	$Ru(bipy)_3ClO_4$ (1 x 10^{-3} M in 0.05 M $HClO_4$ in acetonitrile) oxidised with PbO_2 (0.1 g/20 mL)	10	5-20
Carrier Solution	0.05 M $HClO_4$ in acetonitrile	1000	100

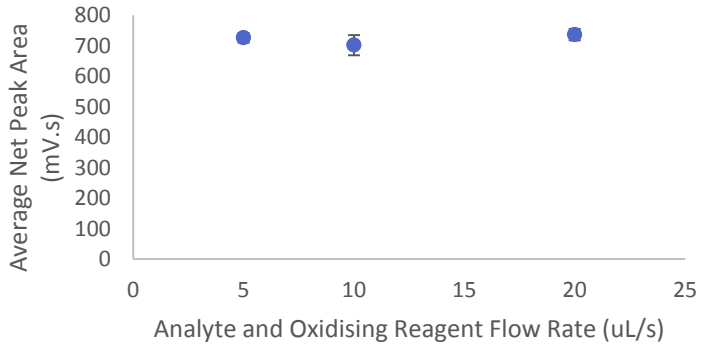

Figure 2-42. Effect of analyte and oxidising reagent aspiration rate on the average net chemiluminescence peak area (n=3) obtained via SIA of imatinib (1 x 10^{-5} M) using $Ru(bipy)_3ClO_4$ (1 x 10^{-3} M in 0.05 M $HClO_4$ in acetronitrile) as the oxidising reagent. Error bars = ± 1 standard deviation.

The effect of the carrier reagent flow rate to the reaction cell was investigated via analysis of imatinib (1 x 10^{-5} M in 50 % acetonitrile) using the conditions in Table 2-37. A flow rate of 100 µL/s produced the highest net peak area (732.7 ± 5 mV.s, Figure 2-43) and the lowest variation (%RSD 0.74 %). Higher flow rates up to 200 µL/s were also investigated, but were found to result in air bubble formation in the line to the detector. 100 µL/s was therefore selected for subsequent analyses.

Table 2-37. SIA reagents, volumes, and flow rates used to investigate effect of analyte and oxidising reagent aspiration flow rate on imatinib chemiluminescence signal using $Ru(bipy)_3ClO_4$ oxidised with PbO_2

Reagent	Composition	Volume (µL)	Flow Rate (µL/s)
Analyte	1 x 10^{-5} M imatinib in 50 % acetonitrile	50	5
Oxidising Reagent	$Ru(bipy)_3ClO_4$ (1 x 10^{-3} M in 0.05 M $HClO_4$ in acetonitrile) oxidised with PbO_2 (0.1 g/20 mL)	10	5
Carrier Solution	0.05 M $HClO_4$ in acetonitrile	1000	50-100

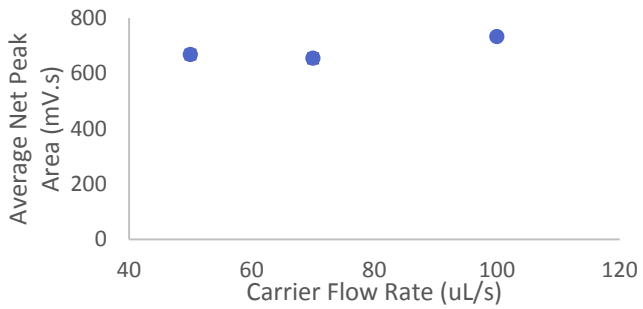

Figure 2-43. Effect of carrier solution flow rate on the average net chemiluminescence peak area (n=3) obtained via SIA of imatinib (1 x 10^{-5} M) using $Ru(bipy)_3ClO_4$ (1 x 10^{-3} M in 0.05 M $HClO_4$ in acetronitrile) as the oxidising reagent. Error bars = ± 1 standard deviation.

The linearity of response obtained using the optimised conditions (Table 2-37) was determined via analysis of imatinib solutions (3 x 10^{-6} M – 1 x 10^{-3} M in 50 % acetonitrile). The resulting net chemiluminescence peak areas obtained are presented plotted against the log_{10} of imatinib concentration Figure 2-44. Chemiluminescence net peak area increased with increasing imatinib concentration up to 5 x 10^{-5} M with reasonable linearity (R^2 0.9818). Above imatinib concentrations of 5 x 10^{-5} M, however, the net chemiluminescence peak area decreased drastically. These solutions were also observed to have a darker translucent yellow colour, compared with the very faint yellow tinge observed in more dilute solutions. It was therefore suggested that high imatinib concentrations may be absorbing the chemiluminescence emission. However, the absorbance profile of imatinib, with maximum at 266 nm, does not overlap with the emission profile of $Ru(bipy)_3$ chemiluminescence, with maximum at 610 nm [122]. It may therefore be more likely that the higher imatinib concentrations resulted in a faster chemiluminescence reaction rate, resulting in the chemiluminescence being detected after the point of maximum emission. At the lowest concentration tested (3 x 10^{-6} M, or 0.002 g/L) a signal lower than the blank was obtained, hence indicating that the limits of detection of the method had been reached. As expected concentrations of cytotoxics in surface waters are in the order of µg/L to ng/L, it is unlikely this detection method would be suitable for imatinib in surface waters. Therefore, imatinib was not persued further as a target analyte in this research.

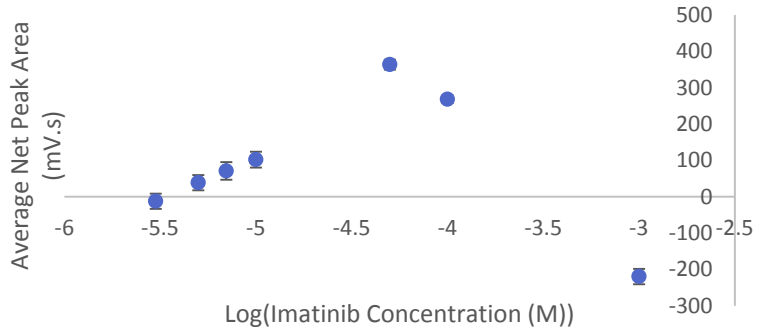

Figure 2-44. Effect of imatinb concentration (on a log_{10} scale) on the average net chemiluminescence peak area (n=3) obtained via SIA of imatinib (1 x 10^{-5} M) using $Ru(bipy)_3ClO_4$ (1 x 10^{-3} M in 0.05 M $HClO_4$ in acetronitrile) as the oxidising reagent. Error bars = ± 1 standard deviation.

2.4 Conclusions

$KMnO_4$, $Ru(bipy)_3Cl_2$, Mn(IV), and $Ce(SO_4)_2$ were investigated for their potential as chemiluminescence oxidising reagents of the cytotoxics cyclophosphamide, 5-fluorouracil, and imatinib using SIA. $Ru(bipy)_3Cl_2$ oxidised with $Ce(SO_4)_2$ produced the most intense chemiluminescence for each cytotoxic, with average net peak areas of 92.4 ± 2 mV.s, 65.0 ± 17 mV.s, and 124 ± 17 mV.s for cyclophosphamide, 5-fluorouracil, and imatinib, respectively. $Ru(bipy)_3Cl_2$ oxidised with PbO_2 also produced intense chemiluminescence from each cytotoxic, with average net peak areas of 62.5 ± 25 mV.s, 110 ± 22 mV.s, and 73.3 ± 26 mV.s for cyclophosphamide, 5-fluorouracil, and imatinib, respectively.

The other oxidising reagents produced less promising results. The maximum average net peak areas obtained when using $KMnO_4$ enhanced with HCl were 2.19 ± 0.8 mV.s, 2.13 ± 2 mV.s, and 37.9 ± 4 mV.s for cyclophosphamide, 5-fluorouracil, and imatinib, respectively. $KMnO_4$ containing sodium thiosulphate produced an average net peak area of 21.2 ± 2 mV.s from imatinib, however signals from cyclophosphamide and 5-fluorouracil were lower than that of the blank. The use of $Ce(SO_4)_2$ alone did not produce chemiluminescence signal greater than the blank for any of the cytotoxics. Mn(IV) produced an average net peak area of 24.5 ± 3 mV.s for imatinib, however signals from cyclophosphamide and 5-fluorouracil were lower than that of the blank.

$Ru(bipy)_3Cl_2$ oxidised with $Ce(SO_4)_2$ was therefore used for method development using SIA. Poor linearity in response was obtained for each cytotoxic. Stopped-flow analysis suggested that this was due to secondary reactions between the cytotoxics and the $Ce(SO_4)_2$. Consequently, this oxidising reagent system was not explored further.

$Ru(bipy)_3Cl_2$ oxidised with PbO_2 was then used in development of chemiluminescence detection of imatinib using SIA. No linearity in response could be obtained, and quenching of the chemiluminescence emission was observed at high imatinib concentrations (> 5 x 10^{-5} M). Consequently, imatinib was not persued further as a target analyte. $Ru(bipy)_3Cl_2/PbO_2$ was then used to develop detection methods for 5-fluorouracil and cyclophosphamide, which will be discussed separately in the following chapters.

Chapter 3:
5-Fluorouracil Detection Using Chemiluminescence

3. 5-Fluorouracil Detection using Chemiluminescence

3.1 Introduction

5-fluorouracil is the active drug of the pro-drug capecitabine, which is one of the most commonly used cytotoxic drugs used for cancer treatment in Australia [11]. 5-fluorouracil acts to indirectly inhibit enzmyes critical in DNA replication and repair, hence leading to cell death. This action is non-specific, affecting both cancerous and non-cancerous cells. 10-20 % of administered 5-fluorouracil is excreted in the urine of patients unchanged, and hence enters wasetwaters [20, 21]. Studies on its removal by wastewater treatment processes have shown mixed results, with some indicating complete removal [35, 48-50, 52], while others suggest high clearance rates [49, 51]. If 5-fluorouracil is indeed able to pass through wastewater treatment it could be present in surface waters, where its non-specific action has the potential to adversely affect aquatic organisms. There have been a few studies on the fate of 5-fluorouracil in surface waters, however this drug was found to be below the limits of detection (0.16-34 ng/L) [50, 59]. This limited knowledge, together with uncertainty as to the removal of 5-fluorouracil from wastewater, gives rise to the need for development of new analysis methodologies for 5-flourouracil in order to answer these questions.

Chemiluminescence is a technique with numerous advantges in environmental analysis, including high sensitivity and selectivity, and capabilities of real-time, in-situ analysis. Chemiluminescence detection of 5-fluorouracil has been reported on three occasions, however none of these have been applied to its detection in surface waters. Sun *et al.* [1, 127] detected 5-fluorouracil in human blood serum using $KMnO_4$ as the chemiluminescence oxidising reagent. The method had limits of detection of 3×10^{-8} g/mL (2.31×10^{-7} M). Dong *et al.* [168] investigated the mechanisms of electrochemiluminescence of 5-fluorouracil and other nitrogen heterocyclic compounds using $Ru(bipy)_3Cl_2$ as the oxidising reagent. As this was an investigative study, however, no limits of detection were reported.

Chapter 2 of this thesis demonstrated that the use of $Ru(bipy)_3Cl_2$ oxidised with either PbO_2 or $Ce(SO_4)_2$ produced the most intense chemiluminescence signal upon reaction with 5-fluorouracil compared to other oxidising reagents. This was most likely due to reaction of the $[Ru(bipy)_3]^{3+}$ with the two secondary amines in 5-fluorouracil, as postulated by Dong *et al.* [168]. Experiments in which $Ce(SO_4)_2$ oxidation of $Ru(bipy)_3Cl_2$ were conducted, however complex chemistry and kinetics were observed, making method development difficult.

This chapter therefore details development of chemiluminescence detection of 5-fluorouracil using $Ru(bipy)_3Cl_2$ oxidised with solid PbO_2 using FIA. Interferences by inorganic cations and anions were assessed, and the method was applied to the detection of 5-fluorouracil in surface waters using solid phase extraction (SPE) clean-up.

3.2 Experimental

3.2.1 Instrumentation

FIA: All experiments were conducted using an in-house-built FIA instrument consisting of a peristaltic pump (John Morris Scientific Pty. Ltd, SA, Australia), a Valco 6-port multiposition valve (Global FIA, Fox Island, WA, USA) as an injection valve, and a 29 mm diameter photomultiplier tube (PMT) (Electron Tubes Limited, 9828SB, Uxbridge, England) encased in a light-proof housing. The PMT voltage was maintained at 800 V by a modular power supply (Electron Tubes Limited, PS1800/12F, Uxbridge, England). A Chebyshev low pass filter was used for all data acquisition, with a cut-off voltage of 20 Hz. The data acquisition sampling rate was 200 Hz. PTFE tubing (1.02 mm I.D.) was used in the peristaltic pump. PTFE tubing (0.02 mm I.D.) (Global FIA, Fox Island, WA, USA) was used as the reaction coil, mixing coil, and for connections between reagents, the valve, and the pump tubing. The reaction coil was prepared by winding PTFE tubing in a planar coil and fixing with blue tack on a piece of cardboard, so that every section of the tubing would be "visible" to the PMT (Figure 3-1). The general instrumental set-up is shown in Figure 3-2.

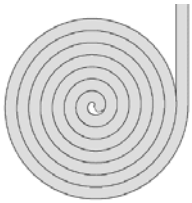

Figure 3-1. Schematic of in-house made reaction coil used for FIA experiments

$Ru(bipy)_3Cl_2$ was injected using a 6-port multiposition valve, as shown in Figure 3-3. The starting position (Position 1) was such that the $Ru(bipy)_3Cl_2$ stream passed through the valve, into a short tube termed the "injection loop", and back out into the $Ru(bipy)_3Cl_2$ pot, while the analyte stream passed straight through the remaining valve ports and through to the PMT. Upon switching of the valve (Position 2), the injection loop became connected to the analyte stream ports, resulting in the contents of the injection loop (the $Ru(bipy)_3Cl_2$) being incorporated into the analyte stream, while the $Ru(bipy)_3Cl_2$ stream continued to flow straight through the valve. The injection loop volume was 23.6 µL.

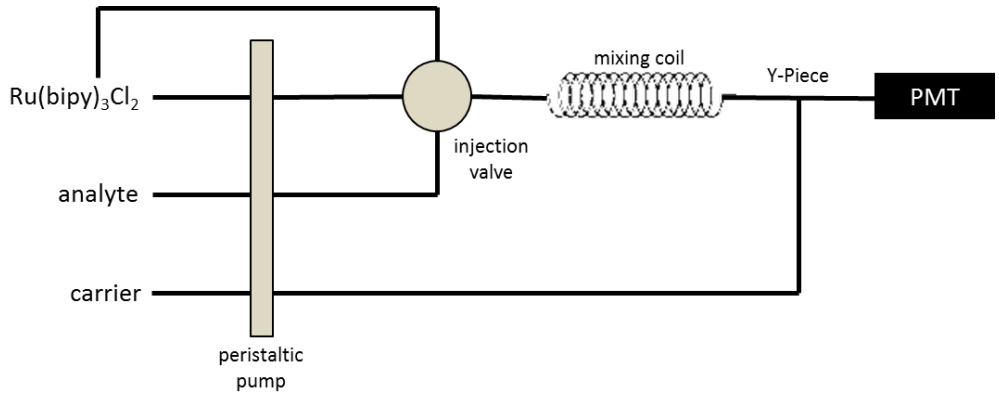

Figure 3-2. Schematic of in-house-built flow injection analysis (FIA) utilised for method development and final detection of 5-fluorouracil

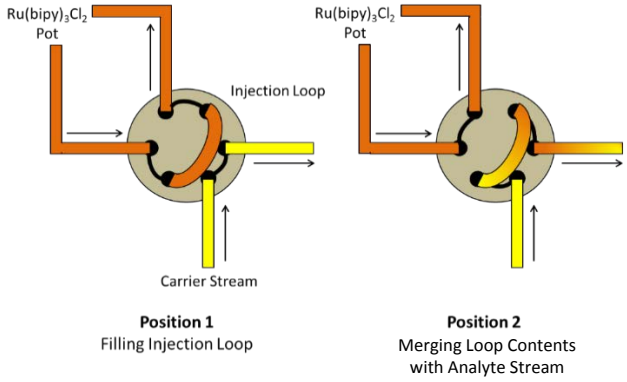

Figure 3-3. Schematic of the multiposition valve used to inject precise volumes of the $Ru(bipy)_3Cl_2$ oxidising reagent into the analyte stream

The instrument was controlled via software written in-house using National Instruments LabVIEW® version 8.2 (Austin, TX, USA). This was based on software written by Osborne *et al.* [181] and Bogdanovic *et al.* [180]. The peristaltic pump flow rate was set manually prior to analysis via control of the pump voltage (Appendix D). The software was then commenced, in which the pump was started. Data acquisition was commenced automatically by the program and continued for 25 seconds unless otherwise stated. After 5 seconds the valve was switched to inject the $Ru(bipy)_3Cl_2$ into the carrier stream. After 25 seconds the data acquisition was halted and the valve switched back to its original position. A time delay of 5 seconds between data acquisition for replicates was utilised, however reagent flow was continual between all replicates. This sequence has been summarised visually in Figure 3-4. Loading of the reagent lines with the desired reagents was conducted prior to each analysis by manually running the pump at 10 mL/min for 30 seconds. After each analysis these lines were flushed with deionised water by manually running the pump 10 mL/min for 30 seconds. During analysis the average flow rate of each reagent was 2.6 mL/min, with a total flow rate through the system of 5.1 mL/min.

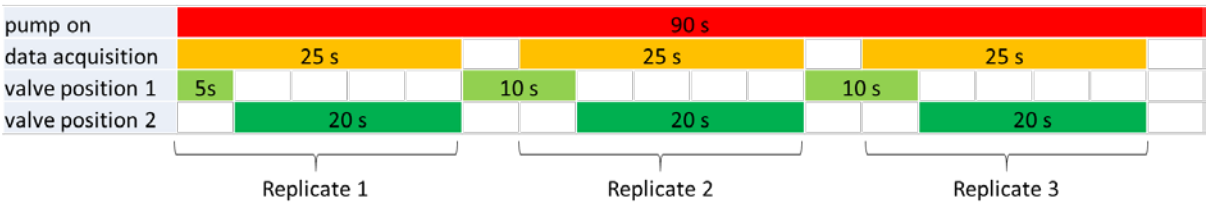

Figure 3-4. Timing of pump, data acquisition, and valve positions during developed FIA run consisting of three replicates

The flow rate of each line used in the peristaltic pump, as well as the total system flow rate, was measured daily. Each line was filled with deionised water by pumping this solution through the pump at 10 mL/min for 30 seconds. The volume of water delivered by a given line in one minute was collected separately in a pre-weighed glass vial and weighed. This was repeated five times for each line and an average mass calculated. The density of the water was taken to be 1 g/mL.

A sodium oxalate calibration was also conducted daily in order to monitor the sensitivity and correct functioning of the instrument. Sodium oxalate solutions (1×10^{-5} M – 1×10^{-4} M) were prepared fresh weekly and analysed in triplicate using the reagent conditions described in Table 3-1.

Table 3-1. FIA-chemiluminescence reagent conditions used for daily analysis of sodium oxalate

Reagent	**Composition**
Analyte	Sodium oxalate (1×10^{-5} – 1×10^{-4} M) in 0.05 M H_2SO_4
Oxidising Reagent	$Ru(bipy)_3Cl_2$ (1×10^{-3} M in 0.05 M $HClO_4$ in acetonitrile) oxidised with solid PbO_2 (0.1 g/20 mL)
0.05 M H_2SO_4	0.05 M H_2SO_4

The raw chemiluminescence signal of voltage (mV) over data acquisition time (s) was imported into Origin® version 9.0 (Northampton, MA, USA). Baseline subtraction using a constant value of the minimum recorded voltage of that replicate was conducted before plots were constructed. The peak area and maximum peak intensity of each baseline-subtracted plot was calculated and the average and standard deviation of these values for each experiment were determined (n=3). All analyses were performed in triplicate.

UHPLC: UHPLC analysis was conducted using a Thermo Scientific UHPLC+ Focused system coupled with a UV diode Array detection (Thermo Scientific, Australia). The column was a Perkin Elmer Phenyl-Hexyl column (particle size: 2.7 µm, ID: 2.1 x 100 mm, Australia). Gradient elution using 0.1 % formic acid in water (A) and methanol (B) was utilised with the following program: 0-0.5 min: 95 % A, 0.5-2.5 min: ramp to 5 % A, 2.5-15 min: 5 % A. Flow rate was 0.4 mL/min. Detection wavelength was 266 nm. Injection volume was 2.0 µL. Column temperature was 25.0 °C. Samples were filtered through 0.22 µm PTFE syringe filters (Adelab Scientific, Thebarton, SA) prior to analysis.

3.2.2 Chemicals and Reagents

All reagents were analytical grade unless otherwise stated. 5-fluorouracil, Triton X100, sodium oxalate, calcium chloride dehydrate, and humic acids (technical grade) were purchased from Sigma Aldrich Pty, Ltd (Castle Hill, NSW, Australia). Tris-2,2'-bipyridyl ruthenium (II) chloride hexahydrate was purchased from Strem Chemicals (Newburyport, MA, USA). Sulfuric acid (98 %), lead dioxide, formaldehyde, formic acid, orthophosphoric acid, sodium thiosulfate, potassium chloride, sodium chloride, iron (III) chloride hexahydrate, and disodium hydrogen phosphate were purchased from Chem-Supply (Gillman, SA, Australia). Hydrochloric acid (37 %) was purchased from Choice Analytical (Thornleigh, NSW, Australia). Tris(hydroxymethyl)aminomethane, magnesium chloride, sodium hydrogen carbonate, and sodium dihydrogen phosphate were purchased from Merck Pty. Ltd (Bayswater, Victoria, Australia). Sodium borate decahydrate was purchased from Amersham Australia Pty. Ltd (Baulkham Hills, NSW, Australia). All solutions were prepared using deionised water unless otherwise stated. Acetonitrile (HPLC grade) was purchased from Rowe Scientific Pty. Ltd (Lonsdale, SA, Australia). Potassium iodide and potassium bromide were purchased from Ajax Chemicals (Sydney, NSW, Australia).

3.2.3 Standards

5-fluorouracil stock solutions (1×10^{-3} M in distilled water) were prepared daily and stored in sealed glass bottles in the absence of light. Standard solutions of 5-fluorouracil (1×10^{-7} M to 1×10^{-3} M) were prepared immediately prior to analysis by serial dilution of the stock in deionised water using glassware.

3.2.4 Oxidising Reagent

All solutions were prepared using ultra-pure water (18 MΩ) unless otherwise stated. $[Ru(bipy)_3]Cl_2$ was prepared by mixing tris(2,2'-bipyridyl)ruthenium(II) chloride (1×10^{-3} M in 0.1 M H_2SO_4) with solid lead dioxide (0.1 g/20 mL), resulting in a colour change from orange to green, followed by removal of the solid material via filtration using a 0.45 µm PFTE syringe filter (Adelab Scientific, Thebarton, SA).

3.2.5 Carrier Solutions

The effect of the carrier solution pH was investigated by preparation of distilled water adjusted to pH between 1 and 12 using either H_2SO_4 or NaOH. The effect of the carrier composition was investigated via preparation of various basic aqueous buffers, namely phosphate buffer, borate buffer, tris buffer, and bicarbonate buffer. pH 7 phosphate buffer was prepared by mixing 115.4 mL of 0.1 M Na_2HPO_4 with 84.6 mL 0.1 M NaH_2PO_4. pH 8 phosphate buffer was prepared by mixing 233 mL of 0.1 M Na_2HPO_4 with 17 mL 0.1 M NaH_2PO_4. Bicarbonate buffer (pH 11) was prepared by diluting a mixture of 100 mL 0.1 M $NaHCO_3$ and 45.4 mL 0.2 M NaOH to 200 mL with distilled water. Borate buffer (pH 10) was prepared by diluting a mixture of 100 mL of 0.1 M $Na_2B_4O_7.10H_2O$ (borax) and 36.6 mL of 0.4 M NaOH

to 200 mL with distilled water. Tris buffer (pH 9) was prepared by diluting a mixture of 100 mL of 0.1 M tris(hydroxymethyl)aminomethane (tris) and 11.4 mL of 0.1 M HCl to 200 mL with distilled water. This is summarised in Table 3-2. The pH of each buffer was confirmed after each preparation using a Mettler Toledo S220 SevenCompact™ pH metre (Rowe Scientific Pty. Ltd, Adelaide, Australia).

Table 3-2. Stock solutions and their corresponding volumes used to prepare various basic buffer carrier solutions

	Solution	Concentration (M)	Volume (mL)	Solution	Concentration (M)	Volume (mL)
phosphate pH 7	Na_2HPO_4	0.1	115.4	NaH_2PO_4	0.1	84.6
phosphate pH 8	Na_2HPO_4	0.1	233	NaH_2PO_4	0.1	17
tris pH 9	tris	0.1	100	HCl	0.1	11.4
Borate pH 10	borax	0.1	100	NaOH	0.4	36.6
Bicarbonate pH 11	$NaHCO_3$	0.1	100	NaOH	0.2	45.4

3.2.6 Interference Studies and Real Sample Analysis

Separate 1 x 10^{-3} M stock solutions of NaCl, $MgCl_2$, $FeCl_3$, $CuCl_2$, $CaCl_2$, KI, KBr, and KCl were prepared via dissolution in deionised water. 5-fluorouracil solutions (1 x 10^{-6} M) were spiked separately with these stocks to final salt concentrations between 1 x 10^{-8} M to 1 x 10^{-4} M. Lake water was obtained as a grab sample (1 L) from the Flinders University Lake (Adelaide, South Australia) and stored in a sealed glass bottle in the absence of light. Tap water (1 L) was obtained from Flinders University and stored in a sealed glass bottle in the absence of light. 25 µL of a 1 x 10^{-3} M 5-fluorouracil stock was then spiked into 250 mL aliquots of the lake and tap water to give final 5-fluorouracil concentrations of 1 x 10^{-6} M in each. Solid phase extraction (SPE) of each solution was conducted off-line prior to analysis using STRATA-X-A polymeric strong anion exchange resins or STRATA-X-C strong cation exchange resin from Phenomenex (Lane Cove, NSW, Australia). These resins were conditioned with 3 mL methanol and washed with 3 mL deionised water prior to addition of 3 mL of the analyte solution. This was repeated 3 times for each replicate to obtain a final analyte volume of 9 mL for chemiluminescence analysis.

3.3 Results and Discussion

3.3.1 Method Development

3.3.1.1 Effect of Carrier Composition and pH

Chemiluminescence reactions are strongly influenced by solution pH [195], and hence the effect of the pH of the carrier solution was investigated. This was achieved via analysis using carrier solutions adjusted to pH levels between 1.39 and 11.18 using H_2SO_4 or NaOH, with the resulting net peak areas given in Figure 3-5. There was no significant difference in peak areas obtained using pH 3-10.5. pH 1.39, however, produced a signal lower than the blank, while pH 11.18 produced the largest net peak area of 2544 ± 84 mV.s. $[Ru(bipy)_3]^{3+}$ chemiluminescence is generally thought to occur via production

of hydroxide ions capable of reacting with the Ru^{3+} species, and hence most experiments using this reagent are conducted at pH levels of less than 7 [195]. Oxidation of amines, such as amino acids, however, has been shown to occur through the anion of the amino acid, and hence for these analytes the $[Ru(bipy)_3]^{3+}$ reaction is faster when conducted at pH levels greater than or equal to the pKa of the analyte [195]. This is due to the higher ionisation potential associated with the protonated form of an amine compared to the neutral form, as is also demonstrated by the greater sensitivity of the technique to tertiary amines than secondary amines [195]. The pKa of 5-fluorouracil is 8.02, therefore at pH levels greater than this value the 5-fluorouracil would be present in protonated form, which has a higher ionisation potential than the neutral form, and hence would be expected to produce a larger chemiluminescence signal. At pH 11.8, however, peak-splitting was observed (Figure 3-6). This was most likely the result of poor miscibility between the highly alkaline carrier solution and the acidic oxidising reagent, resulting in the formation of two separate mixing zones. pH 10.36 was therefore selected for subsequent analyses.

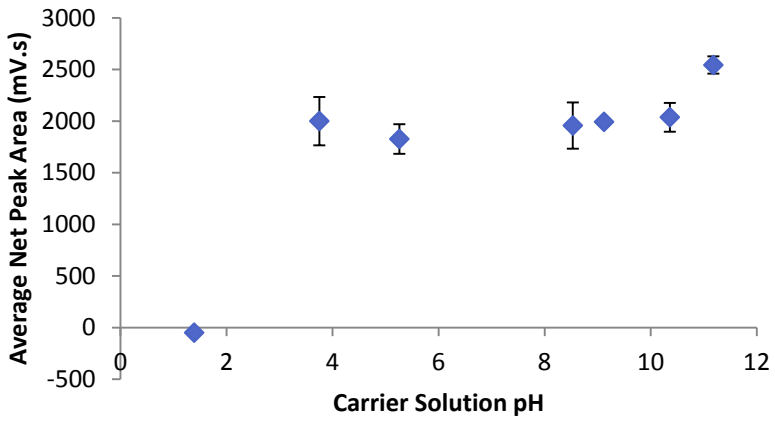

Figure 3-5. Effect of carrier solution pH (deionised water adjusted with either NaOH or H_2SO_4) on the average net peak area (n=3) obtained via FIA chemiluminescence of 5-fluorouracil ($1x10^{-5}$ M in deionised water) using $Ru(bipy)_3Cl_2$ (1 x 10-3 M in 0.075 M H_2SO_4) as the oxidising reagent. Error bars = ± 1 standard deviation.

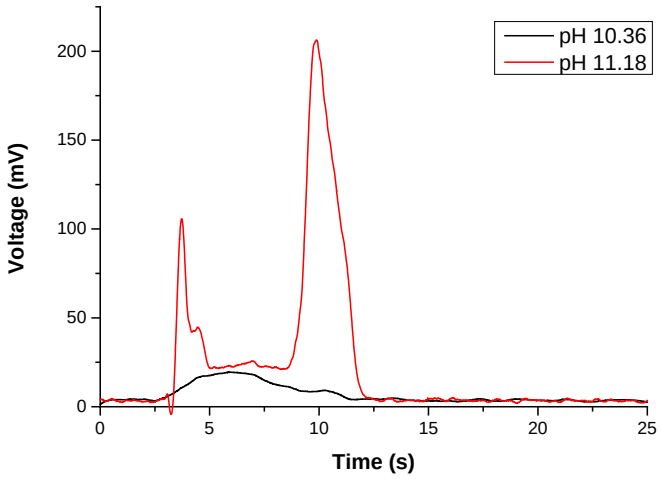

Figure 3-6. Comparison of chemiluminescence peaks obtained via FIA chemiluminescence analysis of deionised water using $Ru(bipy)_3Cl_2$ (1×10^{-3} M in 0.075 M H_2SO_4) as the oxidising reagent and deionised water adjusted to either pH 10.36 or 11.18 using NaOH

Despite the large net peak areas observed when using a carrier with pH of 10.38, no linear relationship between 5-fluorouracil concentration and peak area could be obtained. This could have been due to changes in the pH of the reaction mixture upon mixing with different concentrations of 5-fluorouracil, resulting in varying chemiluminescence reactions. Buffered carriers that can tightly control the reaction mixture pH more effectively were therefore explored. Various basic buffers were tested, namely phosphate (pH 7 and 8), tris (pH 9), borate (pH 10), and bicarbonate (pH 11) buffers, all with a concentration of 0.05 M. The resulting average net peak areas are given in Figure 3-7.

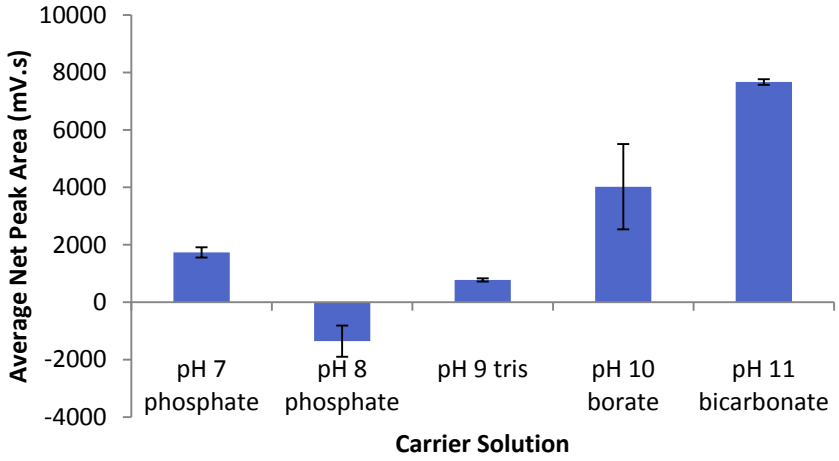

Figure 3-7. Average signal-to-blank ratios of peak area of FIA chemiluminescence signals from aqueous 5-fluorouracil (1×10^{-6} M) obtained using $Ru(bipy)_3Cl_2$ (1×10^{-3} M in 0.075 M H_2SO_4) as the oxidant and various aqueous buffers (0.05 M) as the carrier solution. Error bars = ± 1 standard deviation.

Again, pH 11 produced the largest signal, with a net peak area of 7668 ± 99 mV.s, however no peak splitting was observed. pH 11 bicarbonate buffer was therefore used as the carrier solution for all subsequent analyses.

3.3.1.2 *Effect of Carrier Concentration*

Bicarbonate buffer (pH 11) concentrations from 0.01 M to 0.05 M were then tested, with resulting average net peak areas given in Figure 3-8. The maximum net chemiluminescence peak area of 6849 mV.s was obtained when using a buffer concentration of 0.035 M. However, at this concentration and below a double peak was obtained, as demonstrated in Figure 3-9. This indicated that the buffering capacity of the solution had been reached and hence non-uniform mixing was occurring between the carrier solution, sample, and oxidising reagent. This could result in decreased reproducibility between replicates. 0.05 M was the lowest phosphate concentration at which a single peak was obtained, and hence, in order to optimise reproducibility, this concentration was selected for all subsequent analyses.

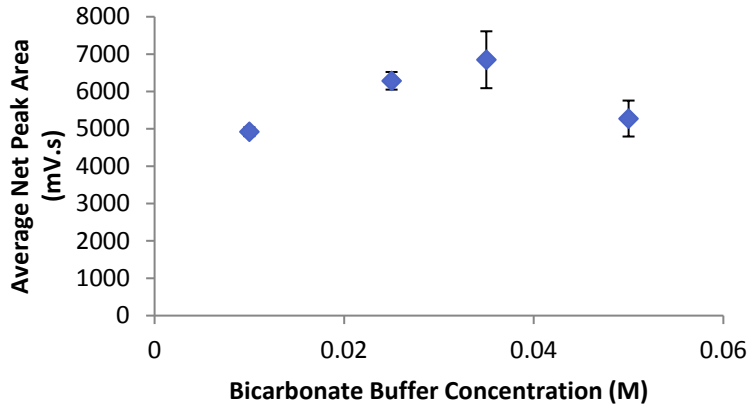

Figure 3-8. Effect of bicarbonate buffer (pH 11) concentration (M) on the average net chemiluminescence peak area (n=3) obtained via FIA of 5-fluorouracil (1 x10^{-6} M in distilled water) using $Ru(bipy)_3Cl_2$ (1 x 10^{-3} M in 0.05 M H_2SO_4) as the oxidising reagent. Error bars = ± 1 standard deviation.

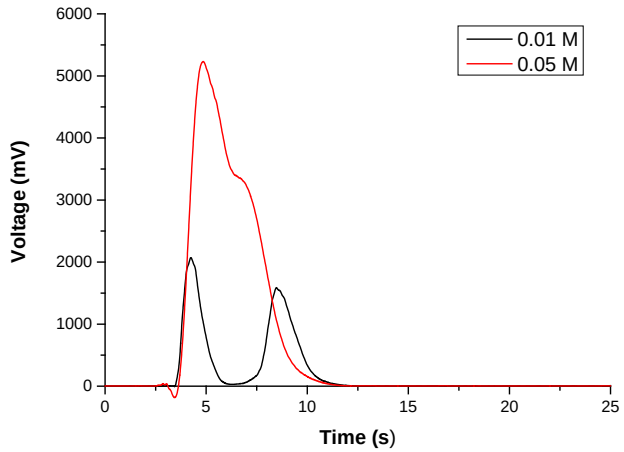

Figure 3-9. Comparison of chemiluminescence peak shape obtained FIA of 5-fluorouracil (1 x10^{-6} M in distilled water) using $Ru(bipy)_3Cl_2$ (1 x 10^{-3} M in 0.05 M H_2SO_4) as the oxidising reagent.

3.3.1.3 *Effect of $Ru(bipy)_3Cl_2$ Concentration*

The effect of the concentration of $Ru(bipy)_3Cl_2$ on the 5-fluorouracil chemiluminescence signal was investigated using $Ru(bipy)_3Cl_2$ concentrations from 1 x 10^{-4} M to 2 x 10^{-3} M, with resulting net peak areas given in Figure 3-10. As the $Ru(bipy)_3Cl_2$ concentration was increased the net

chemiluminescence peak area increased. At concentrations above 4 x 10^{-4} M splitting of the peaks into two began to occur. In order to prevent this 4 x 10^{-4} M $Ru(bipy)_3Cl_2$ was selected for all subsequent analyses.

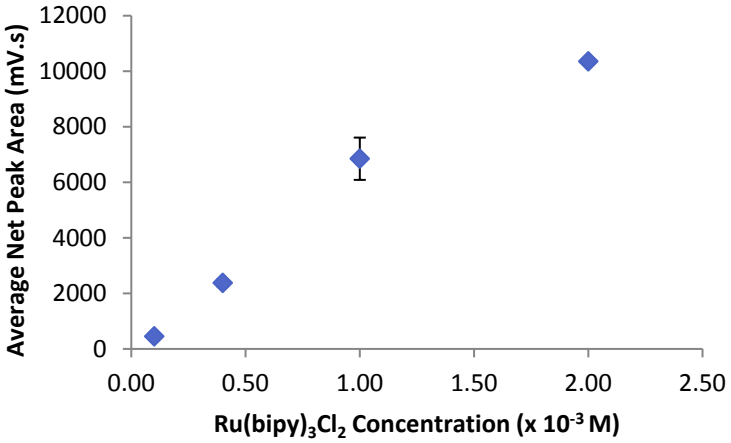

Figure 3-10. Effect of $Ru(bipy)_3Cl_2$ concentration on average net peak area obtained via FIA-chemiluminescence of 5-fluorouracil (1x10^{-6} M) using $Ru(bipy)_3Cl_2$ (1 x 10^{-3} M in 0.05 H_2SO_4) as the oxidising solution and bicarbonate buffer (0.05 M, pH 11) as the carrier solution. Error bars = ± 1 standard deviation.

3.3.1.4 Effect of $Ru(bipy)_3Cl_2$ Acid Concentration

The effect of the acid concentration in the $Ru(bipy)_3Cl_2$ solution was investigated via analysis of 5-fluorouracil using $Ru(bipy)_3Cl_2$ prepared in H_2SO_4 concentrations from 0.01 M and 0.1 M, with resulting signal-to-blank ratios of peak area given in Figure 3-11. As the H_2SO_4 concentration increased the net peak area decreased. It was also observed that when using H_2SO_4 concentrations higher than 0.01 M chemiluminescence peak splitting occurred as shown in Figure 3-12. This was most likely due to a high pH gradient between the oxidising reagent and the basic carrier solution preventing complete mixing of the reagents. It was therefore decided that 0.01 M H_2SO_4 be used for subsequent analyses. Concentrations below 0.01 M were also tested, however at these concentrations conversion to the $[Ru(bipy)_3]^{2+}$ to $[Ru(bipy)_3]^{3+}$ did not occur, as observed by the solution remaining orange in colour.

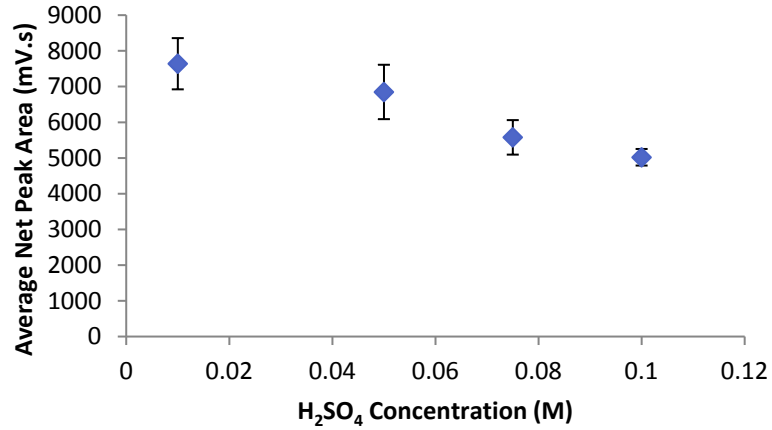

Figure 3-11. Effect of $Ru(bipy)_3Cl_2$ acid concentration on the average net peak area (n=3) obtained via FIA-chemiluminescence analysis of 5-fluorouracil (1x10^{-6} M) using $Ru(bipy)_3Cl_2$ (1 x 10^{-3} M in H_2SO_4) as the oxidiser and bicarbonate buffer (0.01 M, pH 11) as the carrier solution. Error bars = ± 1 standard deviation.

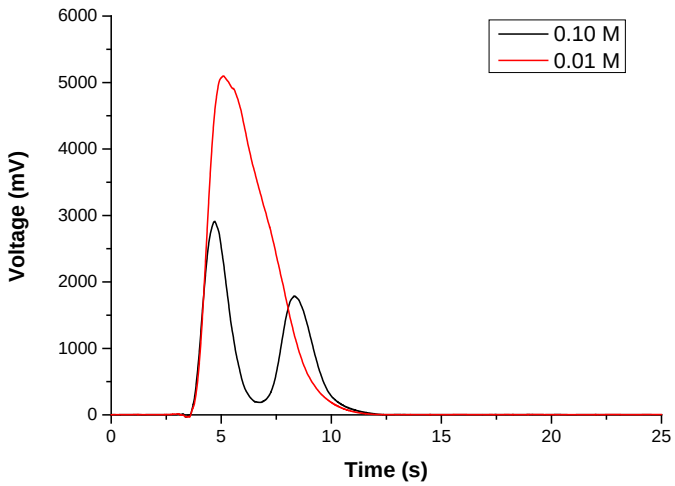

Figure 3-12. Comparison of chemiluminescence peak shape obtained via FIA-chemiluminescence analysis of 5-fluorouracil ($1x10^{-6}$ M) using $Ru(bipy)_3Cl_2$ (1×10^{-3} M in H_2SO_4) as the oxidiser and bicarbonate buffer (0.01 M, pH 11) as the carrier solution.

3.3.2 Method Validation

Aqueous 5-fluorouracil solutions (1×10^{-7} M to 1×10^{-3} M) of various concentrations were than analysed using the developed conditions (Table 3-3). The resulting calibration curve of the average peak area versus 5-fluorouracil concentration, both on a log-scale, is given in Figure 3-13. The blank signal was found to be constant over time, hence allowing for raw peak areas, rather than signal-to-blank ratios, to be utilised. In general, the peak area increased with increasing 5-fluorouracil concentration, however at concentrations above 1×10^{-5} M the signal-to-blank ratio decreased rapidly with increasing concentration (data not shown). It was hypothesised that this was due to quenching of the chemiluminescence reaction, which is known for uracil compounds [196]. When decreasing the 5-fluorouracil concentration below 4×10^{-7} M the chemiluminescence peak areas began to level off, despite still being larger than that of the blank, and hence a linear range between 4×10^{-7} M and 1×10^{-5} M, was established. This corresponded to a limit of detection (LOD) of 6.06×10^{-8} M (blank + 3σ) or 7.89×10^{-9} g.mL^{-1} , which is approximately 4 times lower than the LOD of 3×10^{-8} g/mL previously reported by Sun *et al.* using $KMnO_4$ [1]. The limit of quantification (LOQ) was determined to be 1.16×10^{-6} M (blank + 10σ) or 1.51×10^{-7} g.mL^{-1}.

Table 3-3. Final FIA-chemiluminescence reagent conditions found to be optimal for 5-fluorouracil detection

Reagent	Composition
Analyte	5-fluorouracil (1×10^{-7} – 1×10^{-3} M) in deionised water
Oxidising Reagent	$Ru(bipy)_3Cl_2$ (4×10^{-4} M in 0.01 M H_2SO_4) oxidised with solid PbO_2 (0.1 g/20 mL)
Carrier Solution	Bicarbonate buffer (pH 11, 0.05 M)

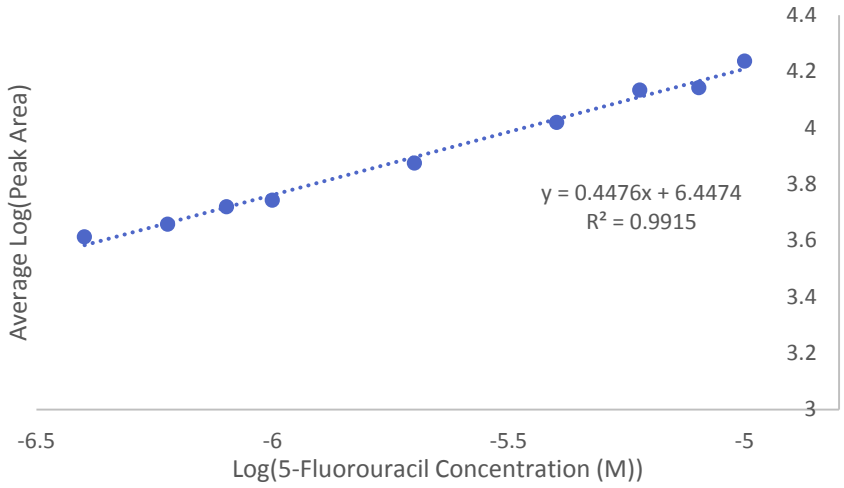

Figure 3-13. Average chemiluminescence signal versus 5-fluorouracil concentration (M), each on a log-scale, obtained via FIA-chemiluminescence analysis of 5-fluorouracil in deionised water, using $Ru(bipy)_3Cl_2$ ($4x10^{-4}$ M in 0.01 M H_2SO_4) oxidised in-line using PbO_2 (0.1 g/20 mL) as the oxidising reagent and bicarbonate buffer (0.05 M, pH 11) as the carrier solution. Error bars = ± 1 standard deviation.

The intra- and inter- day precision were determined by calculating the relative standard deviation (%RSD) of net peak areas obtained from analysis of 5-fluorouracil solutions (4×10^{-7} M – 1×10^{-5} M in distilled water) using the developed conditions on the same day and on different days, using freshly-prepared oxidant, 5-fluorouracil, and carrier solutions, and were found to be 0.08-1 % and 0.006-3 %, respectively.

Table 3-4. Figures of merit for 5-fluorouracil analysis using the developed FIA-chemiluminescence detection method utilising $Ru(bipy)_3Cl_2$ ($4x10^{-4}$ M in 0.01 M H_2SO_4) oxidised with solid PbO_2 (0.1 g/20 mL) as the oxidant and bicarbonate buffer (0.05 M, pH 11) as the carrier solution. This is based on the plot of the average net peak area versus 5-fluorouracil concentration, both on a log10 scale.

Calibration Function	Correlation Coefficient	Linear Range (M)	Intra-day Precision (%RSD)	Inter-day Precision (%RSD)	LOD (M)	LOQ (M)
$\log_{10}A = 0.4476\log[5\text{-fluorouracil}] + 6.4474$	0.9915	$4x10^{-7} – 1x10^{-5}$	0.08 - 1	0.006 - 3	6.06×10^{-8}	1.16×10^{-6}

The accuracy of the developed method was assessed via analysis of blind 5-fluorouracil solutions (1×10^{-7} – 1×10^{-5} M in distilled water) and calculation of their concentrations using a calibration curve constructed using 5-fluorouracil standard solutions prepared on the same day. The percentage recoveries of the lower and upper limits of the 95 % confidence interval calculated for the blind samples are given in Table 3-5.

Table 3-5. Comparison of expected 5-fluorouracil concentrations of unknown solutions and their calculated 95 % confidence intervals (α=0.05)

	Calculated 95 % Confidence Interval (M)		Recovery (%)	
Expected 5-fluorouracil Concentration (M)	**Lower Limit**	**Upper Limit**	**Lower Limit**	**Upper Limit**
8×10^{-6}	8.15×10^{-6}	8.16×10^{-6}	102	102
2×10^{-7}	2.02×10^{-7}	2.05×10^{-7}	101	102
1×10^{-6}	7.48×10^{-7}	7.53×10^{-7}	74.8	75.3

The percentage recoveries obtained for the 8×10^{-6} M and 2×10^{-7} M 5-fluorouracil solutions were between 101 and 102 %, which indicated that the developed method and calibration curve had high accuracy. The recovery obtained for the 1×10^{-6} M standard, however, was much lower, being between 74.8 and 75.3 %. This standard was prepared by using a 1-10 mL glass graduated pipette to dilute 1 mL of a 1×10^{-4} M stock solution to 100 mL, and hence the volume delivered was at the lowest limit of the accuracy of this pipette. This may have introduced error in the dilution, and hence could have contributed to the accuracy of the recoveries determined.

3.3.3 Interference Studies

Chemiluminescence is often affected by the presence of cations and anions in the sample matrix [197]. Consequently, 5-fluorouracil solutions (1×10^{-6} M in deionised water) spiked with increasing concentrations common interfering ions were analysed using the developed method (Table 3-3) in order to assess these possible interferences. The net peak areas relative to an un-spiked 5-fluorouracil solution (1×10^{-6} M) are given in Appendix E. The tolerable ratio of 5-fluorouracil to ion concentration that resulted in a decrease in net chemiluminescence peak area of at least 5 % compared with an un-spiked 5-fluorouracil solution are given in Table 3-6 and Table 3-7. Of the cations tested, K^+ produced the lowest interference, needing to be present at a 10-fold concentration compared with 5-fluorouracil to decrease the net chemiluminescence peak area by 5 %. Fe^{3+} and Na^+ resulted in stronger interference, needing to be present at 0.1-fold the concentration of 5-fluorouracil to decrease the signal by 5 %. Ca^{2+} produced a different trend to the other ions, with all concentrations tested (down to 1×10^{-7} M, 0.1-fold of 5-fluorouracil concentration) resulting in an increase in chemiluminescence signal by at least 140 % (see Appendix E). Of the anions, Cl^- and I^- produced similar results, both needing to be present 10-fold with respect to 5-fluorouracil concentration to cause chemiluminescence quenching. All concentrations of Br^- tested (1×10^{-7} M to 1×10^{-3} M) produced quenching of at least 36 % (see Appendix E). This was an unexpected result because halides are generally thought to produce negligible interferences in chemiluminescence detection [197, 198]. This is therefore an area than needs further research.

Table 3-6. Tolerable ratio of 5-fluorouoracil to cation concentration resulting in a decrease in net chemiluminescence peak area of at least 5 %.

	Tolerable Ratio (5-fluorouracil:Ion)
Na^+	0.1
K^+	10
Mg^{2+}	1
Ca^{2+}	0.1*
Fe^{3+}	0.1

*all concentrations tested (1 x 10^{-7} M to 1 x 10^{-3} M) resulted in an increase in chemiluminescence signal

Table 3-7. Tolerable ratio of 5-fluorouoracil to anion concentration resulting in a decrease in net chemiluminescence peak area of at least 5 %.

	Tolerable Ratio (5-fluorouracil:Ion)
Cl^-	10
Br^-	0.1*
I^-	10

*all concentrations tested (1 x 10^{-7} M to 1 x 10^{-3} M) resulted in quenching of the chemiluminescence signal

As both anions and cations appeared to cuase interferences when detecting 5-fluorouracil using chemiluminescence, SPE clean-up of the sample was investigated. 5-fluorouracil (1 x 10^{-6} M) spiked with NaCl (1 x 10^{-4} M) was filtered through a strong anion exchange SPE filter (STRATA-X-A) followed by a strong cation exchange SPE filter (STRATA-X-A) prior to chemiluminescence analysis using the conditions in Table 3-3. The net chemiluminescence peak area was increased from 43 % of that of un-spiked 5-fluorouracil to 120 % using this SPE clean-up (Figure 3-14). This indicated that the strong anion and strong cation exchange had succesffully removed the ionic interferences. The relative signal of greater than 100 % obtained using the SPE filter was most likely due to residual methanol from the SPE conditioning step remaining in the sample.

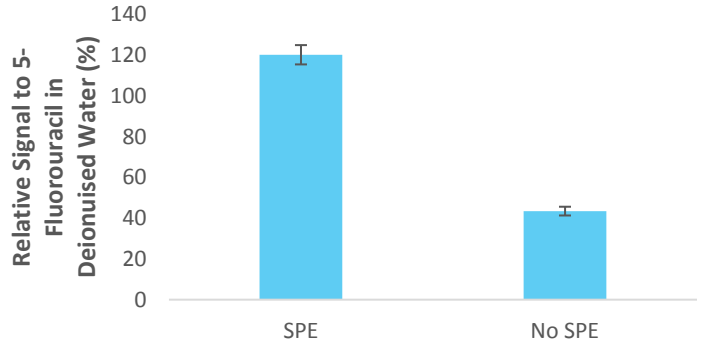

Figure 3-14. Chemiluminescence peak areas of 5-fluorouracil (1 x 10^{-6} M in deionised water) spiked with NaCl (1 x 10^{-4} M in deionised water) and analysed before and after sequential strong anion exchange SPE (STRATA-X-A) and strong cation exchange SPE (STRATA-X-C resin), relative to that of 5-fluorouracil in non-spiked deionised water. Error bars = ± 1 standard deviation.

3.3.4 Application to Surface Waters

The developed FIA-CL method was then applied to the analysis of tap water and lake water samples spiked with a known concentration of 5-fluorouracil (1 x 10^{-6} M). When no SPE clean-up procedure

was used both water samples produced blank signals lower than those obtained from 5-fluorouracil prepared in deionised water, with relative signals of 33.0 % and 51.1 %, respectively (Figure 3-15). The use of strong anion exchange SPE followed by strong cation exchange SPE prior to chemiluminescence analysis was found to increase the signals from 5-fluorouracil in tap water and lake water up to 73.5 % and 65.9 % of 5-fluorouracil in deionised water. This suggested the SPE clean-up was effective in removing inorganic ion interferences, but that there may still be organic interferences present in the samples.

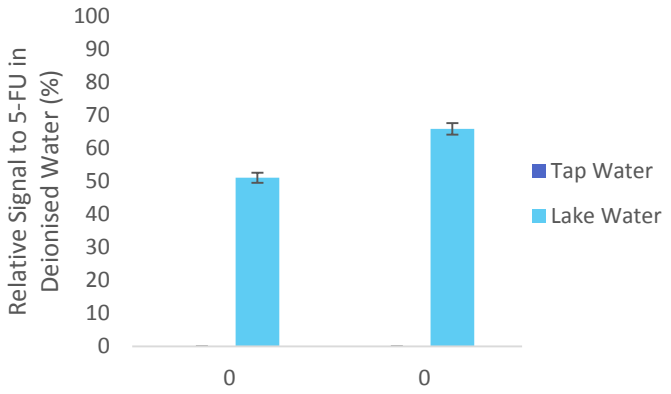

Figure 3-15. Chemiluminescence peak areas of 5-fluorouracil (1 x 10^{-6} M) in tap water and lake water analysed before and after sequential anion and cation exchange SPE, relative to that of 5-fluorouracil in deionised water. Error bars = ± 1 standard deviation.

UHPLC separation of tap and lake water spiked with 5-fluorouracil was then conducted to determine if the 5-fluorouracil could be separated from these interferences. 5-fluorouracil was eluted at 0.95 minutes, which was well separated from all other compounds; being eluted predominantly after 5 minutes (Figure 3-14). It would therefore be reasonable to separate 5-fluorouracil from organic interferences chromatographically, hence indicating that chemiluminescence detection would be viable for use in real surface water samples.

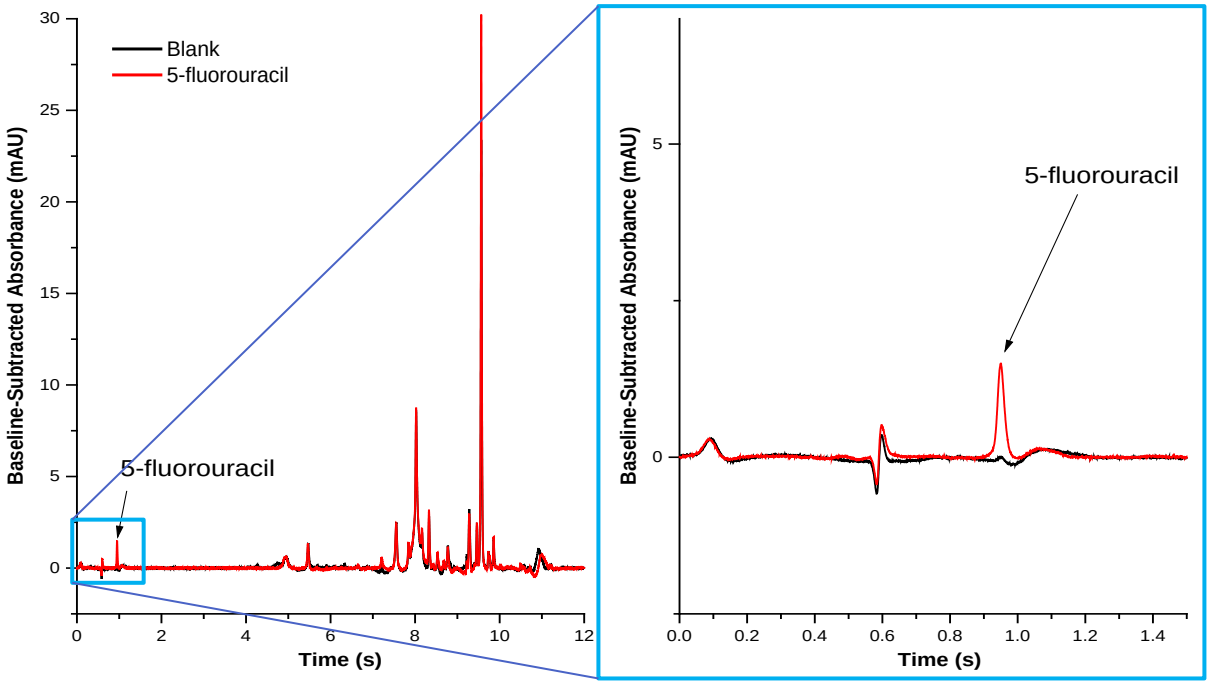

Figure 3-16. UHPLC separation of 5-fluorouoracil (1 x 10^{-6} M) from organic components of lake water

3.4 Conclusions

A new chemiluminescence detection method for 5-fluorouracil was developed using FIA and the tris-2,2'-bipyridyl ruthenium (II) chloride ($Ru(bipy)_3Cl_2$) oxidising reagent prepared using PbO_2. The limit of detection was 6.06 x 10^{-8} M, which is a 4-fold decrease compared with previously reported methods using permanganate-based reagents [1]. Quenching of the chemiluminescence signal obtained using this method was observed in the presence of cations and anions, which could be effectively removed using sequential strong cation and anion exchange SPE. 5-fluorouracil spiked into lake and tap water samples could be easily separated from remaining organic interferences using UHPLC, and hence this method would be highly applicable to the determination of 5-fluorouracil in surface waters.

Chapter 4:

Cyclophosphamide Detection Using Chemiluminescence

4. Cyclophosphamide Detection using Chemiluminescence

4.1 Introduction

Cyclophosphamide is one of the most commonly used cytotoxic drugs used world-wide, being used to treat Hodgkins lymphoma, various types of leukaemia, ovarian, breast, and lung cancers [12]. It brings about its effect via alkylation of nitrogen bases in the DNA structure, resulting in disruptions to DNA replication and translation, and hence cell death. This action is non-specific, affecting both canerous and non-cancerous cells [5, 10]. Cyclophosphamide is therefore classified as a restricted carcinogen in Australia. In the body cyclophosphamide is metabolised to 4-hydroxycyclophosphamide as the major metabolite [13]. However, 5-25 % and 31-66 % of administered cyclophosphamide is excreted unchanged in the urine and faeces, respectively, hence resulting in its presence in wastewater. Its removal in wastewater treatment plants (WWTPs) has been found to be poor, being resistant to biodegradation and photodegradation [29]. This results in the release of cyclophosphamide into surface waters, where it has been detected at concentrations between 50 pg/L and 65 ng/L up to 6 km downstream from WWTP release points [9, 25, 28, 41, 55-58]. Here the non-specific action of cyclophosphamide has the potential to cause harm to adversely affect aquatic organisms. Only one study on the stability if cyclophosphamide in surface waters has been conducted, in which cyclophosphamide was shown to be resistant to photodegradation [50]. Other transformation, degradation, distribution, or interaction mechanisms of cyclophosphamide have not yet been investigated, and hence the true risk of this drug in surface waters is still unclear [9]. This is in-part due to lack of instrumentation suitable for real-time, in-situ analysis. There is therefore need for development of new, simple, sensitive, and potentially portable analysis methods for environmental monitoring of cytotoxic drugs.

Chemiluminescence analysis is a technique highly suited to environmental analysis due to simple instrumentation, low detection limits, high selectivity, and capabilities of in-situ real-time analysis [66-68]. Despite its advantages chemiluminescence detection has not yet been applied to monitoring of cytotoxic drugs in the environment. In Chapter 2 the suitability of various oxidising reagents for chemiluminescence detection for cyclophosphamide was investigated. Tris-2,2'-bipyirdyl ruthenium ($Ru(bipy)_3$), which is known to react readily with amine functionalities [122], was found to produce the most intense signals. This reagent exists as $[Ru(bipy)_3]^{2+}$ and must first be oxidised to the active $[Ru(bipy)_3]^{3+}$, which then undergoes the chemiluminescence reaction. This initial oxidation step can be conducted either chemically or electrochemically. Electrochemical methods, in which the 3+ state is generated at the surface of an electrode, have been shown to be more elegant, but offer equivalent analytical utility as the simpler chemical methods. Chemical generation of $[Ru(bipy)_3]^{3+}$ is typically achieved via mixing of $Ru(bipy)_3Cl_2$ with either $KMnO_4$, $Ce(SO_4)_2$, and PbO_2. The choice of oxidant has

been shown to be highly influential on the sensitivity, selectivity, and linearity in response of chemiluminescence signals from a particular analyte, as well as on the stability of the 3+ oxidation state [153]. $[Ru(bipy)_3]^{3+}$ is known to react with any water present in the reaction mixture to form $[Ru(bipy)_3]^{2+}$, and hence over time the chemiluminescence signal detected from $Ru(bipy)_3Cl_2$ can decrease [179]. Removal of PbO_2 via on-line filtration immediately before analysis has been shown to produce stable signals over long time periods [122]. Alternatively, the stability of the $[Ru(bipy)_3]^{3+}$ state can be increased via preparation of the oxidising reagent in a solvent other than water, however $Ru(bipy)_3Cl_2$ has a very low solubility in organic solvents. Gerardi *et al.* [152] therefore developed a method of converting $Ru(bipy)_3Cl_2$ into its perchlorate salt to allow it to be solubilised in acetonitrile, which, upon mixing with PbO_2, produces a much more stable 3+ oxidation state.

Preliminary studies (Chapter 2) into cyclophosphamide detection using $Ru(bipy)_3$ showed that preparation of $Ru(bipy)_3$ using either $Ce(SO_4)_2$ or PbO_2 produced the most intense signals. The occurrence of secondary reactions with $Ce(SO_4)_2$, however, made use of this reagent preparation system too complicated to offer analytical utility. This chapter is therefore focussed on development of chemiluminescence detection for cyclophosphamide using $[Ru(bipy)_3]^{3+}$ prepared using PbO_2.

4.2 Experimental

4.2.1 Instrumentation

All experiments were conducted using the in-house-built FIA instrument described in Chapter 3. The manifold differed from that in Chapter 3 in that the $Ru(bipy)_3Cl_2$ reagent was injected into the carrier stream rather than into the analyte solution, as shown in Figure 4-1. Data analysis was conducted in the same way as in Chapter 3. All analyses were performed in triplicate. The total reagent flow rate was 1.7 mL/min unless otherwise stated.

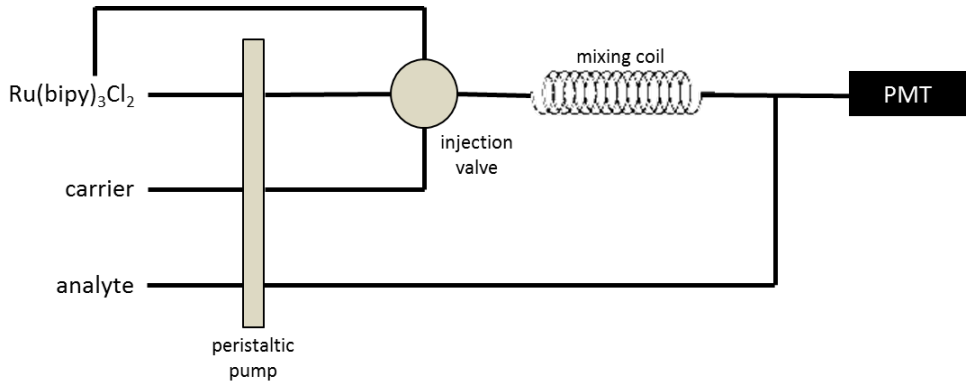

Figure 4-1. Schematic of the FIA chemiluminescence manifold used for development of detection method for cyclophosphamide

4.2.2 Chemicals and Reagents

All reagents were analytical grade unless otherwise stated. Cyclophosphamide monohydrate was purchased from Sigma Aldrich Pty. Ltd (Castle Hill, NSW, Australia). Tris-2,2'-bipyridyl ruthenium (II) chloride hexahydrate was purchased from Strem Chemicals (Newburyport, MA, USA). Sulfuric acid (98 %), lead dioxide (PbO_2), sodium hydroxide, perchloric acid (70 % w/w), and disodium hydrogen phosphate were purchased from Chem-Supply (Gillman, SA, Australia). Sodium dihydrogen phosphate was purchased from Merck Pty. Ltd (Bayswater, Victoria, Australia). Sodium borate decahydrate was purchased from Amersham Australia Pty. Ltd (Baulkham Hills, NSW, Australia). Hydrochloric acid (37 % w/w) was purchased from Choice Analytical (Thornleigh, NSW, Australia). Acetonitrile (LC-MS/MS-grade) was purchased from Rowe Scientific Pty. Ltd (Lonsdale, SA, Australia).

4.2.3 Standards

Cyclophosphamide stock solutions (1×10^{-3} M) were prepared daily in one of deionised water, acetonitrile, or phosphate buffer (0.05 M, pH 7) and stored in sealed glass bottles in the absence of light. Standard solutions of cyclophosphamide ($1x10^{-7}$ M to $1x10^{-4}$ M) were prepared immediately prior to analysis by serial dilution of the stock in deionised water, acetonitrile, or phosphate buffer (0.05 M, pH 7). These solutions were also stored for up to 24 hours in sealed glass bottles in the absence of light for later analysis.

4.2.4 Oxidising Reagents

All solutions were prepared using deionised water (18 MΩ) unless otherwise stated. $[Ru(bipy)_3]Cl_2$ (1×10^{-4} – 3×10^{-3} M) solutions were prepared by dissolution of tris(2,2'-bipyridyl)ruthenium(II) chloride in H_2SO_4 (0.01 – 0.1 M). This solution was then mixed with solid lead dioxide (0.1 g/20 mL), resulting in a colour change from orange to green. The solid material was removed via online filtration through glass wool during analysis. Solid $[Ru(bipy)_3]ClO_4$ was prepared according to the method described by McDermott *et al.* [179]. $[Ru(bipy)_3]ClO_4$ solutions (1.0×10^{-3} M) were prepared in $HClO_4$ (0.05 M in acetonitrile) and oxidised with PbO_2 (0.1 g/ 20 mL). The solid was allowed to settle to the bottom, and the resulting deep green solution was filtered online through glass wool during analysis.

4.2.5 Carrier Solutions

H_2SO_4 (5×10^{-4} - 0.1 M) was prepared by dissolution in deionised water. pH 6 phosphate buffer was prepared by mixing 12.0 mL of 0.05 M Na_2HPO_4 with 88.0 mL 0.05 M NaH_2PO_4. pH 7 phosphate buffer was prepared by mixing 115.4 mL of 0.1 M Na_2HPO_4 with 84.6 mL 0.1 M NaH_2PO_4. pH 8 phosphate buffer was prepared by mixing 233 mL of 0.1 M Na_2HPO_4 with 17 mL 0.1 M NaH_2PO_4. Bicarbonate buffer (pH 11) was prepared by diluting a mixture of 100 mL 0.1 M $NaHCO_3$ and 45.4 mL 0.2 M NaOH to 200 mL with distilled water. Borate buffer (pH 10) was prepared by diluting a mixture of 100 mL of 0.1 M $Na_2B_4O_7.10H_2O$ (borax) and 36.6 mL of 0.4 M NaOH to 200 mL with distilled water. Tris buffer

(pH 9) was prepared by diluting a mixture of 100 mL of 0.1 M tris(hydroxymethyl)aminomethane (tris) and 11.4 mL of 0.1 M HCl to 200 mL with distilled water. This is summarised in Table 4-1. The pH of each buffer was confirmed after each preparation using a Mettler Toledo S220 SevenCompact™ pH metre (Rowe Scientific Pty. Ltd, Adelaide, Australia).

Table 4-1. Stock solutions and their corresponding volumes used to prepare various basic buffer carrier solutions in 200 mL deionised water

	Solution	Concentration (M)	Volume (mL)	Solution	Concentration (M)	Volume (mL)
phosphate pH 7	Na_2HPO_4	0.1	115.4	NaH_2PO_4	0.1	84.6
phosphate pH 8	Na_2HPO_4	0.1	233	NaH_2PO_4	0.1	17
tris pH 9	tris	0.1	100	HCl	0.1	11.4
Borate pH 10	borax	0.1	100	NaOH	0.4	36.6
Bicarbonate pH 11	$NaHCO_3$	0.1	100	NaOH	0.2	45.4

4.3 Results and Discussion

4.3.1 Method Development

4.3.1.1 Stability of $[Ru(bipy)_3]^{3+}$

In the preliminary studies into the suitability of various oxidising reagents for chemiluminescence detection of each cytotoxic (Chapter 2) the $Ru(bipy)_3Cl_2$ reagent was prepared via mixing with solid PbO_2 that was then removed via filtration prior to analysis. When using this approach it was observed that the chemiluminescence signal from the blanks and the analytes continually decreased throughout the day (Appendix F). It is known that the $[Ru(bipy)_3]^{3+}$ species is unstable in aqueous solution, readily converting back to $[Ru(bipy)_3]^{2+}$ upon reaction with water [122]. Although providing adequate intra-experimental reproducibility (%RSD 5.02-10.9 %), variations in signal throughout the day would not allow for comparisons between different experiments. Consequently, removal of the PbO_2 via on-line filtration immediately prior to analysis was trialled as a means of minimising the time allowed for the back reaction to $[Ru(bipy)_3]^{2+}$ to occur. Sodium oxalate was as used as the model analyte to test this approach because it is known to be stable in solution and give intense emission upon reaction with $Ru(bipy)_3^{3+}$. On-line filters made using filter paper or PTFE syringe filters were trialled, however they were found to restrict flow and were prone to fouling. A custom filter made using a plastic pipette tip filled with compacted glass wool was found to be the most effective, because it did not restrict the flow of the pump and was observed to effectively remove all visible PbO_2. Sodium oxalate was analysed every 5 minutes for 2.5 hours using this filter system in the SIA manifold in Chapter 2, using the experimental conditions in Table 4-2. The chemiluminescence peak area was found to be stable

over the 2.5 hours (Figure 4-2), however the variation between trials appeared to increase slightly after 140 minutes.

Table 4-2. SIA reagent compositions, volumes, and flow rates used to assess stability of chemiluminescence signal from sodium oxalate over time using $Ru(bipy)_3Cl_2$

Aspiration Order	Reagent	Composition	Volume (µL)	Flow Rate (µL/s)
2	Oxidising Reagent	$Ru(bipy)_3Cl_2$ (1 x 10^{-3} M in 0.05 M H_2SO_4)	50	15
1	Analyte	Sodium oxalate (1 x 10^{-7} M in 0.05 M H_2SO_4)	50	5
3	Carrier Solution	0.05 M H_2SO_4	300	100

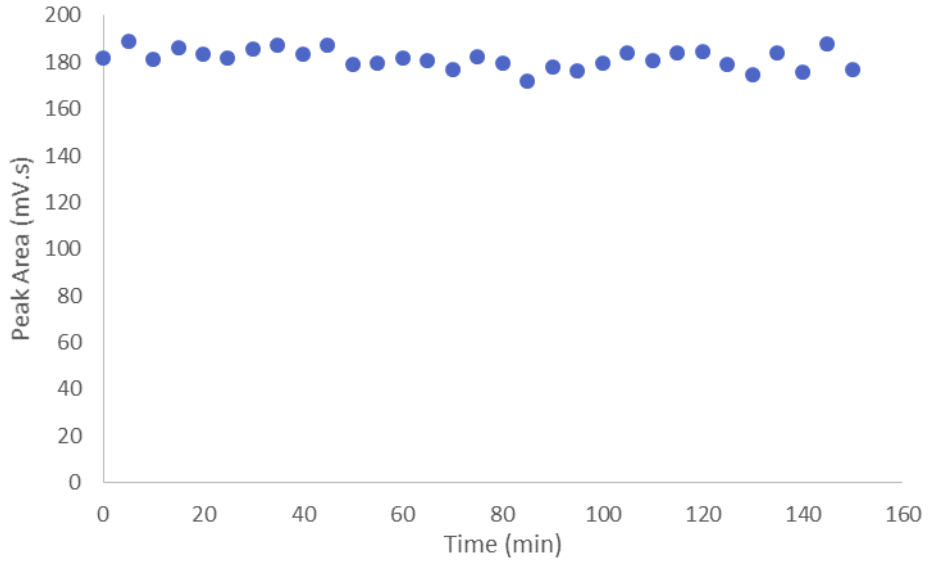

Figure 4-2. Chemiluminescence peak area obtained via SIA of sodium oxalate (1 x 10^{-7} M in 0.05 M H_2SO_4) every 5 minutes over 2.5 hours using $Ru(bipy)_3$ (1 x 10^{-3} M in 0.05 M H_2SO_4) as the oxidiser and H_2SO_4 (0.05 M) as the carrier solution.

Use of $Ru(bipy)_3ClO_4$ in acetonitrile as the 3+ oxidation state of the perchlorate salt, which is reportedly much more stable than $Ru(bipy)_3Cl_2$ [152], was also investigated, and found to produce stable chemiluminescence signals for up to 160 hours (Appendix G). When then investigating the effect of carrier solution pH, however, the use of this reagent caused miscibility issues between the acidic oxidising reagent (pH ≈ 1) and basic carrier solutions, resulting in the formation of two chemiluminescence peaks. $Ru(bipy)_3Cl_2$, which was stable for up to 2.5 hours, was therefore selected for all subsequent method development.

4.3.1.2 Effect of Carrier pH:

The pH of the reaction mixture can have a large effect on the chemiluminescence signal [68]. pH can be varied by varying the pH of the carrier solution. Consequently, cyclophosphamide (1 x 10^{-4} M) was analysed using carrier solutions with pH between 1 and 11 using the conditions in Table 4-3. Overall, acidic pH levels between 1 and 6 produced the weakest signals (net peak area between -135.7 ± 99

mV.s to 105.6 ± 44 mV.s) (Figure 4-3). Neutral and slightly basic pH levels (7-9) produced the most intense chemiluminescence, with pH 7 giving the highest net peak area of 6785 ± 311 mV.s. This was most likely due to cyclophosphamide requiring a high pH to be deprotonated (pKa of 2.84), giving rise to a high ionisation potential. As $Ru(bipy)_3$ chemiluminescence with amines occurs via electron transfer from the amine to $[Ru(bipy)_3]^{3+}$ [199], the first ionisation potential of the non-bonding orbital in the amine is inversely proportional to the intensity of the chemiluminescence produced. Basic pH levels would therefore result in more intense chemiluminescence than acidic pH. As pH 7 produced the most intense signal this carrier pH was selected for subsequent analyses. During this study peak shouldering in the chemiluminescence signals was observed when using carrier solutions with pH greater than 7. This indicated incomplete mixing of the reagents, and was most likely due to the large pH gradient between the basic carrier solutions and the acidic oxidising reagent (pH ≈ 1). Higher buffer concentrations (up to 0.1 M) were tested in order to more tightly control the solution pH, however this resulted in high background signals and flooding of the detector. In general, at high pH the chemiluminescence signal decreased with increasing pH. When increasing from pH 8 to 9, and then from pH 10 to 11, however, the chemiluminescence peak area increased slightly. This was most likely due to changing the composition of buffer from phosphate to tris buffer between pH 8 and 9, and borate to bicarbonate buffer from pH 10 to 11. This changed the background emission obtained, and hence the net chemiluminescence peak area. Overall, pH 7 phosphate buffer produced the most intense chemiluminescence signal, and hence was selected for all subsequent analyses.

Table 4-3. Reagents used to investigate the effect of carrier pH on chemiluminescence signals obtained via FIA of cyclophosphamide (1×10^{-4} M)

Reagent	Composition
Analyte	Cyclophosphamide (1×10^{-4} M) in deionised water
Oxidising Reagent	$Ru(bipy)_3Cl_2$ (1×10^{-3} M in 0.05 M H_2SO_4)
Carrier Solution	Phosphate buffer (pH 6, 0.05 M) Phosphate buffer (pH 7, 0.05 M) Phosphate buffer (pH 8, 0.05 M) Tris buffer (pH 9, 0.05 M) Borate buffer (pH 10, 0.05 M) Bicarbonate buffer (pH 11, 0.05 M)

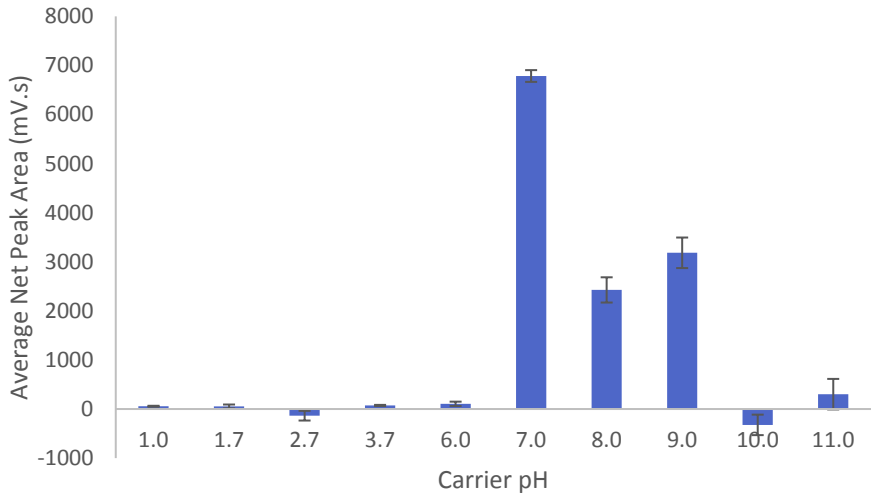

Figure 4-3. Effect of carrier pH (1-11) on the average net chemiluminescence peak area (n=3) from FIA of cyclophosphamide (1 x 10^{-4} M in deionised water) obtained using $Ru(bipy)_3Cl_2$ (1 x 10^{-3} M in 0.05 M H_2SO_4) as the oxidising reagent. Error bars = ± 1 standard deviation.

4.3.1.3 Effect of FIA Manifold:

Reagent mixing can often be improved via manipulation of the mixing geometry in the FIA system. Consequently, the effect of the geometry of the point at which the sample was merged with the carrier and oxidiser stream on chemiluminescence signal was investigated. The FIA manifolds investigated are depicted in Figure 4-4, where Manifold B describes that used previously, and Manifolds A and D differ only in the length (and hence volume) of the tubing between the T-piece and the PMT inlet (18.75 µL and 75 µL, respectively). The reagent conditions are detailed in Table 4-4. The resulting net peak areas are given in Figure 4-5, and the shapes of the chemiluminescence peaks obtained using each manifold are shown in Figure 4-6. It was found that the largest net peak area was obtained when the analyte was delivered perpendicular to the carrier and oxidant flow (Manifold B). This manifold also produced slightly less peak shouldering than the other manifolds.

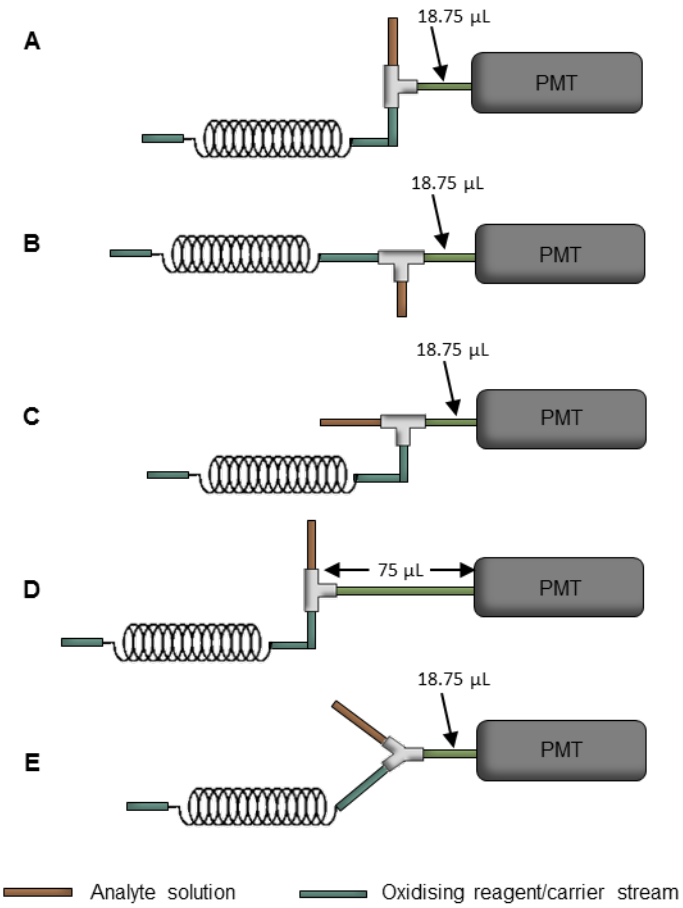

Figure 4-4. Schematics of FIA manifolds tested; varying the geometry of sample merging with the oxidiser and carrier stream

Table 4-4. Reagents used to investigate the effect of the geometry of the point of analyte and carrier stream merging on the shape and intensity of chemiluminescence peaks obtained via FIA of cyclophosphamide (1 x 10^{-4} M)

Reagent	Composition
Analyte	Cyclophosphamide (1 x 10^{-4} M) in deionised water
Oxidising Reagent	$Ru(bipy)_3Cl_2$ (1 x 10^{-3} M in 0.05 M H_2SO_4)
Carrier Solution	Phosphate buffer (pH 7, 0.05 M)

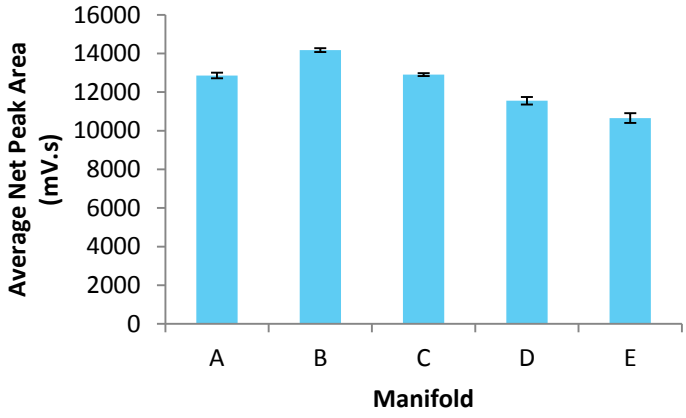

Figure 4-5. Average net chemiluminescence peak area (n=3) from FIA of cyclophosphamide (1 x 10^{-4} M in deionised water) obtained using $Ru(bipy)_3Cl_2$ (1 x 10^{-3} M in 0.05 M H_2SO_4) as the oxidising reagent and phosphate buffer (0.05 M, pH 7) as the carrier solution, using the analyte-carrier solution merging geometries depicted in Figure 4-4.

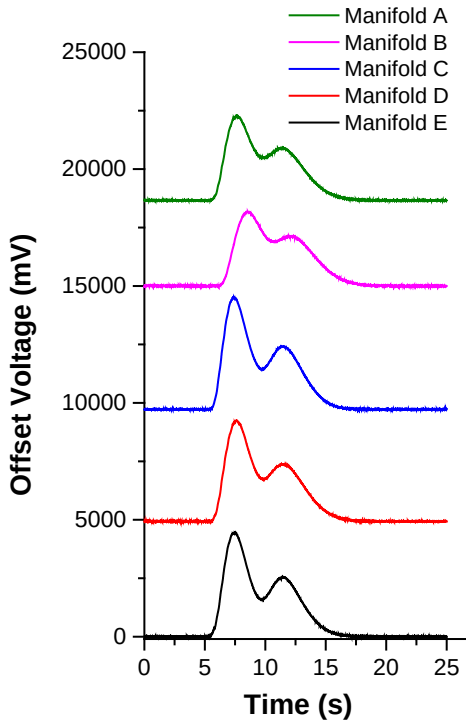

Figure 4-6. Offset FIA chemiluminescence peak obtained via analysis of cyclophosphamide (1×10^{-4} M in deionised water) obtained using $Ru(bipy)_3Cl_2$ (1×10^{-3} M in 0.05 M H_2SO_4) as the oxidising reagent and phosphate buffer (0.05 M, pH 7) as the carrier solution, using the analyte-carrier solution merging geometries depicted in Figure 4-4.

It was also observed that Manifolds A and D, which only differed in the length of the tubing between introduction of the analyte and the PMT, produced different net peak areas. Manifold A, with a shorter tubing length, produced an average net peak area of 12860 ± 147 mV.s, compared with 11553 ± 194 mV.s obtained using the longer tubing in Manifold D. This suggested that the shorter tubing allowed for detection of the emitted light closer to the time of maximum emission. Various lengths of tubing between T-piece and the PMT inlet were therefore tested using the Manifold that produced the least peak shouldering (Manifold B). Again the reagent conditions used are those in Table 4-4. The resulting net peak areas versus tubing length (expressed as tube volume) are given in Figure 4-7, where 0 µL tube volume indicates direct connection of the T-piece to the PMT inlet. It was observed that with increasing tubing length/volume the net peak area increased and then decreased. This correlated well with the idea that when using lower tubing volumes the emitted light would be detected prior to maximum emission. As the tube volume increased the light detection would be closer and closer to the time of maximum emission. The signal would then decrease again once the maximum emission had been passed. The maximum net peak area of 16872 ± 7 mV.s was obtained with a tube volume of 37.5 µL. A tube volume of 37.5 µL in Manifold B was therefore utilised for all subsequent analyses.

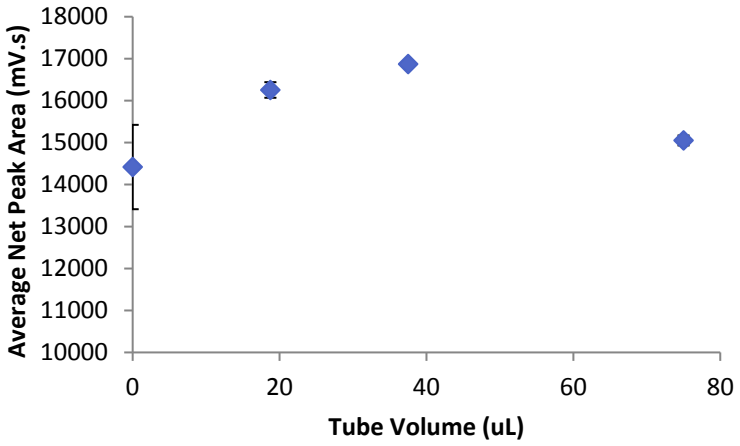

Figure 4-7. Average net chemiluminescence peak area (n=3) from FIA of cyclophosphamide (1 x 10^{-4} M in deionised water) obtained using $Ru(bipy)_3Cl_2$ (1 x 10^{-3} M in 0.05 M H_2SO_4) as the oxidising reagent and phosphate buffer (0.05 M, pH 7) as the carrier solution, using various T-piece-to-PMT tubing volumes. Error bars = ± 1 standard deviation.

4.3.1.4 Effect of Total Flow Rate:

The total flow rate of an FIA system is also highly important because it determines at which point in the chemiluminescence reaction the light reaches the detector. Total flow rates from 0.86 to 3.4 mL/min were therefore tested using the reagent conditions in Table 4-4. The resulting net peak areas are given in Figure 4-8. Similarly to when varying the tubing length, athe chemiluminescence peak area increased and then decreased as the total flow rate was increased. A flow rate of 1.6 mL/min produced the highest net peak area of 6944 ±143 mV.s, and hence was used for subsequent analyses. The reproducibility of the chemiluminescence peak area obtained at the lowest flow rate tested (0.86 mL/min) was larger than that obtained at other flow rates, with a %RSD of 10.8 %. This could have been due to poorer mixing of reagents at this lower flow rate.

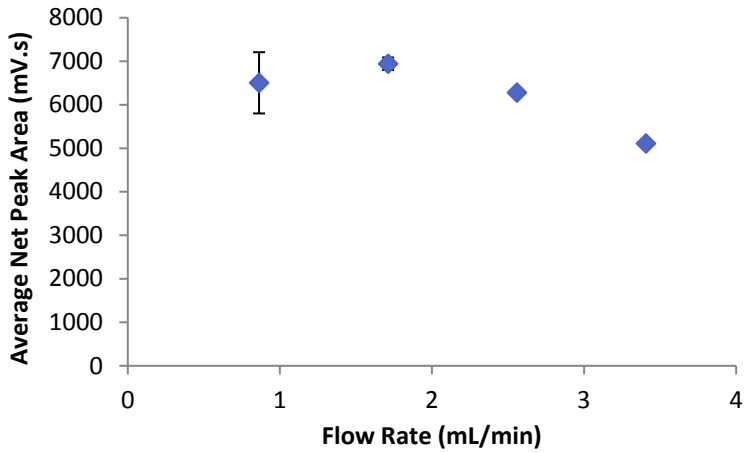

Figure 4-8. Effect of total flow rate on average net chemiluminescence peak area (n=3) from FIA of cyclophosphamide (1 x 10^{-4} M in deionised water) obtained using $Ru(bipy)_3Cl_2$ (1 x 10^{-3} M in 0.05 M H_2SO_4) as the oxidising reagent and phosphate buffer (0.05 M, pH 7) as the carrier solution. Error bars = ± 1 standard deviation.

4.3.1.5 *Effect of Analyte Matrix:*

During these experiments peak shouldering was still being observed. It was hypothesised that preparation of the cyclophosphamide in the same medium as the carrier solution could improve miscibility between the reagents, hence minimising this shouldering. Cyclophosphamide (1×10^{-4} M) prepared in either deionised water or phosphate buffer (pH 7, 0.05 M) was analysed using the reagent conditions in Table 4-5. The resulting net chemiluminescence peak areas are given in Figure 4-9. It was observed that signals obtained using the buffered analyte displayed peak splitting to a much lesser extent (Appendix H), hence indicating that the pH gradient had been decreased. The average net peak area, however, decreased substantially from 3266 ± 131 mV.s to 735.6 ± 165 mV.s upon buffering of the analyte. It is possible that this was due to instability of the cyclophosphamide, as the solution in deionised water was approximately 3 hours older than that prepared in phosphate buffer. However, cyclophosphamide has been shown to be stable for up to 24 hours at room temperature in aqueous solution [200]. In order to ensure adequate signal reproducibility by producing single chemiluminescence peaks buffered analyte solutions were used for the remaining method development.

Table 4-5. Reagents used to investigate the effect of analyte solvent on chemiluminescence peaks obtained via FIA of cyclophosphamide (1×10^{-4} M)

Reagent	Composition
Analyte	Cyclophosphamide (1×10^{-4} M) in deionised water or phosphate buffer (pH 7, 0.05 M)
Oxidising Reagent	$Ru(bipy)_3Cl_2$ (1×10^{-3} M in 0.075 M H_2SO_4)
Carrier Solution	Phosphate buffer (pH 7, 0.05 M)

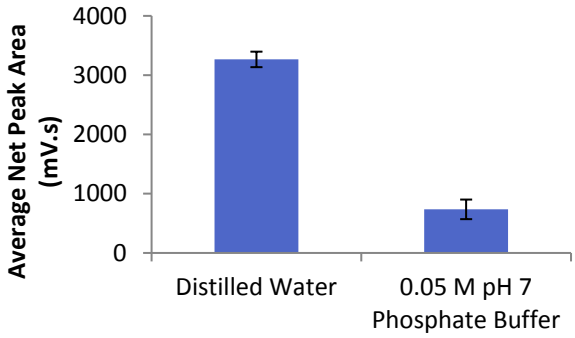

Figure 4-9. Comparison of average net peak area (n=3) obtained via FIA chemiluminescence analysis of cyclophosphamide (1×10^{-4} M) prepared in deionised water or phosphate buffer (0.05 M, pH 7) using $Ru(bipy)_3Cl_2$ (1×10^{-3} M in 0.05 M H_2SO_4) as the oxidising reagent and phosphate buffer (0.05 M, pH 7) as the carrier solution. Error bars = ± 1 standard deviation.

4.3.1.6 *Effect of Carrier Concentration:*

Various concentrations of the phosphate buffer (pH 7) were then tested as the carrier solution and analyte solvent simultaneously using the reagent conditions in Table 4-6. The resulting average net peak areas obtained are given in Figure 4-10. It was observed that the largest average net peak area of 1819 ± 70 mV.s was obtained using a phosphate buffer concentration of 25×10^{-3} M. At this

concentration and below, however, a double peak was obtained (Appendix I). This indicated that the buffering capacity of the solution had been reached and a pH gradient between the phosphate buffer and oxidising reagent may have still existed. This resulted in decreased reproducibility between replicates, as demonstrated by the larger error bars. 50 x 10^{-3} M was the lowest phosphate concentration at which a single peak was obtained, and hence, in order to optimise reproducibility, this concentration was selected for all subsequent analyses.

Table 4-6. Reagents used to investigate the effect of phosphate buffer carrier concentration on chemiluminescence obtained from cyclophosphamide (1 x 10^{-4} M)

Reagent	Composition
Analyte	Cyclophosphamide (1 x 10^{-4} M) in pH 7 phosphate buffer (2 x 10^{-3} - 0.05 M)
Oxidising Reagent	$Ru(bipy)_3Cl_2$ (1 x 10^{-3} M in 0.075 M H_2SO_4)
Carrier Solution	Phosphate buffer (pH 7, 2 x 10^{-3} - 0.05 M)

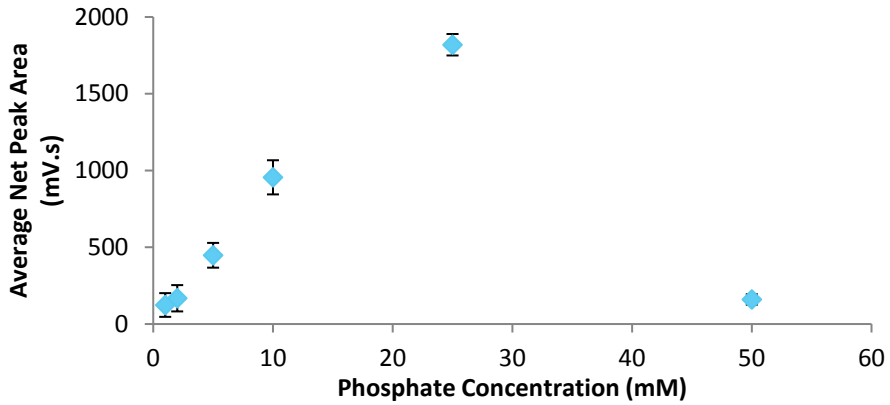

Figure 4-10. Effect of phosphate carrier concentration on the average net chemiluminescence peak area (n=3) obtained via FIA of cyclophosphamide (1 x 10^{-4} M) using $Ru(bipy)_3Cl_2$ (1 x 10^{-3} M in 0.05 M H_2SO_4) as the oxidising reagent. Error bars = ± 1 standard deviation.

4.3.1.7 Effect of $Ru(bipy)_3Cl_2$ Concentration:

The effect of the concentration of $Ru(bipy)_3Cl_2$ was then investigated via analysis of cyclophosphamide (1 x 10^{-4} M in deionised water) using $Ru(bipy)_3Cl_2$ concentrations between 1 x 10^{-4} M and 3 x 10^{-3} M (in 0.05 M H_2SO_4), that had each been oxidised with PbO_2 (0.1 g/ 20 mL). The reagent conditions are given in Table 4-7 and the resulting average net peak areas are given in Figure 4-11. As the $Ru(bipy)_3Cl_2$ concentration was increased up to 1 x 10^{-3} M the average net peak area also increased, before decreasing at concentrations above 1 x 10^{-3} M, and hence 1 x 10^{-3} M $Ru(bipy)_3Cl_2$ was selected for all subsequent analyses.

Table 4-7. Reagent conditions used to determine the effect of $Ru(bipy)_3Cl_2$ concentration on cyclophosphamide chemiluminescence signal

Reagent	Composition
Analyte	Cyclophosphamide (1 x 10^{-4} M) in phosphate buffer (pH 7, 0.05 M)
Oxidising Reagent	$Ru(bipy)_3Cl_2$ (1 x 10^{-4} – 3 x 10^{-3} M in 0.05 M H_2SO_4)
Carrier Solution	Phosphate buffer (pH 7, 0.05 M)

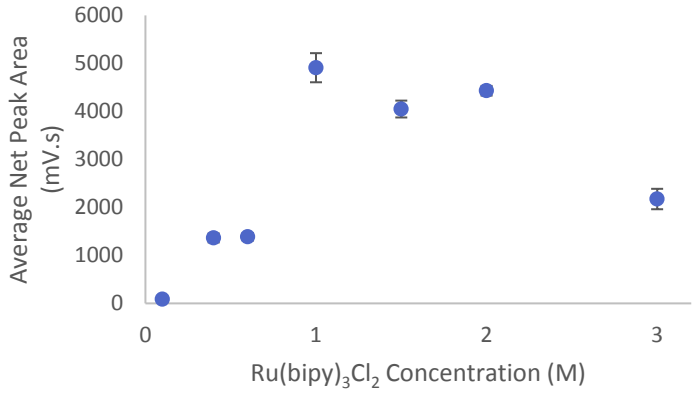

Figure 4-11. Effect of $Ru(bipy)_3Cl_2$ concentration on the average net chemiluminescence peak area (n=3) obtained via FIA of cyclophosphamide (1 x 10^{-4} M) using $Ru(bipy)_3Cl_2$ (in 0.05 M H_2SO_4) as the oxidising reagent and phosphate buffer (0.05 M, pH 7) as the carrier solution. Error bars = ± 1 standard deviation.

4.3.1.8 Effect of $Ru(bipy)_3Cl_2$ Acid Concentration:

The effect of the concentration of the H_2SO_4 used to prepare the $Ru(bipy)_3Cl_2$ was then investigated. Cyclophosphamide (1 x 10^{-3} M in deionised water) was analysed using $Ru(bipy)_3Cl_2$ prepared in H_2SO_4 of concentrations between 1 x 10^{-4} M and 3 x 10^{-3} M, prior to being oxidised with PbO_2 (0.1 g/ 20 mL). The reagent conditions are given in Table 4-8 and the resulting net peak areas are given in Figure 4-12. As the H_2SO_4 concentration increased, so did the average net peak area. This was to be expected because the blank signal obtained is known to be caused by the reaction between $[Ru(bipy)_3]^{3+}$ and ^{-}OH ions, which are generated from the dissociation of water molecules. This dissociation occurs more readily at higher pH, due to the lower abundance of hydrogen ions, and hence lower pH solutions result in a lower background signal, and hence generally a larger signal-to-blank ratio from the analyte [201]. At the highest concentration of 100 mM, however, the chemiluminescence signal was comprised of two peaks (Appendix J). This was most likely due to the high pH gradient caused by the high acid content, resulting in the formation of two reaction zones. This would introduce error into the peak integration and reduce reproducibility, as demonstrated by the increased error bar size at this concentration, and hence it was decided that a sulphuric acid concentration of 75 mM would be optimal.

Table 4-8. Reagent conditions used to determine the effect of the H_2SO_4 concentration used to prepared $Ru(bipy)_3Cl_2$ on cyclophosphamide chemiluminescence

Reagent	Composition
Analyte	Cyclophosphamide (1 x 10^{-4} M) in phosphate buffer (pH 7, 0.05 M)
Oxidising Reagent	$Ru(bipy)_3Cl_2$ (1 x 10^{-3} M in 0.01 - 0.1 M H_2SO_4)
Carrier Solution	Phosphate buffer (pH 7, 0.05 M)

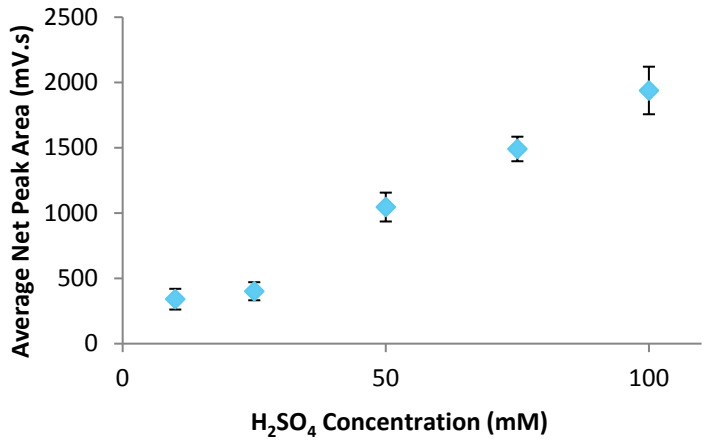

Figure 4-12. Effect of $Ru(bipy)_3$ acid concentration on the average net peak area obtained via FIA-chemiluminescence analysis of cyclophosphamide ($1x10^{-4}$ M) using $Ru(bipy)_3$ (1 mM in 75 mM H_2SO_4) as the oxidiser and Na_2HPO_4/NaH_2PO_4 (50 mM, pH 7) as the carrier and sample solvent. Error bars = ± 1 standard deviation.

4.3.2 Method Validation

Overall, the reagent conditions found to produce the most intense and reproducible chemiluminescence signal were found to be those in Table 4-9.

Table 4-9. Reagent conditions found to be optimal for FIA chemiluminescence detection of cyclophosphamide

Reagent	Composition
Analyte	Cyclophosphamide (1×10^{-6} – 1×10^{-3} M) in phosphate buffer (pH 7, 0.05 M)
Oxidising Reagent	$Ru(bipy)_3Cl_2$ (1×10^{-3} M in 0.075 M H_2SO_4)
Carrier Solution	Phosphate buffer (pH 7, 0.05 M)

During the method development experiments it became clear that the chemiluminescence responses being obtained varied substantially between separate experiments. For instance, the average net peak area obtained from cyclophosphamide (1×10^{-4} M) using $Ru(bipy)_3Cl_2$ (1×10^{-3} M in 0.05 M H_2SO_4) and phosphate buffer (0.05 M, pH 7) during the study on the effect of phosphate concentration was 160.1 ± 34 mV.s. The average net peak area obtained using identical reagent conditions (cyclophosphamide: 1×10^{-4} M, $Ru(bipy)_3Cl_2$: 1×10^{-3} M in 0.05 M H_2SO_4, phosphate buffer: 0.05 M, pH 7) during the study on the effect of $Ru(bipy)_3Cl_2$ concentration, however, was 4910 ± 303 mV.s. This indicated that there was large variation between the response obtained during different sets of experiments.

It was suspected that this variation may be due to differences in room temperature at the times each experiment was conducted. Consequently, the room temperature was measured every 2 hours over a 12 hour day and was found to have a %RSD of 1.4 %. This variation was too low to be solely responsible for the observed variation in chemiluminescence signal.

Another possible explanation for the inter-experimental variation was differences in the PbO_2 mass weighed for each experiment. The %RSD of mass weighed during each of the experiments conducted

during method development was 4.6 %, and hence, again, was decided to not be the sole contributing factor.

The stability of the $[Ru(bipy)_3]^{3+}$ reagent had already been demonstrated during the initial method development (Section 4.3.1.1), hence suggesting this was not the cause of the observed signal fluctuations. The stability of the cyclophosphamide itself was therefore assessed via analysis of a single cyclophosphamide solution (4×10^{-5} M) immediately after preparation and 24 hours after preparation. Sodium oxalate was also analysed 0 and 24 hours after preparation as a control. The reagent conditions used are given in Table 4-10. The net peak area obtained from sodium oxalate analysis did not change (within ± 1 standard deviation) 24 hours after preparation (Figure 4-13). The signal from 24-hour-old cyclophosphamide solution, however, was increased 1.91-fold compared with the fresh solution. This indicated that, while the reagents were stable over 24 hours, the cyclophosphamide solution was not. The cyclophosphamide could have been degrading over time to form a product or products with higher chemiluminescence activity than the parent drug. This would explain the observed fluctuations in chemiluminescence response between different experiments, which would have been conducted using cyclophosphamide solutions of different ages throughout the day.

Table 4-10. Reagents used to determine the inter-day reproducibility of the developed FIA chemiluminescence detection method for cyclophosphamide

Reagent	Composition
Analyte	Cyclophosphamide (4×10^{-5} M) in phosphate buffer (pH 7, 0.05 M) Sodium oxalate (1×10^{-5} M) in deionised water
Oxidising Reagent	$Ru(bipy)_3Cl_2$ (1×10^{-3} M in 0.075 M H_2SO_4)
Carrier Solution	Phosphate buffer (pH 7, 0.05 M)

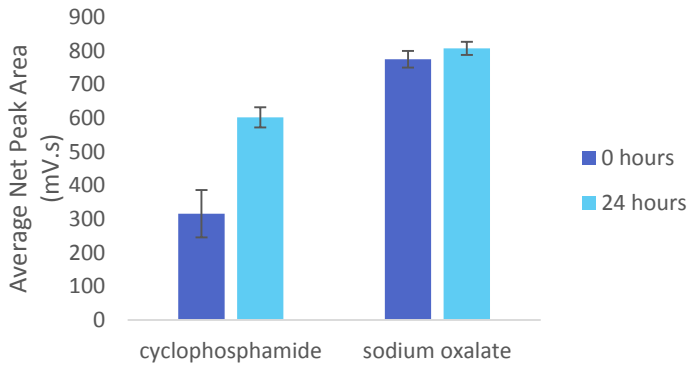

Figure 4-13. Comparison of average net peak area (n=3) obtained via FIA chemiluminescence of cyclophosphamide (4×10^{-5} M in 0.05 M pH 7 phosphate buffer) and sodium oxalate (1×10^{-5} M in deionised water) using $Ru(bipy)_3Cl_2$ (1×10^{-3} M in 0.075 M H_2SO_4) as the oxidiser and phosphate buffer (0.05 M, pH 7) as the carrier solution. Error bars = ± 1 standard deviation.

The approximate rate of this degradation was then assessed via anlaysis of a single cyclophosphamide solution (1×10^{-3} M) maintained at room temperature using the reagent conditions in Table 4-10 every

5 hours over 25 hours. It was observed that while the chemiluminescence peak area from the blank remained relatively constant (%RSD 7.81 %), that of cyclophosphamide again increased by a factor of 1.92 in 20 hours (Figure 4-14). This suggested that the observed increase was not due to instrument or reagent instability, but rather due to instability of the cyclophosphamide solution.

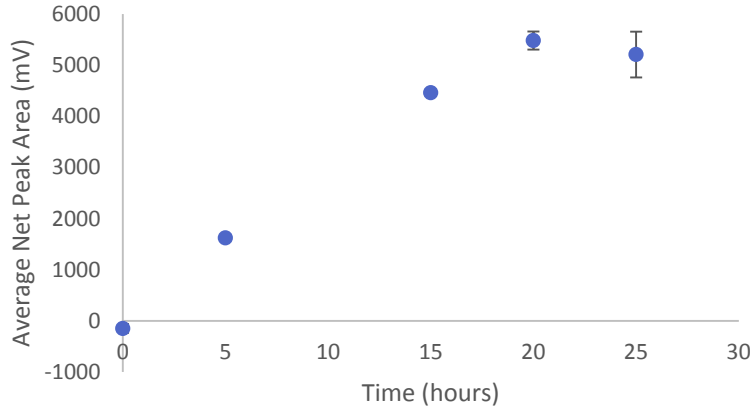

Figure 4-14. Average net peak area (n=3) obtained via FIA chemiluminescence of cyclophosphamide (1 x 10^{-3} M in 0.05 M pH 7 phosphate buffer) peridocially over 25 hours using $Ru(bipy)_3Cl_2$ (1 x 10^{-3} M in 0.075 M H_2SO_4) as the oxidiser and phosphate buffer (0.05 M, pH 7) as the carrier solution. Error bars = ± 1 standard deviation.

The increase in chemiluminescence signal appeared to be relatively linear with time up to 20 hours. This suggested that the degradation of cyclophosphamide may be first-order with respect to cyclophosphamide concentration, with the concentration of the degradation product being directly related to that of the cyclophosphamide. In order to investigate this, cyclophosphamide solutions of various concentrations that had been prepared in phosphate buffer and aged for 24 hours at room temperature were analysed to determine if there was a relationship between these concentrations and chemiluminescence response. The reagent conditions used are given in Table 4-11. Excellent linearity of response was obtained between the original cyclophosphamide concentrations and net chemiluminescence peak area, with an R^2 value of 0.9995 (Figure 4-15). When relating the chemiluminescence signal back to the original concentration of cyclophosphamide in each solution the limit of detection (LOD) and limit of quantitation (LOQ) could be calculated to be 2.23 x 10^{-7} M and 9.24 x 10^{-7} M, respectively. The intra-experimental reproducibility was found to be quite reasonable, with % RSD values of net peak area ranging between 1.63 % and 4.19 %. When analysing the same cyclophosphamide concentrations immediately after preparation, however, no correlation between net chemiluminescence peak area and cyclophosphamide concentration was observed, with an R^2 of 0.023 (Appendix K). Therefore, while not effective for direct cyclophosphamide detection, the developed method could instead be useful for indirect detection of cyclophosphamide via detection of its degradation products. Investigation into the cyclophosphamide degradation was then conducted using the developed chemiluminescence method, as well as NMR, UV analysis, and LC-MS/MS. This will be discussed in Chapter 5.

Table 4-11. Reagents used to determine analyse 24-hour-old cyclophosphamide solutions

Reagent	Composition
Analyte	Cyclophosphamide (2 x 10^{-6} M and 6 x 10^{-5} M) in phosphate buffer (pH 7, 0.05 M), aged for 24 hours in the absence of light at room temperature
Oxidising Reagent	$Ru(bipy)_3Cl_2$ (1 x 10^{-3} M in 0.075 M H_2SO_4)
Carrier Solution	Phosphate buffer (pH 7, 0.05 M)

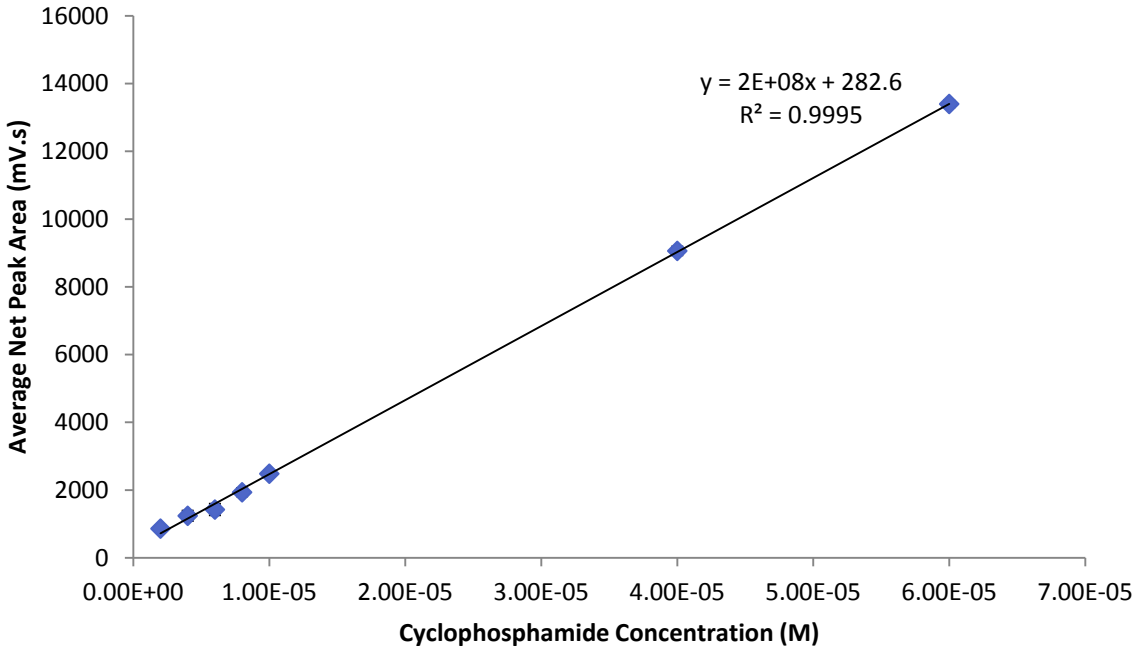

Figure 4-15. Average net peak area (n=3) obtained via FIA chemiluminescence of cyclophosphamide solutions (in 0.05 M pH 7 phosphate buffer) that had been aged for 24 hours at room temperature in the absence of light. $Ru(bipy)_3Cl_2$ (1 x 10^{-3} M in 0.075 M H_2SO_4) was used as the oxidiser and phosphate buffer (0.05 M, pH 7) as the carrier solution. Error bars = ± 1 standard deviation.

Cyclophosphamide is known to undergo hydrolysis in aqueous solution, however this has generally been under extreme conditions of temperature and pH [194, 202-205]. Gilard *et al.* [194] reported that under mild conditions of pH 3.4-8.6 at 20 °C cyclophosphamide solutions showed negligible degradation (≤ 5 %) after 7 days. Similarly, Negreira *et al.* [200] reported cyclophosphamide to be stable (recoveries of 103 %) for up to 24 hours when stored at 25 °C. The degradation observed in this chapter under very similar conditons, however, occurred within a 24 hour period. It is possible that this discrepancy was due to the use of water as the cyclophosphamide solvent in previous papers, compared with the use of pH 7 phosphate buffer here. It is also possible that the degradation products were present at too low concentration to be detected in previsouly reported methods. The approximate LOD obtained for cyclophosphamide when analysing cyclophosphamide solutions 24 hours after preparation was 2.23 x 10^{-7} M, however the true concentration of the degradation products being detected would be expected to be lower than this. It is therefore possible that the degradation products formed in the first 24 hours were present below the detection limits of the ^{31}P NMR and fast atom bombardment mass spectrometry methods used by Gilard *et al.* [194]. Similarly,

the limit of detection for cyclophosphamide in the LC-ESI-MS/MS method used by Negreira *et al.* [200] was in a similar order to that obtained here, being 3.58 x 10^{-8} M. Small changes in cyclophosphamide concentration in the first 24 hours may therefore have not been observable. Chemiluminescence may therefore offer a useful alternative for monitoring of short-term cyclophosphamide degradation.

4.4 Conclusions

Development of chemiluminescence detection for cyclophosphamide was conducted using $Ru(bipy)_3Cl_2$ oxidised with PbO_2. While signals larger than the blank were obtained, a large degree of inter-experimental variation and poor linearity in response was observed for cyclophosphamide concentrations between 2 x 10^{-6} M and 1 x 10^{-4} M. The stability of the chemiluminescence signal from cyclophosphamide was assessed over time, with the net peak area being found to increase 1.9-fold in 20 hours. Instability in reaction temperature and $Ru(bipy)_3Cl_2$ reagent were ruled out as potential causes for the signal increase. It is likely that cyclophosphamide was degrading over time to form products that were more chemiluminescence active. Analysis of cyclophosphamide 24 hours after preparation yielded excellent linearity in response (R^2 0.9995). The developed method could therefore be effective for indirect detection of cyclophosphamide via detection of its degradation products.

Chapter 5:

Cyclophosphamide Hydrolysis Investigation

5. Cyclophosphamide Hydrolysis Investigation

5.1 Introduction

Cyclophosphamide is one of the most commonly used cytotoxics world-wide [12]. There is therefore need for sensitive detection methods for its analysis. In Chapter 4 attempts were made to develop chemiluminescence detection for cyclophosphamide. However, no linearity between cyclophosphamide concentration and net chemiluminescence peak area could be obtained for concentrations between 2 x 10^{-6} M and 1 x 10^{-4} M. Cyclophosphamide did, however, appear to degrade over time to form compounds with a much higher chemiluminescence activity, with the chemiluminescence signal obtained increasing 1.9-fold over 20 hours. When analysing 24-hour-old cyclophosphamide solutions, quite reasonable linearity (R^2 of 0.9995) between original cyclophosphamide concentration and chemiluminescence intensity was obtained. The identity of these products, however, has not yet been determined.

It has been well established that cyclophosphamide undergoes hydrolysis to form a variety of products that differ depending on the reaction conditions. The first reported investigation of the cyclophosphamide hydrolysis reaction was by Arnold and Klose in 1960 [202], who observed cleavage of the P-N bonds when an unbuffered cyclophosphamide solution at pH 8.6 was heated to 70 ^{o}C, resulting in the formation of compounds **2** and **3**, as shown in reaction Scheme A (Figure 5-1). A similar reaction was also found to occur under milder conditions, compounds **3**, **4** and **5** being produced over several days at 37.5 ^{o}C at a pH of 5.0 or 6.9 (Scheme B, Figure 5-1). The group of Gilard *et al.* [194] found that compound **5**, together with another compound (compound **6**), were actually also intermediates in the reaction to form compounds **2** and **3** at pH 1.2, 2.2, and 3.4 at 20 °C (Scheme C, Figure 5-1). The hydrolysis pathway followed, and hence intermediates and final products formed, therefore appeared to be highly dependent on reaction pH and temperature.

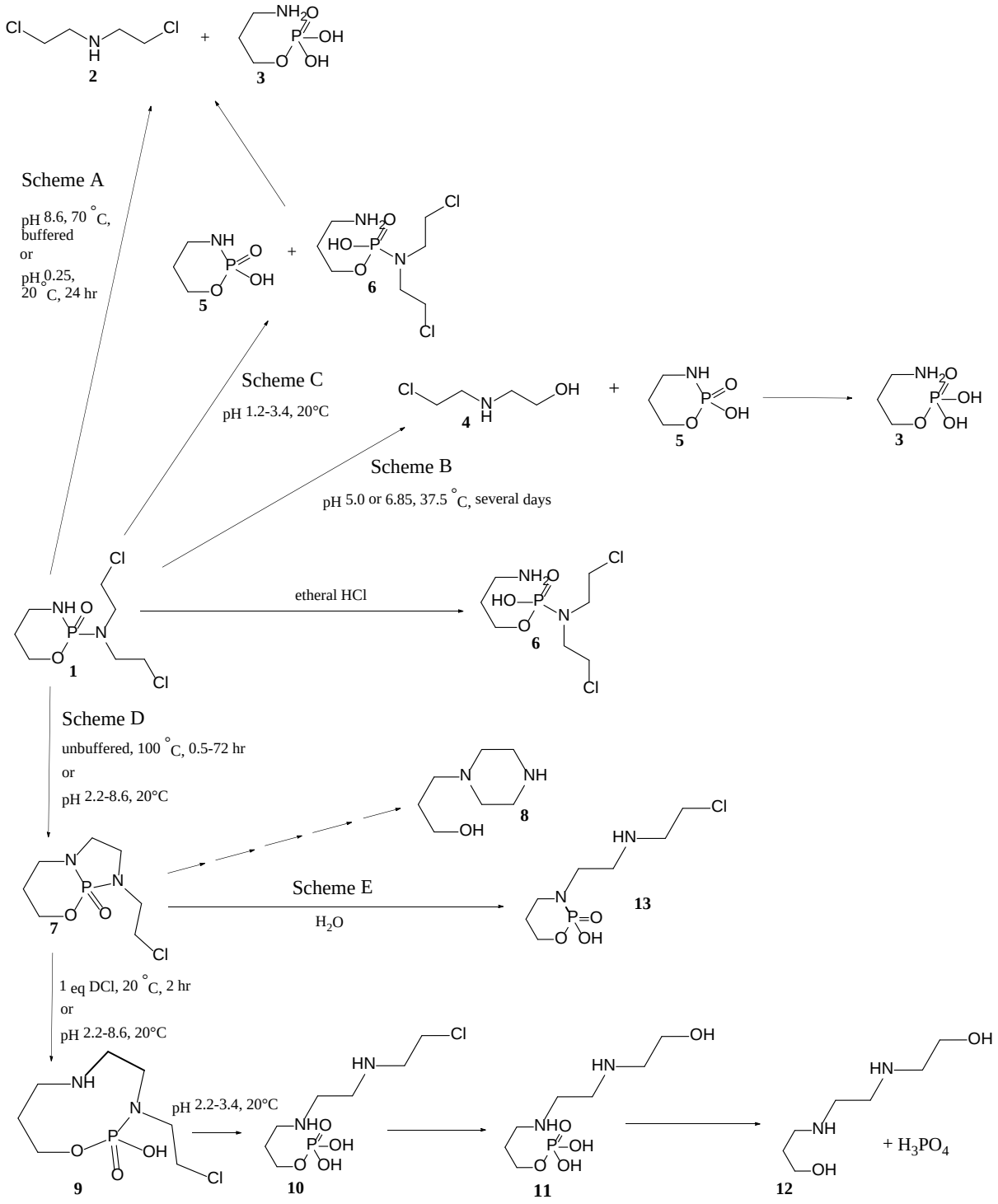

Figure 5-1. Previously reported hydrolysis pathways of cyclophosphamide (1) [194, 203-205]. Compounds 3, 5, and 6 are shown twice to demonstrate the different reaction pathways they have been shown to be involved in.

Friedman *et al.* [203] also investigated the cyclophosphamide hydrolysis reaction by refluxing a 2 % aqueous cyclophosphamide solution for 72 hours. They were able to identify the major and minor products to compound **12** and compound **8**, respectively, via melting points, IR spectroscopy, and octanol-water partitioning coefficients. These findings suggested that cyclophosphamide was reacting via an initial intramolecular alkylation, followed by hydrolysis of the N-P and O-P bonds, and finally a

second N-alkylation, as described in Scheme D in Figure 5-1. This was later referred to by other researchers as the "Friedman Mechanism" [194]. These findings were later confirmed by Zon *et al.* [204] using ^{1}H, ^{13}C, and ^{31}P NMR, via synthesis of compound **7** from **1**, followed by forced hydrolysis to **10** using DCl.

Gilard *et al.* [194] monitored the cyclophosphamide hydrolysis reaction in buffered solutions at room temperature by analysing isolated degradation products using ^{1}H, ^{13}C, and ^{31}P NMR, and fast atom bombardment (FAB) mass spectrometry. This group also synthesised each degradation product individually to confirm the assigned structures. They were able to confirm that the same hydrolysis products produced under the harsh conditions used by previous researchers were formed at room temperature over extended time periods (7-17 days) at various pH levels (Scheme D, Figure 5-1). Zon *et al.* [204] and Pankiewicz *et al.* [205] had also reported the formation of compound **13** upon dissolution of compound **7** in water (Scheme E, Figure 5-1), however Gilard *et al.* [194], were unable to replicate these results.

The first aim of this chapter was therefore to identify which of these reactions schemes was occurring during the experiments conducted in Chapter 4, as well as which compounds were responsible for the observed increase in chemiluminescence signal. The second aim was to force this degradation reaction in order to indirectly detect cyclophosphamide using chemiluminescence. A series of experiments to monitor the hydrolysis reaction simultaneously with chemiluminescence were therefore undertaken. Investigation into the effects of various conditions such as temperature, UV light exposure, and pH were also conducted in order to determine optimal conditions for use in controlled or on-line conversion of cyclophosphamide to the desired product for indirect detection.

5.2 Experimental

5.2.1 Chemicals and Reagents

All reagents were analytical grade unless otherwise stated. Cyclophosphamide monohydrate, deuterium oxide, and sodium oxalate were purchased from Sigma Aldrich Pty. Ltd (Castle Hill, NSW, Australia). Tris-2,2'-bipyridyl ruthenium (II) chloride hexahydrate was purchased from Strem Chemicals (Newburyport, MA, USA). Sulfuric acid (98 %), lead dioxide (PbO_2), sodium hydroxide, orthophosphoric acid (85 %), and disodium hydrogen phosphate were purchased from Chem-Supply (Gillman, SA, Australia). Sodium dihydrogen phosphate and sodium hydrogen carbonate were purchased from Merck Pty. Ltd (Bayswater, Victoria, Australia). Tris(hydroxymethyl)aminomethane and sodium borate decahydrate were purchased from Amersham Australia Pty. Ltd (Baulkham Hills, NSW, Australia). Hydrochloric acid (37 % w/w) was purchased from Choice Analytical (Thornleigh, NSW, Australia).

5.2.2 Cyclophosphamide Degradation Investigation using FIA-Chemiluminescence

5.2.2.1 Sample Preparation and Storage Conditions

Cyclophosphamide solutions (1 x 10^{-3} M) were prepared via dissolution in deionised water (18 MΩ) and sonication for 1 minute (Elmasonic S 30, Elma, Pathtech, Australia). Four of these solutions were incubated in sealed plastic containers (Technoplas, Rowe Scientific Pty Ltd, Australia) in the absence of light at 55, 60, 80, and 98 °C using hot water baths with constant stirring. Four cyclophosphamide solutions were also adjusted to pH 2-11 via addition of NaOH or HCl and stored in sealed plastic containers at room temperature in the absence of light. These solutions were stored in sealed plastic containers (Technoplas, Rowe Scientific Pty Ltd, Australia) at room temperature in the absence of light. 5 mL aliquots of each solution were removed immediately after preparation and then every 5 hours for 25 hours and analysed immediately using FIA-chemiluminescence. Cyclophosphamide solutions (1 x 10^{-3} M) were also prepared in phosphate buffer (pH 7 and 8), tris buffer (pH 9), borate buffer (pH 10), and bicarbonate buffer (pH 11) and sonicated for 1 minute (Elmasonic S 30, Elma, Pathtech, Australia). These solutions were stored in sealed plastic containers (Technoplas, Rowe Scientific Pty Ltd, Australia) at room temperature in the absence of light. 5 mL aliquots of each solution were removed immediately after preparation and then every 5 hours for the first 30 hours, and then every 10 hours for the remaining 60 hours, and analysed immediately using FIA-chemiluminescence. A summary of all storage conditions used is given in Table 5-1.

The original volume of cyclophosphamide incubated was 200 mL. This ensured aliquot removal would be insignificant in comparison to the remaining volume, in order to minimise changes in total volume, heat transfer, and reaction kinetics as the experiment progressed. The room temperature was measured to be 20 °C ± 1 °C.

Table 5-1. Storage conditions used to investigate the degradation of cyclophosphamide (1 x 10^{-3} M) using FIA-chemiluminescence

Temperature (°C)	Sample matrix	Storage Time (hours)
20	deionised water	24
55	deionised water	24
60	deionised water	24
80	deionised water	24
98	deionised water	24
20	pH 2.00 NaOH	24
20	pH 3.80 NaOH	24
20	pH 6.82 HCl	24
20	pH 11.0 HCl	24
20	pH 7 phosphate buffer	100
20	pH 8 phosphate buffer	100
20	pH 9 tris buffer	100
20	pH 10 borate buffer	100
20	pH 11 bicarbonate buffer	100

5.2.2.2 Buffer Preparation

All solutions were prepared using deionised water (18 MΩ) unless otherwise stated. Buffers were prepared fresh daily. H_2SO_4 (5 x 10^{-4} - 0.1 M) was prepared by dissolution in deionised water. pH 6 phosphate buffer was prepared by mixing 12.0 mL of 0.05 M Na_2HPO_4 with 88.0 mL 0.05 M NaH_2PO_4. pH 7 phosphate buffer was prepared by mixing 115.4 mL of 0.1 M Na_2HPO_4 with 84.6 mL 0.1 M NaH_2PO_4. pH 8 phosphate buffer was prepared by mixing 233 mL of 0.1 M Na_2HPO_4 with 17 mL 0.1 M NaH_2PO_4. Bicarbonate buffer (pH 11) was prepared by diluting a mixture of 100 mL 0.1 M $NaHCO_3$ and 45.4 mL 0.2 M NaOH to 200 mL with distilled water. Borate buffer (pH 10) was prepared by diluting a mixture of 100 mL of 0.1 M $Na_2B_4O_7.10H_2O$ (borax) and 36.6 mL of 0.4 M NaOH to 200 mL with distilled water. Tris buffer (pH 9) was prepared by diluting a mixture of 100 mL of 0.1 M tris(hydroxymethyl)aminomethane (tris) and 11.4 mL of 0.1 M HCl to 200 mL with distilled water. This is summarised in Table 5-2. The pH of each buffer was confirmed after each preparation using a Mettler Toledo S220 SevenCompact™ pH metre (Rowe Scientific Pty. Ltd, Adelaide, Australia).

Table 5-2. Stock solutions and their corresponding volumes used to prepare various basic buffer carrier solutions in 200 mL deionised water

	Solution	Concentration (M)	Volume (mL)	Solution	Concentration (M)	Volume (mL)
phosphate pH 7	Na_2HPO_4	0.1	115.4	NaH_2PO_4	0.1	84.6
phosphate pH 8	Na_2HPO_4	0.1	233	NaH_2PO_4	0.1	17
tris pH 9	tris	0.1	100	HCl	0.1	11.4
Borate pH 10	borax	0.1	100	NaOH	0.4	36.6
Bicarbonate pH 11	$NaHCO_3$	0.1	100	NaOH	0.2	45.4

5.2.2.3 Oxidising Reagent Preparation

$[Ru(bipy)_3]Cl_2$ (1 x 10^{-4} M) was prepared by dissolution of tris(2,2'-bipyridyl)ruthenium(II) chloride in H_2SO_4 (0.075 M). This solution was stored in a sealed plastic container (Technoplas, Rowe Scientific Pty Ltd, Australia) in the absence of light for up to 24 hours. Immediately prior to each analysis an aliquot of the stock solution was removed and mixed with solid lead dioxide (0.1 g/20 mL), resulting in a colour change from orange to green. The solid material was removed via online filtration through glass wool during analysis.

5.2.2.4 Instrumentation

FIA-chemiluminescence analysis of each aliquot was conducted immediately after removal using the in-house built instrument described in Chapter 3. Tris-2,2'-bipyridyl ruthenium (II) chloride was used as the oxidising reagent. The active $[Ru(bipy)_3]^{3+}$ oxidation state was produced by mixing with solid PbO_2 (0.1 g per 20 mL) immediately prior to on-line filtering. Bicarbonate buffer (0.05 M, pH 11) was used as the carrier solution. Distilled water was analysed as the blank solution after each aliquot analysis.

5.2.3 Hydrolysis Product Identification

5.2.3.1 Sample Preparation

Three cyclophosphamide solutions (0.1 M in deionised water, 200 mL) were prepared and sonicated for 1 minute using an Elmasonic S 30 ultrasonicator (Elma, Pathtech, Australia). One solution was stored in a sealed plastic container (Technoplas, Rowe Scientific Pty Ltd, Australia) at room temperature in the absence of light. 5 mL aliquots of this solution were removed at 0, 1, 3, 7, 11, 21.5, and 76.5 hours after preparation and analysed immediately using ^{31}P and ^{12}C NMR and FIA-chemiluminescence as described below. The second cyclophosphamide solution was heated at 98 ^{o}C in a water bath with constant stirring for a period of 100 minutes. 5 mL aliquots of the heated solution were taken at 0, 2.5, 9.5, and 18 minutes, and then every 10 minutes up to 100 minutes for FIA-chemiluminescence analysis. 1 mL aliquots of the heated solution were taken at 1, 13, 31, 52, and 73 minutes for ^{31}P NMR analysis (see below). 1 mL aliquots were also taken every 17 minutes for analysis using ion chromatography (see below). The pH and conductivity of the solution were also measured every 10 minutes via direct immersion of the probe into the solution. The third cyclophosphamide solution was stored for 48 hours at room temperature in the absence of light. It was then diluted 1000-fold and analysed using LC-MS/MS (see below).

5.2.3.2 NMR

1 mL of each sample aliquot was transferred to a 5 mm diameter glass NMR tube to which 0.5 mL D_2O was added for locking purposes. These samples were analysed immediately. ^{1}H, ^{31}P, and ^{12}C NMR experiments were conducted using a Bruker 600 MHz spectrometer, 5 mm inverse multinuclear probe,

and autosampler. Probe temperature was maintained at 25 °C. The number of data points for each scan was 65536. Proton decoupling was used for all ^{13}C and ^{31}P NMR experiments. The specific instrument conditions for ^{31}P NMR analysis were as follows: number of scans, 320; spectral width, 96154 Hz; acquisition time, 0.34 seconds; pulse width, 15 µs. The specific instrument conditions for ^{13}C NMR analysis were as follows: number of scans, 700; spectral width, 36058 Hz; acquisition time, 0.91 seconds; pulse width, 12 µs. The specific instrument conditions for ^{1}H NMR analysis were as follows: number of scans, 16; spectral width, 12019 Hz; acquisition time, 2.7 seconds; pulse width, 14 µs. All ^{31}P NMR spectra were referenced to 85 % H_3PO_4. The time points for each spectrum were taken to be the start time of data acquisition.

5.2.3.3 LC-MS/MS

LC-MS/MS analysis was conducted using a Waters Aquity UHPLC® with QTOF detector. The column was a Waters Aquity UHPLC® BEH C18 column (1.7 µm i.d., 3.0 x 50 mm) and a Phenomenex 3 x 4 mm C18 SecurityGuard™ guard cartridge. Gradient elution using 0.1 % formic acid (in 18 MΩ water)(A) and acetonitrile (B) was performed with the following ramp profile: 0-0.5 min: 90 % A; 0.5-7.5 min: ramped to 50 % A; 7.5-10 min: ramped to 5 % A; 10-12 min: ramped to 0 % A. The flow rate was 0/35 mL/min. Column temperature was 30 °C. Injection volume was 10 µL. The conditions for QTOF analysis were as follows: positive ESI mode. 3.0 kV capillary voltage. 125 V fragmentor voltage. Nebuliser pressure 50 psi. Collision gas was nitrogen (350 °C, 10 L/min). Data processing was conducted using Agilent Mass Hunter Qualitative and Quantitaive Analysis version 4.0.

5.2.3.4 FIA-Chemiluminescence

0.1 mL of each sample aliquot was diluted 100-fold in deionised water (18 MΩ) and immediately analysed using the in-house built FIA-chemiluminescence instrument used in Chapter 4 (Figure 5-2), however using a T-piece for analyte-carrier solution merging. The total flow rate was 1.7 µL/min. The reagent conditions used for all analyses are given in Table 5-3. Bicarbonate buffer stock solution (0.05 M, pH 11) was prepared fresh daily and used as the carrier for all FIA-chemiluminescence analyses for a given experiment. All analyses were performed in triplicate.

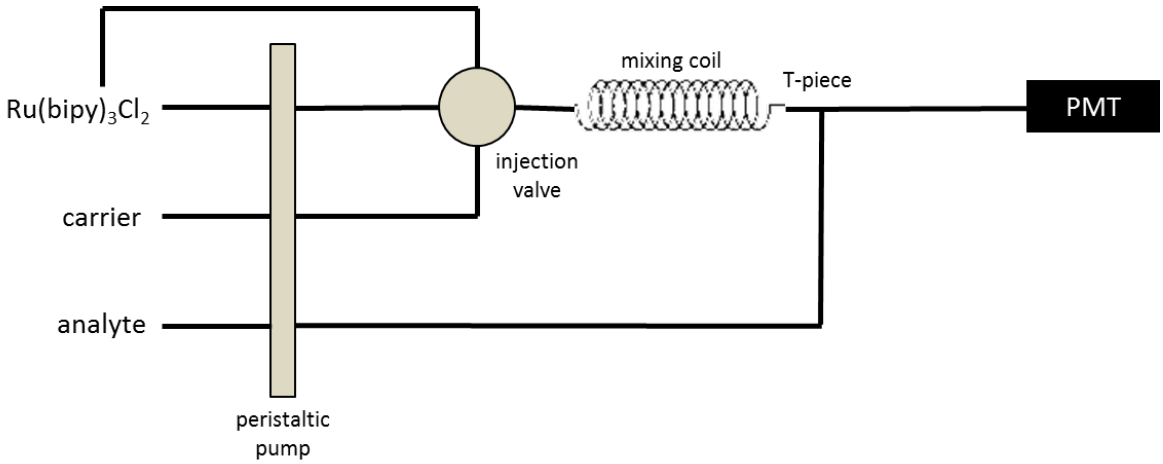

Figure 5-2. Schematic of in-house-built flow injection analysis (FIA) used for investigation into cyclophosphamide degradation

Table 5-3. Reagent conditions used for FIA chemiluminescence analysis of cyclophosphamide (1 x 10^{-5} M) prepared in various matrices and stored under various conditions

Reagent	Composition
Analyte	Cyclophosphamide (1 x 10^{-5} M)
Oxidising Reagent	$Ru(bipy)_3Cl_2$ (1 x 10^{-3} M in 0.075 M H_2SO_4)
Carrier Solution	Bicarbonate buffer (0.05 M, pH 11)

5.2.3.5 Ion Chromatography

0.1 mL of each sample aliquot was diluted 100-fold in distilled water and immediately analysed using a Dionex ICS-1500 Ion Chromatography System (Thermo Fischer Scientific Inc., Melbourne, Victoria). Standard chloride ion solutions of concentration 0.2, 0.4, 0.6, and 0.8 ppm were also analysed in order to identify the chloride peak. The eluent contained 8 x 10^{-3} M sodium carbonate and 1 x 10^{-3} M sodium bicarbonate in distilled water. The column was an IonPac AS22 4 mm column (Thermo Fischer Scientific Inc., Melbourne, Victoria). The injection volume was 20 µL. The flow rate was 1.2 mL/min. All solutions were filtered through 0.2 µm membrane syringe filters (Adelab Scientific, Thebarton, SA) prior to anlaysis.

5.2.3.6 pH and Conductivity Measurements

The pH and conductivity of the heated cyclophosphamide solution were measured every 10 minutes via immersion of the probes directly into the solution while stirring was continued. This was done using a TPS labCHEM-CP Conductivity-TDS-Sal-pH-mV-tempmeter (TPS, Pty Ltd., Springwood, Qld, Australia). The probes were rinsed with deionised water prior to each analysis.

5.2.4 On-line Hydrolysis

On-line treatment of the cyclophosphamide analyte (1 x 10^{-3} M) was conducted using the in-house built FIA chemiluminescence instrument depicted in Figure 5-3. Instrument components and software were the same as those used in Chapters 3 and 4. Two FIA manifolds were tested (1 and 2). The water bath was prepared using a CH1922-001 thermostat hot plate (Industrial Equipment and Control Pty

Ltd., Australia) with constant stirring. Water bath temperatures of 20, 60, 75, and 85 °C were investigated. The heating coil was made of PTFE tubing (0.02 mm I.D.). Heating coil volumes of 263, 393, 400, and 522 µL were investigated. The reagent conditions used are given in Table 5-4.

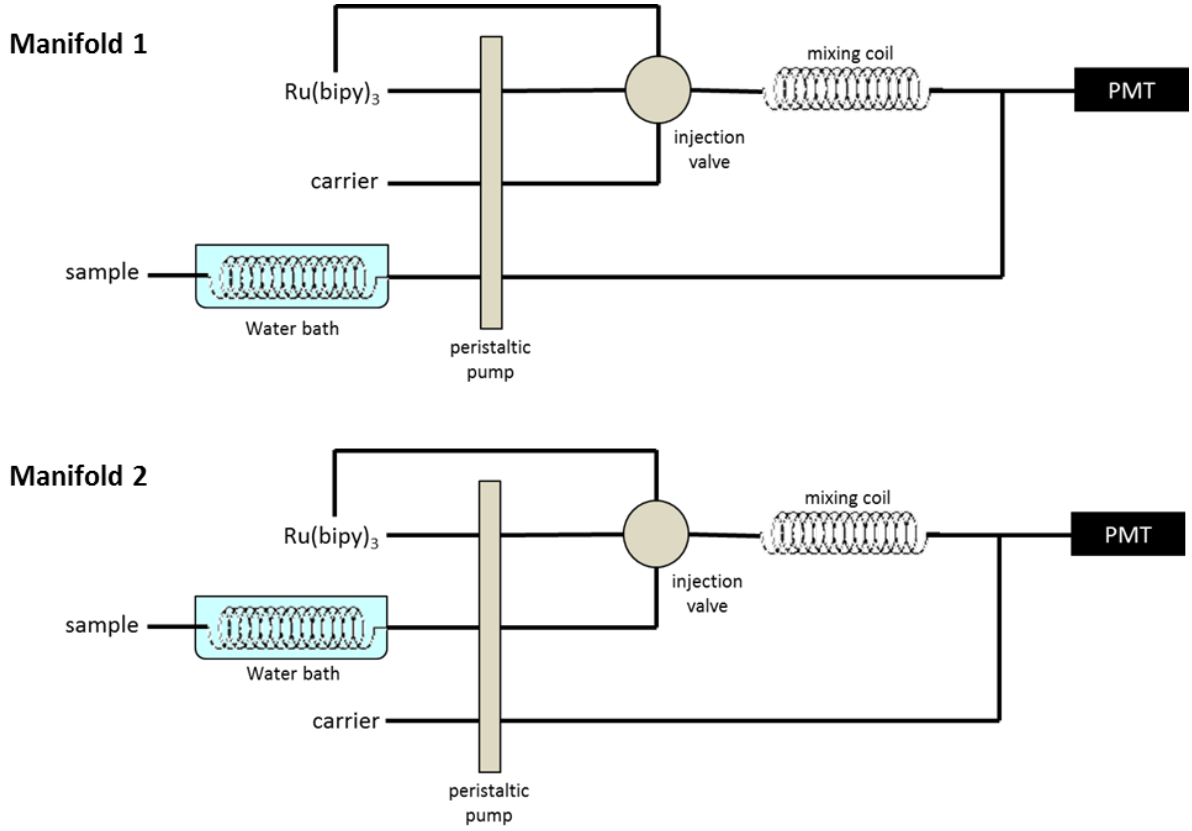

Figure 5-3. FIA-chemiluminescence manifolds tested for on-line treatment of cyclophosphamide

Table 5-4. Reagent conditions used for FIA-chemiluminescence analysis of cyclophosphamide (1 x 10^{-3} M) heated and/or acidified on-line

Reagent	Composition
Analyte	Cyclophosphamide (1 x 10^{-3} M) in deionised water
Oxidising Reagent	$Ru(bipy)_3Cl_2$ (1 x 10^{-3} M in 0.075 M H_2SO_4)
Carrier Solution	Bicarbonate buffer (0.05 M, pH 11)

5.3 Results and Discussion

5.3.1 Cyclophosphamide Degradation Investigation using FIA-Chemiluminescence

In Chapter 4 cyclophosphamide was shown to degrade over time to produce one or more compounds that had a higher chemiluminescence activity than that of the parent drug. The developed FIA-chemiluminescence method was therefore used to investigate the characteristics of this degradation.

5.3.1.1 Effect of Light Exposure:

The effect of light exposure on the rate of change in chemiluminescence signal was investigated via analysis of two cyclophosphamide solutions (1 x 10^{-3} M in 0.05 M pH 7 phosphate buffer) every 5 hours

for 25 hours, with one being held in complete darkness and the other in daylight. The reagent conditions used are given in Table 5-5. The resulting trends in average net chemiluminescence peak area are given in Figure 5-4. While the net chemiluminescence peak area did increase over time, there was no significant difference in signals obtained from cyclophosphamide solutions held in the light or dark. This therefore suggested that a light-induced or catalysed degradation mechanism was unlikely.

Table 5-5. Reagents used for analysis of cyclophosphamide solutions in order to investigate the effect of various parameters on its degradation

Reagent	Composition
Analyte	Cyclophosphamide (1 x 10^{-3} M) in phosphate buffer (pH 7, 0.05 M)
Oxidising Reagent	$Ru(bipy)_3Cl_2$ (1 x 10^{-3} M in 0.075 M H_2SO_4)
Carrier Solution	Phosphate buffer (pH 7, 0.05 M)

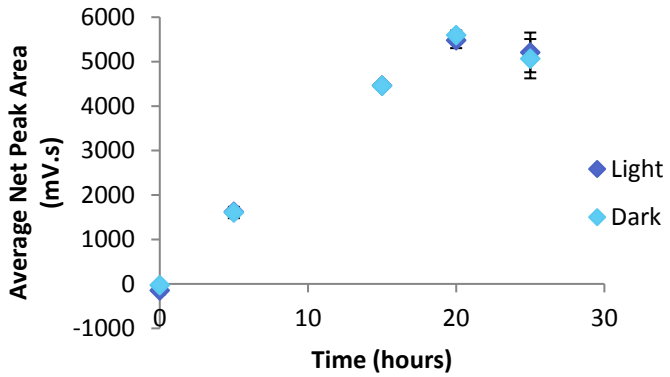

Figure 5-4. Effect of light exposure on the average net peak area (n=3) obtained via FIA-chemiluminescence analysis of cyclophosphamide (1 x 10^{-3} M in 0.05 M pH 7 phosphate buffer) over 25 hours using $Ru(bipy)_3Cl_2$ (1 x 10^{-3} M in 0.075 M H_2SO_4) as the oxidising reagent. Error bars = ± 1 standard deviation.

5.3.1.2 Effect of Temperature:

The effect of temperature on the rate of change in chemiluminescence signal was investigated via analysis of four separate cyclophosphamide solutions (1 x 10^{-3} M in 0.05 M pH 7 phosphate buffer) held at -4, 4, 20, and 35 °C every 5 hours for 25 hours. The reagent conditions used are given in Table 5-5. The resulting trends in chemiluminescence signals are given in Figure 5-5. It was observed that storing cyclophosphamide solutions at temperatures of 4 °C and below lead to stability of the chemiluminescence signal over 24 hours. At 37 °C, however, the chemiluminescence peak area was observed to increase over 25 hours. The rate of this increase was greater at 35 °C than at 20 °C, with the average net peak area increasing by 49 times in 25 hours at 35 °C, compared to 14 times in 25 hours at 20 °C. This therefore indicated that the reaction was thermally driven.

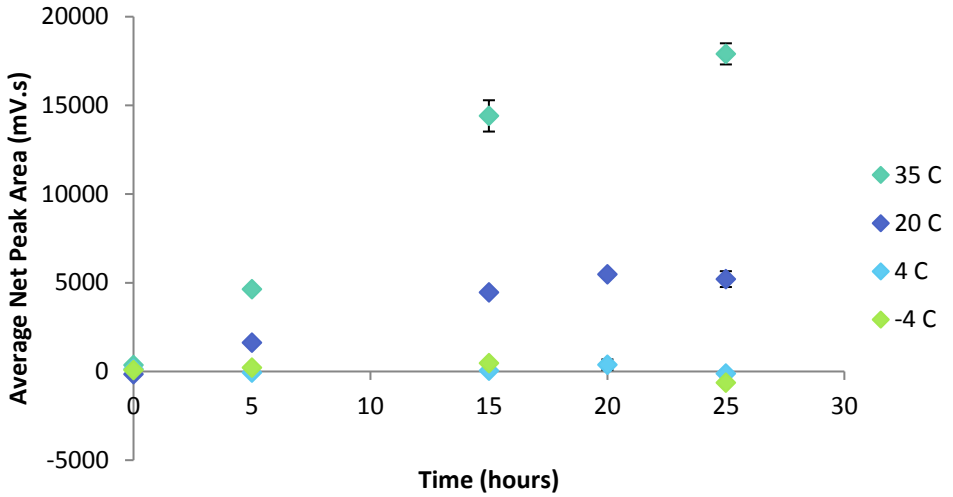

Figure 5-5. Effect of sample storage temperature on the average net peak area (n=3) obtained via FIA-chemiluminescence analysis of cyclophosphamide (1 x 10^{-3} M in 0.05 M pH 7 phosphate buffer) incubated at various temperature over 25 hours using $Ru(bipy)_3Cl_2$ (1 x 10^{-3} M in 0.075 M H_2SO_4) as the oxidising reagent. Error bars = ± 1 standard deviation.

5.3.1.3 Effect of pH

The effect of the pH of the analyte solution on the rate of change in chemiluminescence signal was then investigated. Basic buffers were chosen because the increase in chemiluminescence signal over time observed in Chapter 4 occurred at basic pH. The buffers tested and the reagent conditions used for analysis are given in Table 5-6. Each cyclophosphamide solution (1 x 10^{-3} M) was analysed periodically over 90 hours, with the resulting average net chemiluminescence peak areas given in Figure 5-6. It should be noted that the net peak area at 0 hours for the pH 11 solution was higher than that of the other solutions, being 880.3 ± 86 mV.s, compared to between 30.31 ± 93 mV.s and 288.5 ± 44 mV.s for the other solutions. This was most likely due to slight differences in the cyclophosphamide concentration in this particular solution that occurred during preparation.

It was observed that the chemiluminescence signal increased more quickly at lower buffer pH levels. Buffers with pH above 9 allowed the chemiluminescence signal to remain relatively constant for 24 hours, however after this time the chemiluminescence signal increased for all buffers. The bicarbonate buffer (pH 11) was also observed to give a lower background signal than the other buffers, which would allow for lower limits of detection to be reached. It is therefore recommended that, in order to allow cyclophosphamide samples to be prepared once daily without fear of degradation during analysis, they should be prepared in bicarbonate buffer, rather than the phosphate buffer used previously. The solutions at pH below 8 produced the greatest increase in signal, with net chemiluminescence peak areas of 18438 ± 173 mV.s and 9599.4 ± 55 mV.s after 90 hours for pH 7 and 8, respectively. It was therefore possible that the cyclophosphamide degradation was acid-catalysed.

Table 5-6. Reagents used for the analysis of cyclophosphamide (1 x 10^{-3} M) prepared in various basic buffers to investigate the effect of analyte pH on cyclophosphamide degradation using FIA-chemiluminescence

Reagent	Composition
Analyte	Cyclophosphamide (1 x 10^{-3} M) in 0.05 M: • Phosphate buffer (pH 7.07) • Phosphate buffer (pH 8.43) • Tris buffer (pH 9) • Borate buffer (pH 10) • Bicarbonate buffer (pH 11)
Oxidising Reagent	$Ru(bipy)_3Cl_2$ (1 x 10^{-3} M in 0.075 M H_2SO_4)
Carrier Solution	Phosphate buffer (pH 7, 0.05 M)

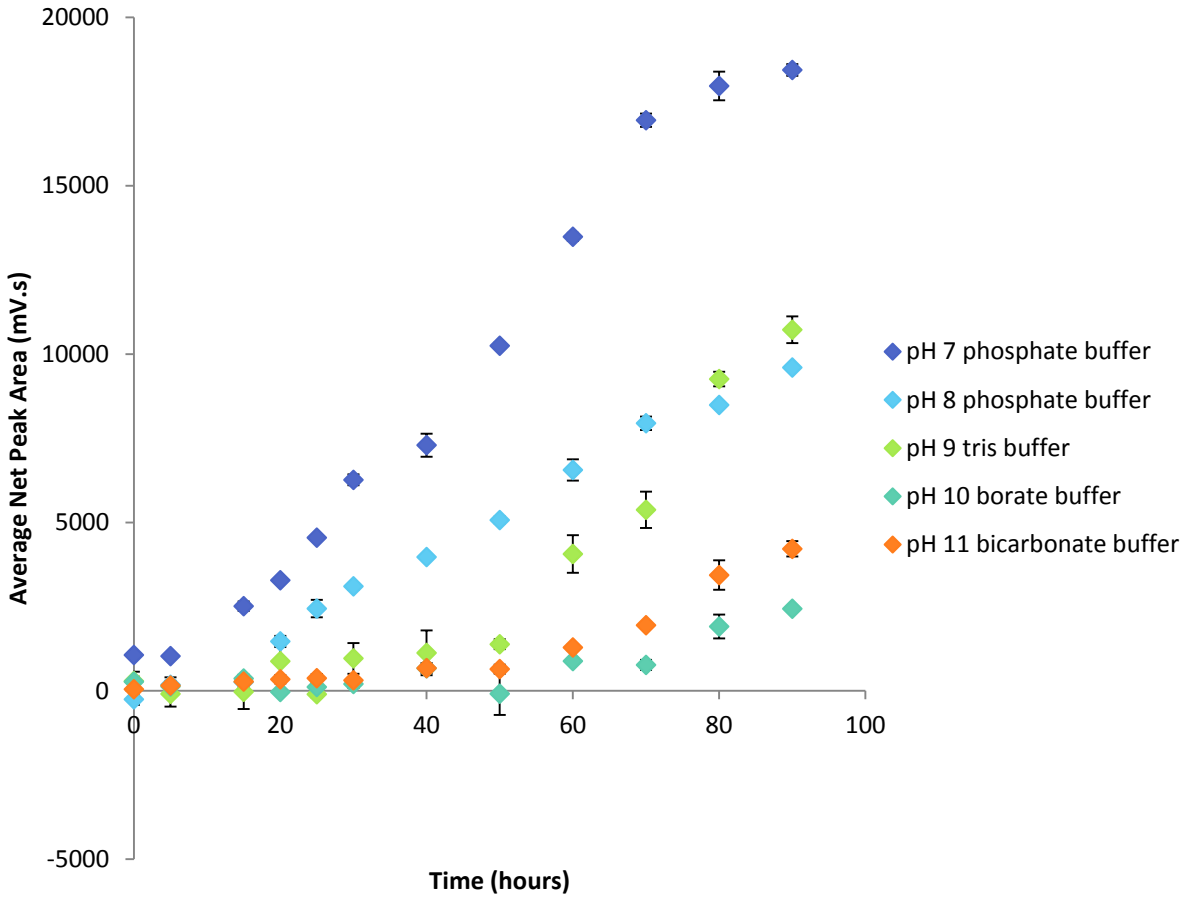

Figure 5-6. Effect of buffered analyte pH on the average net peak area (n=3) obtained via FIA-chemiluminescence analysis of cyclophosphamide (1 x 10^{-3} M in various buffers) over 90 hours using $Ru(bipy)_3Cl_2$ (1 x 10^{-3} M in 0.075 M H_2SO_4) as the oxidising reagent. Error bars = ± 1 standard deviation.

In order to assess if the cyclophosphamide degradation reaction was indeed acid-catalaysed, cyclophosphamide solutions (1 x 10^{-3} M) adjusted to pH values between 2 and 11 using either NaOH or HCl and stored at 20 °C were analysed every 5 hours over 25 hours. These solutions were prepared in deionised water without buffering. The reagent conditions used are given in Table 5-7. The resulting trends in net chemiluminescence peak area are given in Figure 5-7. Different trends were observed for different pH levels. In the first 5 hours the rate of increase in net peak area was highest for the pH 2.00 solution, followed by the pH 3.80 and 6.82 solutions, and then by the pH 11.0 solution, supporting

the idea of an acid-catalysed reaction. After the first 5 hours, however, the net peak area produced by the pH 2.00 solution appeared to level-off. The pH 3.80 and 6.82 solutions produced quite similar increases in net peak area in the first 5 hours, after which the rate of increase was higher for the pH 6.82 solution. At pH 11.0, however, the net peak area decreased slightly over time. The large difference in trends observed at different pH levels suggested that, rather than a simple acid-catalysed reaction, multiple reactions and reaction pathways may have been involved. Zon *et al.* [204] had similar findings, in which the cyclophosphamide hydrolysis kinetics were found to be drastically different when at pH 11 compared to pH 2-8. Gilard *et al.* [194] also found this, with different reaction pathways occurring at different pH levels, as shown in Figure 5-1 from the Introduction. At pH levels between 1 and 3 products **5**, **6**, **3**, and **2** were formed (Scheme A and C). At pH levels between 2 and 8, however, **7** (1*H*,5*H*-[1,3,2]Diazaphospholo[2,1-*b*][1,3,2]oxazaphosphorine, 1-(2-chloroethyl) tetrahydro-, 9-oxide), **9** (3-(2-chloroethyl)octahydro-2-hydroxy-1,3,6,2-oxadiazaphosphine-2-oxide), and **10** (1-propanol,3-[[2-[(2-chloroethyl)amino]ethyl]amino]-, dihydrogen phosphate (ester)) were produced (Scheme D). Figure 5-7 demonstrated that pH levels of 3.80 and 6.82 produced the largest increase in signal in 25 hours, with final net peak areas of 2807 ± 167 mV.s and 3851 ± 61 mV.s, respectively. This suggested that the cyclophosphamide hydrolysis pathway that produced an increase in chemiluminescence was that occurring at pH 2-8 via compounds **7**, **9**, and **10**.

Table 5-7. Reagents used to investigate the effect of analyte pH on the degradation of cyclophosphamide (1×10^{-3} M) using FIA-chemiluminescence

Reagent	**Composition**
Analyte	Cyclophosphamide (1×10^{-3} M) in deionised water adjusted to pH 2-11 using NaOH or HCl
Oxidising Reagent	$Ru(bipy)_3Cl_2$ (1×10^{-3} M in 0.075 M H_2SO_4)
Carrier Solution	Phosphate buffer (pH 7, 0.05 M)

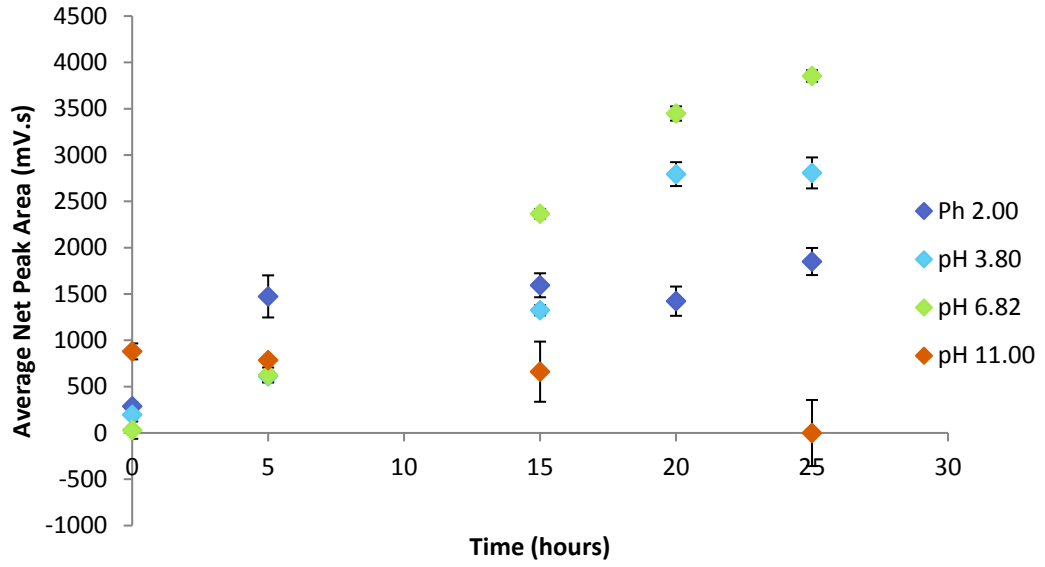

Figure 5-7. Effect of sample pH on the average net peak area (n=3) obtained via FIA-chemiluminescence analysis of cyclophosphamide (1 x 10^{-3} M, adjusted to pH 2-11 using NaOH or HCl) over 25 hours using $Ru(bipy)_3Cl_2$ (1 x 10^{-3} M in 0.075 M H_2SO_4) as the oxidising reagent. Error bars = ± 1 standard deviation.

The increase and then decrease in chemiluminescence signal observed when analysing cyclophosphamide solutions adjusted to various pH levels using NaOH or HCl here was not observed for the buffered solutions earlier. This was most likely due to the buffered solutions more tightly controlling the pH of the reaction mixture. During the reaction of cyclophosphamide the pH of the reaction mixture would be expected to change, due to the production and consumption of H^+ ions. For instance, the degradation of cyclophosphamide to compound **7** (Scheme D, Figure 5-1) would result in the production of HCl, as shown in the mechanism in Figure 5-8. In non-buffered solution this would increase the pH of the reaction mixture, hence affecting which reaction pathway in Figure 5-1 was most favourable. In buffered solutions, however, the production of H^+ ions would be buffered, and hence would affect the pH of the solution to a lesser extent. The favourable cyclophosphamide degradation pathway would therefore remain the same, resulting in a more constant increase in chemiluminescence over time.

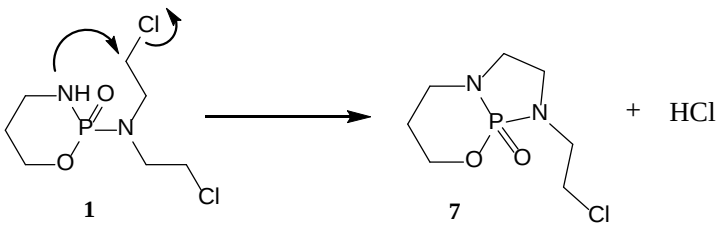

Figure 5-8. Mechanism of cyclophosphamide (1) degradation to compound 7 and production of HCl

5.3.2 Degradation Product Identification

In order to identify the products of the observed degradation of cyclophosphamide, ^{31}P NMR and ^{13}C NMR analysis was conducted. A cyclophosphamide solution (0.1 M in deionised water) was held at room temperature for 100 hours. Periodically over this time 1 mL aliquots were removed and mixed

in a 1:1 (v/v) ratio with D_2O. They were immediately analysed using ^{31}P NMR and ^{13}C NMR as described in Section 5.2.2.4. As the degradation reaction was known to occur quite quickly, the number of scans used for ^{31}P and ^{13}C NMR experiments was decreased from that typically employed down to 320 and 700 scans, respectively. This would increase the number of data points that could be collected over the degradation time, and minimise the degradation that could occur during the NMR analysis itself. This would also decrease the sensitivity of the analyses. Simultaneously, aliquots of the original cyclophosphamide solutions were taken, diluted 100-fold in deionised water, and analysed using FIA-chemiluminescence using the conditions in Table 5-8.

Table 5-8. Reagents used for FIA-chemiluminescence analysis of cyclophosphamide (1 x 10^{-3} M) periodically over 100 hours

Reagent	Composition
Analyte	Cyclophosphamide (1 x 10^{-3} M) in deionised water
Oxidising Reagent	$Ru(bipy)_3Cl_2$ (1 x 10^{-3} M in 0.075 M H_2SO_4)
Carrier Solution	Phosphate buffer (pH 7, 0.05 M)

The ^{31}P NMR analysis gave rise to an intense peak at 15.30 ppm and a much smaller peak at 8.020 ppm (Appendix L). According to Gilard *et al.* [194], the peak at 15.30 ppm most likely corresponded to cyclophosphamide, while that at 8.020 ppm could correspond to compound **9**, as shown in the previously postulated hydrolysis pathways of cyclophosphamide in Figure 5-1. Gilard *et al.* [194] found this compound was formed at neutral pH, and possessed a chemical shift typical of structures containing only one P-N bond. After 10 hours a third peak at 0.5189 ppm appeared and began to increase in intensity with time (Appendix L). This peak likely corresponded to either of compounds **10** or **3** in the postulated cyclophosphamide hydrolysis pathway (Figure 5-1), which were shown to have very similar chemical shifts. It was hypothesised that compound **10** was the most likely identity because compound **3** had only been shown to be formed at a low pH [194], whereas these experiments were conducted at a pH of approximately 6.

The trends in ^{31}P NMR relative peak intensity for the peak at 15.30 ppm are given in Figure 5-9. Trends in intensities of the peaks at 8.020 ppm and 0.5189 ppm, overlaid with the trends in chemiluminescence peak area, are given in Figure 5-10. It was observed that over 80 hours, the percentage of total peak intensity of the peak at 15.30 ppm decreased at an apparently exponential rate, most likely due to the conversion of cyclophosphamide to one or more other compounds, while the peak at 8.020 ppm followed the opposite trend, as shown in Figure 5-9.

Upon inspection of the chemiluminescence trends (Figure 5-10) it was clear that there were two distinct patterns. After 7 hours, the chemiluminescence signal increased at a decreasing rate up to 80 hours; a similar trend to that observed in the intensity of the ^{31}P NMR peaks at 8.020 ppm and 0.5189

ppm. This therefore suggested that either compound **9** (8.020 ppm) or **10** (0.5189 ppm) was responsible for the observed increase in chemiluminescence. Prior to 7 hours, however, the chemiluminescence signal appeared to decrease slightly over time. This was most likely due to compounds **9** or **10** being present at too low a concentration to be detected, and hence the only observable change was that of the decreasing cyclophosphamide concentration as it was degrading. After 7 hours, the hydrolysis products were present in a high enough concentration to be detected using chemiluminescence, and hence the signal trend began to more closely resemble those obtained via ^{31}P NMR analysis. It was hypothesised that compound **9** would have the higher chemiluminescence activity of the two possible hydrolysis products, due to the presence of a tertiary amine, known to produce intense chemiluminescence upon reaction with $[Ru(bipy)_3]^{3+}$, compared with only two secondary amines in compound **10**. It is also possible, however, that neither compound **9** nor **10** is responsible for the increase in chemiluminescence, and the truly more active compound is an intermediate of the reaction to form compounds **9** and **10**, namely compound **7**. Compound **7** was not observed during any NMR experiments, which was also the finding of Gilard *et al.* [194] and Friedman *et al.* [203]. This is most likely a result of very rapid conversion of this product to compound **9**. Compound **7** contains two tertiary amines, and hence would be expected to be more chemiluminescence-active with $[Ru(bipy)_3]^{3+}$ than cyclophosphamide or compounds **9** and **10**. It is therefore possible that this is in-fact the compound responsible for the observed chemiluminescence increase.

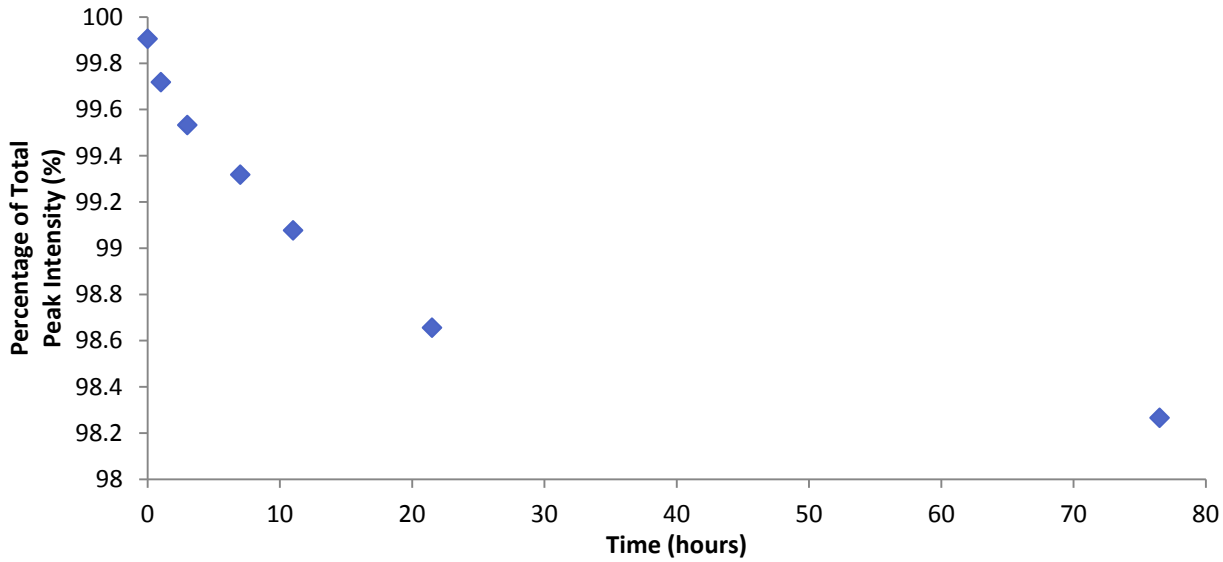

Figure 5-9. Change in percentage of total peak intensity of the ^{31}P NMR peak at 15.30 ppm observed via analysis of cyclophosphamide (0.05 M in deionised water) over 80 hours.

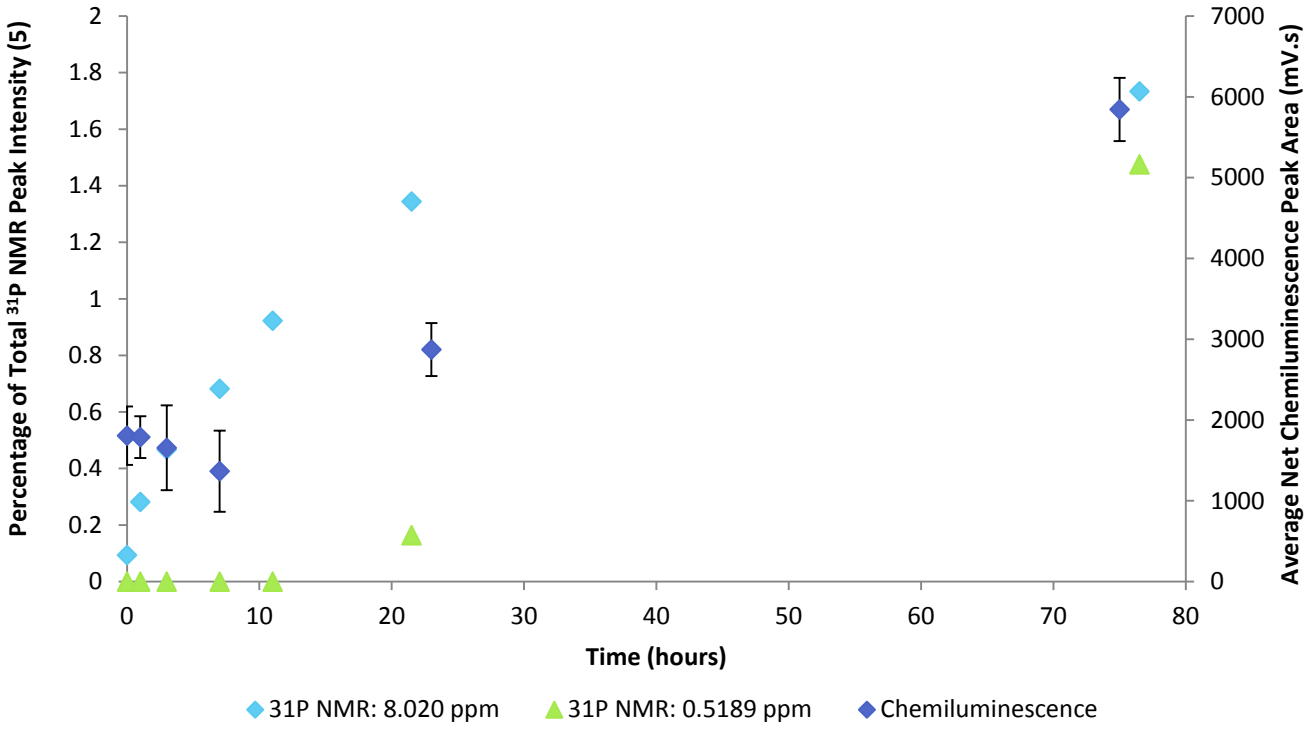

Figure 5-10. Change in percentage of total peak intensity of the ^{31}P NMR peaks at 8.020 ppm and 0.5189 ppm observed via analysis of cyclophosphamide (0.05 M in deionised water) held at room temperature over 80 hours. This is overlaid with the net peak area obtained via chemiluminescence analysis of the aliquots of the same cyclophosphamide solution dilute 10-fold in deionised water and analysed using $Ru(bipy)_3Cl_2$ (1 x 10^{-3} M in 0.075 M H_2SO_4) as the oxidising reagent. Error bars = ± 1 standard deviation.

The trends in peak intensity for the ^{31}P NMR peaks at 15.30 ppm and 8.020 ppm appeared to follow exponential trends, which suggested that the cyclophosphamide degradation reaction may be first order. If a reaction is first order the plot of the natural log of analyte concentration versus time should be linear. Such plots were constructed using ^{31}P NMR and chemiluminescence peak intensity as indicators of analyte concentration (see Appendix M), however no linearity was observed. The cyclophosphamide degradation reaction was therefore unlikely to be first order. Whether the reaction may be second order was also assessed by plotting the inverse of ^{31}P NMR or chemiluminescence signal versus time (Appendix M), however, again, no linearity was obtained. Cyclophosphamide hydrolysis is thought to consist of both first and second order components depending on the pH and step of the reaction [206]. Further investigation into the order of the reaction resulting in the increase in chemiluminescence signal is therefore required.

^{13}C NMR analysis of cyclophosphamide (1 x 10^{-3} M) held at room temperature was also conducted over 72 hours, however no obvious trends in chemical shifts and relative peak integrations were observed (Appendix L). As ^{13}C is a relatively scarce isotope high scan numbers (and hence long analysis times) are required to obtain adequate sensitivity. The cyclophosphamide solution would therefore be decreasing within this analysis time. To minimise conversion during the analyses conducted in this study the number of scans used was decreased to 720 (analysis time of 12 minutes). However, in 12

minutes the cyclophosphamide solution would still be degrading. The ^{13}C NMR spectra obtained would therefore be an average of the degradation products present of the 12 minutes of each analysis, hence making observation of trends quite difficult.

Gilard *et al.* [194] found that compound **9** was converted to compound **10** after 17 days when at low pH, which would be hypothesised to also result in a decrease in chemiluminescence signal intensity due to the loss of the tertiary amine group. Observing a decrease in chemiluminescence signal after an extended time period could therefore provide further support for the identification of the more chemiluminescence-active compound as compound **9**. Considering the rate of the degradation reaction had been shown to increase with increasing reaction temperature (Section 6.3.2.1), experiments in which the sample was constantly heated at 98 °C were conducted in an attempt to observe the full extent of the reaction over a shorter time period. The resulting ^{31}P NMR and chemiluminescence trends are given in Figure 5-11, Figure 5-12, and Figure 5-13.

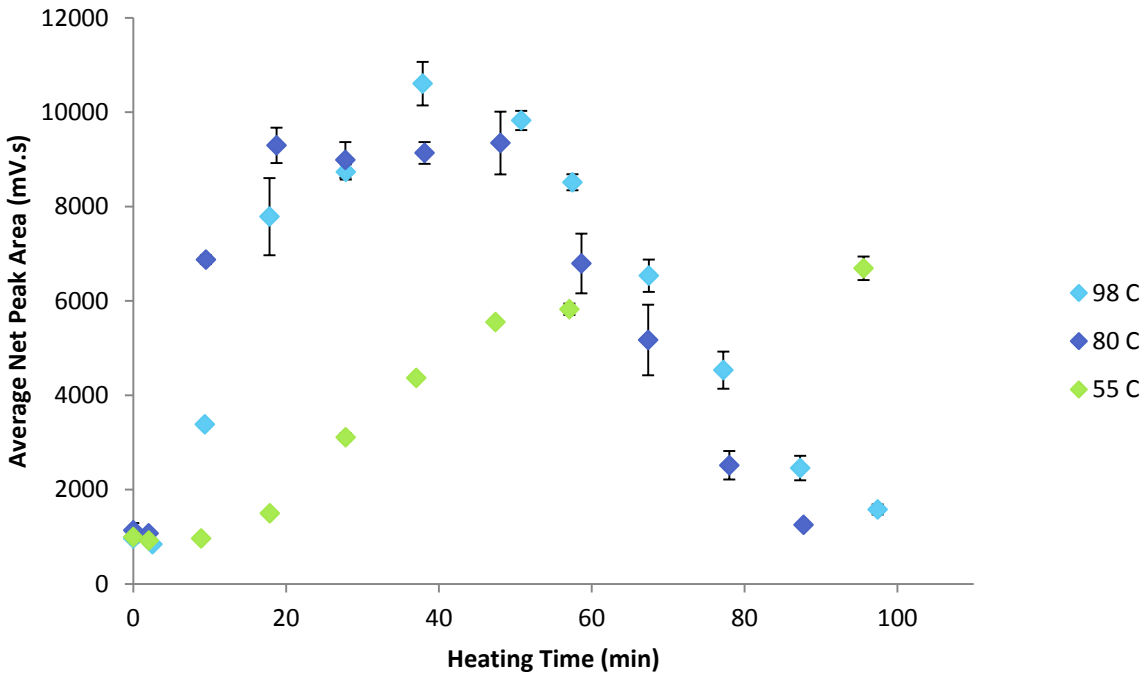

Figure 5-11. Effect of sample heating time on average net peak area (n=3) obtained via FIA-chemiluminescence of cyclophosphamide (1 x 10^{-3} M in deionised water) over 100 minutes using $Ru(bipy)_3Cl_2$ (1 x 10^{-3} M in 0.075 M H_2SO_4) as the oxidising reagent. Error bars = ± 1 standard deviation.

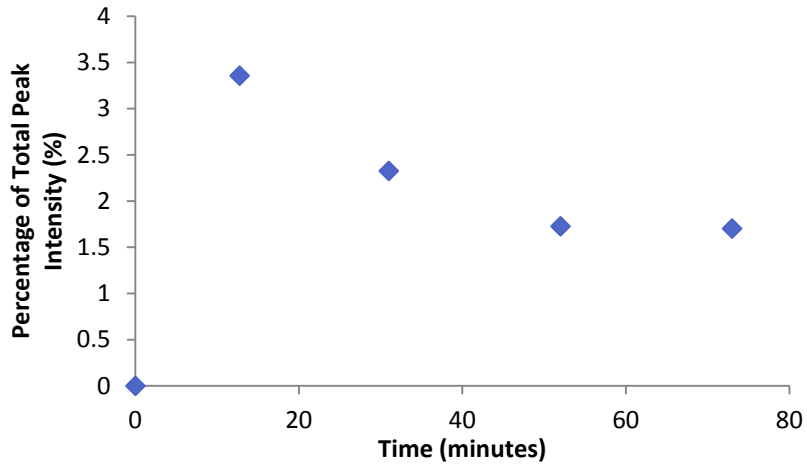

Figure 5-12. Change in percentage of the total peak intensity for the ^{31}P NMR peak at 8.020 ppm in the spectrum of cyclophosphamide (0.1 M in D_2O) heated at 98 °C over 75 minutes

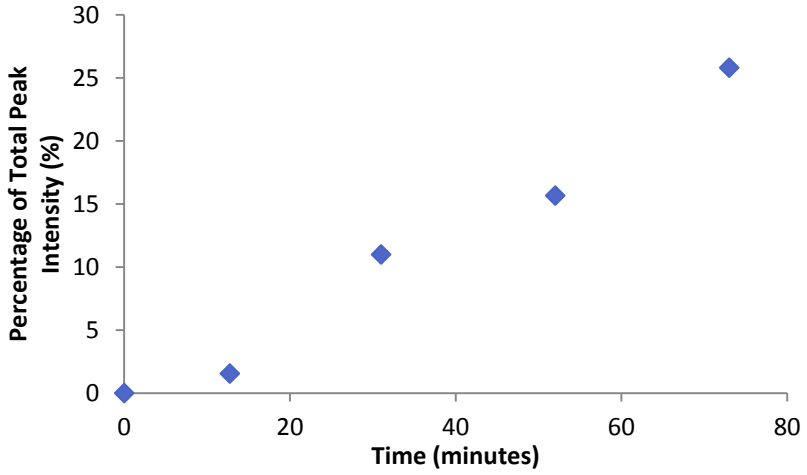

Figure 5-13. Change in percentage of the total peak intensity for the ^{31}P NMR peak at 0.5189 ppm in the spectrum of cyclophosphamide (0.1 M in D_2O) heated at 98 °C over 75 minutes

In these experiments the expected increase and then decrease of signals for both chemiluminescence and the ^{31}P NMR peak at 8.020 ppm was observed, as shown in Figure 5-12. The rate of decrease of the latter, however, was much slower than that of the chemiluminescence signal, hence indicating that compound **9** may not be solely responsible for the observed increasing chemiluminescence. Similarly, the peak at 0.5189 ppm, corresponding to compound **10**, showed a steady increase in intensity over the heating time, as shown in Figure 5-13, hence suggesting this hydrolysis product was also not causing the more intense chemiluminescence signal. It is possible that compound **7** was indeed the more active compound; with its rapid conversion to **9** resulting in a rapid decrease in chemiluminescence. The higher chemiluminescence activity of compound 7 could be due to the presence of two tertiary amine groups, compared to only one in either of cyclophosphamide, compound 9, or compound 10. However, considering each of the postulated hydrolysis products contains secondary or tertiary amines, it is also possible that all of compounds **7**, **9**, and **10** are able to undergo a chemiluminescence reaction, and hence the observed signal is a combination of the

reaction mixture. It would therefore be necessary to separate the components of this mixture to determine which is chemiluminescence-active. This can be achieved using UHPLC coupled to a chemiluminescence detector.

During this investigation, the pH of the cyclophosphamide solution when heated at 98 °C was also monitored over 100 minutes, with resulting trends given in Figure 5-14. It was observed that the pH initially decreased rapidly before reaching a plateau, which correlated well with similar measurements made by Gilard *et al.* [194]. This was most likely due to the formation of HCl during the intramolecular displacement of chloride from the parent drug during formation of compound **7**, hence supporting the assumption of this reaction pathway occurring.

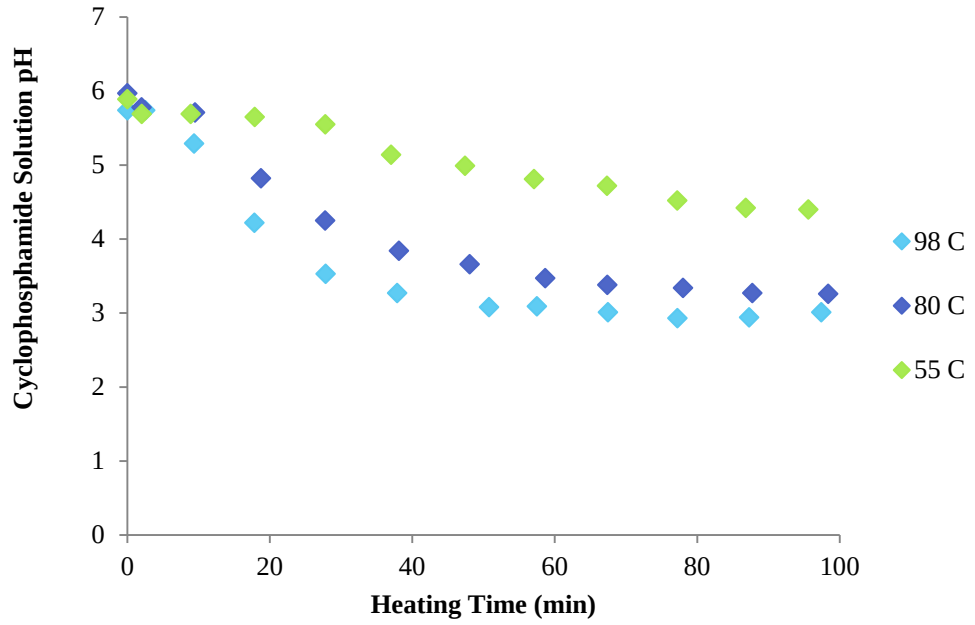

Figure 5-14. pH of cyclophosphamide solution (1 x 10^{-3} M in deionised water) over 100 minutes when heated at various temperatures

The conductivity of the heated solution was also monitored over time, with the thought that the production and consumption of ions during the reactions would result in overall changes in conductivity. As shown in Figure 5-15, it was observed that the conductivity of the solution increased rapidly within the first 5 minutes, but did not change significantly after this time. This supported the idea that the initial reaction step to produce chloride ions (and compound **7**) was quite rapid, and that the chloride ions were not consumed in any subsequent reactions.

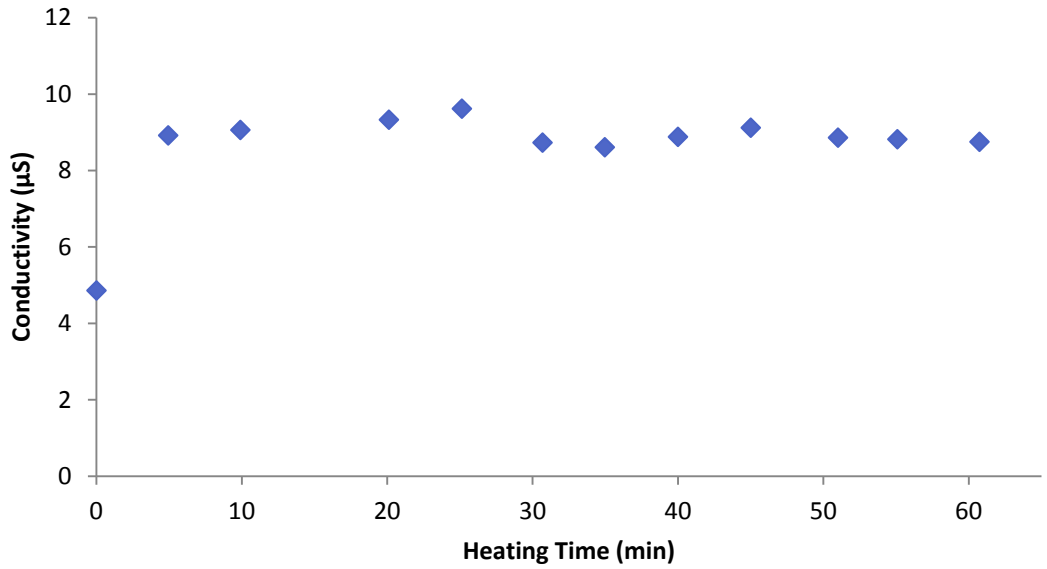

Figure 5-15. Conductivity of cyclophosphamide solution (1 x 10^{-3} M in deionised water) over 1 hour when held at 98 °C

In order to further confirm the formation of chloride ions at this stage of the reaction, ion chromatography (IC) of the cyclophosphamide solution (1 x 10^{-3} M) held at room temperature was conducted every 20 minutes over 10 hours. Chloride ions were able to be detected at concentrations of approximately 1 x 10^{-6} M from 0 minutes after preparation (Figure 5-16) This confirmed that the initial reaction step to form compound **7** (and hence chloride ions) was quite rapid. The chloride ion concentration did not change significantly over the 10 hours, which correlated well with the pH and conductivity measurements. There were, however, three spikes in peak intensity at 40, 120, and 170 minutes. These spikes may have been a result of chloride contamination being present in the glassware used.

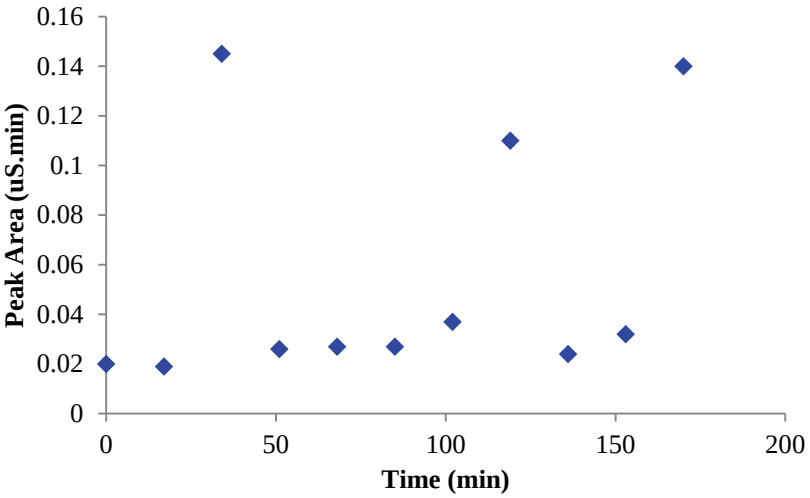

Figure 5-16. Peak area of peaks obtained via ion chromatographic analysis of cyclophosphamide (1 x 10^{-3} M) held at room temperature over time

It would be necessary to confirm which of compounds **7**, **9**, or **10** was responsible for the enhanced chemiluminescence in order to determine which methods of on-line conversion may be necessary for

indirect detection of cyclophosphamide. Consequently, LC-MS/MS analysis using electrospray ionisation (ESI) of a cyclophosphamide solution stored for 24 hours at room temperature in the absence of light was conducted. The resulting chromatogram is given in Figure 5-17, in which 6 peaks were observed. Peak 5 (6.286 min) had a mass spectrum with molecular ions separated by 2 m/z units at 261, 263, and 265 m/z (Figure 5-18). This is typical of the mass spectrum of cyclophosphamide, with the peaks at 263 and 265 m/z being due to the two isotopes of chlorine. This pattern is also typical of compound **10** [194], and hence it is unclear as to which compound this peak corresponded. Peak 1 (2.364 min) had a mass spectrum with a molecular ion with mass to charge ratio (m/z) of 227 (Figure 5-19), which has been shown to be indicative of compound **7** [194]. This therefore confirmed that degradation through the pathway via compound **7** was indeed taking place. Peak 2 (4.792 min) had a molecular ion at 453 m/z (Figure 5-20), which could correspond to a dimer of compound **7**. As there have been no previous reports of dimer formation during cyclophosphamide degradation, this dimerization most likely occurred during the ESI process. Peaks 3, 4, and 6 had molecular ions at 701, 409, and 423 m/z. These ions are much larger than cyclophosphamide or any of its potential degradation products (or their dimers) [194]. Further investigation into the identities of these compounds is therefore required. The detection of compound **7** supported the original hypothesis of cyclophosphamide degradation via this pathway. This was also supported by the fact that degradation products from other pathways were not detected. Compound **9**, however, was not detected, which may have been due to its coelution with other degradation products.

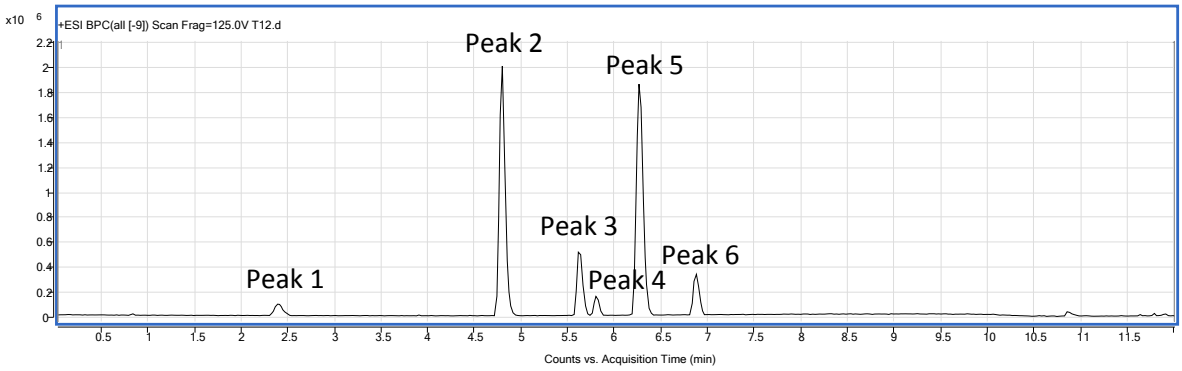

Figure 5-17. LC-MS/MS chromatogram of a cyclophosphamide solution (1 x 10^{-6} M in deionised water) that had been stored for 24 hours at room temperature in the absence of light

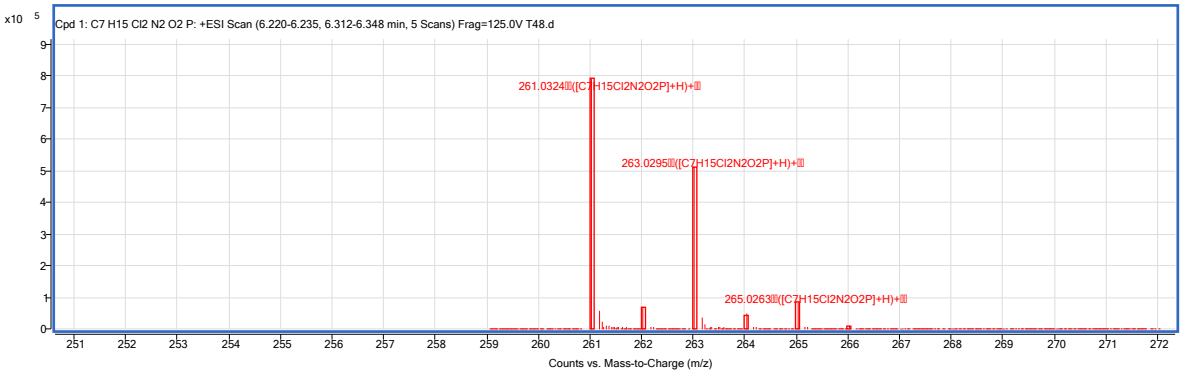

Figure 5-18. Positive ESI mass spectrum of the compound eluted at 6.286 min during LC-MS/MS analysis of cyclophosphamide (1 x 10^{-6} M in deionised water) that had been stored for 24 hours at room temperature in the absence of light

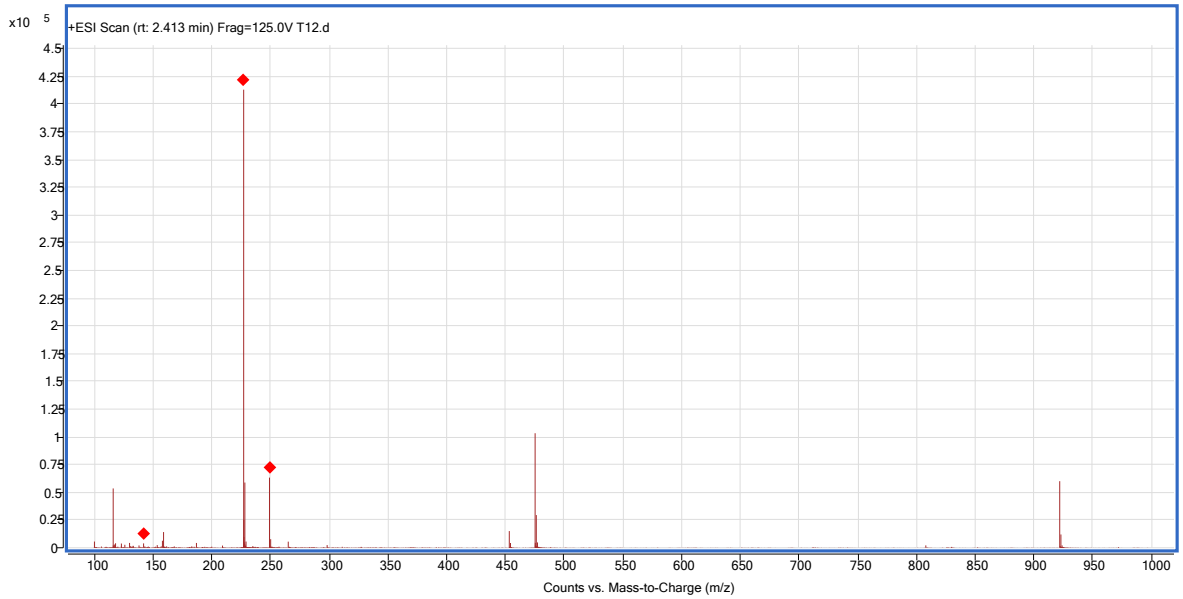

Figure 5-19. Positive ESI mass spectrum of the compound eluted at 2.364 min during LC-MS/MS analysis of cyclophosphamide (1 x 10^{-6} M in deionised water) that had been stored for 24 hours at room temperature in the absence of light

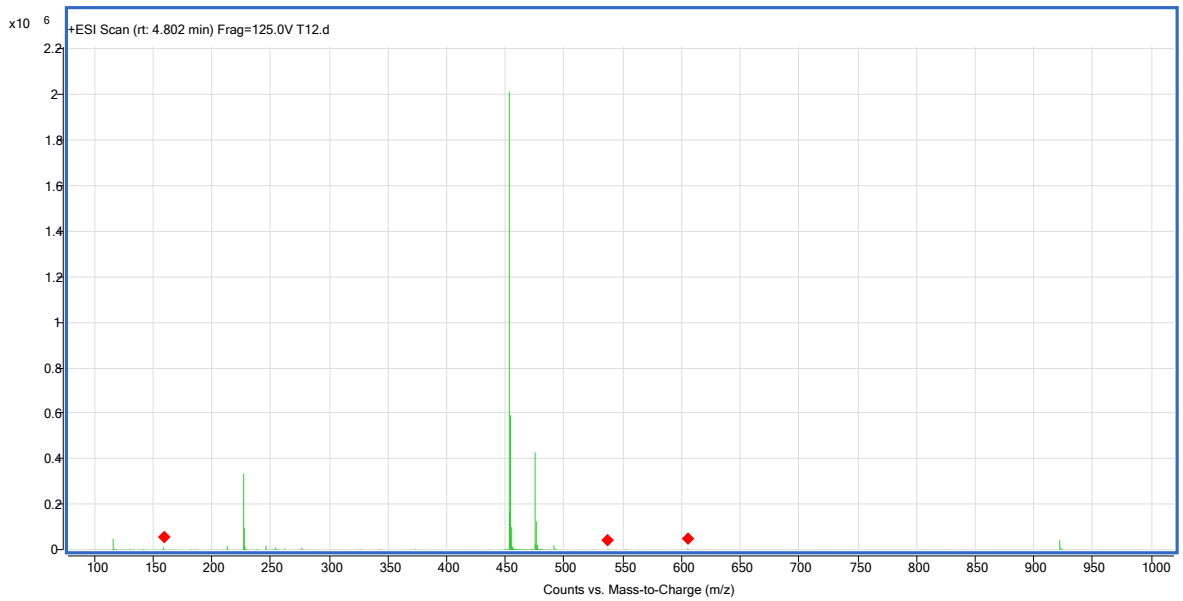

Figure 5-20. Positive ESI mass spectrum of the compound eluted at 4.792 min during LC-MS/MS analysis of cyclophosphamide (1 x 10^{-6} M in deionised water) that had been stored for 24 hours at room temperature in the absence of light

The use of chemiluminescence for the monitoring of cyclophosphamide degradation offers several advantages over the use of NMR techniques. The greatest of these is the far lower sample concentration required for chemiluminescence analysis, as well as the much faster analysis times, which provide a much more accurate representation of the sample at a given point in time, making monitoring of fast reactions more viable.

5.3.3 On-line Cyclophosphamide Treatment

Attempts were then made to utilise the higher chemiluminescence activity of the degradation products to indirectly detect cyclophosphamide via on-line conversion to this product. As determined in Section 5.3.1, the rate of cyclophosphamide degradation could be increased by increasing sample incubation temperature or decreasing sample pH. Various instrument manifolds in which the analyte was heated on-line and/or the analyte was acidified prior to mixing with the other reagents were therefore tested.

5.3.3.1 On-line Heating

Firstly, on-line heating of the sample prior to mixing with the other reagents was trialled by passing the sample through a PTFE heating coil suspended in a water bath before merging with the other reagents, as shown in Manifold 1 (Figure 5-3). The reagent conditions used are given in Table 5-4. The first heating coil trialled was one in which the tubing was woven through a solid plastic support (Figure 5-21) with an internal volume of 400 µL, however this proved to be unsuccessful, with signals no greater than the blank being obtained when using various heating temperatures. This was most likely due to hindered heat transfer between the water bath and the sample tubing due to the plastic support.

Figure 5-21. Woven heating coil tested for on-line conversion of cyclophosphamide

Next, a more loosely-wound tube with an internal volume of 522 µL was utilised with a water bath temperature of 85 °C. It was observed that this heating coil resulted in an increase in the net average chemiluminescence peak area from 1795 ± 51 to 2014 ± 239 mV.s compared with using the same coil held at room temperature. This difference, however, was within ± 1 standard deviation. The large standard deviation in net peak area obtained when heating to 85 °C was most likely a result of non-uniform heating of the analyte through the tube.

Various water bath temperatures were then tested, using the same reagent conditions in Table 5-4. The resulting average net peak areas obtained are given in Figure 5-22. The experiments conducted in Chapter 6.3.1 indicated that the cyclophosphamide reaction occurred over 10 minutes when heated at 98 °C, and at slower rates with decreasing temperature. In the manifold used here, the sample would be in the water bath for approximately 13.6 seconds (based on an average flow rate of 2.3 mL/min, as measured manually), and hence only a very low percentage conversion could be expected. It would therefore be necessary to use as high a temperature as possible. Water bath temperatures up to 98 °C were also tested, however these temperatures resulted in bubbling of the analyte solution in the tubing, due to boiling of the aqueous sample. This resulted in variations in flow rates and volumes delivered, hence resulting in non-reproducible signals. 85 °C was the highest temperature at which smooth flow without bubble formation could be obtained.

It was observed that, of the temperatures tested, only 85 °C was able to increase the chemiluminescence signal compared to passing the sample through the same heating coil but only heating to room temperature (20 °C). Again, however, this increase was within ± 1 standard deviation. Lower net peak areas were obtained when heating to 60 and 75 °C compared with 20 °C. It was hypothesised that this may be due to a decrease in the flow rate through this tube due to the larger volume of the heating coil. The flow rates of each reagent line were therefore measured individually by measuring the average volume of water delivered over 1 minute. The flow rate for the oxidising reagent and carrier solution lines was measured to be 2.7 ± 0.6 mL/min and 2.6 ± .8 mL/min, respectively. That of the analyte line, however, was slightly lower, being 2.3 ± 0.8 mL/min. This decrease, however, was within the 1 standard deviation margin of error. It was therefore unlikely that this difference was the sole reason for the observed decrease in chemiluminescence signal.

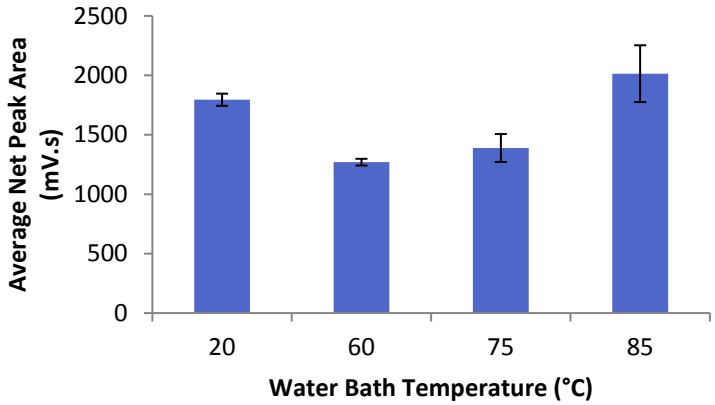

Figure 5-22. Average net peak area (n=3) obtained via FIA-chemiluminescence analysis of cyclophosphamide ($1x10^{-3}$ M in distilled water) heated on-line to various temperatures, using $Ru(bipy)_3Cl_2$ (1×10^{-3} M in 0.075 M H_2SO_4) as the oxidising reagent. Error bars = ± 1 standard deviation.

5.3.3.2 On-line Heating and Acidification

Considering the long reaction times (approximately 10 minutes) required to convert cyclophosphamide to the desired product using high temperatures alone, it was decided that a combination of heat application and acidification would be required. It was hypothesised that this acidification could be achieved on-line by introducing the $Ru(bipy)_3Cl_2$, which had been prepared in 0.075 M H_2SO_4 (pH 0.82), into the sample stream prior to mixing with the basic buffer, as shown in Manifold 2 in Figure 5-3. Cyclophosphamide solutions (1×10^{-3} M) were therefore analysed using Manifold 2 and the reagent conditions detailed in Table 5-4. The resulting average net peak areas are given in Figure 5-23. It was observed that the use of this manifold gave rise to a significant increase in net chemiluminescence peak area from 2014 ± 239 mV.s to 6249 ± 416 mV.s when heating to 85 °C. This manifold was also tested while heating the sample to only room temperature, and again an increase in average net peak area from 1795 ± 51 mV.s to 6249 ± 416 mV.s was observed. This therefore indicated the necessity in using both heat and acidification to generate the increased chemiluminescence signal.

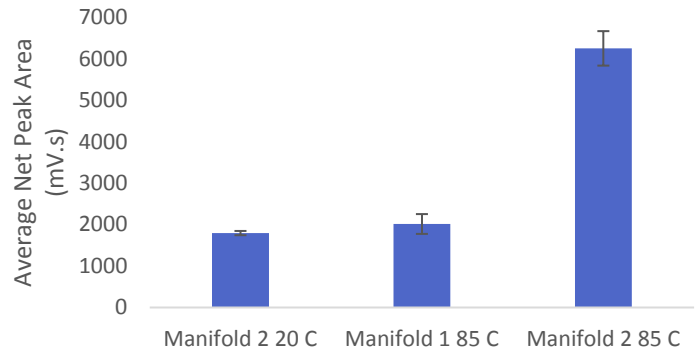

Figure 5-23. Comparison of average net peak area (n=3) obtained via FIA-chemiluminescence of cyclophosphamide ($1x10^{-3}$ M in distilled water) heated on-line to 85 °C using Manifold 1 or 2, using $Ru(bipy)_3Cl_2$ (1×10^{-3} M in 0.075 M H_2SO_4) as the oxidising reagent. Error bars = ± 1 standard deviation.

The effect of volume of the heating coil was then tested by changing the length of the coil, in an attempt to control the length of time the analyte was heated by the water bath. The reagent conditions used are those given in Table 5-4. The resulting average net chemiluminescence peak areas versus the heating coil volume are given in Figure 5-24. It was observed that as the heating coil volume was increased the average net peak area decreased. Again, the flow rate of the analyte solution line was measured when using each heating coil length, with the resulting flow rates given in Table 5-9. The flow rate when using the 522 µL coil was found to be slightly lower than that obtained with the short coils. This was most likely due to a lower total pressure over the longer coil length. The variation in chemiluminescence peak area obtained using the 522 µL coil, however, was lower than that obtained using the short coils, with a %RSD of net peak area of 6.65 % compared to 12.9 and 18.6 % for the 263 and 393 µL coils, respectively. It is possible the longer coil length allowed for a longer temperature equilibration time, resulting in a more uniform heat distribution acorss the solution. This would have ensured the same degree of degradation occurred throughout the solution, hence resulting in less variable chemiluminescence signals. A heating coil volume of 263 µL, however, produced the most intense chemiluminescence signal, and hence was used for subsequent analyses.

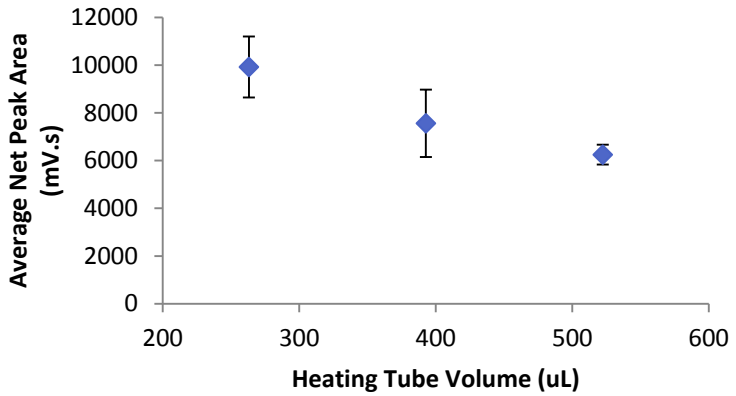

Figure 5-24. Effect of heating coil volume on the average net peak area obtained from FIA-chemiluminescence of cyclophosphamide ($1x10^{-3}$ M in distilled water) heated on-line to various temperatures, using $Ru(bipy)_3Cl_2$ (1×10^{-3} M in 0.075 M H_2SO_4) as the oxidising reagent using Manifold 2. Error bars = ± 1 standard deviation.

Table 5-9. Flow rates (mL/min) of the analyte solution line during FIA using various heating coil volumes

	Flow Rate (mL/min)	
Heating Coil Volume (uL)	**Average**	**Standard Deviation**
263	2.6	0.01
393	2.5	0.02
522	2.3	0.08

These studies showed that the largest net chemiluminescence peak area could be obtained via on-line heating and acidification of cyclophosphamide solutions using Manifold 2 with a heating coil volume of 263 µL and water bath temperature of 85 °C. The detection limits for cyclophosphamide using these developed conditions were then tested. Cyclophosphamide solutions with concentrations

between 1 x 10^{-6} M and 1 x 10^{-4} M were analysed using the reagent conditions in Table 5-8. No correlation between net peak area and cyclophosphamide concentration was observed (Figure 5-25), with concentrations below 1x10^{-5} M producing signals lower than the blank. The cyclophosphamide hydrolysis reactions appeared to be too slow to be forced in the very short time-frames required for on-line reactions. On-line hydrolysis would therefore not be a viable option for indirect detection of cyclophosphamide using chemiluminescence.

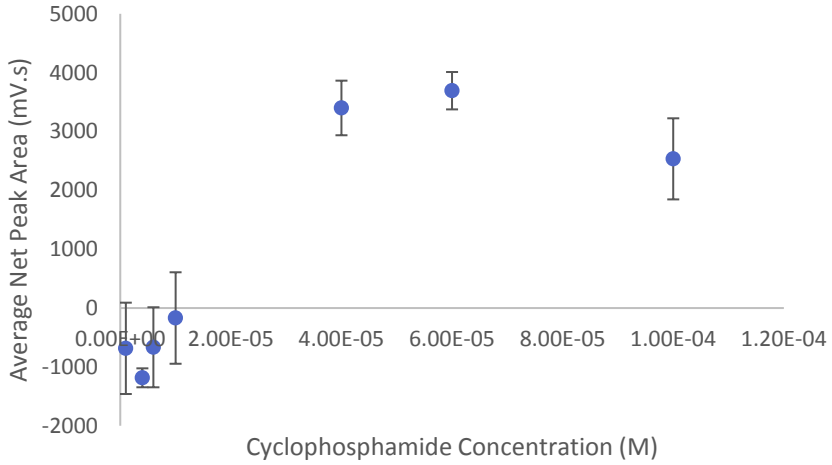

Figure 5-25. Correlation between cyclophosphamide concentration and average signal-to-blank ratio of chemiluminescence peak area obtained via FIA-chemiluminescence analysis of cyclophosphamide solutions heated in-line at 85 °C prior to merging with $Ru(bipy)_3Cl_2$ (1 x 10^{-3} M in 0.075 M H_2SO_4) and a bicarbonate carrier solution (pH 11, 0.05 M)

5.4 Conclusions

Cyclophosphamide was found to degrade in aqueous solution within 24 hours to form compounds with higher chemiluminescence activity than the parent drug. The rate of this reaction increased with increasing temperature and decreasing pH. LC-MS/MS analysis indicated that this degradation progressed through hydrolysis of cyclophosphamide to form compound **7** (Figure 5-3). ^{31}P NMR studies indicated that this compound was then converted to compounds **9** and **10**. On-line forced hydrolysis of cyclophosphamide for its indirect detection via heating to 80 °C and acidification was unsuccessful. This was most likely due to the high temperatures and relatively long reaction times required for the reaction to occur. The developed method could still, however, be effective in detecting cyclophosphamide degradation products as markers for the presence of cyclophosphamide.

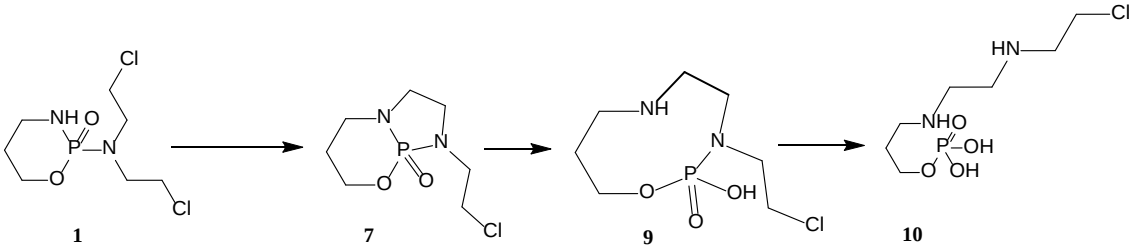

Figure 5-26. Proposed cyclophosphamide degradation scheme resulting in increase in chemiluminescence signal over time

Chapter 6:

Conclusions and Future Work

6. Conclusions and Future Work

6.1 Conclusions

Prior to this research, only two groups had reported chemiluminescence detection for 5-fluorouracil; one using $KMnO_4$ [1, 127] and the other using $Ru(bipy)_3Cl_2$ in electrochemiluminescence [168]. Chemiluminescence detection of cyclophosphamide and imatinib had not been reported previously. Chapter 2 in this thesis therefore provided the first investigation of the suitability of a range of chemiluminescence oxidising reagents for the detection of each of these analytes. $KMnO_4$, $Ru(bipy)_3Cl_2$, Mn(IV), and $Ce(SO_4)_2$ were investigated for their potential as chemiluminescence oxidising reagents of the cytotoxics cyclophosphamide, 5-fluorouracil, and imatinib using SIA. $Ru(bipy)_3Cl_2$ oxidised with $Ce(SO_4)_2$ produced the most intense chemiluminescence for each cytotoxic, with average net peak areas of 92.4 ± 2 mV.s, 65.0 ± 17 mV.s, and 124 ± 17 mV.s for cyclophosphamide, 5-fluorouracil, and imatinib, respectively. $Ru(bipy)_3Cl_2$ oxidised with PbO_2 also produced intense chemiluminescence from each cytotoxic, with average net peak areas of 62.5 ± 25 mV.s, 110 ± 22 mV.s, and 73.3 ± 26 mV.s for cyclophosphamide, 5-fluorouracil, and imatinib, respectively.

The other oxidising reagents produced less promising results. The maximum average net peak areas obtained when using $KMnO_4$ enhanced with HCl were 2.19 ± 0.8 mV.s, 2.13 ± 2 mV.s, and 37.9 ± 4 mV.s for cyclophosphamide, 5-fluorouracil, and imatinib, respectively. $KMnO_4$ containing sodium thiosulphate produced an average net peak area of 21.2 ± 2 mV.s from imatinib, however signals from cyclophosphamide and 5-fluorouracil were lower than that of the blank. The use of $Ce(SO_4)_2$ alone did not produce chemiluminescence signal greater than the blank for any of the cytotoxics. Mn(IV) produced an average net peak area of 24.5 ± 3 mV.s for imatinib, however signals from cyclophosphamide and 5-fluorouracil were lower than that of the blank.

Method development using $Ru(bipy)_3Cl_2$ oxidised with $Ce(SO_4)_2$ was then conducted, however no correlation between cytotoxic concentration and chemiluminescence signal was obtained. This was thought to be due to complex reaction kinetics between the cytotoxics and the $Ce(SO_4)_2$. Investigation into the role of $Ru(bipy)_3Cl_2$, $Ce(SO_4)_2$, and the cytotoxics in the chemiluminescence reactions was conducted using stopped-flow analysis. Cyclophosphamide, 5-fluorouracil, and imatinib were each found to react with $Ce(SO_4)_2$, resulting in a decrease in chemiluminescence peak area over time. The signals from cyclophosphamide and 5-fluorouracil decreased 10-fold and 1.5-fold in 20 hours, respectively, while the imatinib signal decreased 2-fold in 45 minutes. In addition, complete loss of chemiluminescence signal was observed when imatinib concentrations of at least 1×10^{-3} M were analysed. This was hypothesised to be due to absorption of the chemiluminescence emission at pH

levels below 2. Detection of the cytotoxics using $Ru(bipy)_3Cl_2$ reacted with PbO_2 was therefore deemed more effective.

Based on these findings $Ru(bipy)_3Cl_2$ oxidised with PbO_2 was then used in development of chemiluminescence detection of imatinib using SIA. No linearity in response could be obtained, and quenching of the chemiluminescence emission was observed at high imatinib concentrations (> 5 x 10^{-5} M). Consequently, imatinib was not persued further as a target analyte.

A new method for the detection of 5-fluorouracil in surface waters was successfully developed using $Ru(bipy)_3Cl_2$ oxidised with PbO_2. The linear range was 4 x 10^{-7} to 1 x 10^{-5} M, with limits of detection and quantification of 6.06 x 10^{-8} M and 1.16 x 10^{-6} M, respectively. These results were four times lower than that previously obtained using $KMnO_4$ as the oxidising reagent [1]. The effect of the presence of the inorganic ions Na^+, K^+, Mg^{2+}, Ca^{2+}, Fe^{3+}, Cl^-, Br^-, and I^-, which are typically present in surface waters, on the detection of 5-fluorouracil was assessed. Both anions and cations decreased the chemiluminescence signal. The tolerable ratio of 5-fluorouoracil to ion concentration giving rise to no more than 5 % loss of chemiluminescence signal was 0.1-fold for Na^+ and Fe^{3+}, 1-fold for Mg^{2+}, and 10-fold for K^+, Cl^-, and I^-. All Ca^{2+} concentrations tested (1 x 10^{-7} M to 1 x 10^{-3} M) produced an increase in chemiluminescence compared with un-spiked 5-fluorouracil. All Br^- concentrations (1 x 10^{-7} M to 1 x 10^{-3} M) tested resulted in a decrease in chemiluminescence signal. These interferences were found to be removable via sequential strong anion and strong cation exchange SPE prior to chemiluminescence analysis. Organic compounds in surface water samples were also found to decrease the chemiluminescence signal compared to that of 5-fluorouracil. Tap water resulted in a decrease of 73.51 % and lake water resulted in a decreased of 65.94 %, respectively. However, these organic compounds were easily separated from 5-fluorouracil using UHPLC. Therefore this developed method is highly applicable to the detection of 5-fluorouracil in surface waters.

A new method for the chemiluminescence detection of cyclophosphamide in aqueous solution was also developed using $Ru(bipy)_3Cl_2$ oxidised with PbO_2. While poor linearity of response was achieved for fresh cyclophosphamide solutions, high correlation between cyclophosphamide concentration and chemiluminescence signal was obtained when analysing 24-hour-old solutions (R^2 of 0.9995). This was found to be due to hydrolysis of cyclophosphamide to compounds **7**, **9**, and **10** (Figure 5-26) over 24 hours when stored at room temperature in the absence of light. On-line hydrolysis of cyclophosphamide for its indirect detection via heating to 80 °C and acidification was unsuccessful. The developed method could, however, be very useful for investigation of cyclophosphamide hydrolysis, as well as in detection of cyclophosphamide degradation products as markers for the

presence of the parent drug. This has direct applications to investigations of both the aqueous stability of cyclophosphamide, and its fate in surface waters.

6.2 Future Work

6.2.1 Chapter 2 – Preliminary Oxidising Reagent Screen

During the preliminary screen of potential oxidising reagents the use of $Ce(SO_4)_2$ was found to be unsuccessful, with an average net peak area of -0.1673 ± 3 mV.s from cyclophosphamide and 1.957 ± 3 mV.s from 5-fluorouracil, and with imatinib completely quenching the chemiluminescence signal. In later chapters, however, it was discovered that each cytotoxic, particularly imatinib, may be undergoing a reaction with $Ce(SO_4)_2$ during chemiluminescence experiments using $Ru(bipy)_3Cl_2$ as the oxidising reagent. It may therefore be beneficial to conduct further investigation into the use of $Ce(SO_4)_2$ as a chemiluminescence reagent for these analytes. $Ce(SO_4)_2$ is commonly used in combination with enhancing reagents, such as surfactants (particularly Tween-20), benzamides, silver and gold nanoparticles, and carbon dots in order to increase the quantum efficiency of the SO_2* state. Future work could therefore investigate the use of such enhancers for the detection of these cytotoxics.

The original oxidising reagent screen was conducted using SIA, which allows for minimal reagent consumption and precise control over reagent volumes and flow rates. The time delay between reagent mixing and light detection can, however, be too long for some chemiluminescence reactions. It would therefore be interesting to repeat the oxidising reagent screen using FIA, in which this detection delay is minimised.

During the method development conducted in later chapters, it was observed that both cyclophosphamide and 5-fluorouracil could be detected more effectively when using carrier solutions with high pH. During the preliminary oxidising reagent screen, however, only acidic carrier solutions were tested. Further experiments could be performed to test the use of basic carriers for each of the oxidising reagents chosen, in order to examine if higher signals could be obtained.

During the preliminary screen of potential oxidising reagents the chemiluminescence signal was found to be completely lost when analysing imatinib using $Ce(SO_4)_2$, producing only baseline signal. This result was also observed consistently when attempting to develop chemiluminescence detection for imatinib using $Ru(bipy)_3Cl_2$ oxidised with $Ce(SO_4)_2$. One possible explanation for this observation is a rapid reaction between imatinib and the $Ce(SO_4)_2$, resulting in consumption of the $Ce(SO_4)_2$, and hence preventing generation of the active $[Ru(bipy)_3]^{3+}$ state. Another possible explanation could be absorption of the emitted chemiluminescence light by imatinib, which would only occur if the

chemiluminescence emission was from $Ce(SO_4)_2$ rather than $Ru(bipy)_3Cl_2$. $Ru(bipy)_3Cl_2$ chemiluminescence produces spectra with emission maximum at 610 nm [122], while $Ce(SO_4)_2$ produces emissions profiles with maxima between 300 and 450 nm [156]. UV/Vis analysis during the chemiluminescence reaction may therefore provide insight into which mechanisms were occurring [191]. A further examination would then also provide insight into whether quenching, absorption, or another process was the reason for the observed loss in chemiluminescence signal during imatinib analysis. In addition, in order for imatinib to absorb light in the region of SO_2* emission the pH must be less than 2. It would therefore be informative to monitor the pH of the reagent mixtures during the chemiluminescence reaction to confirm if these conditions were met. This could be done using batch methods similar to stopped-flow analysis in which precise volumes of each reagent were injected into a reaction cell at precise times and the pH measured using a pH metre. The loss in chemiluminescence signal from imatinib was found to be highly dependent on imatinib concentration. It is known that the absorption spectrum of imatinib changes with changing imatinib concentration [189]. Future work should therefore involve investigation into whether the observed correlation with imatinib concentration was due to changes in absorption, changes in reaction kinetics and rates, or changes in reagent consumption. It should also be determined whether this change was stable and reproducible. It may then be possible to develop a detection method for imatinib based on this chemiluminescence decrease.

6.2.2 Chapter 4 – Detection of 5-Fluorouracil

During the interference studies in this chapter, the presence of anions and cations was found to decrease the chemiluminescence peak area compared to that of a pure 5-fluorouracil standard. The threshold ratio of ions to 5-fluorouracil found to result in at least 5 % decrease in peak area were between 0.1-fold and 500-fold. For Mg^{2+} the threshold was not determined because even the lowest concentration tested (2×10^{-8} M; 0.02-fold the concentration of 5-fluorouracil) produced a decrease in chemiluminescence peak area of 60 %. This is a very low tolerance to the presence of inorganic ions compared with what is typically reported. Future work should therefore include investigation into why this tolerance was so low. It was also observed that the anions had a strong effect on the chemiluminescence signal, rather than only the cations. This has not been reported previously, as it is generally accepted that the cations, especially Ca^{2+} and Mg^{2+}, that are the major intereferences in chemiluminescence analysis of surface waters. Future work should therefore involve investigation into why this occurred. Investigation into the mechanism of the observed chemiluminescence reaction should also be conducted. This could be done via UV/Vis analysis of batch chemiluminescence experiments.

During the method development in Chapter 4 it was observed that sequential SPE using strong anionic and cationic exchange resins was unable to restore the chemiluminescence signal of 5-fluorouracil in tap water and lake water up to that on 5-fluorouracil in deionised water. This therefore suggested that there may also be interferences from organic compounds in the water samples. The 5-fluorouracil was, however, found to be easily separated from these components using UHPLC. In order for the developed chemiluminescence method to be viable for analysis of real surface water samples it would therefore be necessary to couple chemiluminescence detection to HPLC. This is common practice for many chemiluminescence detection methods [70]. The use of FIA for the method developed in Chapter 3 would make this coupling relatively simple because it allows for easier integration into the HPLC flow. It would be possible for the column eluent to be introduced into the FIA system in place of the analyte line used in this work. The main issue that would need to be resolved is the differences in flow rate requirements between the HPLC and the FIA-chemiluminescence system. The flow rate used in each line of the FIA was 2.6 mL/min, whereas typical UHPLC methods use flow rates between 0.3 and 0.5 mL/min.

The main purpose for the development of new methodologies for cytotoxic analysis is to allow for investigation into their fate in surface waters. Once a suitable HPLC-chemiluminescence detection method had been developed, it would then be possible to use this method to investigate the fate of 5-fluorouracil in such matrices. This would involve first a series of batch experiments, in which 5-fluorouracil was spiked into various water samples (tap water, river/lake water, and in the presence of soils or humic acids). These solutions would be incubated under various light and temperature conditions and the developed method used to periodically analyse for 5-fluorouracil over a defined time period. The developed method should then also be applied to analysis of real surface water samples collected, to determine if environmentally-relevant concentrations of 5-fluorouracil could be detected.

6.2.3 Chapters 5 and 6 – Detection of Cyclophosphamide and Its Degradation Products

The simultaneous ^{31}P NMR and chemiluminescence analyses conducted in Chapter 5 provided excellent insight into the potential degradation products responsible for the observed increases in chemiluminescence signal. Analysis of a 24-hour-old cyclophosphamide solution using LC-MS/MS provided information on the final products of these reactions, but not on any intermediates. It would therefore be quite informative if LC-MS/MS analysis could also be conducted periodically over the 24 hours, rather than only at the end. This would allow for confirmation of the identified intermediates, and hence possibly provide further insight into how to manipulate these reactions for cyclophosphamide detection. Also, there were, several compounds that could not be identified based solely on their ESI mass spectra. Hard ionisation mass spectrometry, such as electron ionisation, may

therefore be required in order to obtain further fragmentation patterns from these compounds to aid in their identification.

The use of a Charged Aerosol Detector (CAD) for HPLC analysis may also provide further insight into the cyclophosphamide degradation. CAD is an almost universal detection method which is independent of the analyte chemical structure [207]. It involves the nebulisation of analytes into an aerosol using a stream of nitrogen. The volatile solvents in the aerosol are then evaporated and the resulting dried particle stream is charged using another nitrogen stream passed over a high voltage platinum wire. The resulting charged particles are then measured using an electrometer, with the response being directly proportional to the number of charged particles [207]. This is independent on the nature and identity of the analyte, and hence the same concentrations of different analytes will give rise to the same intensity in response. Using CAD detection it is therefore possible to gain information on the relative concentrations of unknown components of a mixture without the need for individual standards of each component. This would be highly applicable to the investigation of cyclophosphamide degradation, in which the degradation products are not fully known. This would also allow for the detection of degradation products, as well as cyclophosphamide, which are not UV-active.

The order of the cyclophosphamide degradation reaction should also be investigated further. In Chapter 5 ^{31}P NMR and chemiluminescence signals from cyclophosphamide solutions did not fit first or second order kinetics. Previous studies have shown that cyclophosphamide hydrolysis consists of both first and second order components depending on the pH and step of the reaction [206]. Investigation into reaction rate should therefore be conducted while tightly controlling pH, temperature, and also other factors such as ionic strength that could influence the reaction. Buffered solutions could be used to more tightly control the reaction pH, while ionic strength could be adjusted using sodium sulfate. This may allow for clearer reaction kinetics to be observed, and hence provide insight into the feasibility of forced degradation of cyclophosphamide for indirect detection.

Attempts to convert cyclophosphamide to its more chemiluminescence-active degradation products on-line in the FIA manifold were unsuccessful. This was most likely due to the high temperatures and long reaction times required for the conversion. It would be interesting to determine the end-point of the cyclophosphamide reaction, after which all products were stable with time. If the products required for the increased chemiluminescence were stable over long time periods, this could provide potential for indirect detection of cyclophosphamide. It may be possible for solutions containing cyclophosphamide to be heated for a defined time-period to produce these final products, which could then be detected using the developed chemiluminescence method. In order for this to be a

viable option at least three criteria would have to be met. Firstly, the conversion to the desired products would have to occur reproducibly, to ensure that the chemiluminescence signal could be directly correlated back to the original cyclophosphamide concentration. Secondly, these products would have to be stable over time, to ensure the chemiluminescence signal would remain constant during the analysis time. The use of intermediates of the cyclophosphamide degradation would therefore not be applicable to this detection approach. Finally, the original age of the cyclophosphamide solution would have to have no effect on the production of the desired products. For instance, most surface water samples would contain cyclophosphamide that had been introduced some time previously, and hence would have already had the chance to undergo degradation. Samples analysed would therefore be of different ages and degrees of degradation upon analysis. It would therefore be necessary to treat these samples to form the final products of the degradation reaction to ensure all samples were brought up to the same level of degradation. Correlation back to the original cyclophosphamide concentration, however, would then not be indicative of the cyclophosphamide concentration in the water sample at the time of collection. Rather, it would be an indication of the concentration of cyclophosphamide prior to any degradation.

Chapter 7:

Appendices

7. Appendices

Appendix A – Effect of SIA Parameters on Chemiluminescence Signal using $KMnO_4$, HCl, and formaldehyde

The effect of the volumes of HCl, $KMnO_4$, and formaldehyde on the chemiluminescence signal from 5-fluorouracil were investigated individually using the conditions in Table 7-1, Table 7-2, and Table 7-3 using SIA. No increase in chemiluminescence signal could be obtained when changing each of the parameters (Figure 7-1, Figure 7-2, and Figure 7-3).

Table 7-1. SIA reagents, volumes, and flow rates used for analysis of cyclophosphamide, 5-fluororuacil, and imatinib (1 x 10^{-3} M) using $KMnO_4$ and the oxidising reagent and formaldehyde and HCl as enhancers

Reagent	Composition	Volume (µL)	Flow Rate (µL/s)
Analyte	1 x 10^{-3} M cyclophosphamide, 5-fluorouracil, imatinib in deionised water	50	20
Enhancer 1	Formaldehyde (0.1 M in deionised water)	200	20
Enhancer 2	HCl (2 M)	200	20
Oxidising Reagent	1 x 10^{-3} M $KMnO_4$ in deionised water	50-200	20
Carrier Solution	Deionised water	1000	100

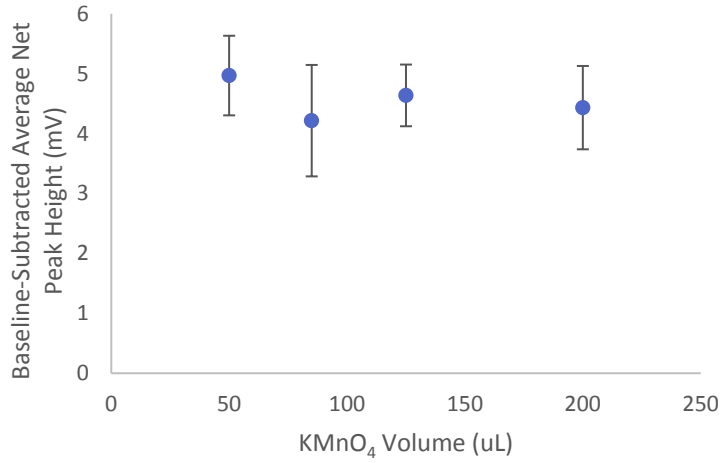

Figure 7-1. Effect of $KMnO_4$ volume on average net chemiluminescence peak area (n=3) obtained via analysis of 5-fluorouracil (1 x 10^{-3} M in deionised water) using $KMnO_4$ (1 x 10^{-3} M in deionised water) as the oxidising reagent and formaldehyde (0.1 M) and HCl (2 M) as sensitisers. Error bars = ± 1 standard deviation.

Table 7-2. SIA reagents, volumes, and flow rates used for analysis of cyclophosphamide, 5-fluororuacil, and imatinib (1 x 10^{-3} M) using $KMnO_4$ and the oxidising reagent and formaldehyde and HCl as enhancers

Reagent	Composition	Volume (µL)	Flow Rate (µL/s)
Analyte	1 x 10^{-3} M cyclophosphamide, 5-fluorouracil, imatinib in deionised water	50	20
Enhancer 1	Formaldehyde (0.1 M in deionised water)	50-200	20
Enhancer 2	HCl (2 M)	200	20
Oxidising Reagent	1 x 10^{-3} M $KMnO_4$ in deionised water	200	20
Carrier Solution	Deionised water	1000	100

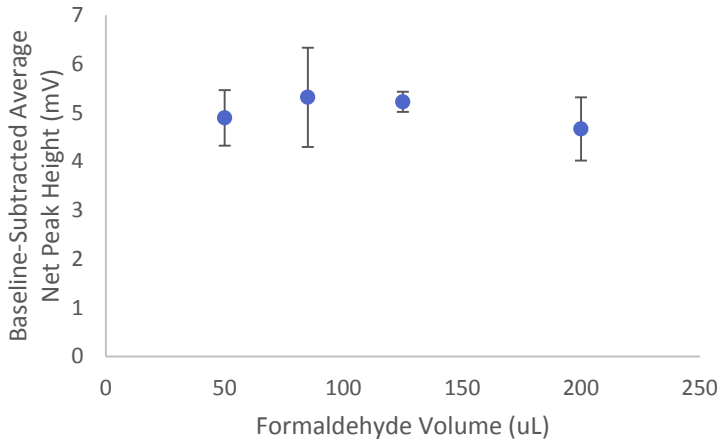

Figure 7-2. Effect of formaldehyde volume on average net chemiluminescence peak area (n=3) obtained via analysis of 5-fluorouracil (1 x 10^{-3} M in deionised water) using $KMnO_4$ (1 x 10^{-3} M in deionised water) as the oxidising reagent and Formaldehyde (0.1 M) and HCl (2 M) as sensitisers. Error bars = ± 1 standard deviation.

Table 7-3. SIA reagents, volumes, and flow rates used for analysis of cyclophosphamide, 5-fluororuacil, and imatinib (1 x 10^{-3} M) using $KMnO_4$ and the oxidising reagent and Formaldehyde and HCl as enhancers

Reagent	**Composition**	**Volume (µL)**	**Flow Rate (µL/s)**
Analyte	1 x 10^{-3} M cyclophosphamide, 5-fluorouracil, imatinib in deionised water	50	20
Enhancer 1	Formaldehyde (0.1 M in deionised water)	200	20
Enhancer 2	HCl (2 M)	50-200	20
Oxidising Reagent	1 x 10^{-3} M $KMnO_4$ in deionised water	200	20
Carrier Solution	Deionised water	1000	100

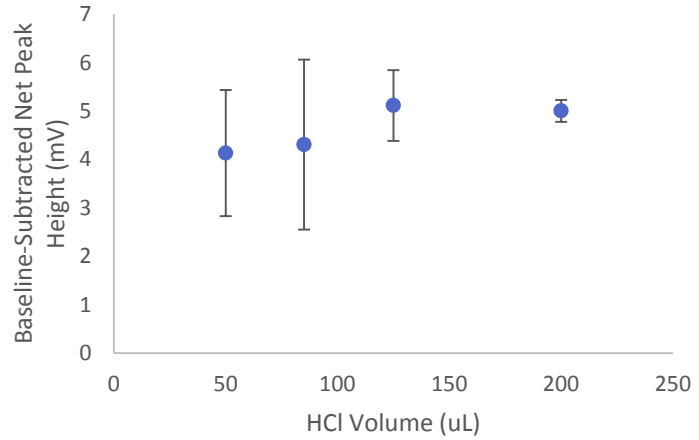

Figure 7-3. Effect of HCl volume on average net chemiluminescence peak area (n=3) obtained via analysis of 5-fluorouracil (1 x 10^{-3} M in deionised water) using $KMnO_4$ (1 x 10^{-3} M in deionised water) as the oxidising reagent and Formaldehyde (0.1 M) and HCl (2 M) as sensitisers. Error bars = ± 1 standard deviation.

Appendix B – Effect of SIA Parameters on 5-Fluorouracil Chemiluminescence Signal using $KMnO_4$ and Sodium Hexametaphosphate

The effect of the volumes of $KMnO_4$ and the analyte on the chemiluminescence signal from 5-fluorouracil were investigated individually using the conditions in Table 7-4 and Table 7-5 using SIA. No increase in chemiluminescence signal could be obtained when changing each of the parameters (Figure 7-4 and Figure 7-5).

Table 7-4. SIA reagents, volumes, and flow rates used to assess the effect of $KMnO_4$ volume on chemiluminescence signal obtained from cyclophosphamide, 5-fluororuacil, and imatinib

Reagent	Composition	Volume (µL)	Flow Rate (µL/s)
Analyte	1 x 10^{-3} M cyclophosphamide, 5-fluorouracil, imatinib in deionised water	50	20
Enhancer	Sodium hexametaphosphate (1 % m/v in 5 x 10^{-3} M H_2SO_4)	100	20
Oxidising Reagent	1 x 10^{-3} M $KMnO_4$ in sodium hexametaphosphate (1 % m/v in 5 x 10^{-3} M H_2SO_4)	10-200	20
Carrier Solution	Sodium hexametaphosphate (1 % m/v in 5 x 10^{-3} M H_2SO_4)	1000	100

Table 7-5. SIA reagents, volumes, and flow rates used to assess the effect of analyte volume on chemiluminescence signal obtained from cyclophosphamide, 5-fluororuacil, and imatinib

Reagent	Composition	Volume (µL)	Flow Rate (µL/s)
Analyte	1 x 10^{-3} M cyclophosphamide, 5-fluorouracil, imatinib in deionised water	25-200	20
Enhancer	Sodium hexametaphosphate (1 % m/v in 5 x 10^{-3} M H_2SO_4)	100	20
Oxidising Reagent	1 x 10^{-3} M $KMnO_4$ in sodium hexametaphosphate (1 % m/v in 5 x 10^{-3} M H_2SO_4)	200	20
Carrier Solution	Sodium hexametaphosphate (1 % m/v in 5 x 10^{-3} M H_2SO_4)	1000	100

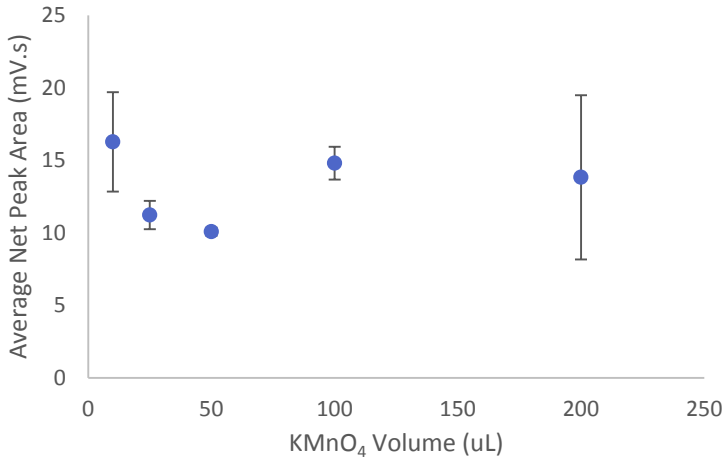

Figure 7-4. Effect of $KMnO_4$ volume on average net chemiluminescence peak area (n=3) obtained via analysis of 5-fluorouracil (1 x 10^{-3} M in deionised water) using $KMnO_4$ (1 x 10^{-3} M in 1 % m/v in 5 x 10^{-3} M H_2SO_4) as the oxidising reagent and sodium hexametaphosphate (1 % m/v in 5 x 10^{-3} M H_2SO_4) as the enhancer. Error bars = ± 1 standard deviation.

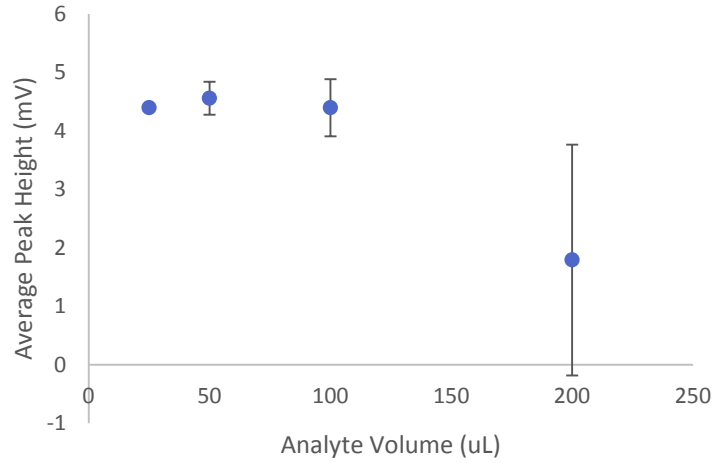

Figure 7-5. Effect of analyte volume on average net chemiluminescence peak area (n=3) obtained via analysis of 5-fluorouracil (1 x 10^{-3} M in deionised water) using $KMnO_4$ (1 x 10^{-3} M in 1 % m/v in 5 x 10^{-3} M H_2SO_4) as the oxidising reagent and sodium hexametaphosphate (1 % m/v in 5 x 10^{-3} M H_2SO_4) as the enhancer. Error bars = ± 1 standard deviation.

Appendix C- $Ru(bipy)_3Cl_2/Ce(SO_4)_2$ Method Development using FIA

Method development for cyclophosphamide, 5-fluorouracil, and imatinib detection was conducted using $Ru(bipy)_3Cl_2$ oxidised on-line with $Ce(SO_4)_2$ using FIA. Firstly, the effect $Ru(bipy)_3Cl_2$ volume was investigated by changing the internal volume of the injection loop. Individual standards of cyclophosphamide, 5-fluorouracil, and imatinib (1 x 10^{-3} M in deionised water) were analysed using the in-house built FIA manifold shown in Figure 7-6 with injection loops of volume 23.6 µL and 55.0 µL. The experimental conditions used are given in Table 7-6. Increasing the $Ru(bipy)_3Cl_2$ increased the chemiluminescence signal, however also resulted in peak splitting (Figure 7-7). This was most likely the result of the higher volume of $Ru(bipy)_3Cl_2$ being injected preventing the uniform mixing of all reagents, hence resulting in the formation of two reaction zones. 23.6 µL was therefore selected for subsequent analyses.

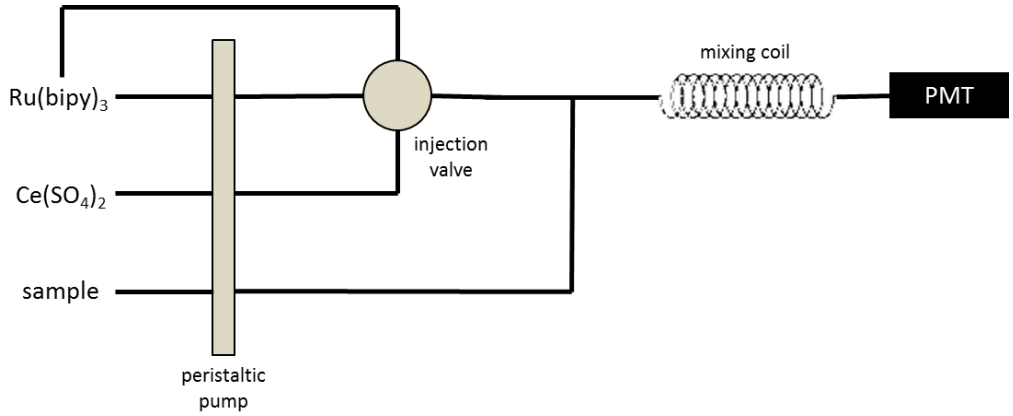

Figure 7-6. Schematic of the FIA manifold utilised for initial detection of sodium oxalate (FIA Manifold 1)

Table 7-6. Reagents used to investigate the effect of the injection loop volume, mixing coil length, and total flow rate on chemiluminescence peaks obtained via FIA of cyclophosphamide (1 x 10^{-4} M)

Reagent	Composition
Analyte	Cyclophosphamide (1 x 10^{-3} M) in deionised water or phosphate buffer (pH 7, 0.05 M)
Oxidising Reagent 1	$Ru(bipy)_3Cl_2$ (1.5 x 10^{-3} M in deionised water)
Oxidising Reagent 2	$Ce(SO_4)_2$ (1x10^{-3} M in 0.4 M H_2SO_4)

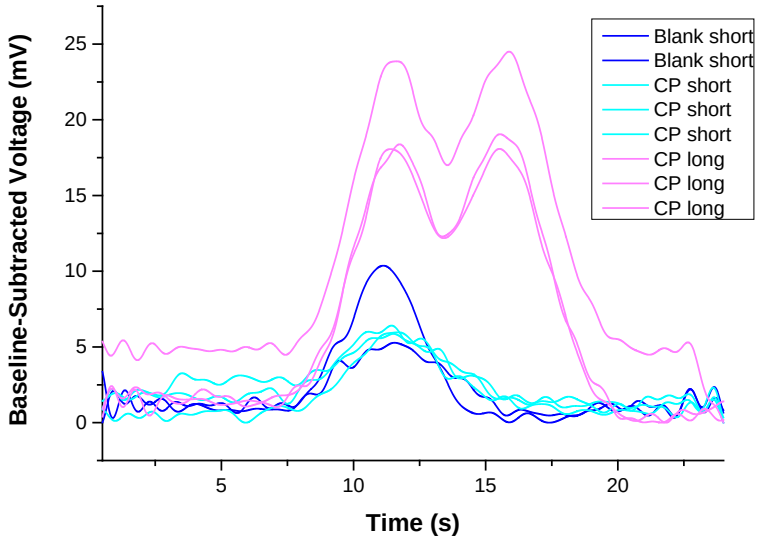

Figure 7-7. Comparison of baseline-subtracted FIA-CL signals obtained via analysis of cyclophosphamide ($1x10^{-3}$ M in distilled water) analysed using on-line mixed $Ru(bipy)_3Cl_2$ (1.5×10^{-3} M in deionised water) and $Ce(SO_4)_2$ ($1x10^{-3}$ M in 0.4 M H_2SO_4).

The effect of the length of the mixing coil was then investigated. 5-fluorouracil was analysed using the conditions in Table 7-6 using two different mixing coil lengths (5 cm and 10 cm). The 10 cm coild produced the highest net peak area (Figure 7-8), most likely by increasing the reaction time between the reagents, and hence this coil was used for subsequent analyses.

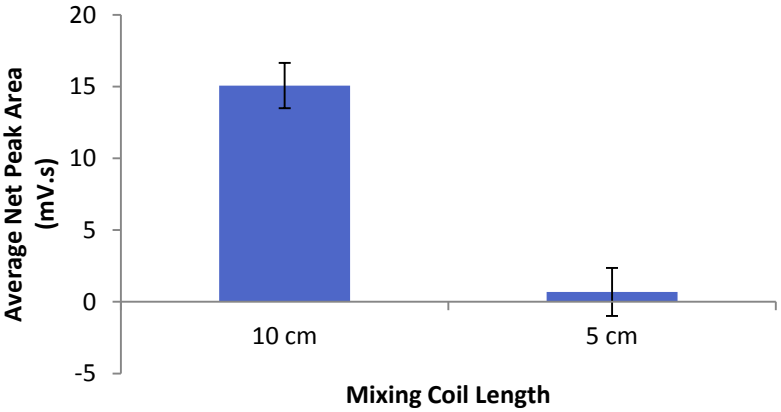

Figure 7-8. Effect of mixing coil length on average net peak area (n=3) for 5-fluorouracil ($1x10^{-3}$ M in distilled water) analysed using on-line mixed $Ru(bipy)_3Cl_2$ (1.5×10^{-3} M in distilled water) and $Ce(SO_4)_2$ ($1x10^{-3}$ M in 0.4 M H_2SO_4). Error bars = ± 1 standard deviation.

The effect of total flow rate on chemiluminescence signal was then investigated. Cyclophosphamide and 5-fluorouracil (1×10^{-3} M) were analysed using the conditions in Table 7-6. The reproducibility obtained was poor due to variation in both the blank and analyte signals, and hence no obvious trends with respect to flow rate could be postulated (Figure 7-9). This was most likely a result of the very low intensities of the signals being obtained, resulting in large interferences due to noise.

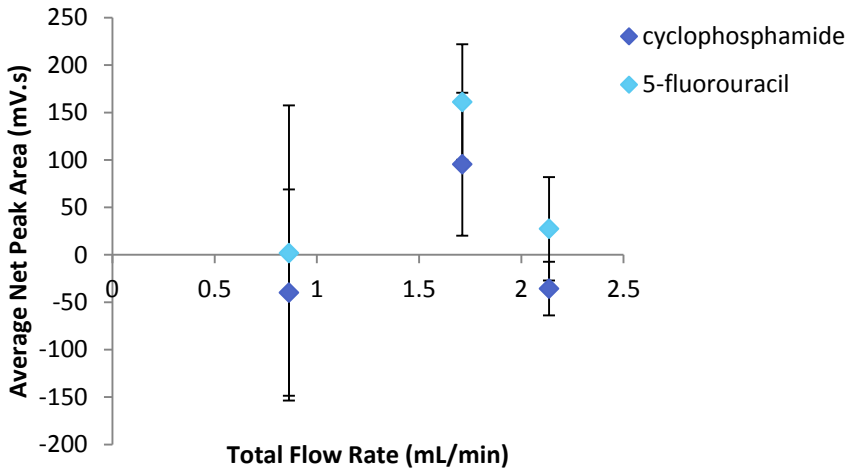

Figure 7-9. Effect of total flow rate (mL/min) on average net peak area (n=3) for cyclophosphamide and 5-fluorouracil ($1x10^{-3}$ M in distilled water) analysed using on-line mixed $Ru(bipy)_3Cl_2$ (1.5×10^{-3} M in distilled water) and $Ce(SO_4)_2$ ($1x10^{-3}$ M in 0.4 M H_2SO_4). Error bars = ± 1 standard deviation.

The effect of $Ce(SO_4)_2$ concentration was then investigated. Cyclophosphamide, 5-fluorouracil, and cyclophosphamide were analysed using the conditions in Table 7-7. Again, reproducibility was poor, and hence no significant variation in signal with $Ce(SO_4)_2$ concentration could be observed (Figure 7-10).

Table 7-7. Reagents used to investigate the effect of the injection loop volume, mixing coil length, and total flow rate on chemiluminescence peaks obtained via FIA of cyclophosphamide (1×10^{-4} M)

Reagent	Composition
Analyte	Cyclophosphamide (1×10^{-3} M) in deionised water or phosphate buffer (pH 7, 0.05 M)
Oxidising Reagent 1	$Ru(bipy)_3Cl_2$ (1.5×10^{-3} M in deionised water)
Oxidising Reagent 2	$Ce(SO_4)_2$ (0.5×10^{-3} - $2x10^{-3}$ M in 0.4 M H_2SO_4)

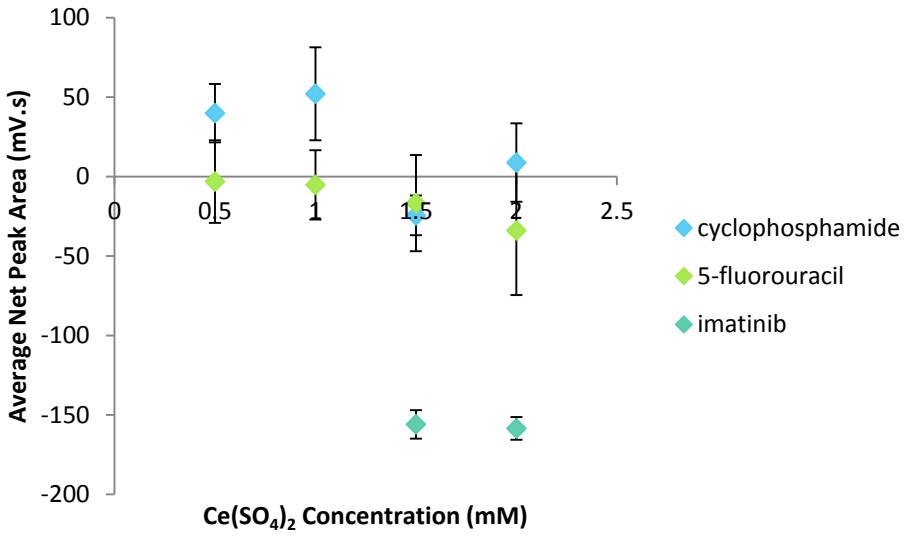

Figure 7-10. Effect of $Ce(SO_4)_2$ concentration (in 0.4 M H_2SO_4) on average net peak area (n=3) for cyclophosphamide, 5-fluorouracil, and imatinib ($1x10^{-3}$ M in distilled water) analysed using on-line mixed $Ru(bipy)_3Cl_2$ (1.5×10^{-3} M in distilled water) and $Ce(SO_4)_2$ ($1x10^{-3}$ M in 0.4 M H_2SO_4). Error bars = ± 1 standard deviation.

It was then hypothesised that pre-mixing the $Ce(SO_4)_2$ with the $Ru(bipy)_3Cl_2$ offline before merging with the sample may allow this initial oxidation step to go to completion, increasing the yield of $Ru(bipy)_3]^{3+}$ obtained and hence increasing chemiluminescence signals. Therefore, separate $Ce(SO_4)_2$ (1.5×10^{-3} M in 0.4 M H_2SO_4) and $Ru(bipy)_3Cl_2$ (1×10^{-3} M in distilled water) solutions were mixed off-line in ratios of 1:1, 2:1, and 1:2 (v/v) and then analysed using the adapted FIA manifold shown in Figure 7-11 (FIA Manifold 2). This manifold allowed for the sample to be "sandwiched" between two streams of pre-mixed oxidising reagent to allow for maximum contact between the reagents. However, signals no larger than the blank were obtained when analysing each of the cytotoxics. This was unexpected as the use of pre-mixed $Ce(SO_4)_2$ and $Ru(bipy)_3Cl_2$ had been shown to produce chemiluminescence with the analytes in Chapter 2. The poor results obtained here were likely due to the ratio of sample to oxidising reagent being too low, resulting in a large background signal relative to the analyte.

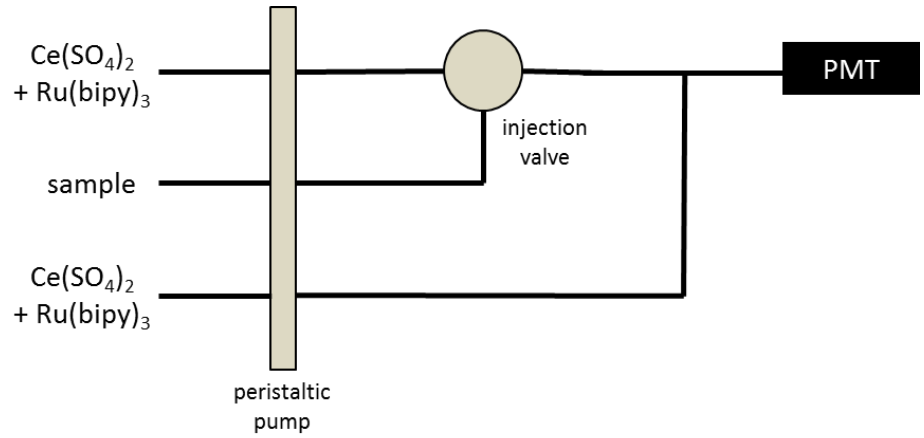

Figure 7-11. FIA Manifold 2

Another manifold (Manifold 3, Figure 7-12), in which only two reagent streams were utilised; one containing the pre-mixed oxidising reagents and one containing the sample, was therefore tested. Various oxidiser ratios, switch-back delays, and total flow rates were tested, however, no signal greater than the blank was obtained.

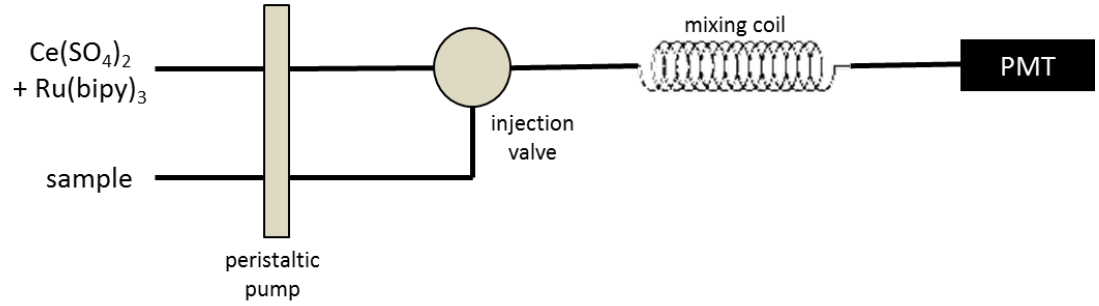

Figure 7-12. FIA Manifold 3

Overall, the use of on-line mixed oxidising reagents was found to be the only method capable of producing signals larger than that of the blank. Finally, cyclophosphamide, 5-fluorouracil, and imatinib (1×10^{-3} M in distilled water) were analysed using the optimal manifold and conditions determined above (Table 7-7). Cyclophosphamide and imatinib produced signals lower than the blank, while 5-fluorouracil produced signals equivalent in intensity to the blank (Figure 7-13). $Ru(bipy)_3Cl_2$ oxidised with $Ce(SO_4)_2$ was therefore decided to be ineffective in detecting each of these cytotoxics, and hence was not persued further.

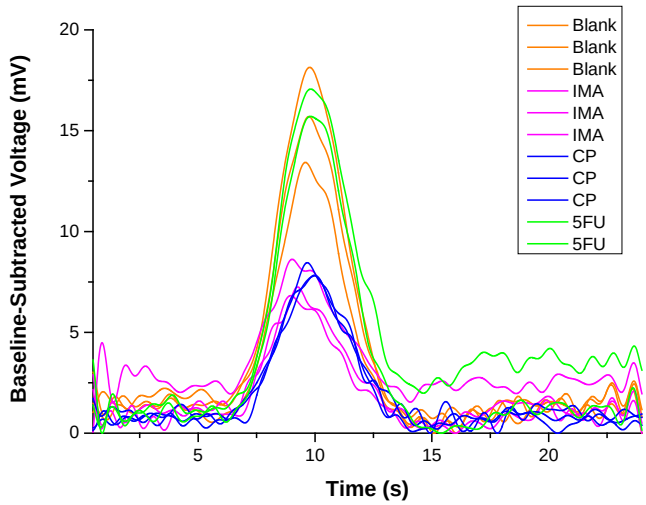

Figure 7-13. Baseline-subtracted chemiluminescence signals obtained via analysis of cyclophosphamide, 5-fluorouracil, and imatinib ($1x10^{-3}$ M in distilled water) analysed using on-line mixed $Ru(bipy)_3Cl_2$ (1.5×10^{-3} M in distilled water) and $Ce(SO_4)_2$ ($1x10^{-3}$ M in 0.4 M H_2SO_4).

Appendix D – Peristaltic Pump Flow Rate Measurement

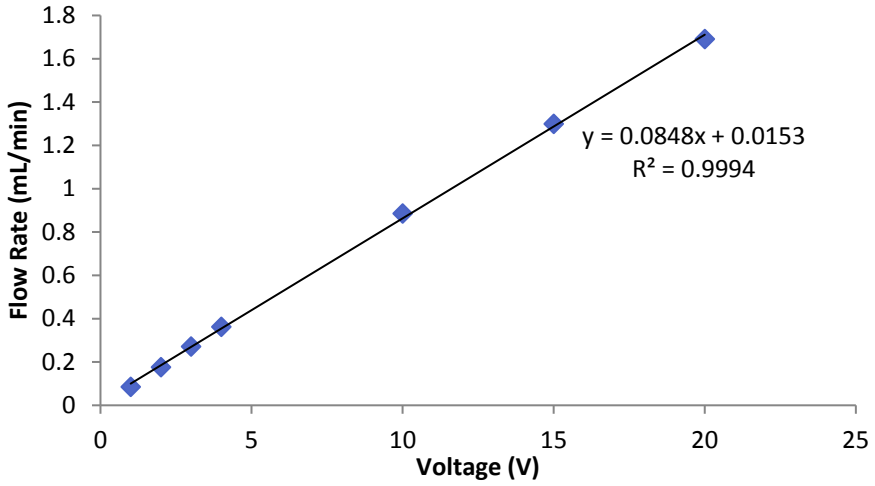

Figure 7-14. Total flow rate corresponding to selected pump voltage in peristaltic pump, determined by measuring the mass of deionised water expelled to waste over 1 minute. 5 replicates of each voltage were conducted.

Appendix E – Inorganic Ions Interference Study Using 5-Flurouracil

The effect of inorganic ions on the chemiluminescence signal of 5-fluorouracil was investigated via analysis of 5-fluorouracil solutions (1 x 10^{-6} M) spiked with various concentrations of inorganic anions and cations using the conditions in Table 7-8. The net chemiluminescence peak areas obtained relative to 5-flurorouracil that had not been spiked with ions are given in Figure 7-17 and Figure 7-18. All cations and anions except Ca^{2+} produced a decrease in chemiluminescence signal relative to unspiked 5-fluorouracil. All Ca^{2+} concentrations tested resulted in an increase in chemiluminescence signal above 100 % of that of unspiked 5-fluorouracil.

Table 7-8. Final FIA-chemiluminescence reagent conditions found to be optimal for 5-fluorouracil detection

Reagent	**Composition**
Analyte	5-fluorouracil (1 x 10^{-6} M) in deionised water and spiked with
Oxidising Reagent	$Ru(bipy)_3Cl_2$ (4 x 10^{-4} M in 0.01 M H_2SO_4) oxidised with solid PbO_2 (0.1 g/20 mL)
Carrier Solution	Bicarbonate buffer (pH 11, 0.05 M)

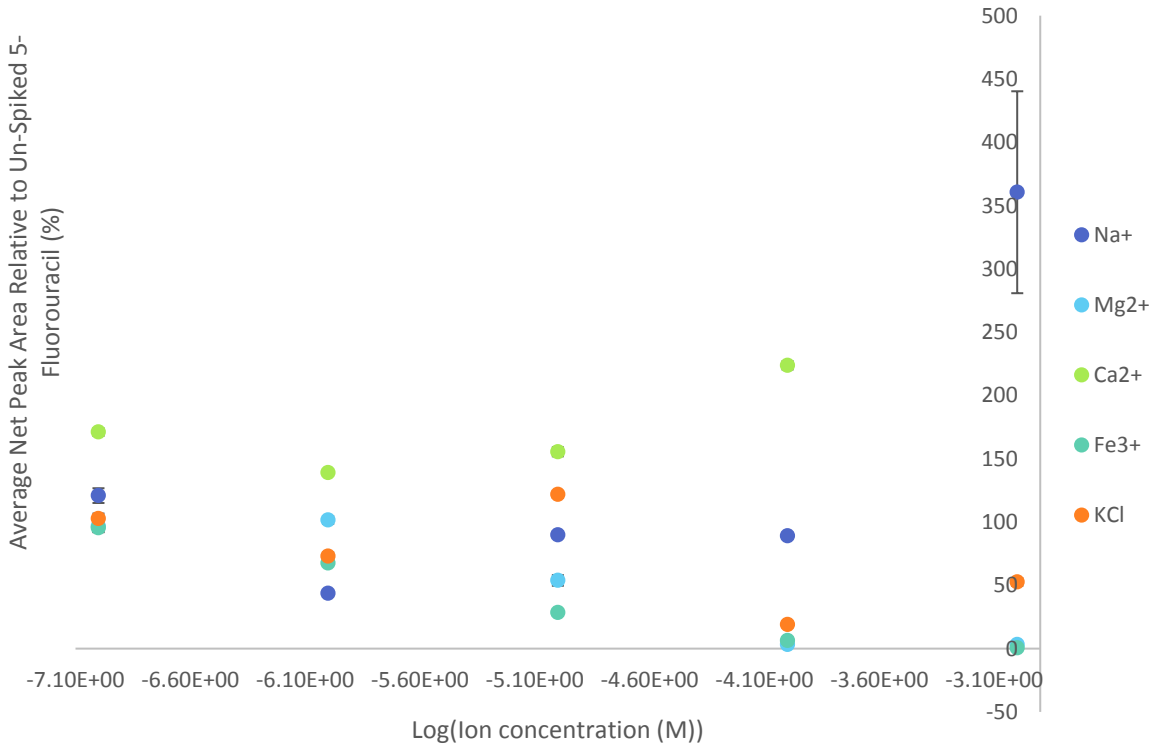

Figure 7-15. Effect of cation concentration on chemiluminescence signal of 5-fluorouracil (1 x 10^{-6} M in deionised water spiked with each chloride salt) relative to that of 5-fluorouracil in un-spiked deionised water. Error bars = ± 1 standard deviation.

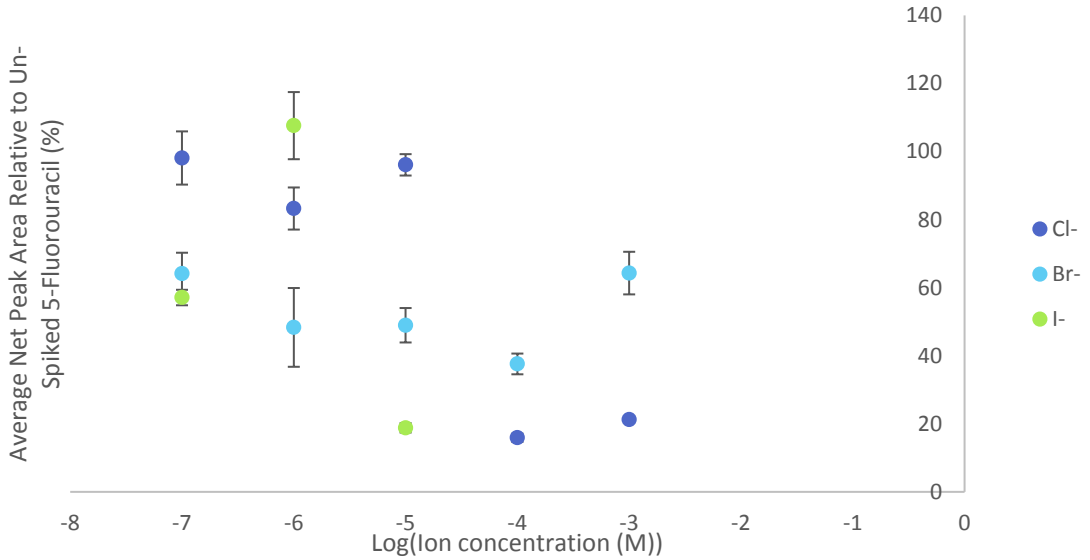

Figure 7-16. Effect of anion concentration on chemiluminescence signal of 5-fluorouracil (1 x 10^{-6} M in deionised water spiked with each potassium salt) relative to that of 5-fluorouracil in un-spiked deionised water. Error bars = ± 1 standard deviation.

Appendix F – $Ru(bipy)_3Cl_2$ Stability

Sodium oxalate and imatinib (1×10^{-7} M and 1×10^{-3} M, respectively) were analysed using the experimental conditions in Table 7-9 over 50 consecutive trials (approximately 3 hours). A clear decrease in net peak area from both analytes was observed over time (Figure 7-17). This suggested the $[Ru(bipy)_3]^{3+}$ reagent was not stable in solution.

Table 7-9. SIA reagent compositions, volumes, and flow rates used to assess stability of chemiluminescence signal from sodium oxalate and imatinib over time using $Ru(bipy)_3Cl_2$

Aspiration Order	Reagent	Composition	Volume (µL)	Flow Rate (µL/s)
2	Oxidising Reagent	$Ru(bipy)_3Cl_2$ (1×10^{-3} M in 0.05 M H_2SO_4)	50	15
1	Analyte	Sodium oxalate (1×10^{-7} M in deionised water) imatinib (1×10^{-3} M in deionised water)	50	5
3	Carrier Solution	0.05 M H_2SO_4	300	100

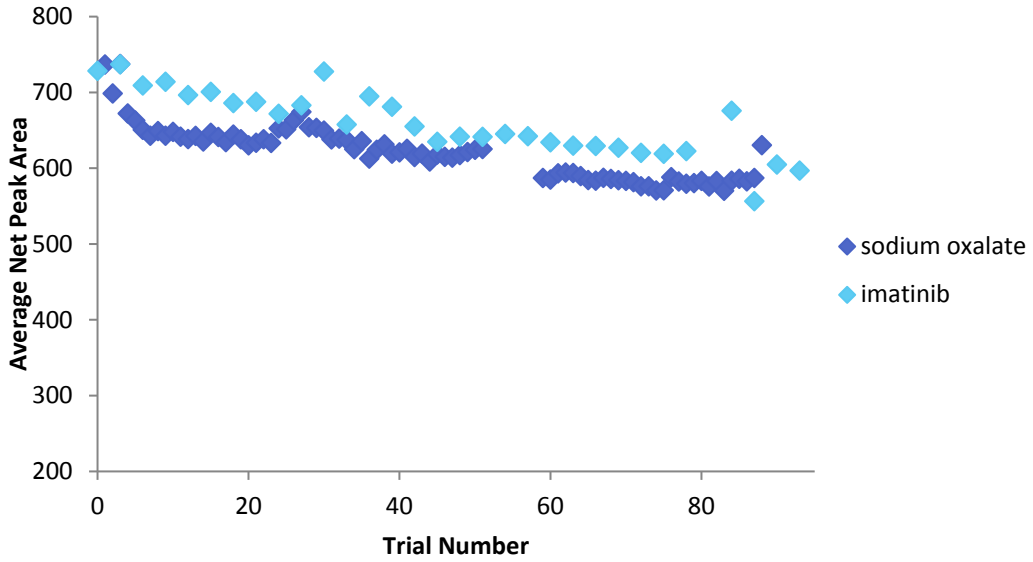

Figure 7-17. Peak areas of SIA-chemiluminescence signals obtained via analysis of imatinib (1×10^{-3} M in deionised water) continually over time, using $Ru(bipy)_3Cl_2$ (1×10^{-3} M in H_2SO_4 (pH 1)) as the oxidising agent and H_2SO_4 (pH 1) as the carrier solution.

Appendix G – $Ru(bipy)_3ClO_4$ Investigation Using Cyclophosphamide

$Ru(bipy)_3ClO_4$ in acetonitrile as the 3+ oxidation state of the perchlorate salt is reportedly much more stable than $Ru(bipy)_3Cl_2$ [152]. Consequently, sodium oxalate was analysed every hour for 40 hours using this stable reagent and the conditions in Table 7-10. The resulting chemiluminescence peak area was found to be stable over 24 hours (Figure 7-18) with slightly more variation being observed after this point. This would allow for comparison between experiments conducted within a 24 hour period, and hence acetonitrile solutions of $Ru(bipy)_3ClO_4$ were used for subsequent cyclophosphamide method development.

Table 7-10. SIA reagent compositions, volumes, and flow rates used to assess stability of chemiluminescence signal from sodium oxalate over time using $Ru(bipy)_3ClO_4$

Aspiration Order	Reagent	Composition	Volume (µL)	Flow Rate (µL/s)
1	Analyte	Sodium oxalate (1 x 10^{-7} M in 0.05 M H_2SO_4)	50	10
2	Oxidising Reagent	$Ru(bipy)_3ClO_4$ (1 x 10^{-3} M in 0.05 M $HClO_4$ in acetonitrile)	30	10
3	Carrier Solution	0.05 M $HClO_4$ in acetonitrile	1000	100

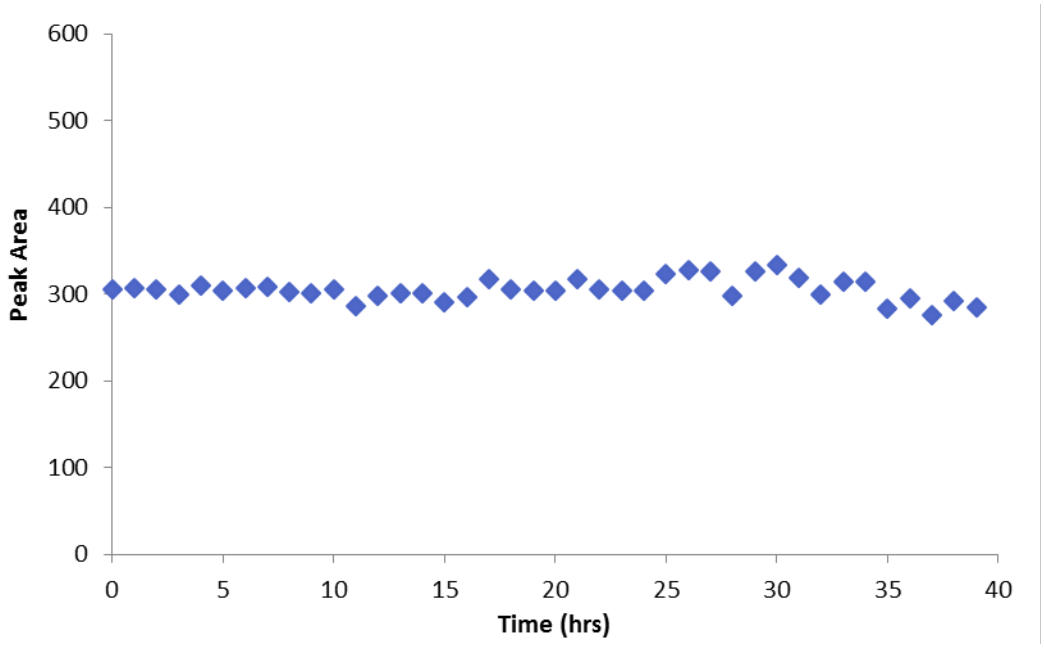

Figure 7-18. Chemiluminescence peak area obtained via SIA of sodium oxalate (1 x 10^{-7} M in 0.05 M H_2SO_4) every 5 minutes over 40 hours using $Ru(bipy)_3$ (1 x 10^{-3} M in 0.05 M $HClO_4$) as the oxidiser and 0.05 M $HClO_4$ as the carrier solution.

Method development for cyclophosphamide was commenced using this reagent. The effect of the pH of various acidic carrier solutions was assessed in the range of 0.1 to 4.1. The reagent details are given in Table 7-11, with the resulting average net chemiluminescence peak heights given in Figure 7-19. When using both $HClO_4$ and H_2SO_4 signals larger than that of the blank could only be obtained at pH levels greater than 1. When increasing the pH beyond this point the chemiluminescence peak height

obtained using H_2SO_4 did not change significantly (within ± 1 standard deviation) with increasing pH. When using $HClO_4$ the maximum peak height was obtained at a pH of 2.10, with an average net peak height of 5.38 ± 2 mV. The variation in chemiluminescence peak heights was high with %RSD up to 47 %. This was most likely due to the low intensities of the signals resulting in large interferences due to noise.

Table 7-11. Reagents used for FIA chemiluminescence of cyclophosphamide (1 x 10^{-3} M) using $HClO_4$ (in acetonitrile), H_2SO_4, or HCl carrier solutions of varying concentration

Reagent	Composition
Analyte	Cyclophosphamide (1 x 10^{-3} M) in deionised water
Oxidising Reagent	$Ru(bipy)_3ClO_4$ (1 x 10^{-3} M in 0.05 M $HClO_4$ in acetonitrile)
Carrier Solution	$HClO_4$ in acetonitrile, H_2SO_4, or HCl (5 x 10^{-4} M – 2.5 x 10^{-2} M)

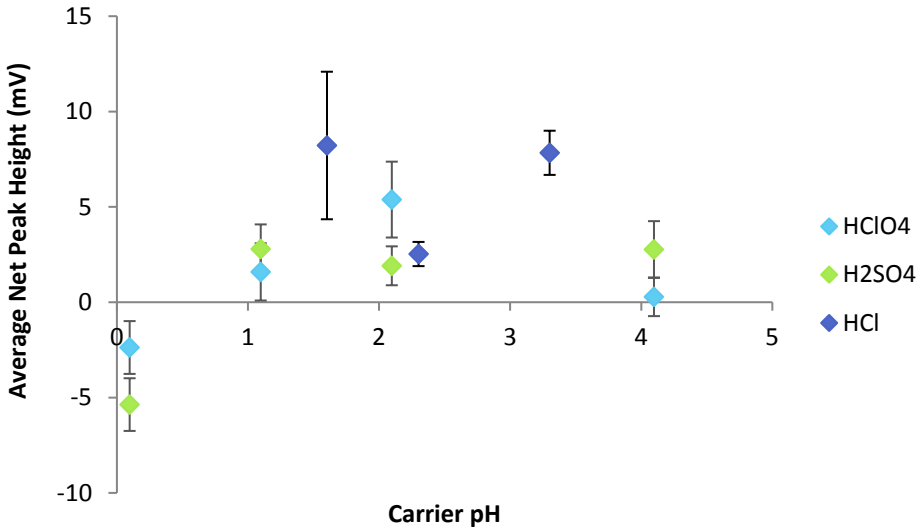

Figure 7-19. Average net peak height (n=3) of chemiluminescence signals obtained via FIA of cyclophosphamide (1 x 10^{-3} M in deionised water) using $Ru(bipy)_3ClO_4$ (1 x 10^{-3} M in 0.05 M $HClO_4$ in acetonitrile) as the oxidising reagent and $HClO_4$ (in acetonitrile), H_2SO_4, and HCl of various concentrations as the carrier solution. Error bars = ± 1 standard deviation.

The chemiluminescence signals obtained using either of the acids were quite small, with net peak heights all below 10 mV. It was therefore suggested that basic carrier solutions may be more effective. Consequently, cyclophosphamide was analysed using borate buffers of pH 8 and 11 as carrier solutions using the conditions in Table 7-13. This resulted in flooding of the detector, observed as flattening of the peaks at the maximum voltage of the PMT (5000 mV). The cyclophosphamide concentration was therefore decreased to 1 x 10^{-4} M, with resulting peaks given in Figure 7-22. The signals were also observed to consist of 2 peaks rather than 1. The average height of the highest peak was 5042 ± 14 mV and 4352 ± 147 mV for the pH 8 and 10.8 buffers, respectively, when analysing cyclophosphamide concentrations of 1 x 10^{-4} M. Peak heights no larger than 10 mV, however, were obtained when using any of the acidic carrier solutions to analyse cyclophosphamide concentrations ten times larger. Basic

carriers would therefore be more effective for cyclophosphamide detection. This was most likely due cyclophosphamide being deprononated at high pH (pKa of 2.84), giving rise to a high ionisation potential. As $Ru(bipy)_3$ chemiluminescence with amines occurs via electron transfer from the amine to $[Ru(bipy)_3]^{3+}$ [199], the first ionisation potential of the non-bonding orbital in the amine is inversely proportional to the intensity of the chemiluminescence produced. Higher pH levels would therefore result in more intense chemiluminescence.

The production of 2 peaks indicated that there was incomplete mixing between the reagents, most likely due to the large pH gradient between the carrier and the highly acidic oxidising reagent. This would have resulted in the formation of two reaction zones, one at either end of the injected oxidising reagent, as described in the schematic in Figure 7-21. This incomplete mixing decreased the intra-experimental variation, as evidenced by the high %RSD of peak area of up to 45.2 % for the pH 8 borate buffer in a single experiment.

Table 7-12. Reagents used for FIA chemiluminescence of cyclophosphamide (1 x 10^{-4} M) using sodium tetraborate buffer (pH 8 or 10.8) as the carrier solution

Reagent	Composition
Analyte	Cyclophosphamide (1 x 10^{-4} M) in deionised water
Oxidising Reagent	$Ru(bipy)_3ClO_4$ (1 x 10^{-3} M in 0.05 M $HClO_4$ in acetonitrile)
Carrier Solution	Sodium tetraborate buffer (0.05 M, pH 8 or pH 11)

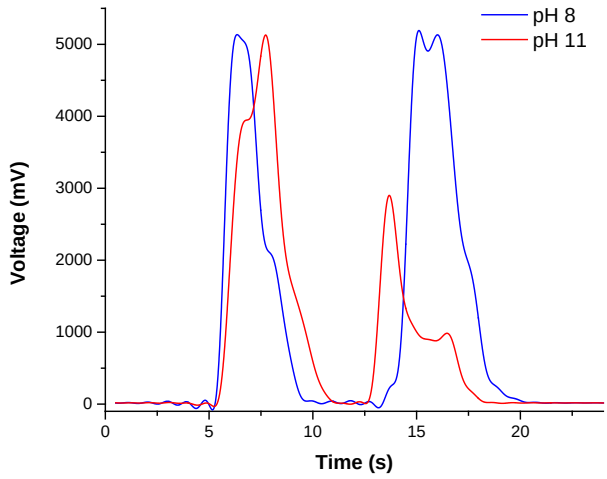

Figure 7-20. Baseline-subtracted FIA chemiluminescence peaks obtained via analysis of cyclophosphamide (1 x 10^{-4} M in deionised water) using $Ru(bipy)_3ClO_4$ (1 x 10^{-3} M in 0.05 M $HClO_4$ in acetonitrile) as the oxidising reagent and sodium tetraborate buffer (0.05 M, pH 8 or 10.8) as the carrier solution.

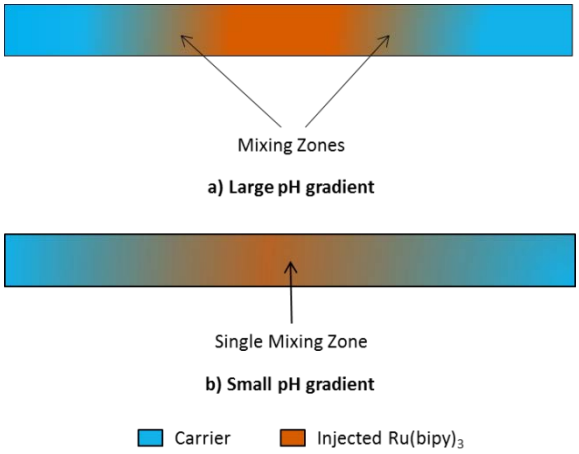

Figure 7-21. Schematic of an FIA tube containing a carrier solution (blue) into which Ru(bipy)3 is injected (orange), comparing a large pH gradient between the solutions (a) to a relatively smaller pH gradient (b)

Attempts were therefore made to reduce this peak splitting by comparing the use of phosphate buffer with borate buffers with the same pH (pH 8) in an attempt to improve miscibility. Cyclophosphamide was analysed using the conditions in Table 7-13. The use of the phosphate buffer carrier decreased the time delay between the two peaks from approximately 10.5 seconds to 3.5 seconds (taken as the time between the point at which the end of peak 1 and the start of peak 2 met the baseline) (Figure 7-22). This was an interesting result because borate buffer is generally thought to be more miscible with acetonitrile than phosphate buffer [208]. It is possible that the phosphate buffer was more effective in buffering the reagent mixture due to its lower effective buffering pH range (5.8-8 compared with 7.4-9.2) [209]. Phosphate buffer was therefore selected for subsequent analyses.

Table 7-13. Reagents used to compare chemiluminescence peak shapes obtained from cyclophosphamide (1×10^{-4} M) when using either phosphate buffer or borate buffer as the carrier solution

Reagent	Composition
Analyte	Cyclophosphamide (1×10^{-4} M) in deionised water
Oxidising Reagent	$Ru(bipy)_3ClO_4$ (1×10^{-3} M in 0.05 M $HClO_4$ in acetonitrile)
Carrier Solution	Sodium tetraborate buffer (0.05 M, pH 8) or phosphate buffer (0.05 M, pH 8)

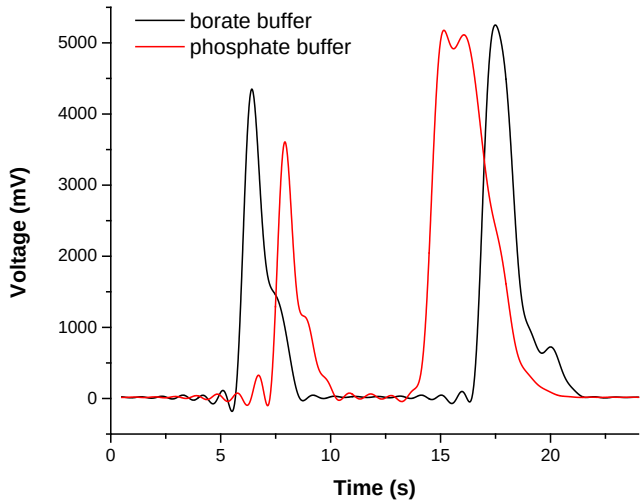

Figure 7-22. Comparison of baseline-subtracted FIA chemiluminescence peaks from cyclophosphamide (1 x 10^{-4} M in deionised water) obtained using $Ru(bipy)_3ClO_4$ (1 x 10^{-3} M in 0.05 M $HClO_4$ in acetonitrile) as the oxidising reagent and sodium tetraborate buffer or phosphate buffer (0.05 M, pH 8) as the carrier solution.

Peak splitting had still not been removed. Another explanation could be due to poor miscibility between the acetonitrile solvent of the $Ru(bipy)_3ClO_4$ reagent and the aqueous buffer. The use of $Ru(bipy)_3ClO_4$, while providing maximal stability of the $[Ru(bipy)_3]^{3+}$ state, would therefore decrease intra-experimental reproducibility. $Ru(bipy)_3Cl_2$ prepared in H_2SO_4, which would be more miscible with aqueous buffers, was therefore revisited in an attempt to improve intra-experimental reproducibility. Cyclophosphamide was analysed using the reagent conditions in Table 7-14, with resulting peak shape in Figure 7-23. A single peak, with some peak-shouldering was produced. The %RSD obtained for peak area was 1.65 %, and hence a large improvement in intra-experimental reproducibility had been achieved. $Ru(bipy)_3Cl_2$ prepared in H_2SO_4 had been shown to be stable for 2.5 hours (Section 4.3.1.1), and hence would provide adequate inter-experimental reproducibility while minimising intra-experimtental variability. $Ru(bipy)_3Cl_2$ prepared in H_2SO_4 was therefore used for all subsequent method development.

Table 7-14. Reagents used to investigate the chemiluminescence peak shape obtained from cyclophosphamide (1 x 10^{-4} M) when using the chloride salt of $Ru(bipy)_3$ in H_2SO_4 as the oxidising reagent and phosphate buffer as the carrier solution

Reagent	Composition
Analyte	Cyclophosphamide (1 x 10^{-4} M) in deionised water
Oxidising Reagent	$Ru(bipy)_3Cl_2$ (1 x 10^{-3} M in 0.05 M H_2SO_4)
Carrier Solution	Phosphate buffer (0.05 M, pH 8)

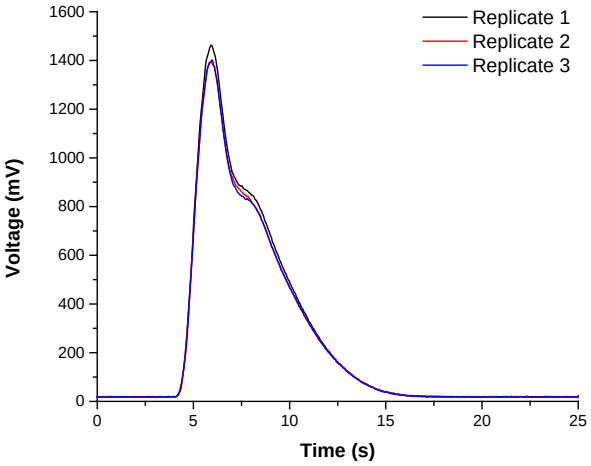

Figure 7-23. Baseline-subtracted FIA chemiluminescence peaks from cyclophosphamide (1 x 10^{-4} M in deionised water) obtained using $Ru(bipy)_3Cl_2$ (1 x 10^{-3} M in 0.05 M H_2SO_4) as the oxidising reagent and phosphate buffer (0.05 M, pH 8) as the carrier solution.

Appendix H – Effect of Cyclophosphamide Matrix on Chemiluminescence Peak Shape

Cyclophosphamide (1 x 10^{-4} M) prepared in either deionised water or phosphate buffer (pH 7, 0.05 M) was analysed using the reagent conditions in Table 7-15. Signals from cyclophosphamide prepared in deionised water had peak-splitting, whereas those from cyclophosphamide prepared in phosphate buffer did not (Figure 7-24).

Table 7-15. Reagents used to investigate the effect of analyte solvent on chemiluminescence peaks obtained via FIA of cyclophosphamide (1 x 10^{-4} M)

Reagent	Composition
Analyte	Cyclophosphamide (1 x 10^{-4} M) in deionised water or phosphate buffer (pH 7, 0.05 M)
Oxidising Reagent	$Ru(bipy)_3Cl_2$ (1 x 10^{-3} M in 0.075 M H_2SO_4)
Carrier Solution	Phosphate buffer (pH 7, 0.05 M)

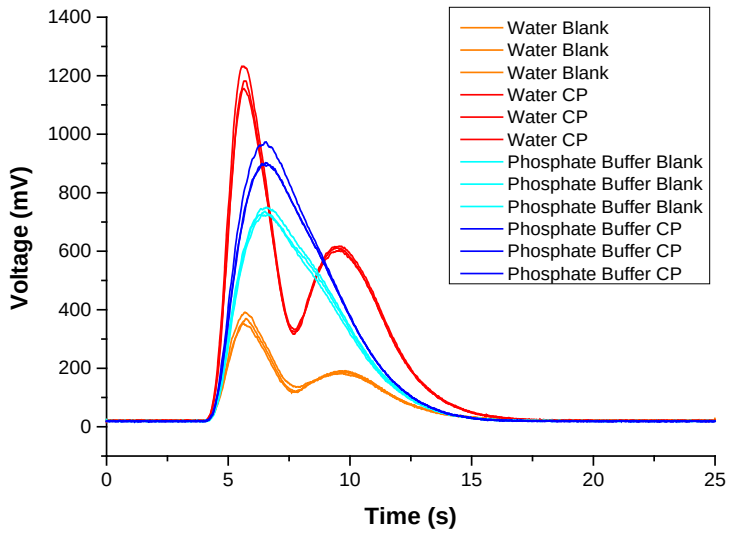

Figure 7-24. Comparison of FIA-chemiluminescence signals obtained via analysis cyclophosphamide (1 x 10^{-4} M) prepared in deionised water or phosphate buffer (0.05 M, pH 7) using $Ru(bipy)_3Cl_2$ (1 x 10^{-3} M in 0.05 M H_2SO_4) as the oxidising reagent and phosphate buffer (0.05 M, pH 7) as the carrier solution.

Appendix I – Effect of Phosphate Carrier Concentration on Cyclophosphamide Peak Shape

The effect of phosphate buffer concentration on chemiluminescence signal was assessed via analysis of cyclophosphamide using the reagent conditions in Table 7-16. A phosphate buffer concentration of 0.05 M (50 mM) was the only concentration that did not result in peak-splitting (Figure 7-25).

Table 7-16. Reagents used to investigate the effect of phosphate buffer carrier concentration on chemiluminescence obtained from cyclophosphamide (1 x 10^{-4} M)

Reagent	Composition
Analyte	Cyclophosphamide (1 x 10^{-4} M) in pH 7 phosphate buffer (2 x 10^{-3} - 0.05 M)
Oxidising Reagent	$Ru(bipy)_3Cl_2$ (1 x 10^{-3} M in 0.075 M H_2SO_4)
Carrier Solution	Phosphate buffer (pH 7, 2 x 10^{-3} - 0.05 M)

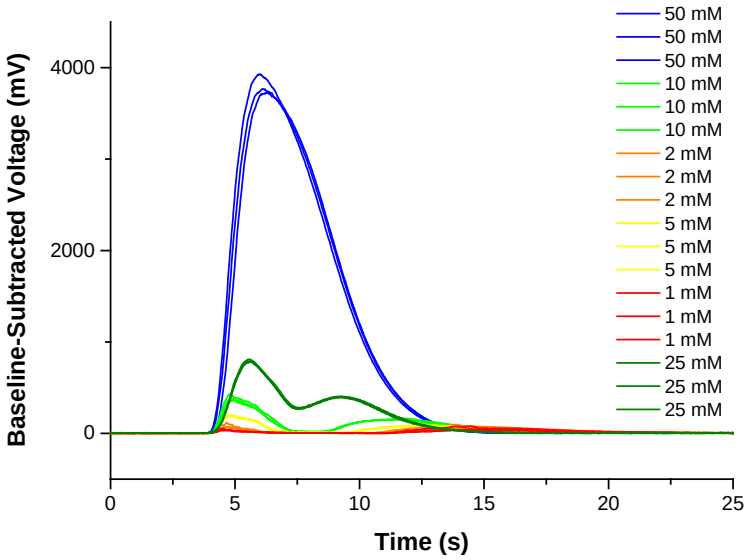

Figure 7-25. Effect of phosphate carrier concentration on the shape of chemiluminescence signals obtained via FIA of cyclophosphamide (1 x 10^{-4} M) using $Ru(bipy)_3Cl_2$ (1 x 10^{-3} M in 0.05 M H_2SO_4) as the oxidising reagent.

Appendix J – Effect of H_2SO_4 Concentration on Cyclophosphamide Chemiluminescence Peak Shape

The effect of the concentration of the H_2SO_4 used to prepare the $Ru(bipy)_3Cl_2$ was then investigated via analysis of cyclophosphamide (1×10^{-3} M in deionised water) using the conditions in Table 7-17. At the highest H_2SO_4 concentration (0.1 M) the chemiluminescence signal was comprised of two peaks (Figure 7-26). This peak splitting did not occur at lower H_2SO_4 concentrations.

Table 7-17. Reagent conditions used to determine the effect of H_2SO_4 concentration used to prepare $Ru(bipy)_3Cl_2$ on cyclophosphamide chemiluminescence

Reagent	Composition
Analyte	Cyclophosphamide (1×10^{-4} M) in phosphate buffer (pH 7, 0.05 M)
Oxidising Reagent	$Ru(bipy)_3Cl_2$ (1×10^{-3} M in 0.01 - 0.1 M H_2SO_4)
Carrier Solution	Phosphate buffer (pH 7, 0.05 M)

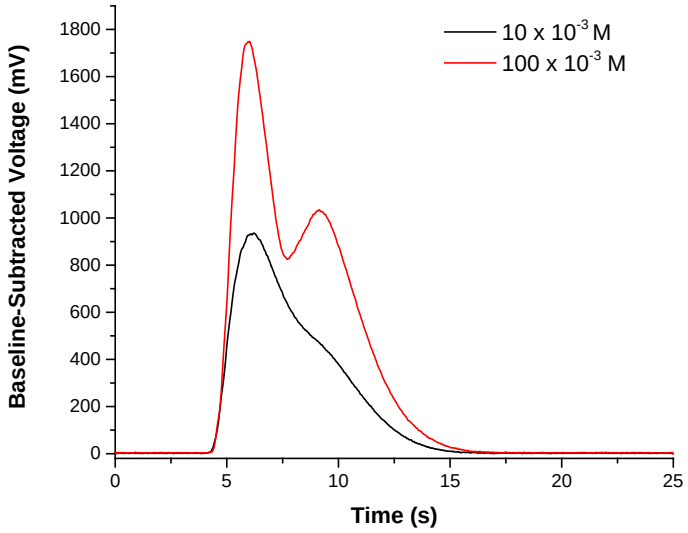

Figure 7-26. Comparison of baseline-subtracted chemiluminescence peaks obtained via FIA of cyclophosphamide (1×10^{-4} M) using $Ru(bipy)_3Cl_2$ prepared in either 10×10^{-3} M or 100×10^{-3} M H_2SO_4 as the oxidising reagent and phosphate buffer (0.05 M, pH 7) as the carrier solution.

Appendix K – Effect of Cyclophosphamide Concentration on Chemiluminescence Signal When Analysed Immediately After Preparation

The linearity of response of the developed FIA chemiluminescence detection method for cyclophosphamide was assessed. Cyclophosphamide solutions (2×10^{-6} M – 1×10^{-4} M in phosphate buffer) were analysed immediately after preparation using the conditions in Table 7-20. No linearity in response was obtained.

Table 7-18. Reagent conditions found to be optimal for FIA chemiluminescence detection of cyclophosphamide

Reagent	Composition
Analyte	Cyclophosphamide (2×10^{-6} – 1×10^{-4} M) in phosphate buffer (pH 7, 0.05 M)
Oxidising Reagent	$Ru(bipy)_3Cl_2$ (1×10^{-3} M in 0.075 M H_2SO_4)
Carrier Solution	Phosphate buffer (pH 7, 0.05 M)

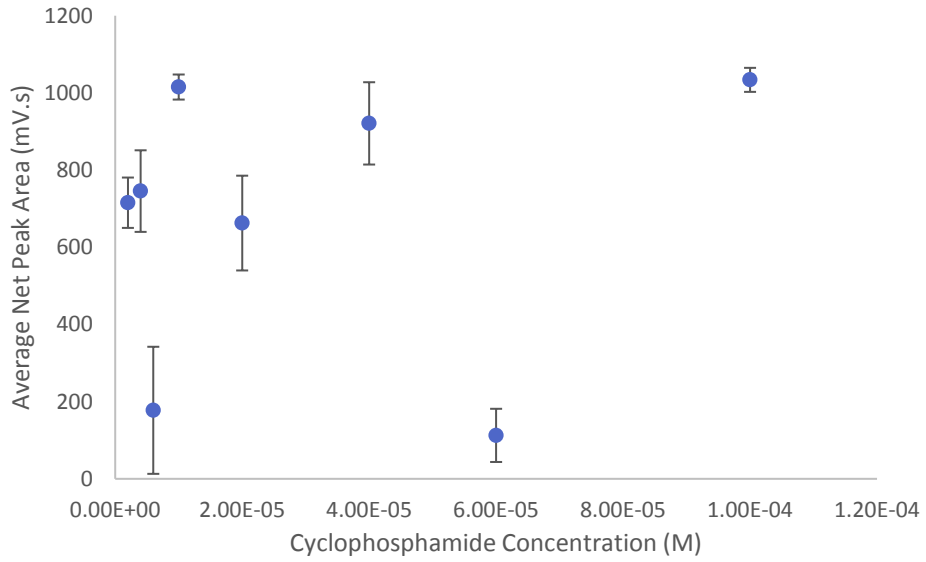

Figure 7-27. Average net peak area (n=3) obtained via FIA chemiluminescence of cyclophosphamide solutions (in 0.05 M pH 7 phosphate buffer). $Ru(bipy)_3Cl_2$ (1×10^{-3} M in 0.075 M H_2SO_4) was used as the oxidiser and phosphate buffer (0.05 M, pH 7) as the carrier solution. Error bars = ± 1 standard deviation.

Appendix L – NMR Spectra

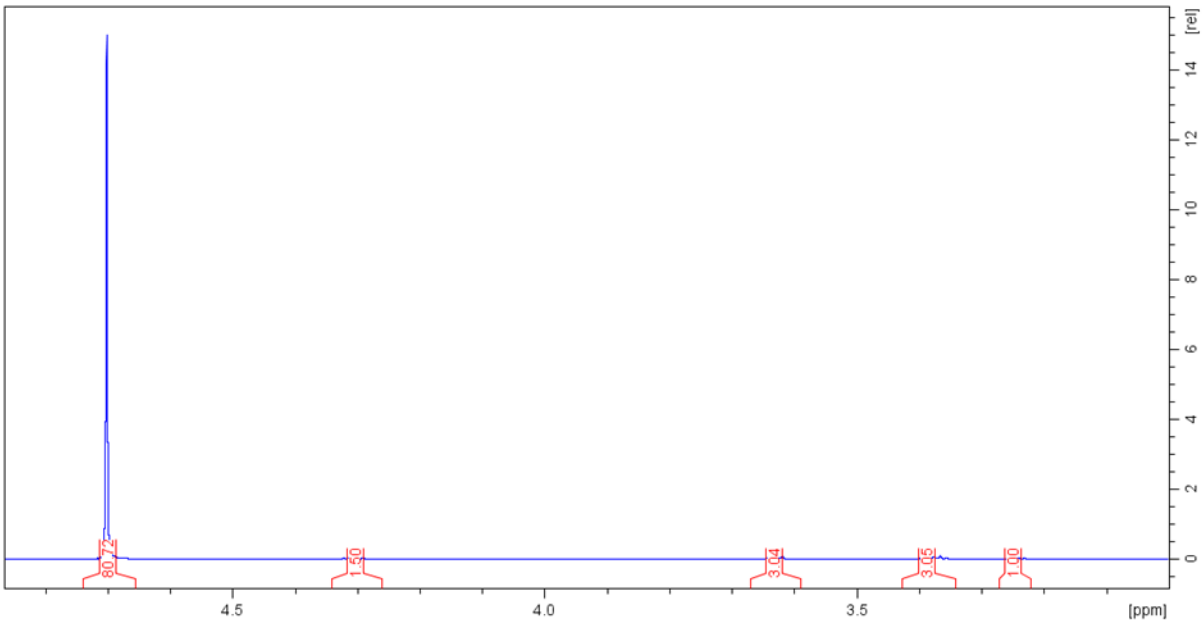

Appendix J 1. ^{1}H NMR spectrum of cyclophosphamide (in D_2O) 0 hours after preparation

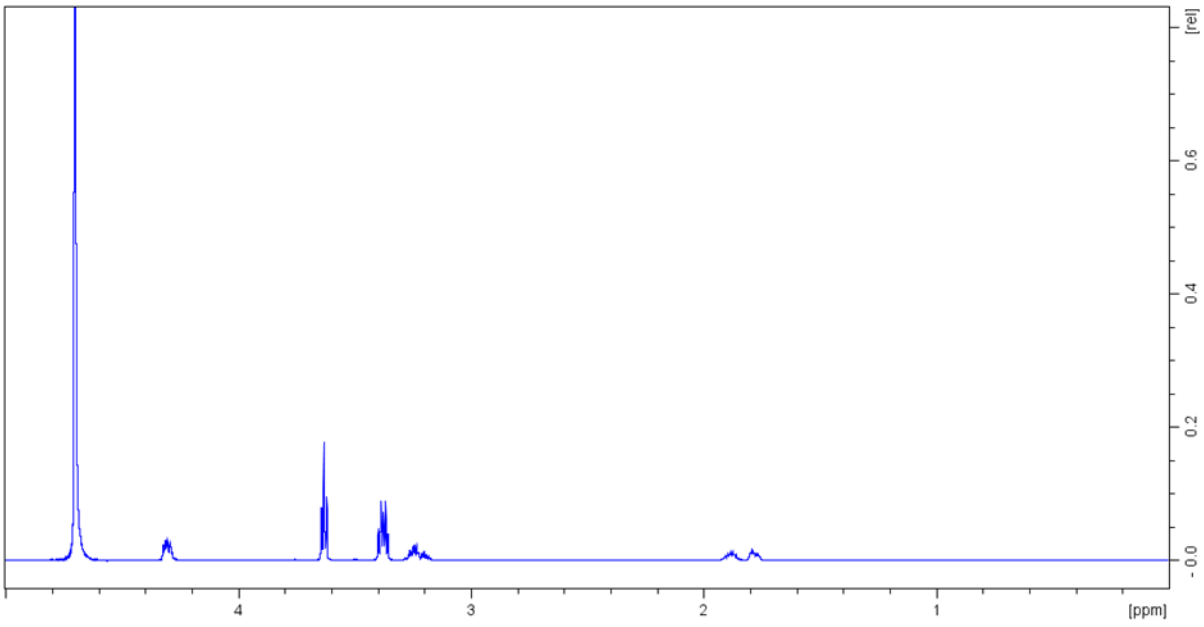

Appendix J 2. ^{1}H NMR spectrum of cyclophosphamide (in D_2O) 0 hours after preparation

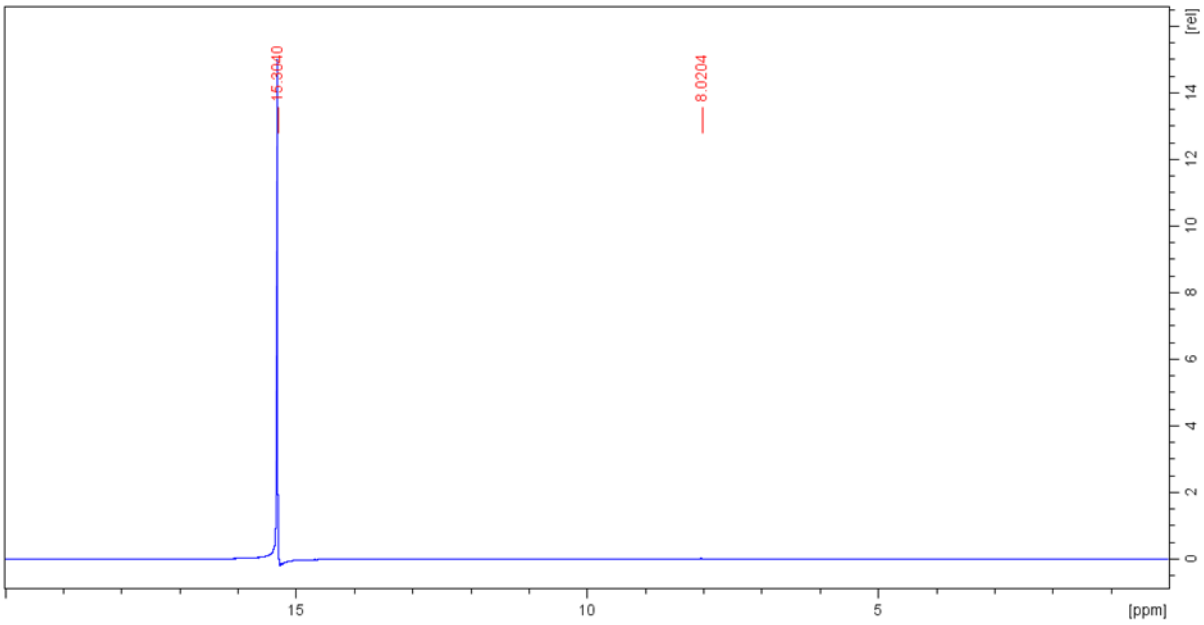

Appendix J 3. ^{31}P NMR of cyclophosphamide (0.05 M in deionised water) 0 hours after preparation

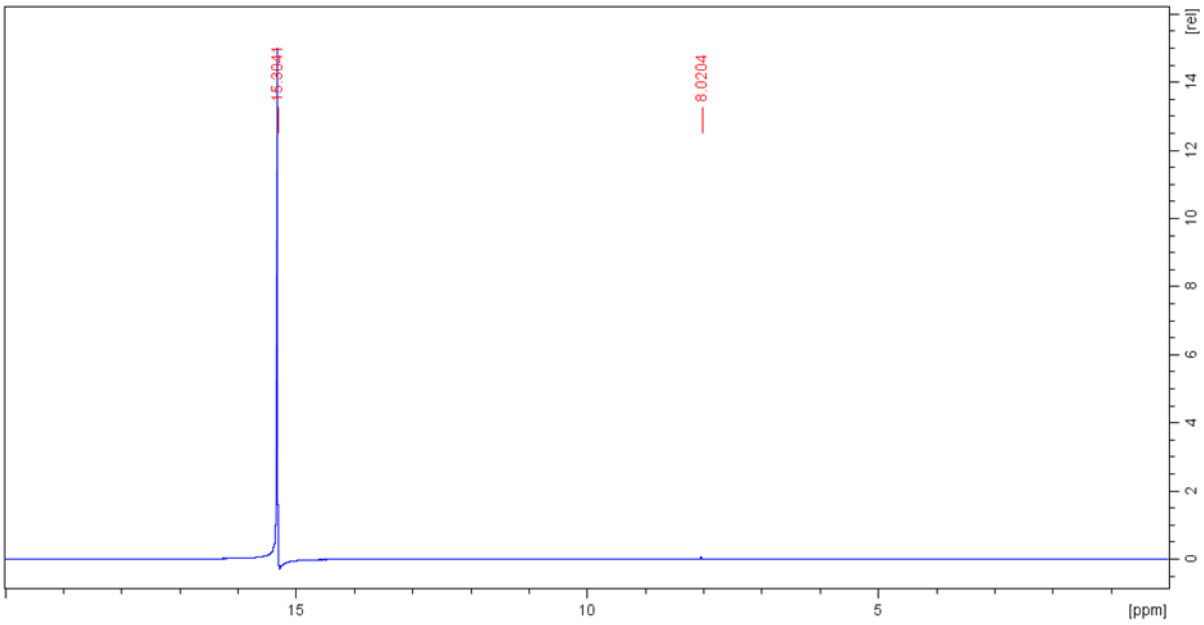

Appendix J 4. ^{31}P NMR of cyclophosphamide (0.05 M in deionised water) 1 hour after preparation

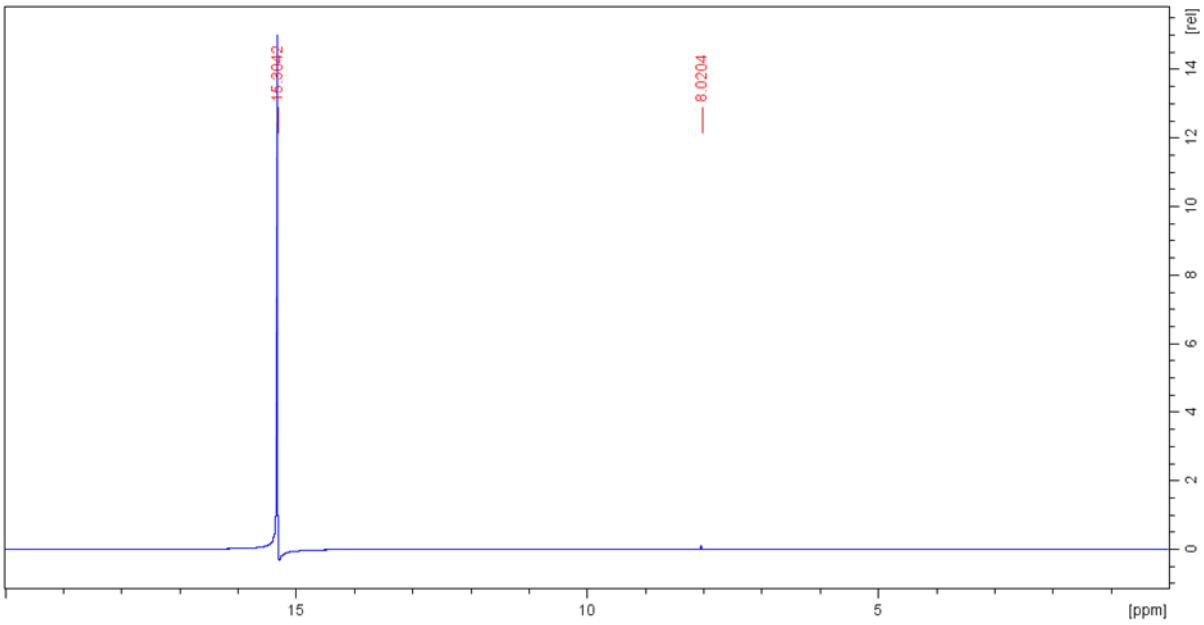

Appendix J 5. ^{31}P NMR of cyclophosphamide (0.05 M in deionised water) 3 hours after preparation

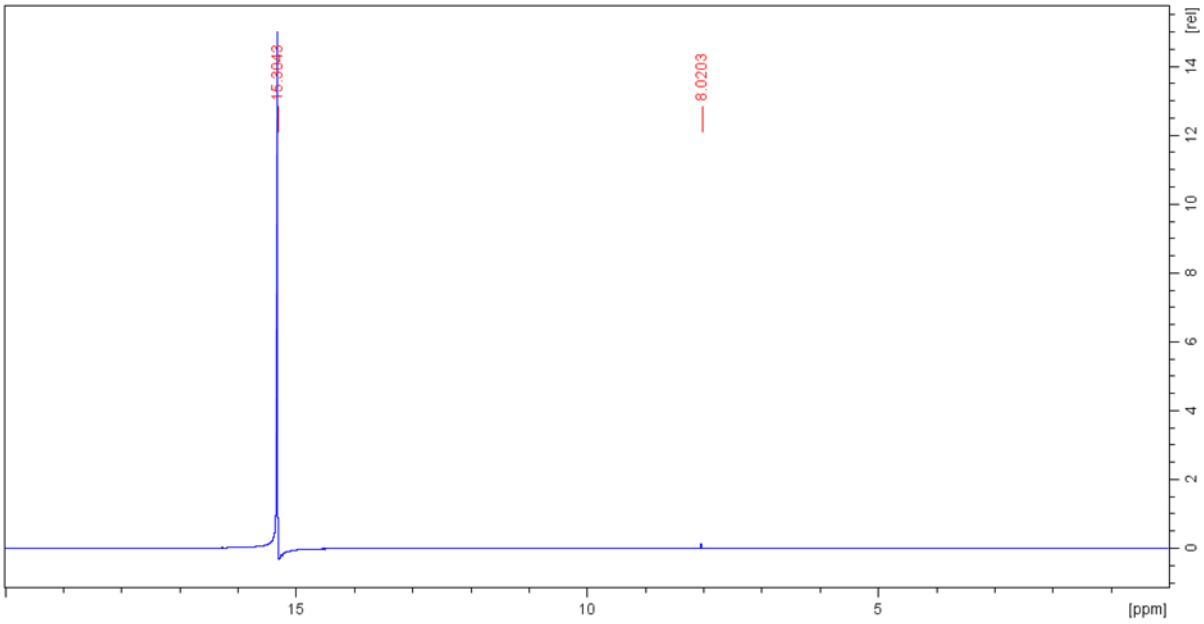

Appendix J 6. ^{31}P NMR of cyclophosphamide (0.05 M in deionised water) 7 hours after preparation

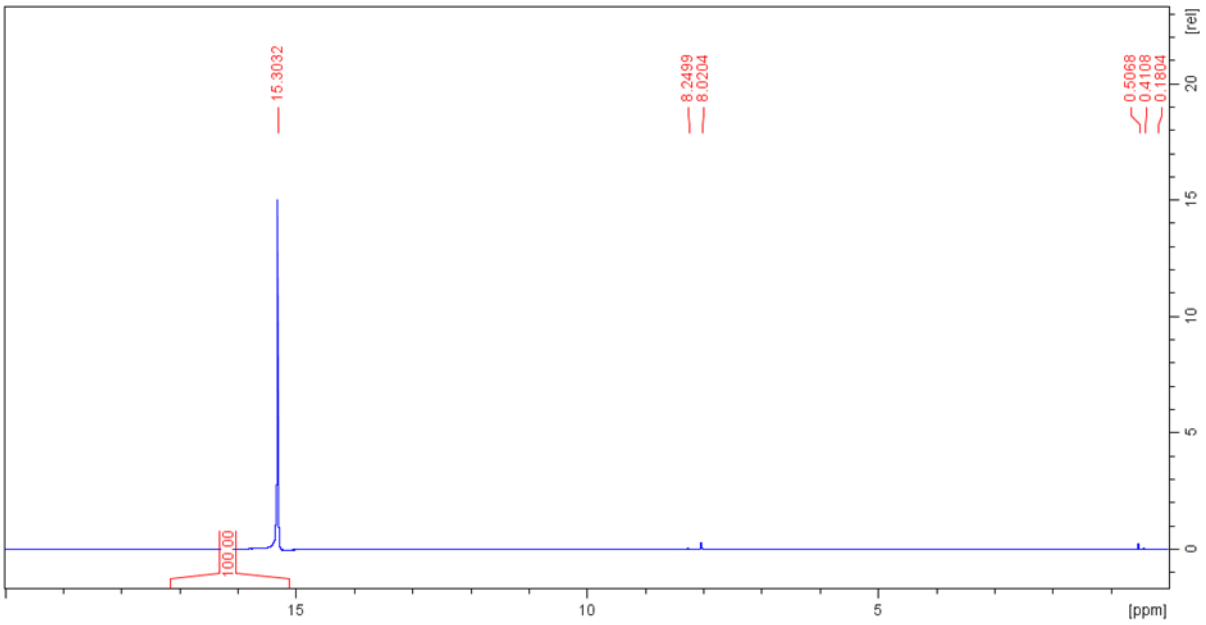

Appendix J 7. ^{31}P NMR of cyclophosphamide (0.05 M in deionised water) 11 hours after preparation

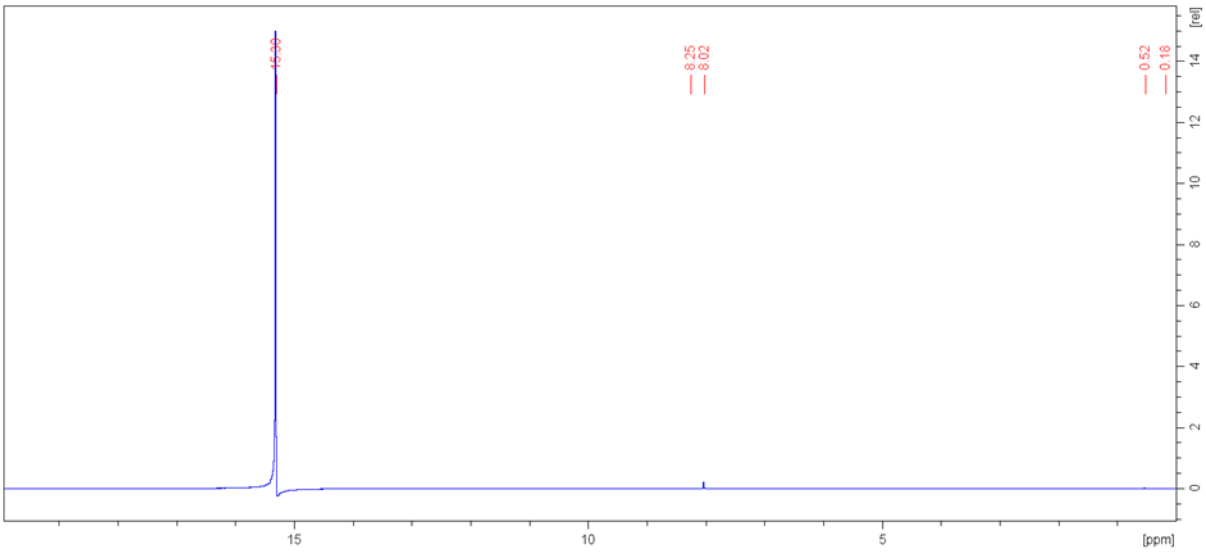

Appendix J 8. ^{31}P NMR of cyclophosphamide (0.05 M in deionised water) 21.5 hours after preparation

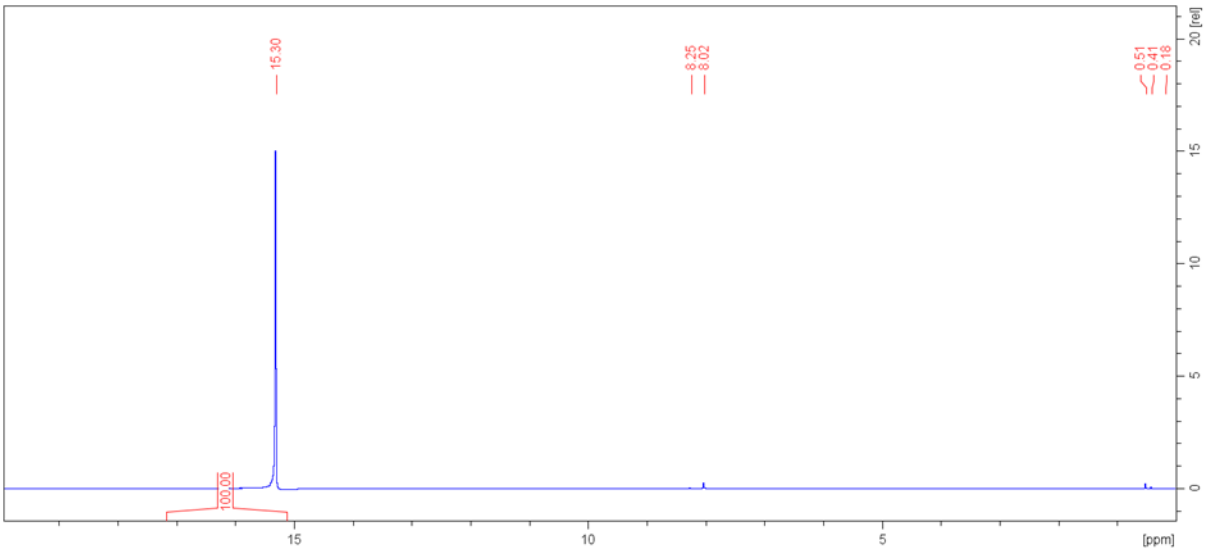

Appendix J 9. ^{31}P NMR of cyclophosphamide (0.05 M in deionised water) 76.5 hours after preparation

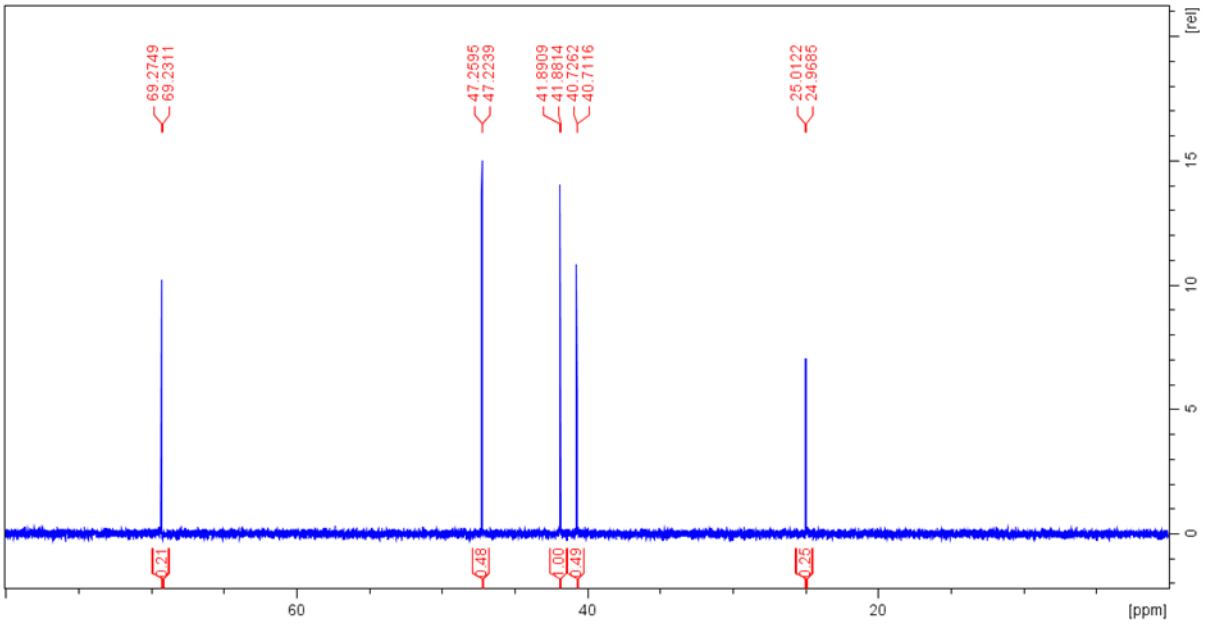

Appendix J 10. ^{13}C NMR of cyclophosphamide (0.05 M in deionised water) 0 hours after preparation

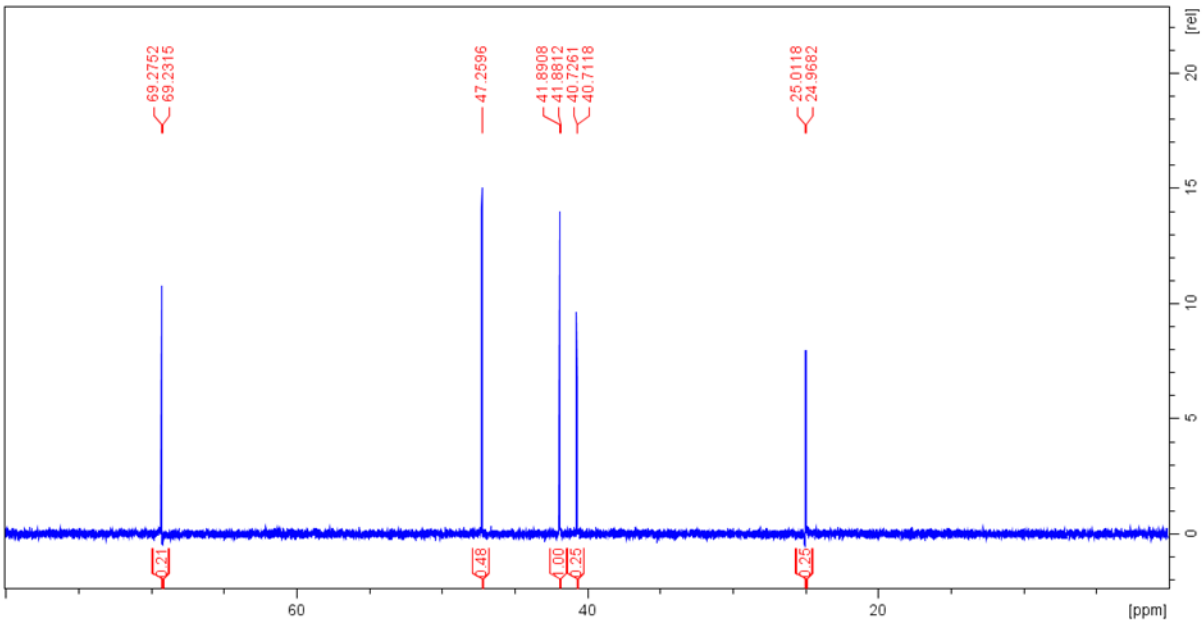

Appendix J 11. ^{13}C NMR of cyclophosphamide (0.05 M in deionised water) 1 hours after preparation

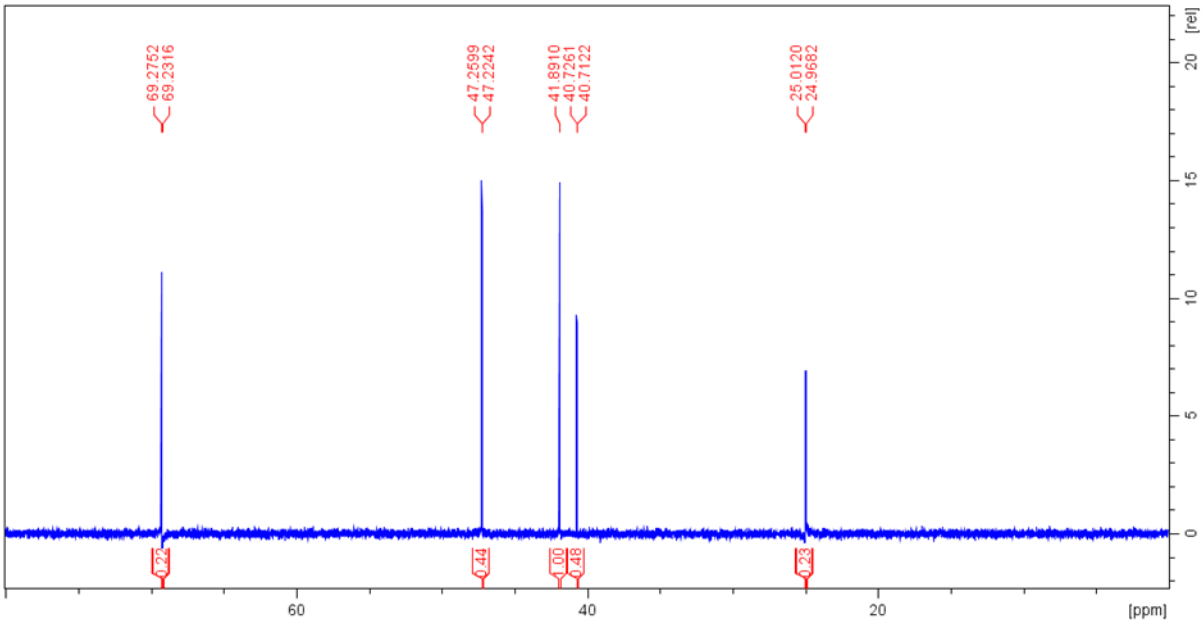

Appendix J 12. ^{13}C NMR of cyclophosphamide (0.05 M in deionised water) 3 hours after preparation

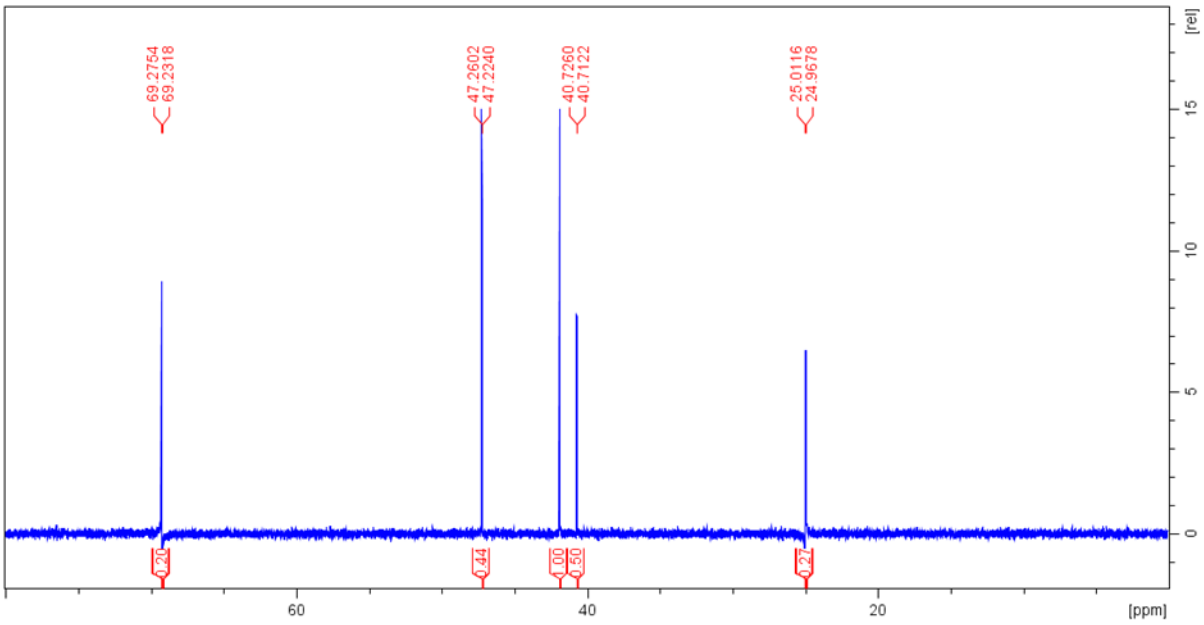

Appendix J 13. ^{13}C NMR of cyclophosphamide (0.05 M in deionised water) 7 hours after preparation

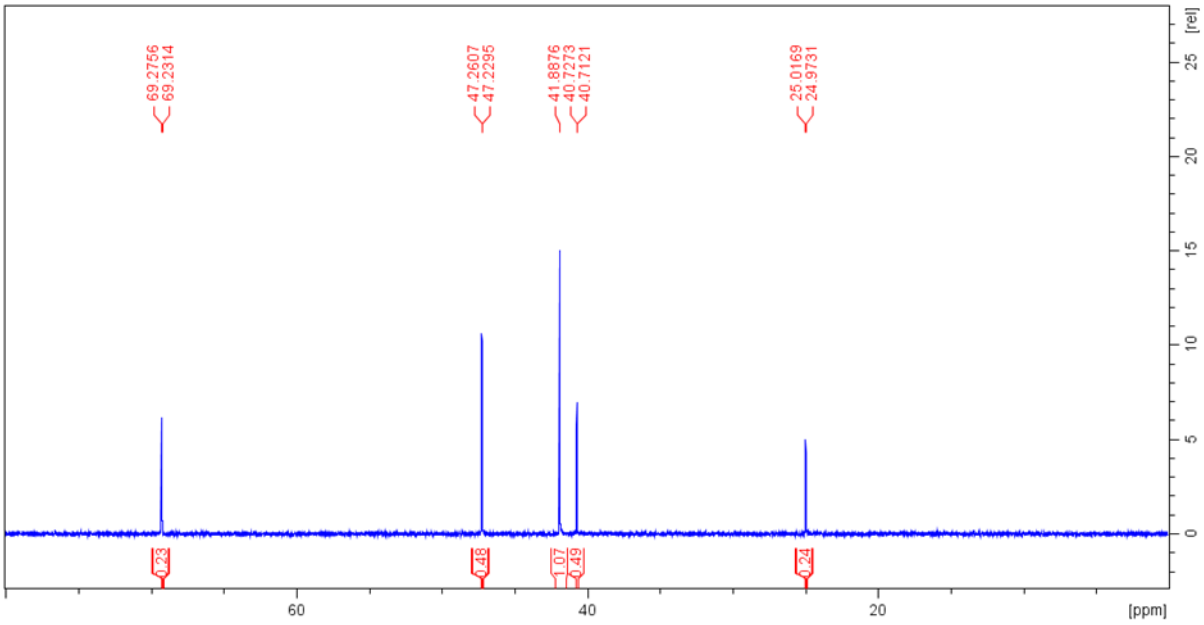

Appendix J 14. ^{13}C NMR of cyclophosphamide (0.05 M in deionised water) 11 hours after preparation

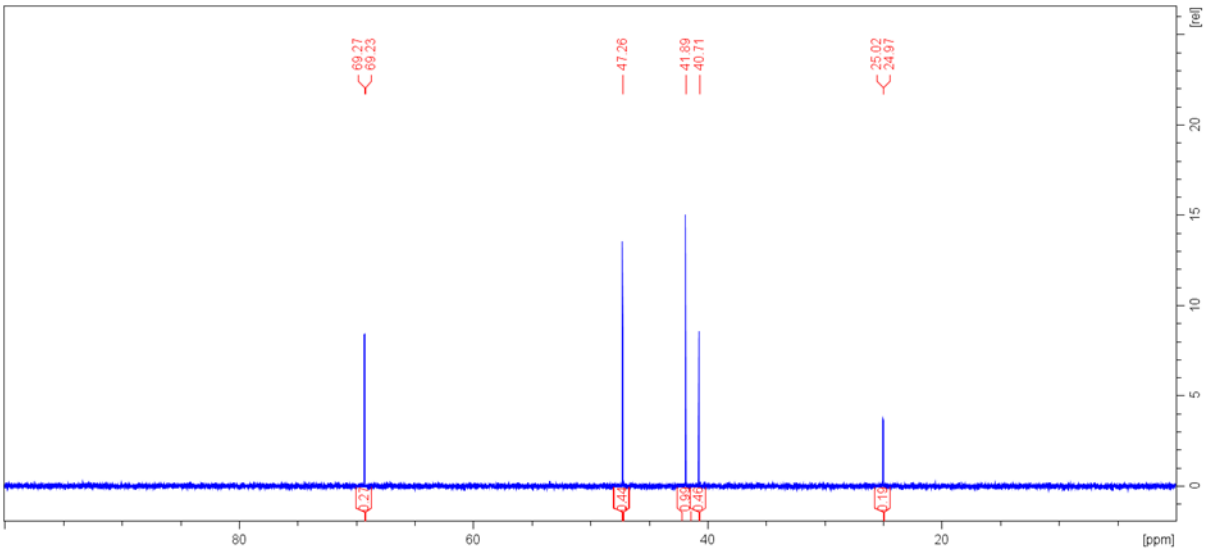

Appendix J 15. ^{13}C NMR of cyclophosphamide (0.05 M in deionised water) 21.5 hours after preparation

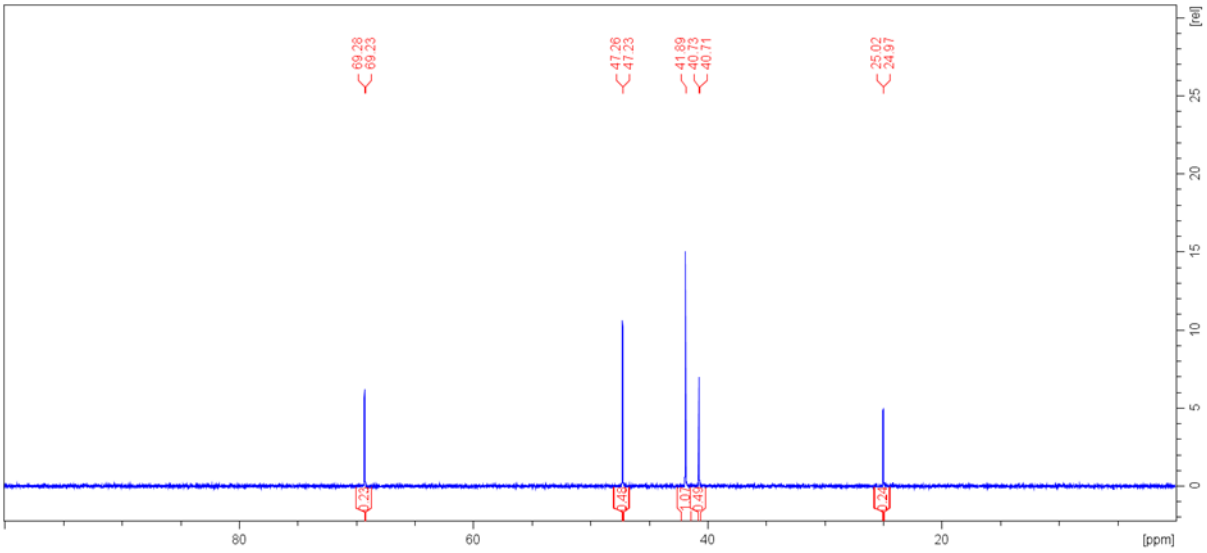

Appendix J 16. ^{13}C NMR of cyclophosphamide (0.05 M in deionised water) 76.5 hours after preparation

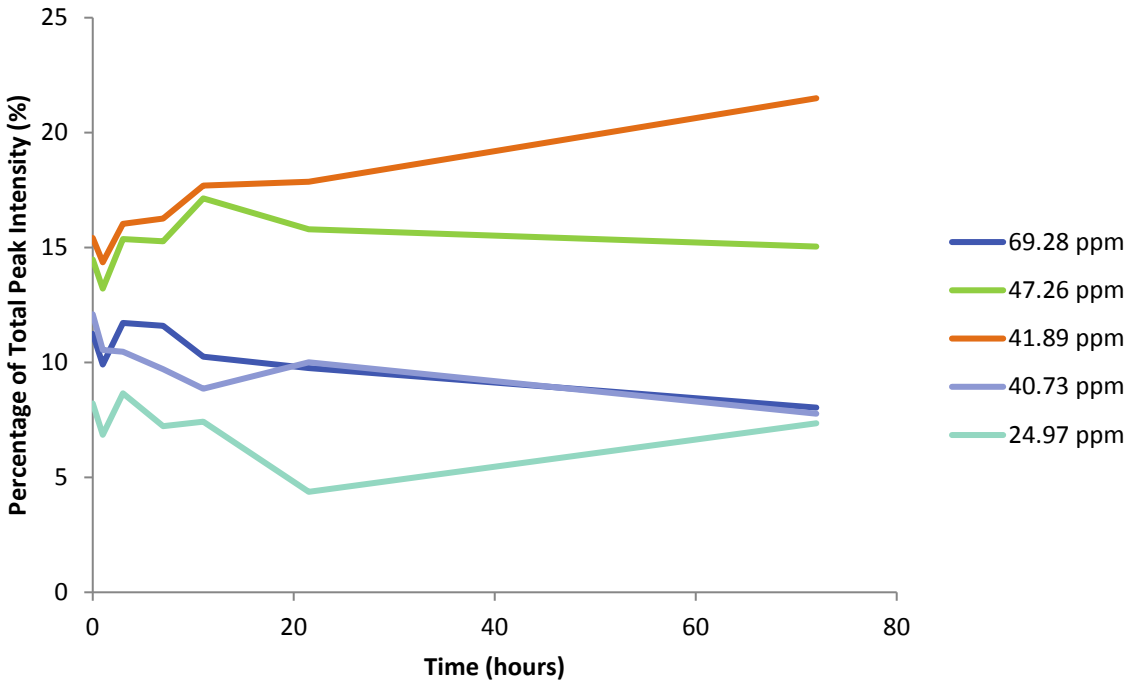

Figure 7-28. Change in percentage of total peak intensity of the ^{12}C NMR peaks observed via analysis of cyclophosphamide (0.05 M in distilled water) over 80 hours.

Appendix M – Investigation of Cyclophosphamide Degradation Reaction Order

Cyclophosphamide (0.1 M in deionised water) was stored at room temperature for 80 hours. Seven aliquots were removed over this time and diluted 2-fold in D_2O prior to immediate ^{31}P NMR analysis. Another cyclophosphamide solution (1 x 10^{-3} M) was prepared in phosphate buffer (pH 7, 0.05 M) and stored at room temperature for 90 hours. 11 aliquots were removed during this time and analysed immediately using FIA chemiluminescence.

The natural logs of the ^{31}P NMR peak intensity of the peaks at 15.30 ppm and 8.020 ppm were plotted against time to determine if the cyclophosphamide degradation reaction was first order. This was also done using the natural log of net chemiluminescence peak area. No linearity in these plots was obtained, hence indicating that the reaction was not first order.

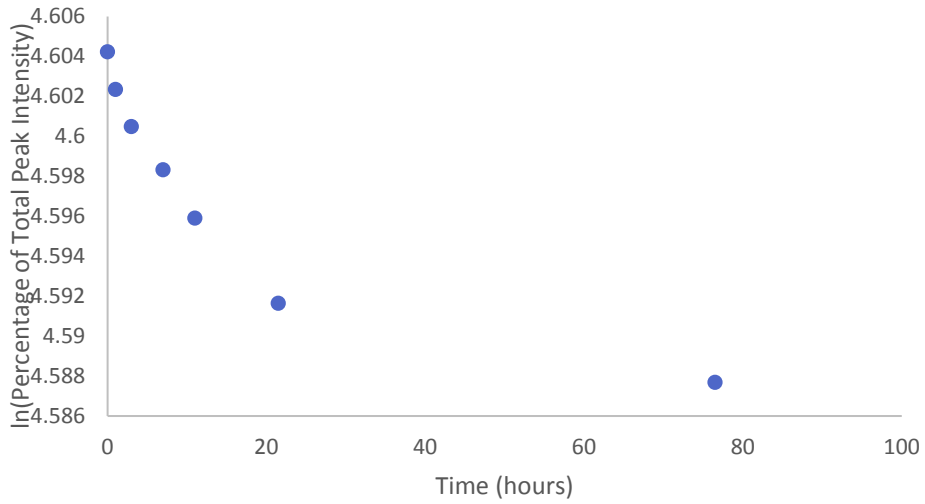

Figure 7-29. ln(percentage of total peak intensity) over time for the ^{31}P NMR peak at 15.30 ppm observed via analysis of cyclophosphamide (0.05 M in deionised water) over 80 hours.

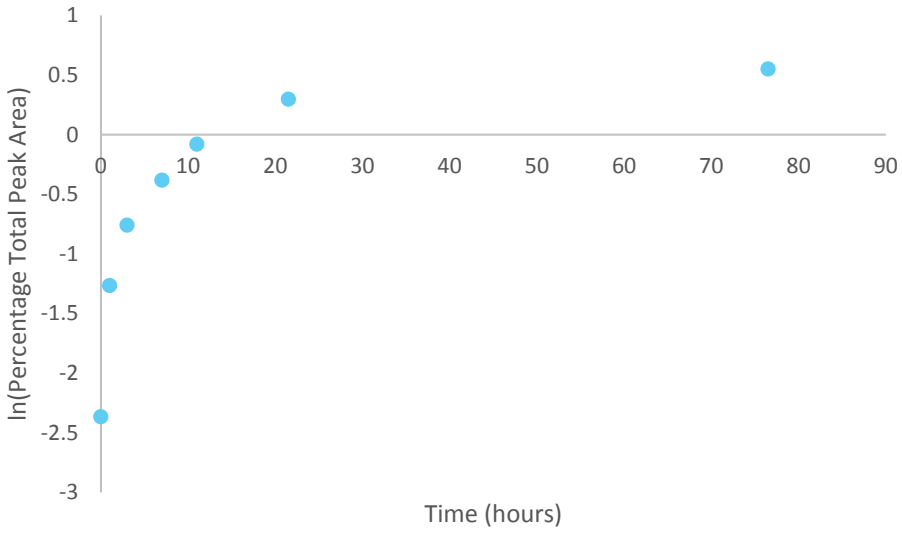

Figure 7-30. ln(percentage of total peak intensity) over time for the ^{31}P NMR peak at 8.020 ppm observed via analysis of cyclophosphamide (0.05 M in deionised water) over 80 hours.

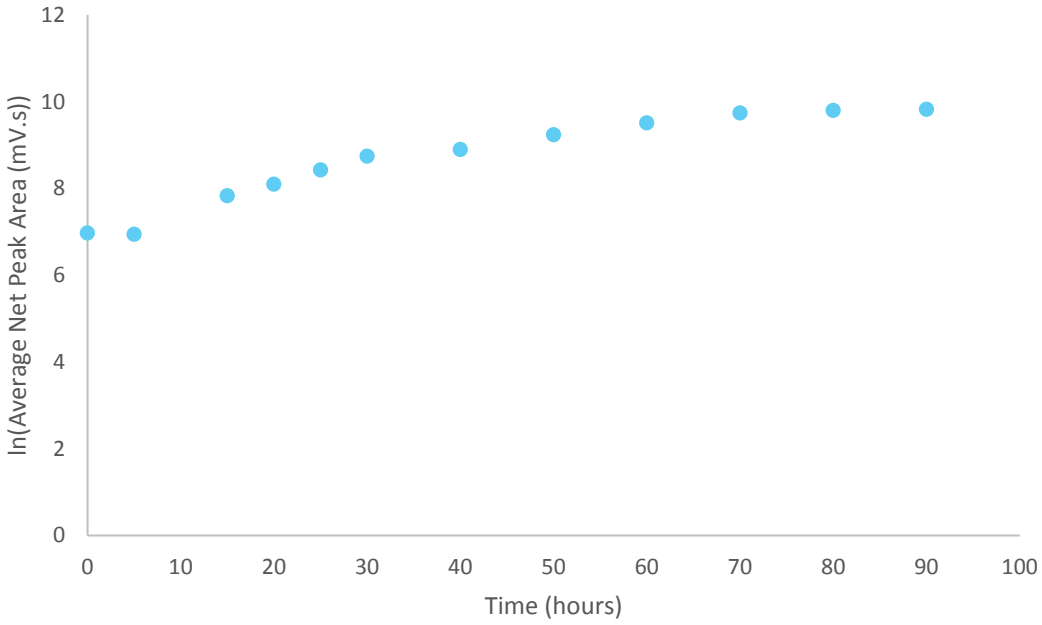

Figure 7-31. ln(average net chemiluminescence peak area) over time obtained via FIA chemiluminescence analysis of cyclophosphamide (1×10^{-3} M in pH 7 0.05 M phosphate buffer) over 90 hours using $Ru(bipy)_3Cl_2$ (1×10^{-3} M in 0.075 M H_2SO_4) as the oxidising reagent.

The inverse of the ^{31}P NMR peak intensity of the peaks at 15.30 ppm and 8.020 ppm were plotted against time to determine if the cyclophosphamide degradation reaction was second order. This was also done using the natural log of net chemiluminescence peak area. No linearity in these plots was obtained, hence indicating that the reaction was also not second order.

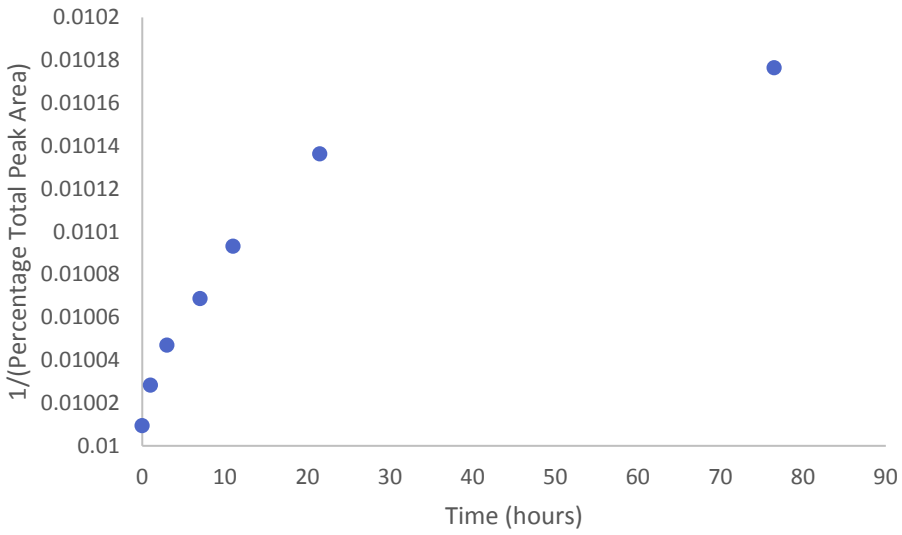

Figure 7-32. 1/(percentage of total peak intensity) over time for the ^{31}P NMR peak at 15.30 ppm observed via analysis of cyclophosphamide (0.05 M in deionised water) over 80 hours.

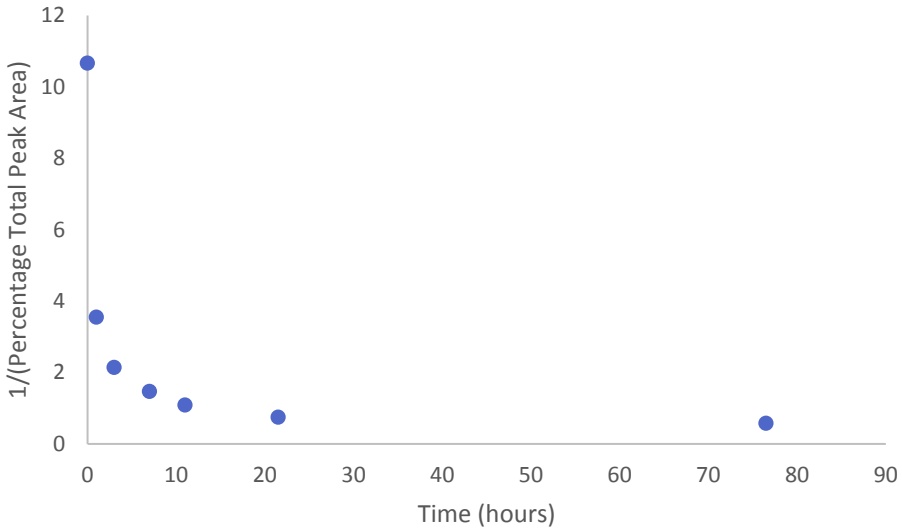

Figure 7-33. 1/(percentage of total peak intensity) over time for the ^{31}P NMR peak at 8.020 ppm observed via analysis of cyclophosphamide (0.05 M in deionised water) over 80 hours.

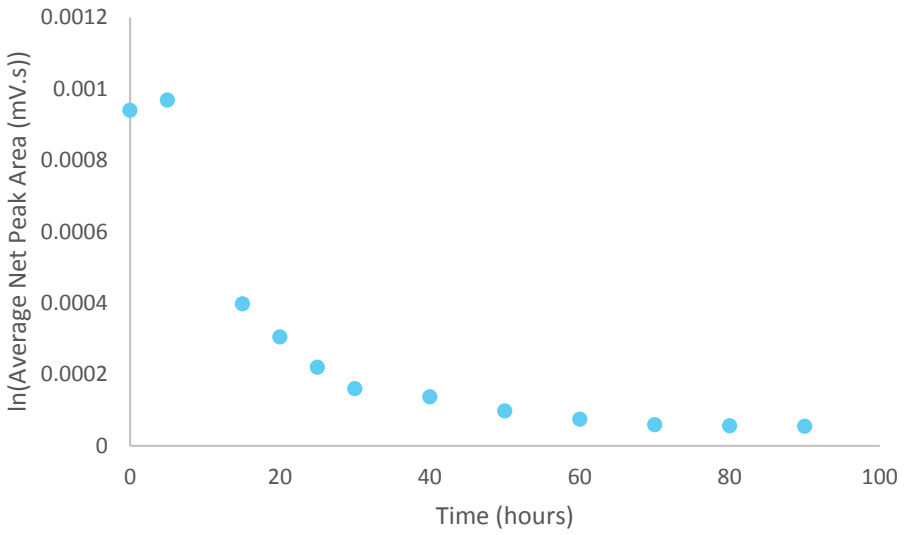

Figure 7-34. 1/(average net chemiluminescence peak area) over time obtained via FIA chemiluminescence analysis of cyclophosphamide (1 x 10^{-3} M in pH 7 0.05 M phosphate buffer) over 90 hours using $Ru(bipy)_3Cl_2$ (1 x 10^{-3} M in 0.075 M H_2SO_4) as the oxidising reagent.

Appendix N – Validation of Stopped-Flow Analysis Instrument

Sodium oxalate (1 x 10^{-7} M in deionised water) was analysed using the stopped-flow instrument described in Chapter 2. Pre-mixed $Ru(bipy)_3Cl_2$ (1 x 10^{-3} M in deionised water) and $Ce(SO_4)_2$ (1.5 x 10^{-3} M in 0.4 M H_2SO_4) in a 50:50 v/v ratio as the oxidising reagent. 11 replicates were conducted, with intense chemiluminescence profiles and good reproducibility obtained (Figure 7-35).

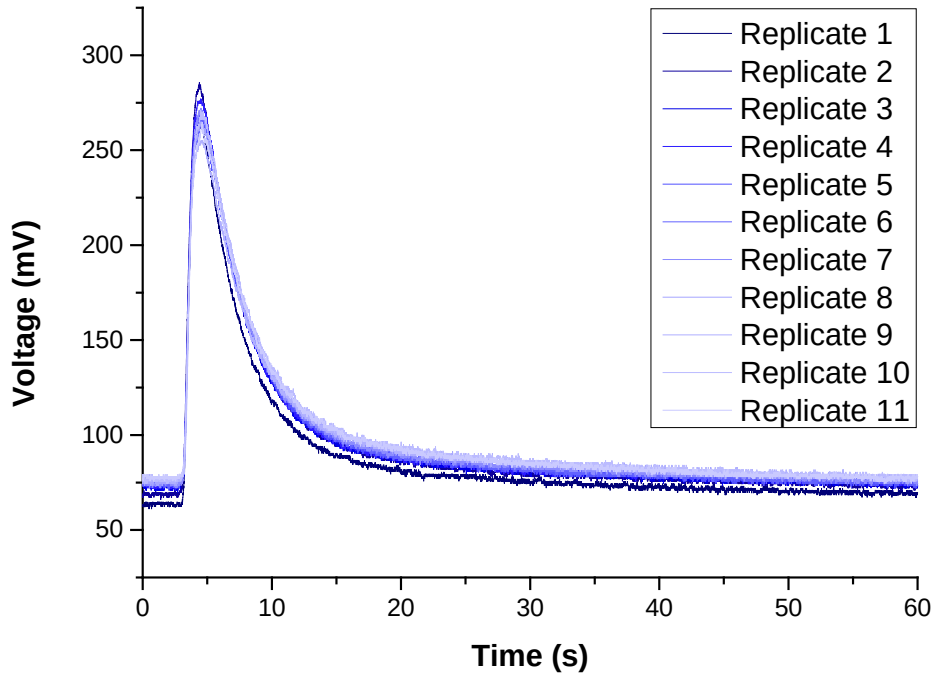

Figure 7-35. Overlaid kinetics profiles of sodium oxalate (1x10^{-7} M in distilled water) reacted with pre-mixed 50:50 (v/v) $Ru(bipy)_3Cl_2$ (1.5 x 10^{-3} M in deionised water) and $Ce(SO_4)_2$ (1 x 10^{-3} M in 0.4 M H_2SO_4) using stopped-flow analysis

Appendix O – Daily Analysis of Sodium Oxalate to Monitor FIA Instrument

Sodium oxalate solutions (1×10^{-6} M – 1×10^{-4} M in 0.1 M H_2SO_4) were analysed daily using the conditions in Table 7-19. The slope of the plot of chemiluminescence peak area versus sodium oxalate concentration increased over time (Figure 7-36), which showed an increase in sensitivity of the method over time.

Table 7-19. Reagents used to monitor the FAI chemiluminescence signals from sodium oxalate each day

Reagent	Composition
Analyte	Sodium oxalate (1×10^{-6} M – 1×10^{-4} M in 0.1 M H_2SO_4)
Oxidising Reagent	$Ru(bipy)_3ClO_4$ (1×10^{-3} M in 0.05 M $HClO_4$ in acetonitrile)
Carrier Solution	H_2SO_4 (0.05 M)

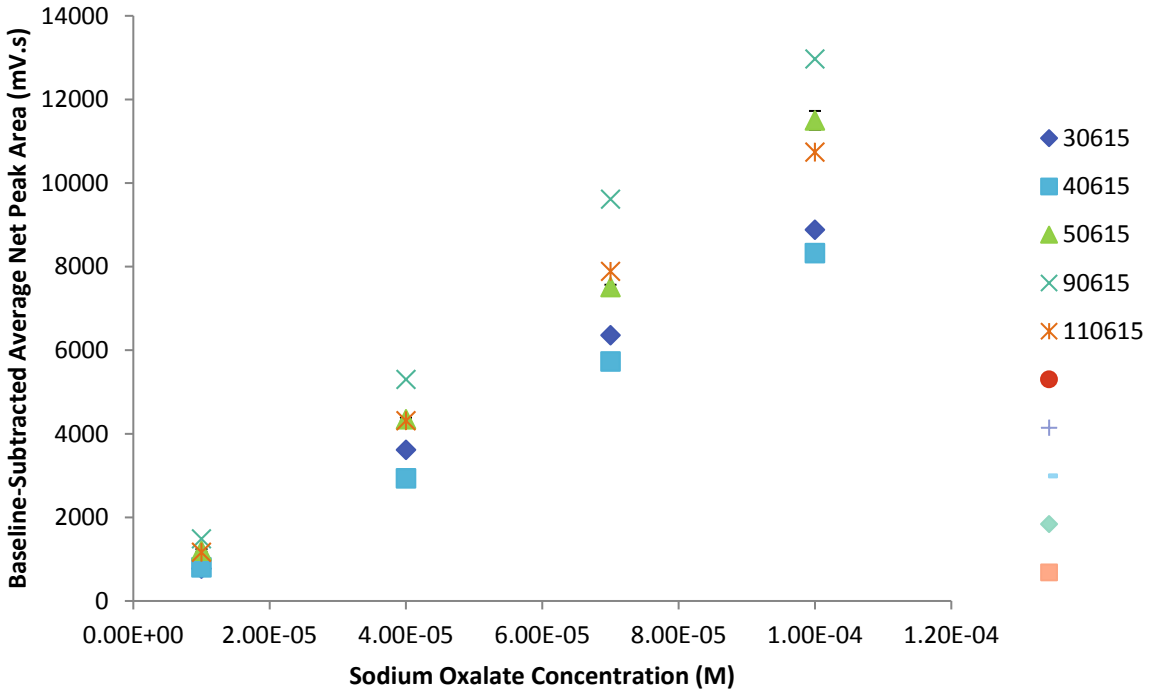

Figure 7-36. Plots of net chemiluminescence peak area versus sodium oxalate concentration (1×10^{-6} M – 1×10^{-4} M in 0.1 M H_2SO_4) collected over several days usinf $Ru(bipy)_3ClO_4$ (1×10^{-3} M in 0.05 M $HClO_4$ in acetonitrile) as the oxidising reagent and 0.05 M H_2SO_4 as the carrier solution. Error bars = ± 1 standard deviation.

Appendix P – Use of Surfactants in Chemiluminescence Method Development Using $Ru(bipy)_3Cl_2/PbO_2$ and SIA

Chemiluminescence can often be enhanced via use of a surfactant to improve miscibility between reagents with large differences in pH, such as the acidic $Ru(bipy)_3ClO_4$ and (relatively) neutral analyte solution in these experiments [210]. The effect of addition of the surfactants sodium dodecyl sulphate (SDS) (0.1 g/L), Triton-X100 (10 % v/v), and Tween-20 (10 % v/v) was therefore tested. Each surfactant was introduced into the reagent stream through a fourth port in the selection valve. The experimental conditions used are given in Table 7-20. Upon addition of each surfactant both cyclophosphamide and imatinib did not produce signals that could be easily integrated, and hence only 5-fluorouracil was used. As the surfactant concentration was increased the 5-fluorouracil chemiluminescence signal decreased and eventually became lower than that of the blank (Figure 7-37). This suggested that either the SDS was not aiding in mixing, or that it was inhibiting or quenching the chemiluminescence emission. Quenching of chemiluminescence can sometimes occur when using anionic surfactants such as SDS, often due to large changes in solution pH due to its addition [210]. This is usually more common, however, for analytes that do not already have a neutral pH. The use of Triton-X100 and Tween-20, which are both non-ionic surfactants, resulted in flooding of the PMT, and hence no accurate peak areas could be calculated. It was therefore decided that a surfactant could not be used to increase the chemiluminescence intensity, and hence no surfactant was used for subsequent analyses.

Table 7-20. Reagents, volumes and flow rates used to assess effect of analyte and oxidising reagent aspiration flow rate on SIA chemiluminescence signal from 5-fluorouracil and imatinib

Aspiration Order	Reagent	Composition	Volume (µL)	Flow Rate (µL/s)
1	Analyte	5-fluorouracil (1 x 10^{-3} M in deionised water)	10	10
2	Surfactant	SDS (0.1 g/L in deionised water), Triton-X100 (10 % v/v), or Tween-20 (10 % v/v)	5-50	10
3	Oxidising Reagent	$Ru(bipy)_3ClO_4$ (1 x 10^{-3} M in 0.05 M $HClO_4$ in acetonitrile)	30	10
4	Carrier Solution	0.05 M $HClO_4$ in acetonitrile	1000	100

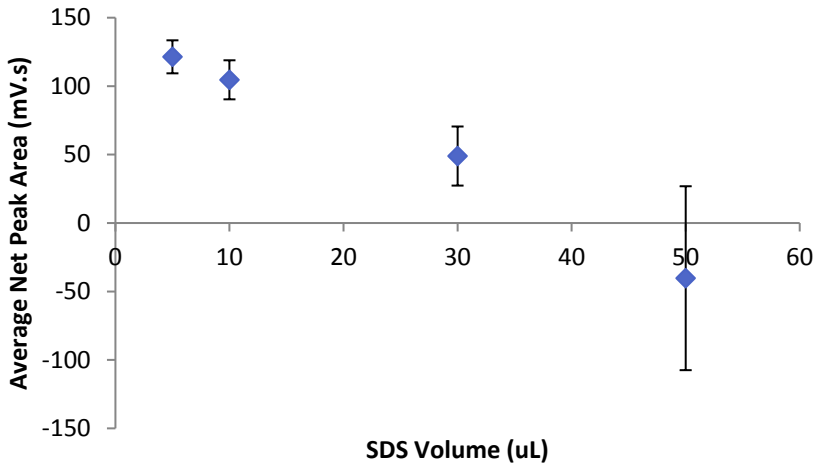

Figure 7-37. Trend in chemiluminescence signal obtained via SIA-chemiluminescence analysis of imatinib ($1x10^{-3}$ M in acetonitrile) analysed using $Ru(bipy)_3ClO_4$ (1×10^{-3} M in 0.05 M $HClO_4$ in acetonitrile) as the oxidising reagent, $HClO_4$ (0.05 M in acetonitrile) as the carrier solution, and with various volumes of SDS (3.5×10^{-4} M). Error bars = ± 1 standard deviation.

Chapter 8:

References

8. References

1. Sun, H., L. Li, and X. Chen, *Sensitized chemiluminescence determination of fluorouracil in pharmaceutical and biological fluids based on potassium permanganate oxidation in the presence of formaldehyde.* Journal of Clinical Laboratory Analysis, 2007. **21**(4): p. 213-219.
2. Kovalova, L., et al., *Removal of highly polar micropollutants from wastewater by powdered activated carbon.* Environmental Science and Pollution Research, 2013. **20**(6): p. 3607-3615.
3. Dubey, D.K., et al., *On-matrix derivatisation–extraction of precursors of nitrogen- and sulfur-mustards for verification of chemical weapons convention.* Journal of Chromatography A, 2005. **1076**(1–2): p. 27-33.
4. Nussbaumer, S., et al., *Analysis of anticancer drugs: A review.* Talanta, 2011. **85**: p. 2265-2289.
5. Kosjek, T. and E. Heath, *Occurrence, fate and determination of cytostatic pharmaceuticals in the environment.* Trends in Analytical Chemistry, 2011. **30**(7): p. 1065-1087.
6. Besse, J. and J. Garric, *Human pharmaceuticals in surface waters - Implementation of a prioritization methodology and application to the French situation.* Toxicology Letters, 2008. **176**: p. 104-123.
7. Hansel, S., et al., *Chemical degradation of wastes of antineoplastic agents: cyclophosphamide, ifosfamide and melphalan.* International Archives of Occupational and Environmental Health, 1996. **69**(2): p. 109-114.
8. Kovalova, L., C.S. McArdell, and J. Hollender, *Challenge of high polarity and low concentrations in analysis of cytostatics and metabolites in wastewater by hydrophilic interaction chromatography tandem MS.* J. Chrom. A, 2009. **1216**: p. 1100-1108.
9. Besse, J., J. Latour, and J. Garric, *Anticancer drugs in surface waters - What can we say about the occurrence and environmental significance of cytotoxic, cytostatic and endocrine therapy drugs?* Environment International, 2012. **39**: p. 73-86.
10. Santana-Viera, S., et al., *Cytostatic drugs in environmental samples: An update on the extraction and determination procedures.* TrAC Trends in Analytical Chemistry, 2016. **80**: p. 373-386.
11. Mabbot, V., et al., *Australian Statistics on Medicine*, A.G.-D.o.H.a. Aging, Editor. 2012, Commonwealth of Australia: Canberra, Australia.
12. American Society of Health-System Pharmacists, I. *Cyclophosphamide*. 2011 [cited 2016 1/07/2016]; Available from: https://www.nlm.nih.gov/medlineplus/druginfo/meds/a682080.html.
13. Joy, M.S., et al., *Cyclophosphamide and 4-hydroxycyclophosphamide pharmacokinetics in patients with glomerulonephritis secondary to lupus and small vessel vasculitis.* British Journal of Clinical Pharmacology, 2012. **74**(3): p. 445-455.
14. Low, J.E., R.F. Borch, and N.E. Sladek, *Conversion of 4-Hydroperoxycyclophosphamide and 4-Hydroxycyclophosphamide to Phosphoramide Mustard and Acrolein Mediated by Bifunctional Catalysts.* Cancer Research, 1982. **42**(3): p. 830-837.
15. Kennedy, R., et al., *Stability of Cyclophosphamide in Extemporaneous Oral Suspensions.* Annals of Pharmacotherapy, 2010. **44**(2): p. 295-301.
16. Chabner, B.A. and D.L. Longo, *Cancer Chemotherapy and Biotherapy: Principles and Practice*. 2011: Lippincott Williams & Wilkins.
17. Walko, C.M. and C. Lindley, *Capecitabine: A review.* Clinical Therapeutics, 2005. **27**(1): p. 23-44.
18. American Society of Health-System Pharmacists, I. *Fluorouracil Injection*. 2012 23 October 2013]; Available from: http://www.nlm.nih.gov/medlineplus/druginfo/meds/a682708.html.
19. Information, N.C.f.B., *TYMS thymidylate synthetase*. 2013, U.S. National Library of Medicine.

20. Bernadou, J., et al., *Complete urinary excretion profile of 5-fluorouracil during a six-day chemotherapeutic schedule, as resolved by 19F nuclear magnetic resonance.* Clin. Chem., 1985. **31**(6): p. 846-848.
21. Solimando, D.A., *Drug Information Handbook for Oncology: A Complete Guide to Combination Chemotherapy Regimes*. 8th ed. 2010, Hudson, OH: Lexi Comp.
22. American Society of Health-System Pharmacists, I. *Imatinib*. 2013 15 January 2013 23 October 2013]; Available from: http://www.nlm.nih.gov/medlineplus/druginfo/meds/a606018.html.
23. Institute, N.C. *Imatinib mesylate*. NCI Drug Dictionary 2013 23 October 2013]; Available from: http://www.cancer.gov/drugdictionary?cdrid=37862.
24. Peng, B., P. Lloyd, and H. Schran, *Clinical pharmacokinetics of imatinib.* Clin. Pharmacokinet., 2005. **44**(9): p. 879-894.
25. Buerge, I.J., et al., *Occurrence and Fate of the Cytostatic Drugs Cyclophosphamide and Ifosfamide in Wastewater and Surface Waters.* Environmental Science and Technology, 2006. **40**: p. 7242-7250.
26. Garcia-Ac, A., et al., *Comparison of APPI, APCI and ESI for the LC-MS/MS analysis of bezafibrate, cyclophosphamide, enalapril, methotrexate and orlistat inmunicipal wastewater.* Journal of Mass Spectrometry, 2011. **46**: p. 383-390.
27. Gomez-Canela, C., et al., *Occurrence of cyclophosphamide and epirubicin in wastewaters by direct injection analysis–liquid chromatography–high-resolution mass spectrometry.* Environmental Science and Pollution Research, 2012. **19**: p. 3210-3218.
28. Kuemmerer, K. and A. Al-Ahmad, *Estimation of the cancer risk to humans resulting from the presence of cyclophosphamide and ifosfamide in surface water.* Environmental Science and Pollution Research International, 2010. **17**(2): p. 486-496.
29. Garcia-Ac, A., et al., *Determination of bezafibrate, methotrexate, cyclophosphamide, orlistat and enalapril in waste and surface waters using online SPE LC coupled to polairty-switching electrospray tandem MS.* Journal of Environmental Monitoring, 2009. **11**: p. 830-838.
30. Steger-Hartmann, T., K. Kümmerer, and A. Hartmann, *Biological Degradation of Cyclophosphamide and Its Occurrence in Sewage Water.* Ecotoxicology and Environmental Safety, 1997. **36**(2): p. 174-179.
31. Castiglioni, S., et al., *A multiresidue analytical method using solid-phase extraction and high-pressure liquid chromatography tandem mass spectrometry to measure pharmaceuticals of different therapeutic classes in urban wastewaters.* Journal of Chromatography A, 2005. **1092**: p. 206-215.
32. Hua, W.Y., et al., *SEASONALITY EFFECTS ON PHARMACEUTICALS AND S-TRIAZINE HERBICIDES IN WASTEWATER EFFLUENT AND SURFACE WATER FROM THE CANADIAN SIDE OF THE UPPER DETROIT RIVER.* Environmental Toxocology and Chemistry, 2006. **25**(9): p. 2356-2365.
33. Yin, J., et al., *Analysis of Anticancer Drugs in SewageWater By Selective SPE and UPLC–ESI-MS–MS.* Journal of Chromatographic Science, 2010. **48**: p. 781-789.
34. Gomez-Canela, C., et al., *Liquid chromatography coupled to tandem mass spectrometry and high resolution mass spectrometry as analytical tools to characterise multi-class cytostatic compounds.* J. Chrom. A, 2013. **1276**: p. 78-94.
35. Kiffmeyer, T.K., et al., *Trace enrichment, chromatographic separation and biodegradation of cytostatic compounds in surface water.* Fresenius' Journal of Analytical Chemistry, 1998. **361**(2): p. 185-191.
36. Avella, A.C., et al., *Effect of cytostatic drug presence on extracellular polymeric substances formation in municipal wastewater treated by membrane bioreactor.* Biosource Technology, 2010. **101**: p. 518-526.
37. Delgado, L.F., et al., *Removal of a cytostatic drug by a membrane bioreactor.* Desalination and Water Treatment, 2009. **9**(1-3): p. 112-118.

38. Brown, A.J., et al., *Soluble manganese(IV) as a chemiluminescence reagent for the determination of opiate alkaloids, indoles and analytes of forensic interest.* Talanta, 2007. **71**(5): p. 1951-1957.
39. Delgado, L.F., et al., *Effect of cytostatic drugs on the sludge and on the mixed liquor characteristics of a cross-flow membrane bioreactor: Consequence on the process.* Journal of Membrane Science, 2010. **347**: p. 165-173.
40. Llewellyn, N., et al., *Determination of cyclophosphamide and ifosfamide in sewage effluent by stable isotope-dilution liquid chromatography–tandem mass spectrometry.* J. Chrom. A, 2011. **1218**: p. 8519-8528.
41. Metcalfe, C.D., et al., *DISTRIBUTION OF ACIDIC AND NEUTRAL DRUGS IN SURFACE WATERS NEAR SEWAGE TREATMENT PLANTS IN THE LOWER GREAT LAKES, CANADA.* Environmental Toxocology and Chemistry, 2003. **22**(12): p. 2881-2889.
42. Busetti, F., K.L. Linge, and A. Heitz, *Analysis of pharmaceuticals in indirect potable reuse systems using solid-phase extraction and liquid chromatography–tandem mass spectrometry.* J. Chrom. A, 2009. **1216**: p. 5807-5818.
43. Wang, L., et al., *Cyclophosphamide removal from water by nanofiltration and reverse osmosis membrane.* Water Research, 2009. **43**: p. 4115-4122.
44. Garcia-Ac, A., et al., *Oxidation kinetics of cyclophosphamide and methotrexate by ozone in drinking water.* Chemosphere, 2010. **79**(11): p. 1056-1063.
45. Fernández, L.A., et al., *Cyclophosphamide degradation by advanced oxidation processes.* Water and Environment Journal, 2010. **24**(3): p. 174-180.
46. Tuerk, J., et al., *Efficiency, costs and benefits of AOPs for removal of pharmaceuticals from the water cycle.* Water Science and Technology, 2010. **61**(4): p. 985-993.
47. Lester, Y., et al., *Removal of pharmaceuticals using combination of UV/H2O2/O3 advanced oxidation process.* Water Science and Technology, 2011. **64**(11): p. 2230-2238.
48. Rowney, N.C., A.C. Johnson, and R.J. Williams, *CYTOTOXIC DRUGS IN DRINKING WATER: A PREDICTION AND RISK ASSESSMENT EXERCISE FOR THE THAMES CATCHMENT IN THE UNITED KINGDOM.* Environmental Toxocology and Chemistry, 2009. **28**(12): p. 2733-2743.
49. Straub, J.O., *Combined Environmental Risk Assessment for 5-Fluorouracil and Capecitabine in Europe.* Integrated Environmental Assessment and Management, 2009. **6**: p. 540-566.
50. Kosjek, T., et al., *Fluorouracil in the environment: Analysis, occurrence, degradation and transformation.* J. Chrom. A, 2013. **1290**: p. 62-72.
51. Kümmerer, K. and A. Al-Ahmad, *Biodegradability of the Anti-tumour Agents 5-Fluorouracil, Cytarabine, and Gemcitabine: Impact of the Chemical Structure and Synergistic Toxicity with Hospital Effluent.* Acta hydrochimica et hydrobiologica, 1997. **25**(4): p. 166-172.
52. Mahnik, S.N., et al., *Fate of 5-fluorouracil, doxorubicin, epirubicin, and daunorubicin in hospital wastewater and their elimination by activated sludge and treatment in a membrane-bio-reactor system.* Chemosphere, 2007. **66**: p. 30-37.
53. Pérez Rey, R., et al., *Ozonation of Cytostatics in Water Medium. Nitrogen Bases.* Ozone: Science & Engineering, 1999. **21**(1): p. 69-77.
54. Negreira, N., M. Lopez de Alda, and D. Barcelo, *On-line solid phase extraction–liquid chromatography–tandem mass spectrometry for the determination of 17 cytostatics and metabolites in waste, surface and ground water samples.* J. Chrom. A, 2013. **1280**: p. 64-74.
55. Moldovan, Z., *Occurrences of pharmaceutical and personal care products as micropollutants in rivers from Romania.* Chemosphere, 2006. **64**(11): p. 1808-1817.
56. Zuccato, E., et al., *Presence of therapeutic drugs in the environment.* The Lancet, 2000. **355**(9217): p. 1789-1790.
57. Martín, J., et al., *Simultaneous determination of a selected group of cytostatic drugs in water using high-performance liquid chromatography–triple-quadrupole mass spectrometry.* Journal of Separation Science, 2011. **34**(22): p. 3166-3177.

58. Valcárcel, Y., et al., *Detection of pharmaceutically active compounds in the rivers and tap water of the Madrid Region (Spain) and potential ecotoxicological risk.* Chemosphere, 2011. **84**(10): p. 1336-1348.
59. Martin, J., et al., *Simultaneous determination of a selected group of cytostatic drugs in water using high-performance liquid chromatography–triple-quadrupole mass spectrometry.* Journal of Separation Science, 2011. **34**: p. 3166-3177.
60. Deblonde, T. and P. Hartemann, *Environmental impact of medical prescriptions: assessing the risks and hazards of persistence, bioaccumulation and toxicity of pharmaceuticals.* Public Health, 2013. **127**(4): p. 312-317.
61. Zhang, J., et al., *Removal of cytostatic drugs from aquatic environment: A review.* Science of The Total Environment, 2013. **445–446**: p. 281-298.
62. Siegrist, H. and A. Joss, *Review on the fate of organic micropollutants in wastewater treatment and water reuse with membranes.* Water Science and Technology, 2012. **66**(6): p. 1369-1376.
63. Lin, A.Y., X. Wang, and W. Lee, *Phototransformation Determines the Fate of 5 -Fluorouracil and Cyclophosphamide in Natural Surface Waters.* Environmental Science and Technology, 2013. **47**: p. 4104-4112.
64. Mamouni, A., et al., *Comparison of different experimental designs to assess the degradability of pharmaceuticals in the environment*, in *SETAC Europe 15th Annual Meeting*. 2005: Lille, France.
65. Lutterbeck, C.A., et al., *Degradation of 5-FU by means of advanced (photo)oxidation processes: UV/H2O2, UV/Fe2 +/H2O2 and UV/TiO2 — Comparison of transformation products, ready biodegradability and toxicity.* Science of The Total Environment, 2015. **527–528**: p. 232-245.
66. García-Campaña, A., M. and W. Baeyens, R.G., *Principles and recent analytical applications of chemiluminescence.* Analusis, 2000. **28**(8): p. 686-698.
67. Rongen, H.A.H., et al., *Chemiluminescence and immunoassays.* Journal of Pharmaceutical and Biomedical Analysis, 1994. **12**(4): p. 433-462.
68. Ocaña-González, J.A., et al., *Application of chemiluminescence in the analysis of wastewaters – A review.* Talanta, 2014. **122**: p. 214-222.
69. Shultz, L.L. and T.A. Nieman, *Stopped-flow analysis of Ru(bpy)(3)(3+) chemiluminescent reactions.* Journal of Bioluminescence and Chemiluminescence, 1998. **13**(2): p. 85-90.
70. Li, F., et al., *Chemiluminescence detection in HPLC and CE for pharmaceutical and biomedical analysis.* Biomedical Chromatography, 2003. **17**(2-3): p. 96-105.
71. Gámiz-Gracia, L., et al., *Chemiluminescence detection in liquid chromatography: Applications to clinical, pharmaceutical, environmental and food analysis—A review.* Analytica Chimica Acta, 2009. **640**: p. 7-28.
72. Iranifam, M., *Revisiting flow-chemiluminescence techniques: pharmaceutical analysis.* Luminescence, 2013. **28**(6): p. 798-820.
73. Adcock, J.L., et al., *Chemiluminescence and electrochemiluminescence detection of controlled drugs.* Drug Testing and Analysis, 2011. **3**: p. 145-160.
74. Liu, M., Z. Lin, and J.-M. Lin, *A review on applications of chemiluminescence detection in food analysis.* Analytica Chimica Acta, 2010. **670**(1–2): p. 1-10.
75. Trojanowicz, M. and K. Kolacinska, *Recent advances in flow injection analysis.* Analyst, 2016. **141**(7): p. 2085-2139.
76. Fereja, T.H., A. Hymete, and T. Gunasekaran, *A Recent Review on Chemiluminescence Reaction, Principle and Application on Pharmaceutical Analysis.* ISRN Spectroscopy, 2013. **2013**: p. 12.
77. Ponhong, K., et al., *Simultaneous injection effective mixing analysis system for the determination of direct bilirubin in urinary samples.* Talanta, 2011. **87**: p. 113-117.

78. Pimenta, A.M., et al., *Application of sequential injection analysis to pharmaceutical analysis.* Journal of Pharmaceutical and Biomedical Analysis, 2006. **40**(1): p. 16-34.
79. Karim, M.M., et al., *A Batch Chemiluminescence Determination of Enoxacin Using a Tris-(1,10-phenanthroline)ruthenium(II)–Cerium(IV) System.* Journal of Fluorescence, 2006. **16**(4): p. 535-540.
80. Pulgarin, J.A.M., L.F.G. Bermejo, and P.F. Lopez, *Sensitive determination of captopril by time-resolved chemiluminescence using the stopped-flow analysis based on potassium permanganate oxidation.* Analytica Chimica Acta, 2005. **546**(1): p. 60-67.
81. Noguchi, N. and E. Niki, *DYNAMICS OF FREE-RADICAL FORMATION FROM THE REACTION OF PEROXIDES WITH HAEMPROTEINS AS STUDIED BY STOPPED-FLOW CHEMILUMINESCENCE.* Free Radical Research, 1995. **23**(4): p. 329-338.
82. Somnam, S., et al., *Hydrodynamic Sequential Injection with Stopped-flow Procedure for Consecutive Determination of Phosphate and Silicate in Wastewater.* Chiang Mai Journal of Science, 2014. **41**(3): p. 606-617.
83. Quintino, M.S.M. and L. Angnes, *Fast BIA-amperometric determination of isoniazid in tablets.* Journal of Pharmaceutical and Biomedical Analysis, 2006. **42**(3): p. 400-404.
84. Tsukagoshi, K., et al., *Consideration on peak shape in a batch-type chemiluminescence detection cell for capillary electrophoresis.* Journal of Chromatography A, 2001. **930**(1-2): p. 165-169.
85. Tsukagoshi, K., et al., *Batch-Type Detection Cell Using a Peroxyoxalate Chemiluminescence System for Capillary Electrophoresis.* Analytical Sciences, 1999. **15**(12): p. 1257-1260.
86. Tsukagoshi, K., et al., *Simple and Convenient Cell for Chemiluminescence Detection in Capillary Electrophoresis.* Analytical Sciences, 1999. **15**(11): p. 1047-1048.
87. Tsukagoshi, K., T. Nakamura, and R. Nakajima, *Batch-Type Chemiluminescence Detection Cell for Sensitization and Simplification of Capillary Electrophoresis.* Analytical Chemistry, 2002. **74**(16): p. 4109-4116.
88. Tsukagoshi, K., Y. Obata, and R. Nakajima, *Miniaturization of batch- and flow-type chemiluminescence detectors in capillary electrophoresis.* Journal of Chromatography A, 2002. **971**(1–2): p. 255-260.
89. Tsukagoshi, K., M. Tahira, and R. Nakajima, *Capillary electrophoresis apparatus equipped with a bioluminescence detector using a batch- or flow-type detection cell.* Journal of Chromatography A, 2005. **1094**(1-2): p. 192-195.
90. Murillo Pulgarín, J.A., L.F. García Bermejo, and J.A. Rubio Aranda, *Development of Time-Resolved Chemiluminescence for the Determination of Antu in River Water, Wheat, Barley, and Oat Grain Samples.* Journal of Agricultural and Food Chemistry, 2005. **53**(17): p. 6609-6615.
91. Oyama, M., T. Higuchi, and S. Okazaki, *Spectroscopic detection and kinetic analysis of short-lived aromatic amine cation radicals using an electron transfer stopped-flow method.* Journal of the Chemical Society, Perkin Transactions 2, 2001(8): p. 1287-1293.
92. Yeh, H.C. and W.Y. Lin, *Stopped-flow study of the enhanced chemiluminescence for the oxidation of luminol with hydrogen peroxide catalyzed by microperoxidase 8.* Talanta, 2003. **59**(5): p. 1029-1038.
93. Gaikwad, A., M. Silva, and D. Perezbendito, *SELECTIVE STOPPED-FLOW DETERMINATION OF MANGANESE WITH LUMINOL IN THE ABSENCE OF HYDROGEN-PEROXIDE.* Analytica Chimica Acta, 1995. **302**(2-3): p. 275-282.
94. Diaz, A.N. and J.A.G. Garcia, *NONLINEAR MULTICOMPONENT KINETIC-ANALYSIS FOR THE SIMULTANEOUS STOPPED-FLOW DETERMINATION OF CHEMILUMINESCENCE ENHANCERS.* Analytical Chemistry, 1994. **66**(7): p. 988-993.
95. Hadd, A.G., A. Seeber, and J.W. Birks, *Kinetics of Two Pathways in Peroxyoxalate Chemiluminescence.* The Journal of Organic Chemistry, 2000. **65**(9): p. 2675-2683.

96. Ma, A.J., Y.T. Chang, and W.Y. Lin, *A kinetic treatment of stopped-flow time courses for multiple chemiluminescence of the KIO4-luminol-Mn2+ system.* Luminescence, 2013. **28**(3): p. 355-362.
97. Hadd, A.G., et al., *Stopped-Flow Kinetics Investigation of the Imidazole-Catalyzed Peroxyoxalate Chemiluminescence Reaction.* The Journal of Organic Chemistry, 1998. **63**(9): p. 3023-3031.
98. Otamonga, J.P., et al., *A kinetic study of the enhancement of solution chemiluminescence of glyoxylic acid oxidation by manganese species.* Luminescence, 2015. **30**(5): p. 507-511.
99. Sanchez, F.G., A.N. Diaz, and J.A.G. Garcia, *STUDY OF THE ENHANCED CHEMILUMINESCENCE FROM THE LUMINOL HORSERADISH-PEROXIDASE HYDROGEN-PEROXIDE P-COUMARIC ACID SYSTEM AT VERY SHORT TIMES - STOPPED-FLOW SELECTIVE DETERMINATION OF P-COUMARIC ACID IN BEERS.* Analytica Chimica Acta, 1995. **310**(3): p. 399-406.
100. Pulgarin, J.A.M., J.M.L. Gallego, and M.N.S. Garcia, *Determination of Tiopronin in Pharmatceutical Preparations by Time Resolved Chemiluminescence Using the Stopped-Flow Technique.* Analytical Letters, 2013. **46**(11): p. 1836-1848.
101. García Sánchez, F., et al., *Determination of asulam by fast stopped-flow chemiluminescence inhibition of luminol/peroxidase.* Talanta, 2008. **77**(1): p. 294-297.
102. Pérez-Ruiz, T., et al., *Chemiluminescence determination of citrate and pyruvate and their mixtures by the stopped-flow mixing technique.* Analytica Chimica Acta, 2003. **485**(1): p. 63-72.
103. Murillo Pulgarin, J.A., et al., *Simultaneous stopped-flow determination of morphine and naloxone by time-resolved chemiluminescence.* Talanta, 2008. **74**(5): p. 1539-46.
104. Pulgarin, J.A.M., et al., *Simultaneous stopped-flow determination of morphine and naloxone by time-resolved chemiluminescence.* Talanta, 2008. **74**(5): p. 1539-1546.
105. Pérez-Ruiz, T., et al., *Chemiluminescence Determination of Glucose, Fructose and their Mixture by the Stopped-Flow Mixing Technique.* Microchimica Acta, 2003. **141**(1): p. 73-78.
106. Quintino, M.S.M., et al., *Amperometric quantification of sodium metabisulfite in pharmaceutical formulations utilizing tetraruthenated porphyrin film modified electrodes and batch injection analysis.* Talanta, 2006. **68**(4): p. 1281-1286.
107. Osullivan, D.W., A.K. Hanson, and D.R. Kester, *STOPPED-FLOW LUMINOL CHEMILUMINESCENCE DETERMINATION OF FE(II) AND REDUCIBLE IRON IN SEAWATER AT SUBNANOMOLAR LEVELS.* Marine Chemistry, 1995. **49**(1): p. 65-77.
108. Gaikwad, A., M. Silva, and D. Perezbendito, *SENSITIVE DETERMINATION OF PERIODATE AND TARTARIC ACID BY STOPPED-FLOW CHEMILUMINESCENCE SPECTROMETRY.* Analyst, 1994. **119**(8): p. 1819-1824.
109. Pulgarin, J.A.M., L.E.G. Bermejo, and J.A.R. Aranda, *Time-resolved chemiluminescence: a novel tool for improved emission sequence in stopped-flow analysis - Application to a kinetic study of the oxidation of naloxone.* Analytica Chimica Acta, 2004. **517**(1-2): p. 111-117.
110. Ventura, S., M. Silva, and D. Perezbendito, *STOPPED-FLOW CHEMILUMINESCENCE SPECTROMETRY TO IMPROVE THE DETERMINATION OF PENICILLINS BASED ON THE LUMINOL IODINE REACTION.* Analytica Chimica Acta, 1992. **266**(2): p. 301-307.
111. Mervartov´a, K., M. Pol´aˇsek, and J.M. Calatayud, *Recent applications of flow-injection and sequential-injection analysis techniques to chemiluminescence determination of pharmaceuticals.* Journal of Pharmaceutical and Biomedical Analysis, 2007. **45**: p. 367-381.
112. Lewis, S.W., et al., *Pulsed flow chemistry: a new approach to solution handling for flow analysis coupled with chemiluminescence detection.* Analyst, 2000. **125**: p. 1869-1874.
113. Francis, P.S., et al., *Flow analysis based on a pulsed flow of solution: theory, instrumentation and applications.* Talanta, 2002. **58**(6): p. 1029-1042.
114. Rodrigues, S.S.M. and J.L.M. Santos, *Chemiluminometric determination of captopril in a multi-pumping flow system.* Talanta, 2012. **96**(0): p. 210-215.

115. Marques, K.L., J.L.M. Santos, and J. Lima, *Application of pulsed flow analysis for chemiluminescent screening of fluoxetine counterfeit pharmaceuticals.* Analytical Letters, 2007. **40**(11): p. 2241-2251.
116. Manera, M., et al., *Rapid chemiluminometric determination of gabapentin in pharmaceutical formulations exploiting pulsed-flow analysis.* Luminescence, 2009. **24**(1): p. 10-14.
117. Lewis, S.W., et al., *Monitoring urea levels during haemodialysis with a pulsed-flow chemiluminescence analyser.* Analytica Chimica Acta, 2002. **461**(1): p. 131-139.
118. Campíns-Falcó, P., L.A. Tortajada-Genaro, and F. Bosch-Reig, *A new flow cell design for chemiluminiscence analysis.* Talanta, 2001. **55**(2): p. 403-413.
119. Yuan, J. and A.M. Shiller, *Determination of Subnanomolar Levels of Hydrogen Peroxide in Seawater by Reagent-Injection Chemiluminescence Detection.* Analytical Chemistry, 1999. **71**(10): p. 1975-1980.
120. Ellis, R.J. and A.G. Wright, *Optimal use of photomultipliers for chemiluminescence and bioluminescence applications.* Luminescence, 1999. **14**(1): p. 11-18.
121. Kiba, N., et al., *Highly sensitive flow-injection determination of glucose in plasma using an immobilized pyranose oxidase and a chemiluminometric peroxidase sensor.* Analytica Chimica Acta, 1997. **354**(1–3): p. 205-210.
122. Gorman, B.A., P.S. Francis, and N.W. Barnett, *Tris(2,2'-bipyridyl)ruthenium(ii) chemiluminescence.* Analyst, 2006. **131**(5): p. 616-639.
123. Adcock, J.L., P.S. Francis, and N.W. Barnett, *Acidic potassium permanganate as a chemiluminescence reagent—A review.* Analytica Chimica Acta, 2007. **601**(1): p. 36-67.
124. Hindson, B.J. and N.W. Barnett, *Analytical applications of acidic potassium permanganate as a chemiluminescence reagent.* Analytica Chimica Acta, 2001. **445**(1): p. 1-19.
125. Hindson, C.M., et al., *Mechanism of permanganate chemiluminescence.* Analytical Chemistry, 2010. **82**: p. 4174-4180.
126. Adcock, J.L., et al., *Advances in the use of acidic potassium permanganate as a chemiluminescence reagent: A review.* Analytica Chimica Acta, 2014. **807**: p. 9-28.
127. Sun, H.W. and L.Q. Li, *Flow-injection-enhanced chemiluminescence method for the determination of four anticancer drugs.* Journal of Analytical Chemistry, 2008. **63**(5): p. 485-491.
128. Li, L. and H. Sun, *A novel sensitized chemiluminescence flow injection system for the determination of adriamycin and mitomycin.* Journal of the Iranian Chemical Society, 2008. **5**(1): p. 140-149.
129. Adcock, J.L., et al., *A review of recent advances in chemiluminescence detection using nano-colloidal manganese(IV).* Analytica Chimica Acta, 2014. **848**: p. 1-9.
130. Barnett, N.W., et al., *Chemically induced phosphorescence from manganese(II) during the oxidation of various compounds by manganese(III), (IV) and (VII) in acidic aqueous solutions.* Analytica Chimica Acta, 2002. **451**(2): p. 181-188.
131. Adcock, J.L., et al., *The characteristic red chemiluminescence from reactions with acidic potassium permanganate: further spectroscopic evidence for a manganese(ii) emitter.* Analyst, 2008. **133**(1): p. 49-51.
132. Wang, L., et al., *Flow injection chemiluminescence determination of 6-mercaptopurine based on a new system of potassium permanganate–thioacetamide–sodium hexametaphosphate.* Luminescence, 2010. **25**(6): p. 431-435.
133. Holland, B.J., et al., *The importance of chain length for the polyphosphate enhancement of acidic potassium permanganate chemiluminescence.* Analytica Chimica Acta, 2014. **842**: p. 35-41.
134. Francis, P.S., et al., *Enhanced permanganate chemiluminescence.* Analyst, 2011. **136**(1): p. 64-66.
135. Perez-Benito, J.F., E. Brillas, and R. Pouplana, *Identification of a soluble form of colloidal manganese(IV).* Inorganic Chemistry, 1989. **28**(3): p. 390-392.

136. Slezak, T., et al., *Autocatalytic Nature of Permanganate Oxidations Exploited for Highly Sensitive Chemiluminescence Detection.* Analytical Chemistry, 2010. **82**(6): p. 2580-2584.
137. Jáky, M. and L.I. Simándi, *Autocatalytic oxidation of propane-1,2-diol by soluble manganese(IV) in aqueous phosphoric acid.* Inorganica Chimica Acta, 1984. **90**(3): p. L39-L41.
138. Jáky, M., *Oxidations with soluble manganese(IV) phosphate.* Polyhedron, 1993. **12**(11): p. 1271-1275.
139. Barnett, N.W., et al., *Soluble manganese(IV); a new chemiluminescence reagent.* Analyst, 2001. **126**(10): p. 1636-1639.
140. Brown, A.J., et al., *Manganese(III) and manganese(IV) as chemiluminescence reagents: A review.* Analytica Chimica Acta, 2008. **624**(2): p. 175-183.
141. Smith, Z.M., et al., *On-line generation of a colloidal manganese(IV) reagent for chemiluminescence detection.* Microchemical Journal, 2013. **111**: p. 67-73.
142. Agater, I.B., *Applications of permanganate chemiluminescence to the anlysis of food components*, in *Department of Chemical and Biological Sciences*. 1999, The University of Huddersfield. p. 248.
143. Du, J. and H. Wang, *Chemiluminescence of nano-colloidal MnO2 with formaldehyde and its analytical applications.* Acta Chimic Sinica (Chin. Ed.), 2012. **70**: p. 537-543.
144. Smith, Z.M., et al., *Ethanol as an alternative to formalydehyde for the enhancement of manganese(IV) chemiluminescence detection.* Talanta, 2014. **130**: p. 221-225.
145. Nalewajko-Sieliwoniuk, E., et al., *Application of direct-injection detector integrated with the multi-pumping flow system to chemiluminescence determination of the total polyphenol index.* Analytica Chimica Acta, 2016. **911**: p. 82-91.
146. Nalewajko-Sieliwoniuk, E., et al., *Determination of polyphenolic compounds in Cirsium palustre (L.) extracts by high performance liquid chromatography with chemiluminescence detection.* Talanta, 2015. **133**: p. 38-44.
147. Nalewajko-Sieliwoniuk, E., et al., *A Novel Multicommuted Flow Method with Nanocolloidal Manganese(IV)-Based Chemiluminescence Detection for the Determination of the Total Polyphenol Index.* Food Analytical Methods, 2016. **9**(4): p. 991-1001.
148. Nalewajko-Sieliwoniuk, E., et al., *A study on the selection of chemiluminescence system for the flow injection determination of the total polyphenol index of plant-derived foods.* Food Chemistry, 2015. **176**: p. 175-183.
149. Tsaplev, Y.B., R.F. Vasil'ev, and A.V. Trofimov, *Phenomenological features of chemiluminescence in manganese(III) reduction reactions.* High Energy Chemistry, 2015. **49**(3): p. 189-192.
150. Tsaplev, Y.B., R.F. Vasil'ev, and A.V. Trofimov, *Quenchers and inhibitors of chemiluminescence in the reduction reactions of Mn3+.* Russian Journal of Physical Chemistry A, 2015. **89**(6): p. 1103-1107.
151. Karavaev, A.D., et al., *Mn(II) chemiluminescence in the belousov-zhabotinskII (BZh) autooscillating reaction.* Bulletin of the Academy of Sciences of the USSR, Division of chemical science, 1987. **36**(5): p. 1105-1105.
152. Gerardi, R.D., N.W. Barnett, and P. Jones, *Two chemical approaches for the production of stable solutions of tris(2,2'-bipyridyl)ruthenium(III) for analytical chemiluminescence.* Analytica Chimica Acta, 1999. **388**(1–2): p. 1-10.
153. Gorman, B.A., et al., *Effect of oxidant type on the chemiluminescence intensity from the reaction of tris(2,2'-bipyridyl)ruthenium(III) with various organic acids.* Talanta, 2007. **72**(2): p. 568-574.
154. Gerardi, R.D., N.W. Barnett, and S.W. Lewis, *Analytical applications of tris(2,2'-bipyridyl)ruthenium(III) as a chemiluminescent reagent.* Analytica Chimica Acta, 1999. **378**(1–3): p. 1-41.
155. Uchikura, K., *Determination of oxalate by FIA with electrogenerated chemiluminescence detection.* Bunseki kagaku, 1990. **39**(6): p. 323-326.

156. Kaczmarek, M., *Energy Transfer Processes of Chemiluminescence Reaction Systems with Cerium(IV) Ions and Their Analytical Application: A Review.* Journal of Fluorescence, 2015. **25**(2): p. 419-431.
157. Marquette, C.A. and L.J. Blum, *Applications of the luminol chemiluminescent reaction in analytical chemistry.* Anal Bioanal Chem, 2006. **385**: p. 546-554.
158. Xu, S., et al., *A chemiluminescence resonance energy transfer system composed of cobalt(II), luminol, hydrogen peroxide and CdTe quantum dots for highly sensitive determination of hydroquinone.* Microchimica Acta, 2016. **183**(2): p. 667-673.
159. Catalá-Icardo, M., et al., *Determination of organothiophosphorus pesticides in water by liquid chromatography and post-column chemiluminescence with cerium(IV).* Journal of Chromatography A, 2014. **1341**(0): p. 31-40.
160. Catala-Icardo, M., J.L. Lopez-Paz, and J. Blazquez-Perez, *Development of a Photoinduced Chemiluminescent Method for the Determination of the Herbicide Quinmerac in Water.* Applied Spectroscopy, 2015. **69**(10): p. 1199-1204.
161. Wang, Z.H., et al., *An ultrasensitive calcein sensor based on the implementation of a novel chemiluminescence system with modified kaolin.* Sensors and Actuators B-Chemical, 2015. **212**: p. 264-272.
162. Linnik, R.P. and O.A. Zaporozhets, *Chemiluminescence determination of dissolved copper(II) in natural waters.* Journal of Analytical Chemistry, 2014. **69**(6): p. 519-524.
163. Durand, A., et al., *Microplate-reader method for the rapid analysis of copper in natural waters with chemiluminescence detection.* Frontiers in Microbiology, 2013. **3**.
164. Liang, H.C., N. Bilon, and M.T. Hay, *Analytical Methods for Pesticide Residues in the Water Environment.* Water Environment Research, 2015. **87**(10): p. 1923-1937.
165. Zhihua, X. and Y. Jiaguo, *A novel solid-state electrochemiluminescence sensor based on Ru(bpy) 3 2 + immobilization on TiO 2 nanotube arrays and its application for detection of amines in water.* Nanotechnology, 2010. **21**(24): p. 245501.
166. Čapka, L., et al., *A portable device for fast analysis of explosives in the environment.* Journal of Chromatography A, 2015. **1388**: p. 167-173.
167. Adcock, J.L., P.S. Francis, and N.W. Barnett, *Emitting Species in Chemiluminescence Reactions with Acidic Potassium Permanganate: A Re-Evaluation Based on New Spectroscopic Evidence.* Journal of Fluorescence, 2009. **19**(5): p. 867-874.
168. Dong, Y., et al., *Spectroelectrochemistry for studying electrochemiluminescence mechanism.* Electrochemistry Communications, 2009. **11**(5): p. 983-986.
169. Jackson, J.K., et al., *Topoisomerase inhibitors as anti-arthritic agents.* Inflammation Research, 2008. **57**(3): p. 126-134.
170. Smit, T., et al., *Comparison of the effects of cisplatin and a novel platinum polymer conjugate on the production of reactive oxygen species by human neutrophils in vitro.* Drug Development Research, 2005. **66**(3): p. 204-209.
171. Czuba, Z.P., et al., *The effects of taxol (paclitaxel) on chemiluminescence of neutrophils, macrophages and J.774.2 cell line.* Acta Biochimica Polonica, 1998. **45**(1): p. 103-106.
172. Ueta, E. and T. Osaki, *Suppression by anticancer agents of reactive oxygen generation from polymorphonuclear leukocytes.* Free Radical Research, 1996. **24**(1): p. 39-53.
173. Barret, J.M., et al., *Evaluation of DNA repair inhibition by antitumor or antibiotic drugs using a chemiluminescence microplate assay.* Carcinogenesis, 1997. **18**(12): p. 2441-2445.
174. Salles, B., et al., *In vitro eukaryotic DNA excision repair assays: An overview.* Biochimie, 1995. **77**(10): p. 796-802.
175. Gray, S., et al., *Flow analysis techniques for spatial and temporal measurement of nutrients in aquatic systems.* Environmental Chemistry, 2006. **3**(1): p. 3-18.
176. Sidlova, P., R. Podlipna, and T. Vanek, *Cytostatic pharmaceuticals in the environment.* Chemistry Sheets, 2011. **105**(1): p. 8-14.

177. Francis, P.S., et al., *Enhanced permanganate chemiluminescence.* Analyst, 2011. **136**: p. 64-66.
178. Terry, J.M., et al., *Chemiluminescence detection of amino acids and related compounds using acidic potassium permanganate, manganese(IV) or tris(2,2'-bipyridine)ruthenium(III).* Talanta, 2012. **99**: p. 1051-1056.
179. McDermott, G.P., et al., *Stable Tris(2,2'-bipyridine)ruthenium(III) for Chemiluminescence Detection.* Analytical Chemistry, 2011. **83**(13): p. 5453-5457.
180. Bogdanovic, D., *Studies into the suitability of acidic potassium permanganate chemiluminescence for determination of inorganic ions*, in *School of Chemical and Physical Sciences*. 2011, Flinders University: Adelaide, South Australia.
181. Osborne, O.D., *Investigations into the natural varaiton of pyrite reactivity*, in *School of Chemical and Physical Sciences*. 2013, Flinders University: Adelaide, South Australia.
182. Venable, F. and D. Jackson, *The reaction between hydrochloric acid and potassium permanganate.* Journal of the American Chemical Society, 1920. **42**: p. 237.
183. Anastos, N., et al., *Comparison of soluble manganese(IV) and acidic potassium permanganate chemiluminescence detection using flow injection and sequential injection analysis for the determination of ascorbic acid in Vitamin C tablets.* Talanta, 2004. **64**(1): p. 130-134.
184. Yang, F., et al., *Determination of captopril with potassium permanganate chemiluminescence system.* Der Pharma Chemica, 2016. **8**(1): p. 289-293.
185. Campiglio, A., *Chemiluminescence determination of naltrexone based on potassium permanganate oxidation.* Analyst, 1998. **123**: p. 1053-1056.
186. Wołyniec, E., et al., *Determination of lipoic acid by flow-injection and high-performance liquid chromatography with chemiluminescence detection.* Talanta, 2012. **96**: p. 223-229.
187. H. Sun, et al., Yaowu Fenxi Zazhi. **28**: p. 219-222.
188. Perez-Benito, J.F., C. Arias, and E. Amat, *A Kinetic Study of the Reduction of Colloidal Manganese Dioxide by Oxalic Acid.* Journal of Colloid and Interface Science, 1996. **177**(2): p. 288-297.
189. Grante, I., A. Actins, and L. Orola, *Protonation effects on the UV/Vis absorption spectra of imatinib: A theoretical and experimental study.* Spectrochimica Acta Part A: Molecular and Biomolecular Spectroscopy, 2014. **129**: p. 326-332.
190. Brown, T.L., H.E. LeMay, and B.E. Bursten, *Chemistry - The Central Science*. 2006, Upper Saddle River, NJ: Pearson Education, Inc.
191. Briois, V., et al., *Time-Resolved Study of the Oxidation of Ethanol by Cerium(IV) Using Combined Quick-XANES, UV−Vis, and Raman Spectroscopies.* The Journal of Physical Chemistry A, 2005. **109**(2): p. 320-329.
192. Lakshmi, S. and R. Renganathan, *Kinetics of oxidation of certain pyrimidines by Ce(IV).* International Journal of Chemical Kinetics, 1996. **28**(10): p. 713-720.
193. Craig, C.R. and R.E. Stitzel, eds. *Modern pharmacology with clinical applications*. 6th ed. 2003, Lippincott Williams & Wilkins: United States of America.
194. Gilard, V., et al., *Chemical and Biological Evaluation of Hydrolysis Products of Cyclophosphamide.* Journal of Medicinal Chemistry, 1994. **37**(23): p. 3986-3993.
195. Brune, S.N. and D.R. Bobbitt, *Effect of pH on the reaction of tris(2,2'-bipyridyl)ruthenium(III) with amino acids: Implications for their detection.* Talanta, 1991. **38**(4): p. 419-424.
196. Khot, M.S., et al., *Spectrofluorimetric determination of 5-fluorouracil by fluorescence quenching of 9-anthracenecarboxylic acid.* Spectrochimica Acta Part A: Molecular and Biomolecular Spectroscopy, 2010. **77**(1): p. 82-86.
197. Mikuška, P. and Z. Vecera, *Simultaneous determination of nitrite and nitrate in water by chemiluminescent flow-injection analysis.* Analytica Chimica Acta, 2003. **495**: p. 225-232.

198. Borges, E.P., A.F. Lavorante, and B. Freire dos Reis, *Determination of bromide ions in seawater using flow system with chemiluminescence detection.* Analytica Chimica Acta, 2005. **528**: p. 115-119.
199. Lee, W., *Tris(2,2'-bipyridyl)ruthenium(II) electrogenerated chemiluminescence in analytical science.* Microchimica Acta, 1997. **127**(1): p. 19-39.
200. Negreira, N., et al., *Multianalyte determination of 24 cytostatics and metabolites by liquid chromatography-electrospray-tandem mass spectrometry and study of their stability and optimum storage conditions in aqueous solution.* Talanta, 2013. **116**: p. 290-299.
201. Greenway, G.M. and S.J.L. Dolman, *Analysis of tricyclic antidepressants using electrogenerated chemiluminescence.* Analyst, 1999. **124**(5): p. 759-762.
202. Arnold, H. and A. Klose, *Die Hydrolyse hexacyclischer N-Lostphosphamidester im gepufferten System (Hydrolysis of hexacyclic N-Mustardphosphamide esters in buffered systems).* Arzneim.-Forsch., 1960. **10**: p. 288-291.
203. Friedman, O.M., S. Bien, and J.K. Chakrabarti, *Studies on the Hydrolysis of Cyclophosphamide. I. Identification of N-(2-Hydroxyethyl)-N'-(3-hydroxypropyl)ethylenediamine as the Main Product1.* Journal of the American Chemical Society, 1965. **87**(21): p. 4978-4979.
204. Zon, G., S.M. Ludeman, and W. Egan, *High-resolution nuclear magnetic resonance investigations of the chemical stability of cyclophosphamide and related phosphoramidic compounds.* Journal of the American Chemical Society, 1977. **99**(17): p. 5785-5795.
205. Pankiewicz, K., et al., *Synthesis and Absolute Configuration Assignments of Enantiomeric Forms of Ifosphamide, Sulfosphamide, and Trofosphamide.* Journal of the American Chemical Society, 1979. **101**(26): p. 7712-7718.
206. Connors, K.A., G.L. Amidon, and V.J. Stella, *Chemical Stability of Pharmaceuticals - A Handbook for Pharmacists*. 2nd ed. 1986, USA: John Wiley & Sons, Inc.
207. Vehovec, T. and A. Obreza, *Review of operating principle and applications of the charged aerosol detector.* Journal of Chromatography A, 2010. **1217**(10): p. 1549-1556.
208. Schellinger, A.P. and P.W. Carr, *Solubility of buffers in aqueous-organic eluents for reversed-phase liquid chromatography.* LCGC North America, 2004. **22**.
209. Dolan, J., *A Guide of HPLC and LC-MS Buffer Selection*. Advanced Chromatography Technologies: Averdeen, Scotland.
210. Wada, M., et al., *Enhancement of peroxyoxalate chemiluminescence intensity by surfactants and its application to detect detergent.* Talanta, 2010. **81**(3): p. 1133-1136.